



THE UNIVERSITY *of* EDINBURGH

This thesis has been submitted in fulfilment of the requirements for a postgraduate degree (e.g. PhD, MPhil, DClinPsychol) at the University of Edinburgh. Please note the following terms and conditions of use:

This work is protected by copyright and other intellectual property rights, which are retained by the thesis author, unless otherwise stated.

A copy can be downloaded for personal non-commercial research or study, without prior permission or charge.

This thesis cannot be reproduced or quoted extensively from without first obtaining permission in writing from the author.

The content must not be changed in any way or sold commercially in any format or medium without the formal permission of the author.

When referring to this work, full bibliographic details including the author, title, awarding institution and date of the thesis must be given.

Health Monitoring of Renewable Energy Systems

Marco Antonio Sepulveda Gutierrez



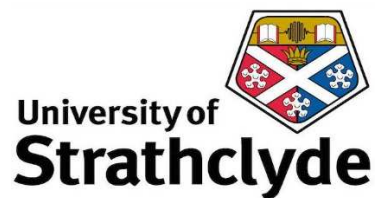
A thesis submitted in partial fulfilment of the requirements for the award on an
Engineering Doctorate

The University of Edinburgh

2018

IDCORE

This thesis is submitted in partial fulfilment of the requirements for the award of an Engineering Doctorate (EngD), jointly awarded by the University of Edinburgh, the University of Exeter and the University of Strathclyde. The work presented has been conducted under the industrial supervision of Lloyd's Register.



Abstract

The offshore wind energy industry has grown exponentially; globally, there is 12GW of installed capacity of offshore wind, of which over 95% has been installed in the past ten years. Access and maintenance in offshore wind farms can be difficult and considerably more expensive than onshore wind farms. Additionally, with low availability levels and greater downtime due to failures, there is a growing interest in the optimisation of operation and maintenance (O&M) activities to maximise profitability.

Traditionally, maintenance activities on critical components and subsystems have deployed two maintenance approaches; time-based preventative or corrective. Time-based preventative or scheduled maintenance approaches are based on intervening at fixed intervals, determined in advance for each component. Scheduling is based on failure statistics such as mean time between failures (MTBF), mean time to repair (MTTR) or mean time to failure (MTTF). These come either from publicly available databases or operational measurements. As part of preventive maintenance activities, there are annual services of the turbine to replace and maintain any component or assembly based on manufacturers' indications. On the other hand, the corrective maintenance approach involves operating equipment until it fails and then restoring it, repairing it, or replacing it.

Due to conservative estimates regarding the probability of failure, preventive and corrective maintenance approaches have financial implications associated with them. In the preventive approach, components are frequently replaced before they reach the end of their working life. In contrast, corrective maintenance guarantees that the serviceable life of a component is maximised, but it is subjected to long downtime, which is expensive regarding energy generation loss. Additionally, failure of the component may cause consequential damage to other parts of the wind turbine system, resulting in even greater repair costs, downtime and loss of revenue.

A comprehensive literature review has been undertaken in the areas of maintenance, turbine reliability, turbine failure modes and causes, physics of failure, condition monitoring techniques, and costs. The limitations and disadvantages of current operation and maintenance practices are identified, and new approaches combining the knowledge of the

condition of components and historical data are proposed and compared to achieve optimal turbine availability and maintenance cost reduction.

A Failure Modes and Effects Analysis (FMEA) was performed for the functional modes of each system, subsystem, assembly and component following the British standard BS EN 60812:2006. Currently, the most common offshore wind turbine uses three blades, a 3-stage gearbox, induction generator and a fully rated power converter. The Siemens 3.6MW -120 turbine is selected for this project as an example of this configuration. The main objectives of undertaking this comprehensive FMEA are to identify critical components and their failures with significant impact on the wind turbine operation in terms of maintainability, safety and availability. The assessment identified 500 components and almost 1000 failure causes. The most critical assemblies identified in terms of severity, occurrence and undetectability of the failure are; the frequency converter, pitch system, yaw system and gearbox.

The implementation of a condition-based maintenance philosophy, including the development of real predictive approaches which estimate the remaining useful life of degrading critical components has been analysed by the recent literature. However, developing such capabilities for the critical assemblies identified is a significant technical challenge. This study aims to develop and demonstrate the implementation of a methodology and appropriate algorithms to optimise O&M of offshore wind farms, by estimating the remaining useful life of critical components with greater accuracy using a combination of physics-based models, statistical-based models and data mining approaches.

A register of trends and likely the main causes of failures of the power converter, gearbox, yaw system and pitch system was generated through a thorough literature search and participation in conferences and workshops during the project. The main sources of failure of the power converter and gearbox have been represented by algorithms and physics-based models developed in Python and proprietary software, respectively. These algorithms comprise two phases: diagnosis or learning phase using historical data (such as SCADA or digital information recorded by condition monitoring systems) and prognosis phase using simulated data (using as a basis the wind turbine aero-elastic software FASTv8). The pitch system failure mechanisms were explored using a combination of data mining approaches and subject matter expert knowledge. Examples of approaches investigated and implemented include: Support Vector Machine (SVM) to define normal behaviour and K

Nearest Neighbour (KNN) to classify new observations regarding operation state (green for normal operation, amber for abnormal operation, red for failure). New observations with amber or red colours need to be analysed further, to diagnose potential failure modes using a decision tree algorithm with more variables related to the pitch system.

The goals of developing a well-defined strategy for maintenance interventions and optimised management of wind farm logistics are required to effectively improve wind farm availability while reducing the cost of operations. Additionally, a clear identification of uncertainties inherent in stochastic processes, necessary for estimating access, failure prognosis and failure probabilities is required for operators to make informed decisions. The final output of this work is an O&M cost model which analyses and compares a conventional O&M strategy using a combination of preventive and reactive maintenance against an O&M strategy using the approaches described above for failure prognosis and diagnosis. The analysis is performed for a fictitious offshore wind farm with one-year operational data. The results include availability, downtime, the cost of repair, loss of production, revenue losses and the hidden CO₂ emissions of the maintenance activities taking into account a combined probability level to account for the uncertainties.

Acknowledgements

First and foremost I would like to thank to my lead supervisor Dr Jonathan Shek for his career and academic advice and unconditional support. Besides my lead supervisor, I would like to thank to Dr Philipp Thies and Dr Erkan Oterkus for their comprehensive comments and hard questions, which help me to widen my research and knowledge from several points of views.

My sincere thanks also go to my industrial supervisor, Peter Davies who provided me an opportunity to join their team in a great organisation. In particular, I am grateful to Dr Mark Spring who, besides Peter, encourage me to push myself to be a better person and engineer.

Last but not the least, I would like to thank my all family, especially to my wife Paulina and my sons Antonio and Sebastian for supporting me on this process throughout writing this thesis and on any aspects of my life. Without their precious support and love, it would not be possible to conduct this project.

Declaration

I declare that this thesis was composed by myself and that the material presented, except where clearly indicated, is my own work. I declare that the work has not been submitted for consideration as part of any other degree or professional qualification.

Signed:

A handwritten signature in blue ink, consisting of a large, stylized initial 'C' followed by a series of connected loops and a final flourish.

Contents

List of Figures	12
List of Tables	15
Abbreviations	17
Definitions of key terms.....	19
CHAPTER 1 - INTRODUCTION	22
1.1 Introduction	22
1.2 Thesis Background	22
1.3 Thesis Description	24
1.3.1 Aims.....	24
1.3.2 Thesis Outline.....	25
1.3.3 Publications.....	27
1.4 Thesis contribution to knowledge	28
CHAPTER 2 – LITERATURE REVIEW	29
2.1 Offshore Wind Turbines – configuration and systems	29
2.1.1 Components Functionality, Materials and Failure Characteristics	31
2.1.2 Critical Components of an Offshore Wind Turbine.....	40
2.1.3 Condition Monitoring Techniques for Offshore Wind Turbines	43
2.1.4 Condition Monitoring using SCADA data	50
2.2 Maintenance of Offshore Wind Farms	52
2.2.1 Reliability Centred Maintenance (RCM)	55
2.2.2 Spare parts management.....	58
2.2.3 O&M Strategy factors	59
2.2.4 Condition Based Maintenance.....	59
2.2.5 Fault Prognostic	60
2.3 Risk Assessment Approach for Offshore Wind Turbines	63
CHAPTER 3 – FAILURE MODES AND EFFECTS ANALYSIS (FMEA)	65
3.1 Introduction	65
3.1.1 Scope.....	66
3.1.2 Wind Turbine System.....	66
3.2 FMEA and FMECA methodology	67
3.2.1 Assumptions and Ground Rules.....	68
3.2.2 Data sources.....	71
3.2.3 Functional Block Diagram	72
3.2.4 FMEA Worksheet	75

3.2.5 Ratings.....	75
3.2.6 Analysis Flowchart	78
3.3 Criticality Analysis	78
3.4 Results Analysis.....	79
3.4.1 RPN and Failure Contribution	79
3.4.2 Consequential Damage	86
3.4.3 Failure Detectability and Criticality.....	87
3.4.4 Criticality Analysis Results.....	89
3.4.5 Top 30 chart for failure mechanisms	91
3.4.5 Sensitivity Analysis	93
3.4.6 3D Risk Matrix	94
3.4.7 FMEA comparison with European projects	95
3.5 Confidence of the Accuracy of the Assigned Ratings (CAAR)	99
3.6 Conclusion.....	102
CHAPTER 4 – FAILURE PROGNOSIS BASED ON PHYSICS-BASED MODELS	104
4.1 Introduction	104
4.2 Prediction methodology	104
4.2.1 Wind Turbine dynamic integrated system in FASTv8	105
4.2.2 Generation of future events for failure prognosis.....	109
4.3 Gearbox physics-model.....	111
4.3.1 Gearbox failure investigation.....	113
4.3.2 Physics-based model of the gearbox	115
4.3.3 Physics-based model outputs: Gearbox.....	121
4.4 Power converter physics-based model.....	122
4.4.1 Failure investigation of power converter.....	123
4.4.2 Induction generator model	124
4.4.3 Power losses calculation	126
4.4.4 Thermal model	129
4.4.5 Physics-based model outputs: Power converter	134
4.5 Conclusion.....	136
CHAPTER 5 – DATA MINING APPROACH FOR THE PITCH SYSTEM.....	138
5.1 introduction	138
5.1.1 Pitch system technology	139
5.1.2 Data mining approach objectives	140
5.2 Data analysis	141

5.2.1 Data mining process.....	141
5.2.2 SCADA data analysis.....	142
5.2.3 Failure investigation outputs	145
5.3 Support Vector Machine (SVM)	147
5.4 Decision Tree Algorithm (DTA).....	150
5.5 K-Nearest Neighbours (KNN)	152
5.6 Data mining approach outputs	154
5.7 Conclusion.....	156
CHAPTER 6 - O&M COST MODEL	158
6.1 Introduction	158
6.1.2 Objectives.....	159
6.1.3 O&M cost model outline.....	160
6.2 O&M of offshore wind farms.....	162
6.2.1 Key offshore wind energy O&M market trends.....	164
6.2.2 O&M logistics.....	165
6.2.3 Spare part management	168
6.3 O&M optimization overview.....	169
6.4 O&M cost model.....	171
6.4.1 General description.....	171
6.4.2 Maintenance classes, repair actions and spare part availability	172
6.4.3 Wind turbine database	175
6.4.4 Digital sensors	176
6.4.5 Maintenance strategies	177
6.4.6 Meteorological conditions	181
6.4.7 Wind turbine power output.....	183
6.4.8 Economic parameters	187
6.4.9 O&M costs model outputs	189
CHAPTER 7 – CONCLUSIONS AND DISCUSSIONS	195
7.1 General.....	195
6.2 Conclusions	196
Physics-based models	198
Gearbox.....	198
Power converter	200
Data mining approach.....	200
O&M cost model.....	202

6.3 Further work	204
FMEA	204
Physics-based models	205
Data mining.....	205
O&M cost model.....	206
REFERENCES.....	209
ANNEX.....	220
Annex 1: FMEA Failure analysis	220
Annex 2: FASTv8 pre-processors.....	223

List of Figures

Figure 1. Thesis structure – flow diagram.....	26
Figure 2. Main parts of a wind turbine. [21,,22]	30
Figure 3. Wind turbine taxonomy [3].....	30
Figure 4. Typical Wind Turbine 3-stage Gearbox [31]	33
Figure 5. Gearbox vulnerability map [31]	35
Figure 6. Gearbox teeth. From healthy tooth (left) to missing tooth (right).....	35
Figure 7. Hydraulic unit of pitching system (Turbine VESTAS V39/V4x/V90). [24].....	37
Figure 8. Example of wind turbine brake system [24]	38
Figure 9. Example of a yaw system.[42]	40
Figure 10. Distribution of failures for wind turbine components [21].	42
Figure 11. Failure rates across wind turbine sub-assemblies [45].....	42
Figure 12. Typical development of a mechanical failure [21].....	46
Figure 13. Vibration condition monitoring system formed by a data acquisition unit and accelerometers (yellow circles) mounted on the drive train and generator. The revolution speed of the generator shaft measured by a proximity switch (purple circle). [55].....	47
Figure 14. Real time data exchange network structure [57].	50
Figure 15. Maintenance strategies. [64,65] [62][3]	52
Figure 16. Corrective Maintenance compared to Scheduled Preventive Maintenance [3].	53
Figure 17. RCM stages [66] [63].....	57
Figure 18. RCM framework [66] [63]	58
Figure 19. Condition based maintenance compared to scheduled and corrective maintenance. [23] [23].....	60
Figure 20. Remaining useful life probability distribution [49].	61
Figure 21. Prognosis techniques [6].....	61
Figure 22. Wind turbine market trends.	67
Figure 23. Siemens Turbine SWT 3.6 -120.	67
Figure 24. Hierarchical Wind Turbine Structure [84,85] [78,79].	68
Figure 25. Wind Turbine System Functional Diagram	73
Figure 26. Gearbox Functional Diagram	74
Figure 27. Generator Functional Diagram	74
Figure 28. FMEA procedure	78
Figure 29. Example of the FMEA spreadsheet.....	79
Figure 30. Average RPN per assembly.	81
Figure 31. Average RPN of critical components.....	82
Figure 32. Failure contribution per assembly.	83
Figure 33. Main failure modes of critical assemblies.....	83
Figure 34. Families of failure modes and their number of events.....	84
Figure 35. Failure modes and average RPN.	85
Figure 36.Sensitivity Analysis	93
Figure 37. Sensitivity Analysis with three variables.....	94
Figure 38. Example of a 3D risk matrix of critical assemblies.....	95
Figure 39. Failure contribution and onshore wind turbine failure rates.	96
Figure 40. Annual failure frequency and downtime per failure of WMEP, LWKF and Swedish survey.	97

Figure 41. Comparison of occurrence and severity values of the FMEA and the Annual failure frequency and downtime per failure of WMEP, LWKF, Swedish survey and ReliaWind technical report [85].	98
Figure 42. Goal decomposition graph	100
Figure 43. CAAR Flow chart.	101
Figure 44. Normal Turbulence Model (NTM): Turbulence standard deviation [91].	107
Figure 45. Normal Turbulence Model (NTM): Turbulence intensity [91].	107
Figure 46. Wind field using FASTv8 pre-processor TurbSim [91].	108
Figure 47. Discrete example of MCMC, transition graph and matrix.	110
Figure 48. Example of the probability distribution of load cases.	110
Figure 49. Example of future scenario generation.	111
Figure 50. Block diagram of RUL estimation.	112
Figure 51. Vulnerability map of a 5MW 3-stage gearbox [31].	114
Figure 52. 3D view of Kissys gearbox model	119
Figure 53. Power converter physics-based approach to estimate accumulated damage.	122
Figure 54. Remaining useful life estimation flow diagram.	123
Figure 55. Power converter module structural details [107] [98][109] [100].	124
Figure 56. Source of stresses with impact on electronic components [108] [99].	124
Figure 57. Induction machine simplified equivalent circuit [110].	125
Figure 58. The circuit for the examination of the IGBT switching and conduction losses [112] [103].	126
Figure 59. IGBT output characteristics. Red lines are used for slope calculation, and blue lines are curve fitting approximations [113] [104].	127
Figure 60. Diode output characteristics. Red lines are used for slope calculation and blue lines are curve fitting approximations [113] [104].	127
Figure 61. Typical energy losses. e_1 and e_2 represent slope [113] [104].	129
Figure 62. Static thermal model (R_{th}) without base plate [109].	130
Figure 63. Transient thermal impedance [109,113] [100,104].	131
Figure 64. Temperature calculation process [109] [100].	131
Figure 65. Process to calculate temperatures incorporating ambient temperature in each step [109] [100].	132
Figure 66. Dependency of the power cycling value n for IGBT4 modules as a function of the temperature cycling amplitude ΔT_j and the mean temperature T_{jm} [109] [100].	134
Figure 67. IGBTs and diode temperature.	135
Figure 68. Probability distribution of the IGBT junction temperature.	135
Figure 69. Three-dimensional analysis of the pitch system using one year of historical data.	139
Figure 70. Idealised typical hydraulic pitch system [121] [111].	140
Figure 71. Data mining approach.	141
Figure 72. Turbine with pitch system failure	144
Figure 73. SCADA data and O&M data analysis	145
Figure 74. Comparison between healthy turbine and turbine with pitch system failure.	146
Figure 75. Main findings of the failure investigation.	147
Figure 76. SVM data separation with feature space [16].	148
Figure 77. SVM output.	149
Figure 78. SVM output analysis.	150
Figure 79. Decision tree to assign a status vector to the training data.	151

Figure 80. Wind turbine variables relationship [40].	152
Figure 81. KNN example.	153
Figure 82. KNN main output	155
Figure 83. O&M optimisation tools and outputs.	159
Figure 84. O&M cost model outline.	162
Figure 85. Asset integrity management of offshore wind turbines.	163
Figure 86. Maintenance team and logistics [117].	166
Figure 87. Maintenance strategies.	168
Figure 88. Prediction of accumulated damage techniques, accessibility and O&M strategy.	170
Figure 89. Optimal maintenance costs, turbine availability, distance to port and turbine age [117].	171
Figure 90. Example of the wind turbine database.	175
Figure 91. Mean waiting time per month [140] [130]	183
Figure 92. Wind speed histogram for one year.	184
Figure 93. Siemens 3.6MW power curve [81].	185
Figure 94. Total theoretical maximum energy production per month.	187
Figure 95. Electricity sales price [145]	188
Figure 96. Repair cost breakdown for WT1.	193

List of Tables

Table 1. Number of grid connect turbines in Europe, 2016. [12]	23
Table 2. Operational performance of four UK round 1 offshore wind farms. [14]	24
Table 3. Composites and binders used in manufacturing wind turbine blades [5]	31
Table 4. Share of total failure costs in the gearbox [34]	34
Table 5. Distribution of Failures per main component of rotating machines [35]	36
Table 6. WT construction types.	36
Table 7. Average failure frequency for each subassembly of three databases. [19]	41
Table 8. Characteristics of condition monitoring systems [50]	44
Table 9. Possible failures, monitoring techniques and WT measured parameters. [49][20] [21][50] [40]	49
Table 10. Maintenance strategies comparison	55
Table 11. Generic OWT Failure Modes.[78][79]	69
Table 12. Prevention methods. [1][74]	70
Table 13. Detection Methods associated with the type of failure modes. [21][20][3][50]	71
Table 14. Gearbox Functional Diagram Description	73
Table 15. Severity Levels	76
Table 16. Failure rates from WSD, WSDK and LWK databases.	77
Table 17. Occurrence Levels	77
Table 18. Detection Levels	77
Table 19. Criticality Analysis Categories	79
Table 20. FMEA summary	80
Table 21. Minimum, average and maximum values of RPN of the components of each assembly....	80
Table 22. Undetectable Identified Failure Modes	86
Table 23. Affected Components associated with failure modes	87
Table 24. Undetectable and Critical failure Modes	88
Table 25. Criticality analysis results – Safety ranking	90
Table 26. Criticality analysis results – Environment ranking.	90
Table 27. Criticality analysis summary.	91
Table 28. Top 30 chart for wind turbine failure mechanism.	92
Table 29. Comparison with an available database of failure rates and downtime of onshore WT.	97
Table 30. Confidence factor.	100
Table 31. CAAR percentages	101
Table 32. Average CAAR per assembly	102
Table 33. Design load cases. NTM (Normal turbulence model), NWP (Normal wind profile model)	105
Table 34. Wind turbine classes [82].	107
Table 35. Example of FASTv8 outputs	109
Table 36. Gearbox speed ratios [30].	114
Table 37. Gearbox failure cost share.	115
Table 38. 3.6MW Gearbox specification	116
Table 39. HSS and LSS diameter calculation results.	119
Table 40. Load spectrum as an input for KISSsoft using SCADA data.	120
Table 41. Gearbox physics-based model: damage of HSS bearings B1 and B2.	121
Table 42. Material commonly used on power converters [98].	130
Table 43. Estimated damage of the IGBT.	136
Table 44. Pearson correlation coefficient.	143

Table 45. SVM advantages and disadvantages [114].....	149
Table 46. New dataset with the status vector.	152
Table 47. OpEx breakdown[117].....	165
Table 48. Vessels utilization features [120].	167
Table 49. Maintenance classes' description (continuous) [79][124][125]	173
Table 50. Maintenance classes' description[79][124][125].....	174
Table 51. Repair actions per maintenance class[79].	174
Table 52 Failure rate based on FMEA occurrence rating.....	176
Table 53. Digital sensors as inputs of the O&M cost model.....	177
Table 54. Wind farm characteristics.	178
Table 55. Percentage of scheduled and unscheduled maintenance hours.	178
Table 56. O&M information [126].	179
Table 57. Planned maintenance based on component condition and risk.	180
Table 58. Case study: scheduled maintenance WT1.	181
Table 59. Case study: unscheduled maintenance WT1.	181
Table 60. Case study: digital sensors application.	181
Table 61. Mean waiting time and daylight hours	183
Table 62. Wind speed frequency per month.	184
Table 63. Power output per wind speed and month.....	186
Table 64. Average energy production per day.....	187
Table 65. Economic parameters	188
Table 66. O&M outputs: downtime, loss of production and revenue losses due to scheduled maintenance.	190
Table 67. O&M outputs: spare part, labour and vessel cost due to scheduled maintenance.	190
Table 68. O&M outputs: downtime, loss of revenue and costs due to unscheduled maintenance. .	192
Table 69. O&M outputs: summary of the case study.....	193
Table 70. Comparison between the case study and the optimised case study.....	194

Abbreviations

A	Availability
AEP	Annual Energy Production
CBM	Condition-Based Maintenance
CM	Condition Monitoring
CAAR	Confidence of Accuracy of Assigned Ratings
CMS	Condition Monitoring System
CoE	Cost of Energy
DAQ	Data Acquisition
DFIG	Doubly Fed Induction Generator
DFT	Discrete Fourier transform
DAU	Data Acquisition Units
EWEA	European Wind Energy Association
FM	Failure Mode
FC	Failure Cause
FFT	Fixed Charge Rate
FMEA	Failure Mode and Effect Analysis
FMECA	Failure Mode and Effect Criticality Analysis
ICC	Initial Capital Cost
IG	Induction Generator
LCCA	Life Cycle Cost Analysis
LRC	Levelized Replacement Cost

LWK	Survey Performed by the Schleswig Holstein LandWirtschaftskammer
MTBF	Mean Time Between Failures
MTTF	Mean Time to Failures
MTTR	Mean Time to Repair
NAREC	National Renewable Energy Centre
O&M	Operation and Maintenance
OEM	Original Equipment Manufacturer
OWT	Offshore Wind Turbine
PM	Preventive or Scheduled Maintenance
RPN	Risk Priority Number
SCADA	Supervisory Control Alarm and Data Acquisition
SHM	Structural Health Monitoring
WSDK	Windstats Surveys in Denmark and Germany
WSD	Windstats Surveys in Germany
WT	Wind Turbine

Definitions of key terms

Reliability 'is the ability of an item to perform a required function under given conditions for a given time interval. Reliability represents the probability of items to perform their required functions for a desired period of time without failure in specified environments; however reliability does not account for any repair actions that may take place' (IEC 60050-191) [1].

Risk is "defined as the combination of the probability of an event and its consequences (ISO/IEC Guide 73)" [2].

Maintainability 'is the probability that a given active maintenance action for an item under given conditions of use can be carried out within a stated time interval, when the maintenance is performed under stated conditions and using stated procedures and resources'.

Accessibility 'is a qualitative or quantitative measure of the ease of gaining access to a component for the purposes of maintenance'.

Availability 'is the ability of an item to be in a state to perform a required function under given conditions at a given instant of time or over a given time interval, assuming that the required external resources are provided. In other words, availability represents the probability that a system is capable of conducting its required function when it is called upon, given that it is not failed or undergoing a repair action. Therefore, not only is availability a function of reliability, but it is also a function of maintainability' [1][3].

Life Cycle Cost Analysis 'is the quantification of the expenses in different phases of the project. This is important due to capital costs and risk placement involved in offshore wind farms' [4].

CAPEX (capital expenditures) are one-time expenditures and comprise the cost of planning, manufacturing and installing the offshore energy project.

OPEX are expenditures occurring for marine energy project operation e.g. inspection, maintenance, repair.

Failure is the inability of a sub-assembly to perform its required function under defined conditions [3].

Failure Mode is the specific manner or way by which a failure occurs[3].

Failure Root what caused the failure mode to occur[3].

Maintenance Optimisation is a process that attempts to balance the maintenance requirements (legislative, economic, technical, etc.) and the resources used to carry out the maintenance program (people, spares, consumables, equipment, facilities, etc.) [5].

Prognosis and Diagnosis differ in the nature of the analysis; diagnosis involves posterior event analysis identifying the occurrence of an event which has already happened. Prognosis is concerned with prior event analysis predicting the future behaviour of a system under observation [6] [6].

Failure Mode and Effects Analysis is used to determine what parts fail, why they usually fail and what effect their failure has on the system[7].

Repair action can be an addition of a new part, exchange of parts, removal of a damaged part, changes or adjustment to settings, software update, lubrication or cleaning [8].

Non-repairable system is discarded after a failure. Examples of non-repairable systems are small batteries or light bulbs [8].

Repairable system: A system that, when a failure occurs, can be restored into operational condition after any action of repair, other than replacement of the entire system. Examples of repairable systems are WTs, car engines, electrical generators and computers [8].

Mean time between failures defines the mean time between failures expressed in hours of operations for a specific module population. It does NOT mean that a module will operate for that many hours before failure [3].

Mean time to failure is used when evaluating non-repairable systems. MTBF assumes that a device is to experience multiple failures in a lifetime, and after each failure a repair occurs. For non-repairable systems, there is no repair. Therefore, in the lifetime of a non-repairable device, the device fails once and MTTF represents the average time until this failure occurs [3].

Weather window is a period of time during which if a given maintenance operation is started, it can be completed [9].

CHAPTER 1 - INTRODUCTION

“In the last 20 years turbines have increased in power by a factor of 100, the cost of energy has reduced, and the industry has moved from an idealistic fringe activity to the edge of conventional power generation”

“A modern wind turbine operates for about 13 years in a design life of 20 and is almost always unattended. A motor vehicle, by comparison, is manned, frequently maintained and its design life of about 150,000 kilometres is equivalent to just 4 months of continuous operation.”

European Wind Energy Assoc., Wind Energy - The Facts, 2005

1.1 Introduction

This chapter aims to provide a general understanding of the project and current the methodologies to optimise the O&M of offshore wind turbines; section 1.2 describes the current state of the offshore wind industry, procedures and challenges. Section 1.3 describes the objectives of the project, thesis structure and publications, and finally, section 1.4 describes the contribution to the knowledge of the thesis.

1.2 Thesis Background

Renewable energy resources that directly or indirectly come from the sun and moon have different operational availabilities, which is the ability of a system to perform its function under certain operational conditions and time. Currently, among renewable energy technologies, wind energy technology is the most available and mature. The contribution of offshore wind energy has made an impact on the energy systems during recent years compared with other technologies [10]. In Europe, 18GW of offshore wind has been installed since 2008, of which over 95% has been installed in the past ten years [11].

The largest offshore wind market is in the UK with 36% of the global installed capacity, followed by Germany with 29%. In 2016, China took third place with 11% leaving Denmark in

the fourth place with 8.8% [12]. Table 1 shows the total number of offshore wind turbines connect to the grid in European countries.

Table 1. Number of offshore grid connect turbines in Europe, 2016. [12]

Country	Belgium	Germany	Denmark	Spain	Finland	Ireland	Netherlands	Norway	Sweden	UK	Total
No. of Farms	6	18	13	1	2	1	6	1	5	28	81
No. of turbines connected	182	947	517	1	11	7	365	1	86	1472	3589
Capacity Installed (MW)	712	4108	1271	5	32	25	1118	2	202	5156	12631

The offshore wind industry has grown in the past years in European waters, and further growth is expected in Europe with the target of 20% of renewable energy by 2020. Wind energy plays a key role around the world to satisfy future energy demand [13]. The UK government considers that offshore wind power should play a major part in meeting the UK's renewable energy and carbon emission targets by 2020. Therefore, it is developing a strategy of having a diverse mix of low-carbon energy sources [14].

In offshore wind turbines, the cost of maintenance is a considerable part of the total life-cycle cost, between 20 – 35% of the lifetime power generation cost [15]. Studies have shown that most of the downtime is due to some critical components of the turbines. Reliability and productivity can be improved by optimising maintenance practices and focused condition-based maintenance for those critical components ewhile reducing costs and improving safety [8].

One of the major targets of the marine energy industry is to reduce the cost of energy. When considering future wind farms located far offshore, in remote locations, with increased power rating, maintenance strategies and advanced O&M tools are likely to be expensive, requiring large resources and will be technically challenging [1][16]. According to the International Energy Agency (IEA), US\$380 trillion are needed to meet the projected worldwide energy demand until 2035, and a significant portion is due to maintenance and operation of wind energy systems [17]. Typical maintenance costs for the offshore situation, including costs for maintaining the farm infrastructure, civil structures, etc. are given below [18]:

- Preventive maintenance 0.003 to 0.006 (€/kWh)
- Corrective maintenance 0.005 to 0.010 (€/kWh)

Table 2 below shows the operational performance in the early operation in 2010 of four UK offshore wind farms. The annual average technical availability for reporting the UK round 1 offshore wind farms is 80.2%, much less than the average availability of 97% achieved by onshore wind farms in the UK or the availability at 93.3% achieved by an established EU offshore wind farm [14]. In 2018, the UK's offshore wind farms showed an operational availability above 94% [19]

Table 2. Operational performance of four UK round 1 offshore wind farms. [14]

Offshore Wind Farm	Annual average wind speed (hub height): m/s	Specific energy yield: kWh/m/year	Capacity factor: %	Performance factor: %	Availability: %
Barrow	9.15	996	24.1	68.9	67.4
North Hoyle	8.36	1220	35.0	100.0	87.7
Scroby Sands	8.08	943	27.1	77.4	81.0
Kentish Flats V90	7.88	1146	27.7	79.1	80.4
Annual average					80.2

1.3 Thesis Description

1.3.1 Aims

The main aim of this work is to reduce the cost of maintenance activities and to improve turbine availability through the development of new methodologies for failure prognosis and diagnosis. The failure prognosis will be based on a deterministic model in combination with a risk-based assessment. The proposed project will be delivered by the completion of the following objectives:

- Initial literature review of failure rates, mode and analysis of critical components of offshore wind turbines.
- To create a risk model to analyse structural, mechanical and electrical failure modes of critical components of the offshore wind turbine.

- To create a physical model of the device to calculate loads associated with identified failure modes.
- To create a deterministic model with algorithms of individual damage accumulation based on a combination of measurements and numerical model simulations.
- To develop a cost function for maintenance tasks and data processing system.

The datasets used for this project come from disparate data sources. The following lists some key inputs:

- FMEA of a generic wind turbines
- Recognised and peer-reviewed long-term reliability data (for instance from the EU Framework 7 Project, Reliawind)
- Lloyd's Register experience built up from working with wind farm operators
- Operational data of a UK's offshore wind farm: Maintenance task reports, technicians' logs, marine coordinators' records, vessel skippers records, personnel tracking systems, Automatic Identification System records (AIS), showing vessel movements
- Reliability data from SCADA databases (UK's offshore wind farm)
- Reliability data from other industrial sectors for similar components under equivalent conditions of operation.

1.3.2 Thesis Outline

Figure 1 describes the thesis structure:

Chapter 1 and Chapter 2 introduce the research problem and present a literature review of the factors impacting Operation and Maintenance (O&M) optimisation of offshore wind farms. Furthermore, these chapters explore key findings, outputs and definitions related to the research problem of key offshore wind industry stakeholders.

Chapter 3 describes a risk assessment using the tool Failure Mode and Effect Analysis (FMEA). The risk assessment is performed for the turbine Siemens 3.6MW-120. The chapter describes the procedure based on standards, data sources, a new methodology for data and uncertainty control, results and final discussion. The main output of this section is the definition of the four most critical assemblies in the Siemens 3.6MW-120, which are explored further in the following chapters.

Chapter 4 describes the physics-based models of the gearbox, power converter and yaw system, respectively. The models determine the accumulated damage and the remaining useful life. This chapter also introduces the methodology proposed to generate future events for prognostic purposes. The aero-elastic computer-aided engineering tool for horizontal axis wind turbines FASTv8 developed by NREL is used to represent the turbine structural and mechanical behaviour. The outputs of this section are several variables such as torque, wind turbulence, wind speed and rotational speed. A methodology is proposed to predict these variables for several months in advance.

Chapter 5 aims to describe a data mining approach to detect any abnormal behaviour in the pitch system using subject matter expert knowledge. The approach proposes a decision tree algorithm to diagnose failure mode using a combination of SCADA data variables.

Finally, Chapter 6 presents the development of the O&M cost function, which includes outputs such as cost of repair, downtime, availability, Mean Time to Repair, etc.. The cost model is able to analyse the most salient aspects of the O&M strategy including turbine availability, spare parts logistic, access, cost of components and others.

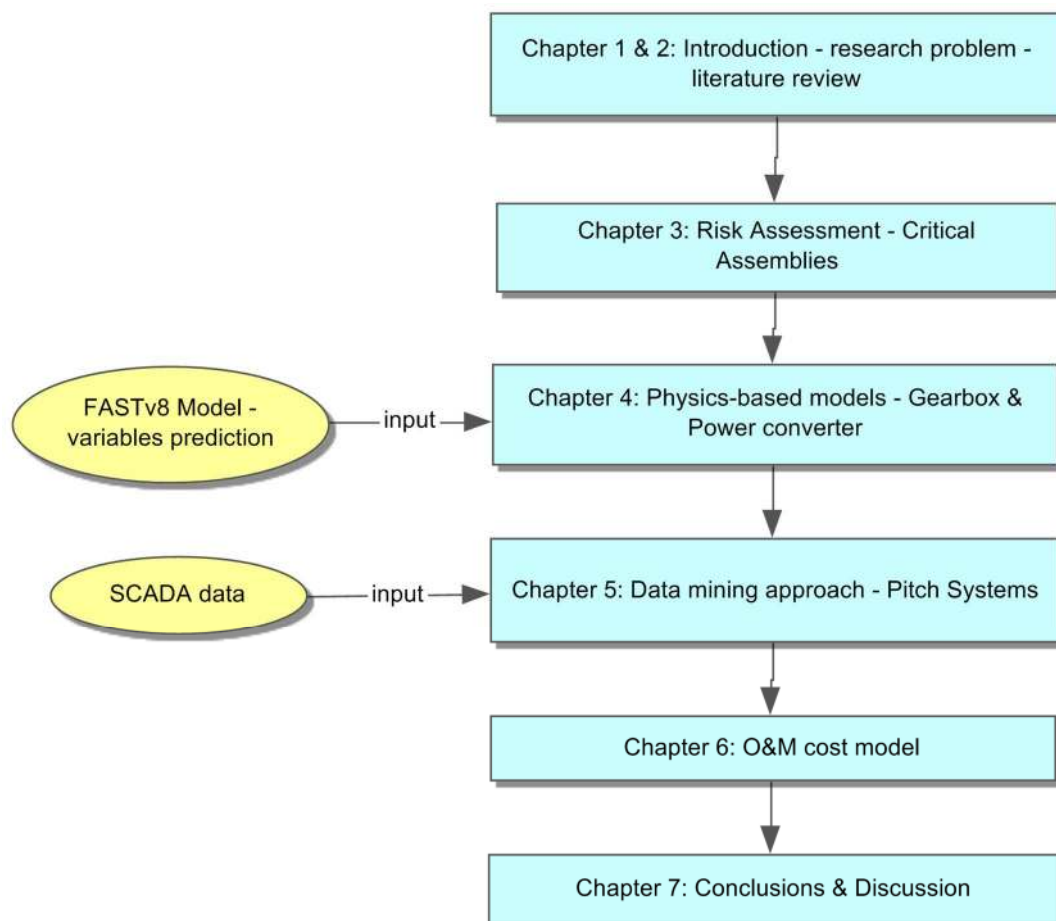


Figure 1. Thesis structure – flow diagram

1.3.3 Publications

The following publications were presented during this project:

Chapter 3: Failure mode and effects analysis (FMEA)

- Marco Sepulveda, Dr Jonathan Shek, Dr Philipp R. Thies. Risk assessment of an offshore wind turbine and development of a physics of failure based approach to estimate the remaining useful life (RUL) of the power converter. International Conference on Offshore Renewable Energy CORE 2016. Glasgow, UK.
- Marco A. Sepulveda, Dr. Jonathan Shek, Dr. Philipp Thies, Dr. Erkan Oterkus, Mr. Peter Davies, Dr. Mark Spring, Cengiz Yilmaz. Remaining Useful Life Estimation of Gearboxes through Combined Statistical and Physics-based Offshore Wind Turbine Modelling. American Wind Energy Association (AWEA) Conference, Warwick USA, 2016.
- Marco Sepúlveda, Mark Spring, Peter Davies, Dr Jonathan Shek, Dr Philipp R. Thies, Dr Erkan Oterkus. Risk Management in O&M for Offshore Wind Generation. Offshore Wind Operations & Maintenance Forum BIS Group, London, 2016.
- Mark Spring, Marco Sepúlveda, Peter Davies, Gerard Gaal. Top 30 Chart for wind turbine failure mechanisms. European Wind Energy Association (EWEA) Conference 2015. Paris.

Chapter 4: Failure prognosis based on physics-based models

- Marco A. Sepulveda, Dr. Jonathan Shek, Dr. Philipp Thies, Dr. Erkan Oterkus, Mr. Peter Davies, Dr. Mark Spring. Physics-based gearbox failure model for multi-MW offshore wind turbines. Proceedings of the 36th International Conference on Ocean, Offshore & Arctic Engineering ASME OMAE17, Trondheim, Norway, 2017.
- Marco A. Sepulveda, Dr. Jonathan Shek, Dr. Philipp Thies, Dr. Erkan Oterkus, Mr. Peter Davies, Dr. Mark Spring, Cengiz Yilmaz. Remaining Useful Life Estimation of Gearboxes through Combined Statistical and Physics-based Offshore Wind Turbine Modelling. American Wind Energy Association (AWEA) Conference, Warwick USA, 2016.
- Marco Sepulveda, Dr Jonathan Shek, Dr Philipp R. Thies. Risk assessment of an offshore wind turbine and development of a physics of failure based approach to estimate the remaining useful life (RUL) of the power converter. International Conference on Offshore Renewable Energy CORE 2016. Glasgow, UK.

- Krishnamoorthi Sivalingam, Dr Mark Spring, Peter Davies, Marco Sepulveda. A Review and Methodology Development for Remaining Useful Life Prediction of Offshore Fixed and Floating Wind turbine Power Converter with Digital Twin Technology Perspective. IEEE, 2nd International Conference on Green Energy and Applications (ICGEA), Singapore, 2018. DOI: 10.1109/ICGEA.2018.8356292.

Chapter 5: Data mining approach of the pitch system

- Marco A. Sepulveda, Dr. Jonathan Shek, Dr. Philipp Thies, Dr. Erkan Oterkus, Mr. Peter Davies, Dr. Mark Spring. Pitch system failure identification using a combination of subject matter expert knowledge of offshore wind turbines and machine learning techniques. Offshore Wind Energy Conference WindEurope, London, 2017.

Chapter 6: O&M Cost Model

- Marco A. Sepulveda, Dr. Jonathan Shek, Dr. Philipp Thies, Dr. Erkan Oterkus, Mr. Peter Davies, Dr. Mark Spring. Offshore wind farm O&M optimisation: using an integral approach for failure diagnosis and prognosis. All-Energy Conference and Exhibition, Glasgow, 2017.

1.4 Thesis contribution to knowledge

The main contribution of this project is the identification, development and demonstration of methodologies applied in the optimisation of offshore wind farm O&M. It is based on the synthesis, combination and demonstration of established approaches of previous studies, which have combined deterministic and probabilistic methods to identify factors contributing to the O&M costs and turbine availability. The specific contributions are:

- Development of a rigorous, systematic and consistent index to manage data and uncertainties in the risk assessment of the offshore wind turbine.
- Application of methods and software routinely used in design analysis for O&M diagnostics including the calculation of damage accumulation and remaining useful life for critical assemblies.
- Development of a comprehensive approach for O&M cost analysis including outputs such as turbine downtime, cost of repair, logistic delay time; and inputs such as virtual sensors, failure rates and weather windows, cost of spare part, spare part availability and time to repair.

CHAPTER 2 – LITERATURE REVIEW

This chapter critically reviews publications relevant to O&M of offshore renewable energy systems, particularly literature related to offshore wind turbine reliability and maintenance optimisation. Maintenance optimisation is a key part of the research, and it is described from different point of views. In order to understand the component's functionalities and materials used in the construction and design of offshore wind turbines, Section 2.1 presents a turbine description and analysis of components and failure characteristics.

In Section 2.2, current maintenance strategies for wind farms and relevant factors for their optimisation are presented. A review of failure detection approaches are presented in this section, which is the base for Section 2.3; a risk based assessment for wind turbines.

2.1 Offshore Wind Turbines – configuration and systems

The differences of the terms used to describe the several parts of the wind turbine are a common problem when different wind turbine failure surveys are analysed. The following terminology used in [20] [20] will be adopted in this work:

- System: for the entire wind turbine and the connection infrastructures.
- Subsystem: to generically indicate part of the wind turbine that deals with the same form of energy, for example the entire drive train.
- Subassembly: to indicate devices performing more specific functions for which the failure data are recorded separately, for example, the gearbox.
- Component: to indicate small devices typically non repairable constituting the subassemblies, for example, the gearbox/generator coupling.

This section discusses the functions, design materials and condition monitoring of the main components, subassemblies and subsystems of a wind turbine shown in Figure 2. It also identifies from the literature critical components, probabilities, causes of failure, consequences of failures and, diagnosis techniques.

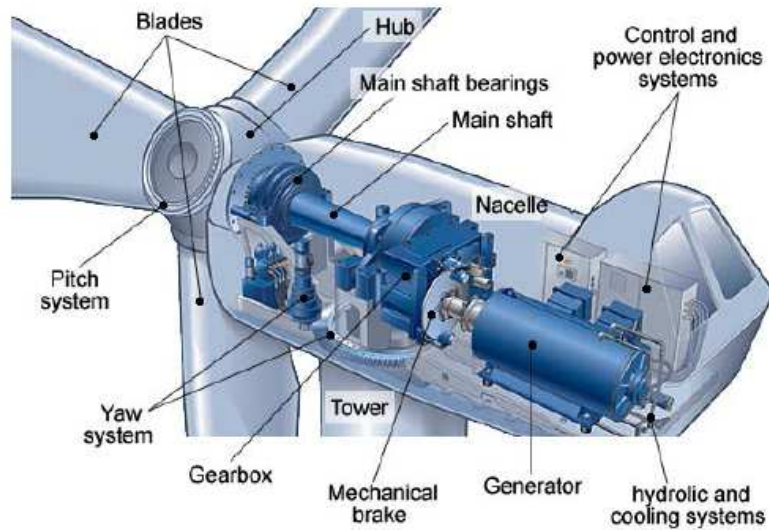


Figure 2. Main parts of a wind turbine. [21,,22]

In [3], the author defines taxonomy as the structure that names the main features of a WT in standard terminology. An example of the adopted taxonomy for this thesis is shown in Figure 3.

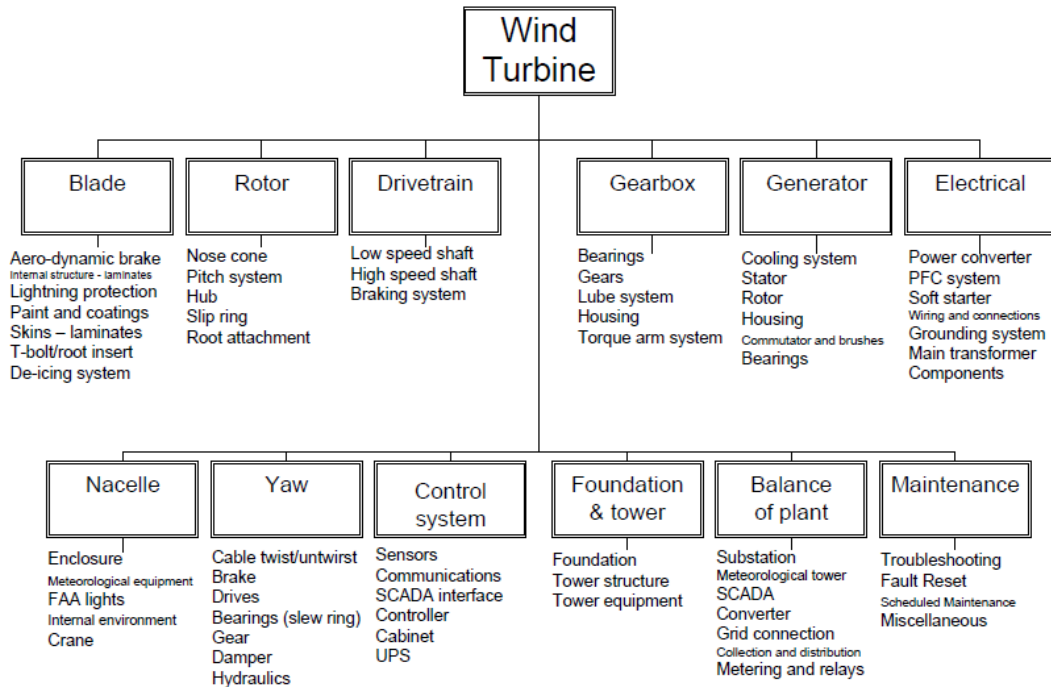


Figure 3. Wind turbine taxonomy [3]

2.1.1 Components Functionality, Materials and Failure Characteristics

Rotor and Blades

Due to their physical characteristics such as achieving high strength and stiffness to weight ratio, blades are usually made from composite materials in Table 3. They have good corrosion resistance for the hostile environment and good electrical insulation [23].

Table 3. Composites and binders used in manufacturing wind turbine blades [5]

Composites	Binders or Resins
Fibreglass	Polyester (unsaturated)
Carbon fibre	Vinyl ester
Wood	Epoxy

Blades comprises two main parts: the spar and the skin. The spar gives the structural stiffness and, the skin shapes the airfoil. The three most common shapes of blades are defined based on wind turbine technology and aerodynamic considerations; near optimum, linear taper and constant chord [5]. Blades also have bushes glued into their root which copes with the dynamic loads, and are linked to the hub by bolts [5,20,24] [5,20,24].

Usually, blades failures are produced by cycling loading which comes from the interaction between centrifugal, gravitational forces and, wind thrust and turbulence. Blades can fail due to cracks arising from fatigue during normal operation as well as materials defects, lightning strikes and icing [5]. The author in] [25] describes the four main failure mechanisms of composite materials: fibre fracture, fibre/matrix debonding, matrix cracking and delamination.

Other rotor faults are described by the authors in [26] and [27]: blade surface roughness due to pollution such as dirt and insects, damages of the painting in the surface such as cracks and blowholes and, icing. The imbalance in the rotor and aerodynamic asymmetry may be caused by the following reasons: manufacturer defects, non-uniform accumulation of ice or moisture, or accumulated damage to the rotor blades. It is necessary to stop the turbine when

there is a severe imbalance. Production tolerances or permanent deformation during operation could be another cause of imbalance.

Main Shaft

The drive train is a crucial subsystem for the reliability of the wind turbine. It includes the main shaft, the main bearings, the coupling, the generator and the gearbox. The main shaft connects the hub with the gearbox supported by the main bearing and transmitting rotational forces. Usually, the main shaft is made from forged alloy steel or graphite iron to allow more complex shapes. It also has a hole bored down the centre to enable communications and monitoring and to reduce the overall weight [5,20,24]

Failures of the main shaft will be analysed separately in the following sub-sections.

Main Bearings

The purpose of the main bearing is to decrease friction in the connection of hub and the main-shaft. The main bearing is attached to the nacelle. It is typically designed specifically for wind energy applications with spherical roller shape. To deal with radial loads and axial forces, the main bearing has two sets of rollers. The spherical shape allows the rings of the bearing in operation to have a maximum of a half degree of misalignment without damaging [5] [5].

Among the main causes of failure in the main bearings are poor lubrication, wear, pitting and deformation of bearing components [26].

Gearbox

The gearbox is the heaviest and most expensive parts of the turbine. It constitutes 13% of the value of a typical onshore wind turbine. There are 175,000 geared turbines in operation with 1,200 failures reported each year with a cost in the range of US\$200,000 to US\$300,000 [28]. The replacement of the complete gearbox, including equipment, crane time, labour and lost production, can reach up to \$500,000 [29]. The author in [30] states that gearboxes cause only 6.7% of total turbine stops but 55% of the downtime.

The gearbox increases the low speed of the rotor in the main shaft to high speed in the generator, usually around 1500 to 1800 rpm. A three-stage planetary gearbox is usually used in a multi-megawatts turbine, see Figure 4 [31]. The first two stages are planetary configuration, and the third one is a parallel. The planetary parts comprise a ring wheel which is an interior toothed gear wheel, three or more planet wheels which are smaller toothed

gear wheels and the sun wheel, a toothed gear wheel in the centre [5]. The high speed shaft of the gearbox is connected to the generator through a flexible coupling made from rubber to absorb and allow misalignments between the gearbox and the generator [32].

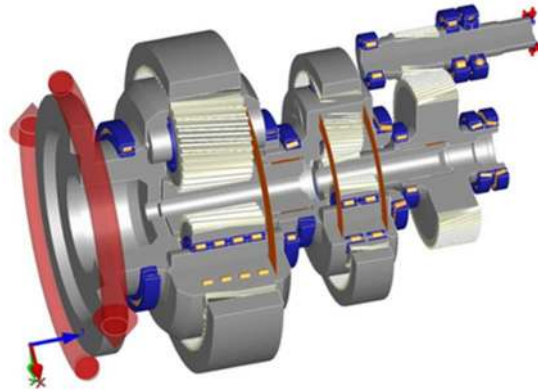


Figure 4. Typical Wind Turbine 3-stage Gearbox [31]

The gearbox as one of the most problematic critical components based on the latest literature. Mean time between failures (MTTF) of gearboxes is projected to be approximately ten years [33]. The most important issue in the reliability in the drive train is the wear of the gear teeth and bearings in the gearbox [27]. The main causes of failure of the gearbox include: particles in the oil owing to contamination during assembly, corrosion and wear; variations in rotor speed owing to imbalance, variations in wind speed, etc., The main failure modes are: the gear teeth to chatter, causing fretting and generating particles; stress concentrations in gear teeth due to wear or machining; mechanical interference or other manufacturing problems such as heat treatments or surface finish out of specification; loss of oil or oil circulation, see figure 5, 6 and 7. Additionally to the mentioned causes of failure, it is also possible to add false brinelling due to vibrations of small loads or small contact areas with very large local stress that can arise during transport or long periods of "parked-braked-status". For that reason, the main shaft of the gearbox can be rotated slowly during transport to vary contact location and distribute lubrication over rolling elements of bearings and gear teeth.

Common gearbox failures identified in [28] are manufacturing defects, cracking of bearing coatings, and ineffective lubrication. Based on [34], one major cause of -bearing failures in

the gearbox is axial cracking, identified with irregular white areas that appear when affected bearing surfaces are examined. Axial bearing cracking are lengthwise cracks on the bearing's inner ring along the roller path. Axial-cracking failures are common in bearings of the intermediate and high-speed stages.

The main causes of failure identified in [35] are insufficient or contaminated lubrication, the share of total failure costs are shown in Table 4. The author also concluded that half of the failures were caused by the bearings and caused by poor fitting, poor lubrication, contamination and fatigue. On the other hand, gearwheel failures represent the highest downtime. The causes of the main failures of the gears are fretting corrosion and bending fatigue.

Table 4. Share of total failure costs in the gearbox [35] [35]

Failure Mode	Failure cost as percentage of total cost
High speed shaft bearing failure	27.8%
Broken intermediate shaft	21.2%
Intermediate shaft bearing failure	10.1%
Planet bearing failure	9.6%
Broken centre post	6.2%
High speed shaft bearing black spot	5.4%
Sun gear - Broken teeth	5.3%
Low-speed shaft bearing failure	5.0%
Intermediate shaft bearing failure	4.8%
High speed shaft grinding temper failure	2.3%
Broken low-speed wheel	1.2%
Oil pump failure	0.8%
Intermediate shaft splash plate failure	0.2%

The author in [30] represents the criticality of the gearbox components in a vulnerability map, Figure 5. This map is based on the fatigue damage of gears and bearings [31]. The most critical components are the high-speed bearings and the high-speed gears.

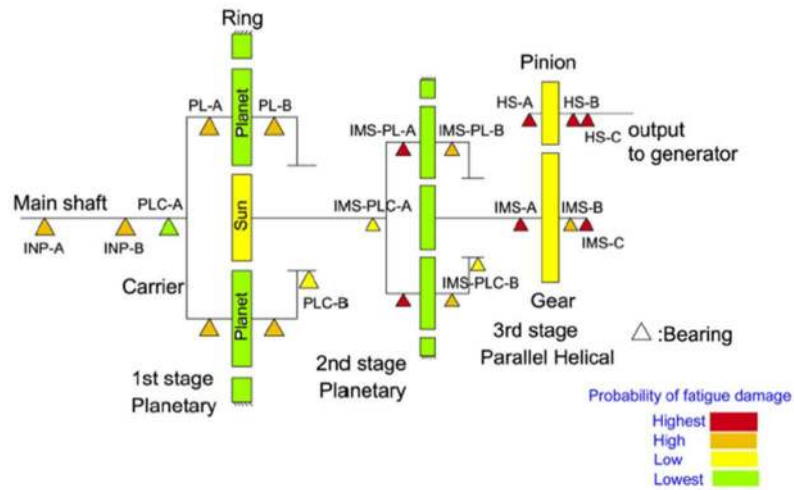


Figure 5. Gearbox vulnerability map [31]

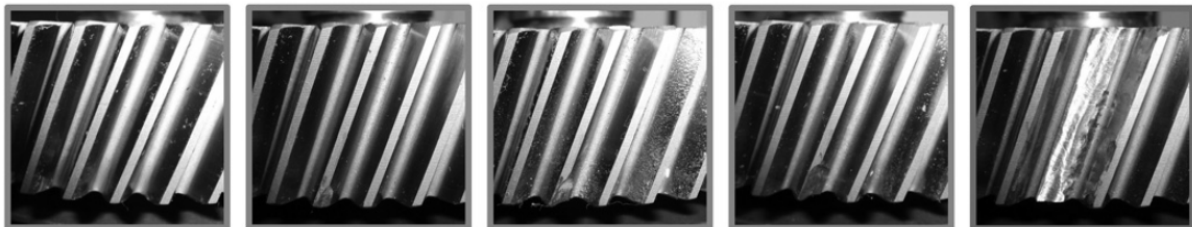


Figure 6. Gearbox teeth. From healthy tooth (left) to missing tooth (right)

Generator

Due to its advantages of mature technology, low cost and compact structure, induction generators are commonly used in wind and marine turbines. Studies present that wind turbine generators show a higher failure rate than steam turbo-generators. The author in [36], shows the distribution of failure (stator, rotor, and bearings) summarised in Table 5. Failure in rotating machines depends on size, voltage and type of machine. It is also possible to conclude, based on the surveys described in this study that the larger the wind turbine generator, the less reliable it is as dielectric stress and vibration are more significant than in small machines [37].

Table 5. Distribution of Failures per main component of rotating machines [36]

	Types of Machines			
	<150kW	<750kW	>150KW- MV & HV Generators	>11kW
Bearings	75%	95%	41%	42%
Stator	9%	2%	37%	13%
Rotor	6%	1%	10%	8%
Other	10%	2%	12%	38%

The main cause of failure of an induction generator occurs in the bearings, so maintenance is mainly focused on lubrication. Generators can operate at different power frequencies, however, overheating and torque pulsations may occur if it is connected to a weak grid with an unbalanced three-phase load [5][23].

There are different types of WT configurations therefore; there are different types of generators with different reliability and failure modes. A common configuration is WT with gearbox, high-speed asynchronous generator and partially rated converted DFIG. On the other hand, a less common configuration is a direct drive WT without gearbox, low-speed synchronous generator and a fully rated converter.

Table 6. WT construction types.

Type of generation system	Turbine concept	Gearbox	Converter
Single Cage Induction Generator (SCIG)	fixed speed	multiple stages	
	variable speed	multiple stages	full scale
Permanent Magnet Synchronous Generator (PMSG)	variable speed		full scale
	variable speed	single or multiple stage	full scale
Doubly Fed Induction Generator (DFIG)	variable speed	multiple stages	partial scale
Electrically Excited Synchronous Generator (EESG)	variable speed		partial and full scale
Wound Rotor Induction Generator (WRIG)	limited variable speed	multiple stages	partial scale
Brushless Doubly Fed Induction Generator (BDFIG)	variable speed	multiple stages	partial scale

Pitching System

The blade pitching system is one of the control systems of a wind turbine to maximise energy conversion, limits power extraction and, evade stress or damage in the components due to variable wind. The pitch system is designed to work within a minimum and maximum wind speed. The pitching system has two purposes; aerodynamic power control and aerodynamic braking [24][38].

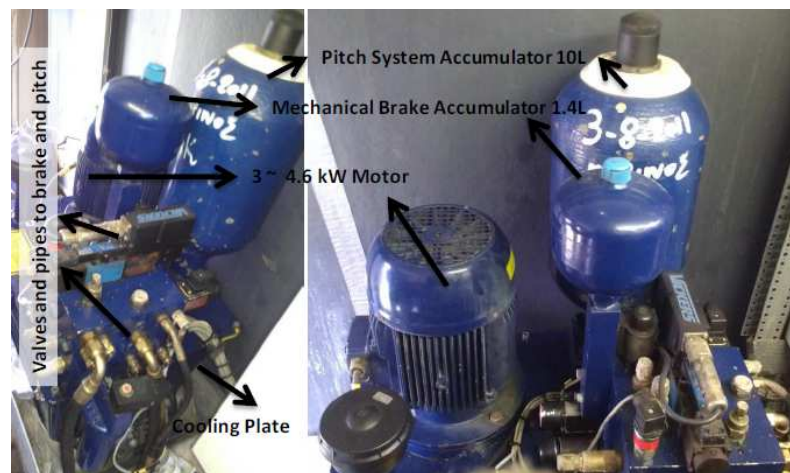


Figure 7. Hydraulic unit of pitching system (Turbine VESTAS V39/V4x/V90). [24] [24]

Each blade has an independent pitching actuator which comprises a hydraulic cylinder and piston rod [5]. An example of the hydraulic unit of the pitching system is shown in Figure 7. Unexpected distribution of stress within the bearing due to raceways flexibility is the main cause of failure. The hydraulic system can show failure modes such as leakages, overpressure and corrosion [38].

Mechanical Brakes

A mechanical brake is essential for any turbine since a fault in braking the wind turbine rotation may result in loss of the whole structure or catastrophic failure [24].

The mechanical braking system has two objectives: to support the function of the pitch system and its aerodynamic brake when the rotational speed of the drive train reaches intolerable levels and, to brake the wind turbine when it is not operating. The mechanical brake is usually located on the high speed shaft, between the gearbox and the generator and it comprises a brake disc, brake pads and callipers [5] [23]. See figure below.



Figure 8. Example of wind turbine brake system [24] [24]

Mechanical brake failures can be caused by excessive wear on brake linings. The hydraulic system pump can present failures caused by contamination of hydraulic fluid, wrong oil viscosity, premature failure of cylinders as a result of high hydraulic fluid temperature, hydraulic valve failure caused by cavitation, faulty circuit protection devices, and seal failure [5].

Control System

The control system is defined in IEC 612400-2 as “...a sub-system of wind turbine that receives information about the condition of the wind turbine and/or its environment and adjusts the turbine in order to maintain it within its operating limit”. The design requirements of the control system can be found in the standard IEC 61400-1 [5]. The main objective of the control system is to avoid excessive mechanical load, to maximise power output and power quality [39].

There two main control strategies in variable speed wind turbines: below-rated power where the speed controller will adjust the rotor speed to maintain the maximum power coefficient at that speed level. The second strategy occurs above the rated wind speed, where the pitch angle is controlled to maintain a constant rotor speed [40].

Despite the fact that the sensors, cables, software and hardware have a high quality, damaged sensors giving false positive or false negative can result in WT shutdown. National Renewable Energy Laboratory (NREL) states that software reliability is not estimated and its failure modes are not predictable. It is extremely difficult to test all in-input sequences therefore; a large number of harmful faults in the software will not be detected [5].

Electrical System

In addition to the generator which constitutes a different subassembly, the electrical system comprises all the electro-mechanical devices that allow the connection of the generator to the network. The electric system of a wind turbine is by far the most complex subassembly. The complexity of the electric system is reflected in the frequency of failure, which is generally high, if not the highest in the wind turbine systems of the selected databases.

The main components of this subsystem are: power converter, transformer, switchgear, power cables, protection relays, power factor correction units, circuit breaker and the earthing system. Failures in these components depend on different mechanical or electrical failure modes [20].

Structure: Tower, Foundation and Nacelle

The structure comprises four main parts: the foundation, the tower, nacelle and the yaw system [20]. The nacelle is the housing for most of the main components of the WT: gearbox, generator, brake system, low and high-speed shaft, and others. The nacelle also provides the proper environmental conditions in terms of temperature, pressure, humidity and salinity, to allow the normal operation of the components [23].

It is worthy to mention the scour activity around the offshore wind turbine foundations, which comprises many technical challenges related to the following issues [41]:

- Reduction of the structure's stability
- Vertical, horizontal and angular misalignment of the tower
- Increased hydraulic loading on the vertical face of the structure
- Increased maximum moments at the foundation structure
- Decrease and variation in the natural frequency of the turbine
- Need for more complicated foundation design requirements
- Increased bending stresses on cables, which may exceed the design limits.

Yaw System

The yaw system allows the nacelle to align with the wind direction, and it is essential to the functioning of a turbine with an upwind rotor [20]. The specific type of yaw system is defined based on the topology of the rotor, there are two types of yawing systems; active and free. Active yaw consists of a motor that actively aligns the turbine with the wind direction, see

Figure 9 [5]. A WT could have, depending on the WT types and construction, between 4 and 8 independent hydraulic or electric yaw drive systems. See figure below.

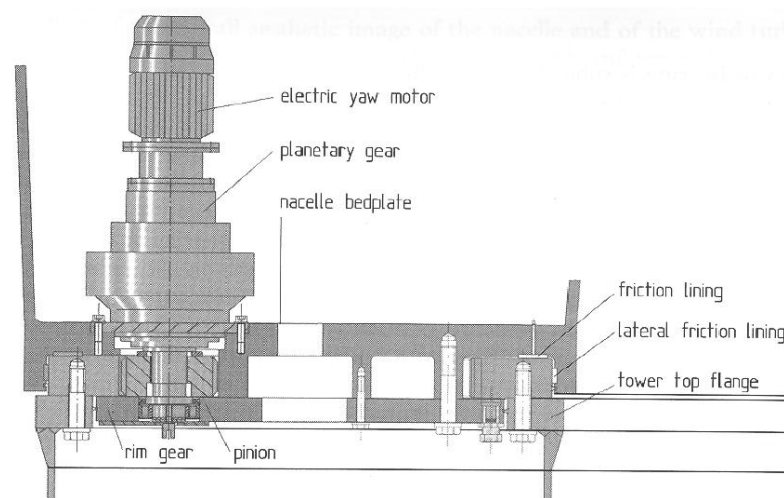


Figure 9. Example of a yaw system.[42] [42]

Bearing failures, pinion and bull gear teeth pitting, yaw brake failure, pinion and bull gear teeth wear-out are the main causes of failure of a yaw system [5][43].

2.1.2 Critical Components of an Offshore Wind Turbine

A reliability study can be useful in areas of risk analysis, optimisation of operations and maintenance. Reliability data is analysed to provide information as a basis for the decision. This work identifies critical wind turbine components based on the analysis of reliability data in previous studies. These identified critical components will optimise the necessary resources to performed risk-based assessment of the wind turbine. The risk analysis is a way of identifying probability of causes and consequences of failure events, and the optimization is a way of telling how failures can be prevented, where to focus the efforts on and how to improve the availability of a system [23].

This section identifies critical components based on cost, failure rates, consequences of failure that represent significant financial loss and downtime. One of the hardest matters of reliability engineering is obtaining accurate failure data. Offshore wind turbines are a technology highly specialised and due to the commercial sensitivity of failure data of wind turbines, operators and manufacturers are reluctant to disclose data about reliability or failure patterns. Consequently, the sources of information are restricted to databases of onshore wind farms publicly available [10,20].

WindStats D (WSD), WindStats DK (WSDK) and LWK are three examples of publications collecting failure data of different populations of wind turbines and constitute the main source of information to select critical components [23].

Table 7. Average failure frequency for each subassembly of three databases. [20]

	WSD (1291-4285 WTs) failures/turbine/year	WSDK (851-2345 WTs) failures/turbine/year	LWK (158-643 WTs) failures/turbine/year
Electrical system / Grid / Electrics	0.294	0.0468	0.32
Rotor or blades / Hub / Blades	0.191	0.0486	0.19
Electrical control / Electronics	0.182	0.15	0.239
Yaw system	0.108	0.0645	0.116
Generator	0.105	0.0497	0.139
Hydraulic system	0.0958	0.0451	0.131
Gearbox	0.0929	0.0425	0.134
Pitch control / Mechanical Control	0.0893	0.0141	0.0834
Air brakes / Rotor Brake	0.0411	0.0164	0.0397
Mechanical brake	0.033	0.0289	0.0554
Main shaft / Bearing	0.0212	0.0145	0.0311
Anemometry, Sensors, Other / Other	0.188	0.209	0.367

The failures frequency of wind turbines varies with the scale and type, and it is only possible to find in failure analysis based on onshore wind turbine databases as it is shown in Table 7. There is an overall tendency of an increasing failure rate with turbine size, so it is possible to assume the initial failure rate as the turbine size will increase for offshore applications. Studies showed the distribution of failures of the main components divided into five groups; electrical system, control system, hydraulic system, sensors, and rotor blades, are responsible for 67% of failures as shown in Figure 10 and Figure 11 [21][16].

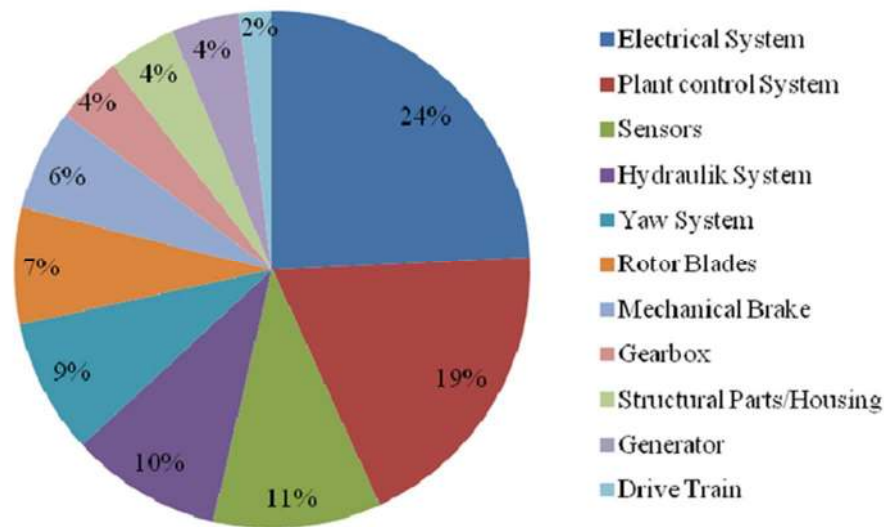


Figure 10. Distribution of failures for wind turbine components [21].

It is not possible to detect all the faults occurring in an offshore wind turbine using a limited number of sensors and huge amount of data to be analysed. The study done by Wisznia, shows a criterion to select critical components of offshore wind turbines. It states that faults must be detectable using simple, reliable and demonstrated instrumentation; failures have to be detected in the early stages to allow maintenance plan and, this early detection must lead to a significant cost reduction in maintenance activities [44].

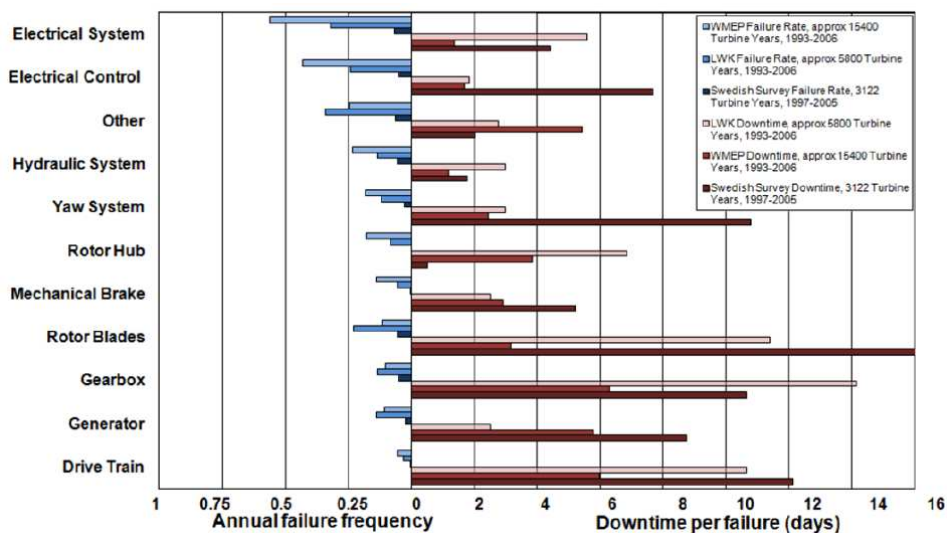


Figure 11. Failure rates across wind turbine sub-assemblies [45].

The consequence of a failure event can be measured according to numerous criteria, commonly failure modes effects analysis (FMECA or FMEA) is used to evaluate the criticality.

Unfortunately, the failure data do not allow a practical and rather accurate criticality index such as the total cost of the repair however; downtime information is available and can be used as a criticality index. Availability of spare parts, availability of personnel, accessibility to the WT site, weather conditions and the corrective maintenance policy are factors that might affect downtime of the turbine [20].

The author in [15] concluded that the failure contribution of critical assemblies out of the total is: pitch system (16%), frequency converter (12%), yaw system (12%), control system (14%), generator (6%) assembly and gearbox (5%).

Blades, gearbox, generator, yaw system, hydraulic system, electrical and control system are shown in Figure 11, as the main sources of failure. Likewise, the blades, gearbox, generator, electrical, drive train and control system are cost significant items within a wind turbine in terms of downtime. Therefore, it is essential to focus the maintenance efforts on the identified critical components [5][21].

2.1.3 Condition Monitoring Techniques for Offshore Wind Turbines

An efficient condition monitoring system relies on the correct understanding of the machine and its subassemblies, objective and analysis of reliability data, correct selection of critical components or subassemblies, proper data acquisition techniques, correct analysis of monitored data and reasonable strategy for machine condition assessment [46].

Due to clear benefits of offshore wind energy compared with the industry onshore, including a greater capacity factor, there is a wide number of condition monitoring techniques currently available [47][16].

Condition monitoring techniques have been used in many industrial sectors. Different systems have become commercially available for application to wind turbines, such as vibration monitoring systems for bearings and gearboxes, online oil monitoring systems as well as the temperature of bearings, generator windings, etc. [47] [48].

The reduced offshore availability and accessibility and increasing trend for offshore wind deployment require an effective and reliable condition based maintenance process with condition monitoring systems instead of the combination of reactive and scheduled maintenance strategy. The goal of a condition monitoring system is to enhance the availability of expensive critical assets and reducing overall O&M costs. Condition based maintenance

approach aims to reduce maintenance costs by reducing the number of planned PM actions; thus only when there is evidence of irregular behaviour, maintenance staff will perform actions [49][50]. Furthermore, insurance companies give another reason for installing a condition monitoring system. Insurance companies require for example, that the complete drive train of the wind power plant has to be overhauled after 40.000 hours of operations. The exception to this clause is if a condition monitoring system recognised by the insurance company is installed. The leading insurance companies within wind power have created requirements for condition monitoring systems on wind power plants [23].

CMS, detection and diagnosis of failures techniques have been increasingly used in the offshore wind energy sector. CMS has been regarded as a crucial tool for achieving their expected availability as a result of the economic loss caused by the unexpected breakdown. Furthermore, the added values of their CM can be further extended to guarantee the quality of the power they generated [24,37]. The main reasons to use CMS are:

- Maintenance cost reduction
- Detection and prediction of faults in the early stages
- Reliability and availability improvements

The importance of monitoring system due to its characteristics are listed in Table 8:

Table 8. Characteristics of condition monitoring systems [51]

Characteristics	Advantages	Benefits
Early warning	-Avoid breakdowns -Better planning of maintenance	-Avoid repair costs -Minimise downtime
Identification of problem	-Right service at the right time -Minimising unnecessary replacements. -Problems resolved before the time of guarantee expires	-Prolonged lifetime -Lowered maintenance costs -Quality-controlled operations during time of guarantee
Continuous monitoring	-Constant information that the wind power system is working	-Security. Less stress

Condition monitoring system (CMS) involves several sensors gathering physical data from the functional subsystems of the offshore wind or tidal turbine. Sensors also transfer the data to

a centralised node for processing. The final aim of the CMS is to predict the fault of a critical component to optimise the required actions and improve the reliability and availability of the OWT. It is important to mention that any failure within the sensors creates an extra maintenance cost for the installed system.

CMS can be divided into three stages, first detecting an unusual operation condition that is outside of the right theoretical behaviour or healthy range. The second stage is diagnosing the failure root responsible for the unusual operation condition and third forecasting the remaining life of the component based on physics of failure or probabilities [44].

Wind turbine CMS commercially available shown in surveys [22] [43][50] show a clear trend towards vibration signals based techniques. The vibration monitoring mainly covers the turbine drive train where rotating machinery is involved. Other techniques such as fibre optic based strain measurement for blades and oil debris analyses for gearboxes are also used to monitor key subsystems and components of offshore wind turbines.

Based on [52], CMS with the basis of a significant change is a symptom of a developing failure, include combinations sensors and signal processing equipment that provide constant signs of the component, subsystem and system condition. CMS could be performed on-line to provide real-time condition feedback or, off-line where data are collected at regular time intervals using measurement systems that are not integrated with the equipment. The following techniques possibly applicable for offshore wind turbine have been identified based on the literature [43] [50][51]:

Vibration analysis

Vibration analysis is the most known technology applied for rotating equipment. The types of sensors used depend on some degree on the frequency range relevant for the monitoring. Some sensors of this technique are position transducers for the low-frequency range, velocity sensors in the middle frequency area, accelerometers in the high-frequency range and spectral emitted energy sensors for very high frequencies (acoustic vibrations). Vibration analysis is used in wind turbines to monitor the wheels and bearings of the gearbox, bearings of the generator and the main bearing [51,53].

Fast Fourier transformation is the signal processing technique commonly used to convert a time-domain signal into a frequency-domain signal. The vibration analysis technique is

applied to shafts, bearings, gearboxes, and blades, and it is standardised in ISO10816 which defines the positioning and use of sensors. Vibration analysis methods are easy to implement in existing equipment and have a high level of interpretation, making it easy to locate the exact damaged component, see Figure 12. However, this approach comprises the use of additional hardware and software, which increases the production costs [21].

In [54], the author explores the problem of automatic signal validation. A number of typical signal inaccuracies encountered in large databases were shown. As a result of the research, the authors show an algorithm for automatic validation of vibration signals. The algorithm for automatic signal validation was extended to the statistical signal description, followed by a short discussion on additional vibration signal constrains concerning random impacts, transient states and signal offset.

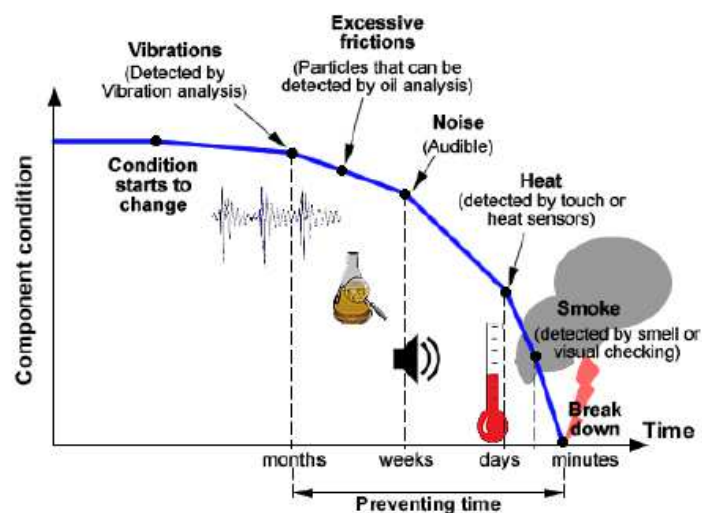


Figure 12. Typical development of a mechanical failure [21].

An example of implementation and allocation of accelerometers of a Vestas turbine is shown in Figure 13. Sensors measure absolute position of the rotor to perform phase sensitive narrow band analysis, the nacelle oscillation induced by the rotational speed of the rotor with static accelerometers and the vibration induced by bearings and gearwheels [51].

Oil analysis

Oil debris monitoring is a practical condition monitoring technique for the early detection of faults in bearing and gears of the gearbox. 80% of gearbox problems can be attributed to the bearings with consequential damage to the gearing [21].

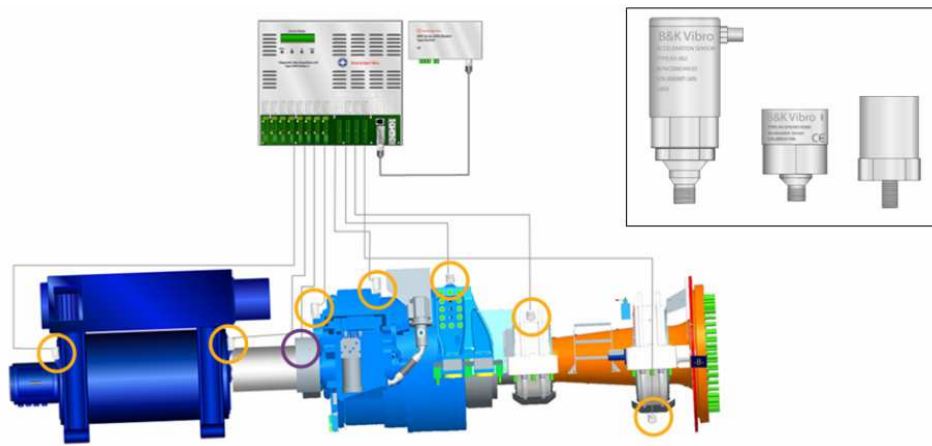


Figure 13. Vibration condition monitoring system formed by a data acquisition unit and accelerometers (yellow circles) mounted on the drive train and generator. The revolution speed of the generator shaft measured by a proximity switch (purple circle). [55]

This technique could have two aims; protection of the oil quality which can be contaminated by parts or moist and, protection the components involved. It is typically performed off-line, by taking samples but, for protecting the oil quality on-line sensors application is increasing. Condition monitoring of oil filter state by measuring the pressure loss over the filter now is mostly applied for hydraulic as well as for lubrication oil. Excessive filter pollution, oil contamination or change in component characteristics can give an indication of components with excessive wear [22,51].

This analysis uses the pumped oil in a closed-loop system of the component, and metal debris from cracked gearbox wheels or bearings is caught by a filter. The amount and type of metal debris can indicate the health of the component. Six main tests are mentioned in [21]: Viscosity analysis, oxidation analysis, water content or acid content analysis, particle count analysis, component condition (wear) analysis and temperature.

The technology for on-line detection can be broadly divided into three subcategories depending on the sensing techniques applied: electromagnetic sensing, flow or pressure-drop sensing, and optical debris sensing. In terms of cost, size, accuracy, and development, suitable oil monitoring technologies are online ferrography, selective fluorescence spectroscopy, scattering measurements, Fourier transform infrared (IR) spectroscopy, photo acoustic spectroscopy, and solid-state viscometry [33][50]. In [56] the author presented a high-throughput, high-sensitivity inductive sensor for the detection of micro-scale metallic debris in nonconductive lubrication oil. The device is able to detect and differentiate ferrous and non-ferrous metallic debris in lubrication oil with high efficiency. The main disadvantages of

this technique are that it is very expensive, and it is only focused to detect a failure in the gearbox [50].

Thermography and Temperature Measurement

Thermography technique is usually applied in electronic and electric components. Deterioration, damage or bad contact of these type of components generate higher temperatures (hot spots) that can be identified with this technique. It is applied offline, and often involves visual understanding. Currently, it is not particularly designed for online condition monitoring however, the necessary equipment, such as cameras and software, are starting to become available [22][51]

On the other hand, temperature measurement technique is able to detect excessive mechanical friction due to faulty bearings and gears, insufficient lubricant properties, and loose or bad electrical connections [42]. It provides an indication of the ongoing deterioration process. Due to each component or equipment has a limited operational temperature this technique is considered reliable however, as the temperature develops slowly, the temperature measurement technique is not sufficient for early failure prognosis and diagnosis. It can also be affected by ambient conditions [50].

Electrical effects

Condition monitoring of electrical equipment such as power converter, generators and transformer is typically performed using voltage and current analysis. Discharge measurements are used for medium and high voltage grids. A spectral analysis of the stator current in the generator can be used for detecting isolation faults in the cabling without influencing WT operation [22].

Nuisance Alarms

Nuisance alarms have been an issue for operators due to the additional cost that they might cause. The author in [54] developed an algorithm for the automatic validation of vibration signals in the condition monitoring system to minimise the risk of anomalies in a wind farm. Based on amplitude validation, the vibration data are validated via an original implementation of Parseval's theorem. The "N-point" rule is a simple and powerful technique for automatic signal error detection [21,54].

Summary of CMS for wind turbines

Table 9 summarises condition-monitoring techniques for each of the main assemblies

Table 9. Possible failures, monitoring techniques and WT measured parameters. [50][21] [22] [51] [41]

Wind Turbine			Condition Monitoring Method		
Subsystem	Component	Failures	Component	Subsystem	Analysis Method
Rotor	Blades	Deterioration, cracking, and adjustment error	Ultrasound, fibre optic and active thermography	Torque, acoustic and strain measurement, visual inspection, proximity probe	FFT frequency domain
	Bearings	Spalling, wear, defect of bearing shells and rolling element	Vibration, oil analysis, acoustic emission, shock pulse method, and performance monitoring		FFT frequency domain, Acceleration enveloping
	Shaft	Fatigue, and crack formation, shaft displacement	Vibration analysis		Time domain and FFT
Drive Train	Main haft bearing	Wear, and high vibration	Vibration, shock pulse method, temperature, and acoustic emission	Torque, power signal analysis, thermography, acoustic emission, and performance monitoring	Time domain based on initial 'fingerprint'
	Mechanical Brake	Locking position	Temperature		
	Gearbox	Wearing, fatigue, oil leakage, insufficient lubrication, braking in teeth, displacement, and eccentricity of toothed wheels	Temperature, vibration, shock pulse method, particles in oil, and acoustic emission		FFT frequency domain analysis, Envelope analysis, Time domain analysis
Generator		Wearing, electrical problems, slip rigs, winding damage, rotor asymmetries, bar break, overheating, and over speed	Generated effect, temperature, vibration, SPM, OM, torque, power signal analysis, electrical effects, process parameters, performance monitoring, and thermography		FFT amplitude spectra FFT envelope spectra Time domain magnitude Comb filtering, whitening, Kurtogram analysis
Auxiliary Systems	Yaw system	Yaw motor problem, brake locked, and gear problem	Motor current		
	Pitch system	Pitch motor problem	O&M		
	Hydraulic system	Pump motor problems, and oil leakage	O&M, process parameter, performance monitoring		
	Sensors	Broken, and wrong indication	Thermography		
Electrical System	Control system	Short circuit, component fault, and bad connection	Current consumption, and temperature	Thermography, and visual inspection	
	Power electronics	Short circuit, component fault, and bad connection	Current consumption, and temperature		
	High voltage	Contamination, and arcs	Arc guard, temperature		
Tower	Nacelle	Fire, and yaw error	Smoke, temperature and noise measurement, flame detection	Vibration, shock pulse method, strain measurement, temperature and acoustic measurement and	Time Domain, FFT frequency analysis
	Tower	Crack formation, fatigue, vibration, and foundation weakness			
Transformer		Problem with contamination, breakers, disconnectors, and isolators	Thermography		

2.1.4 Condition Monitoring using SCADA data

The Standard IEC61400-25 is used as a basis for the data exchange and communication software and procedures between condition monitoring techniques, the wind turbine controller, the SCADA System, Farm Server and human users. Data has to be made available without any time delay, "real-time data". For this type of data, hardware signals must be made available according to analogue and digital bus system. Figure 14 shows an exchange network structure for real-time data [57].

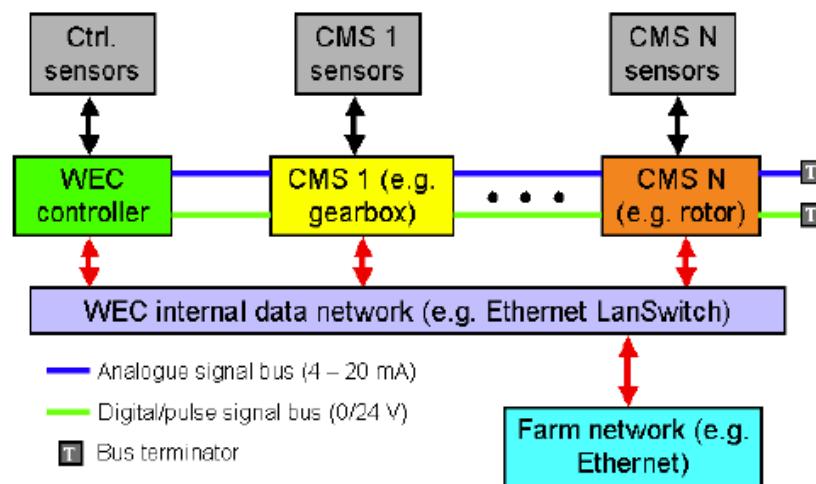


Figure 14. Real time data exchange network structure [57].

The SCADA system has been used in the wind industry for more than 35 years. SCADA sends turbine operational and meteorological data, usually in a 10-minute averaged, in real-time to a remote central computer via a communication system [50][52]. SCADA system provides data of the rotational speed and pitch angle of the rotor, information of the drive train such as the gearbox oil and bearing temperatures, power output from the generator, wind speed and ambient temperature. This operational health data of the turbines can be used as part of a general turbine condition monitoring system [16].

Condition monitoring based SCADA has the advantage over traditional CMS of significantly lower cost due to the lack of need of expensive sensors. Using accelerometers to obtain vibration signals is an example of expensive systems. Furthermore, CMS has a significantly greater volume of data to be analysed than the SCADA system and also a greater requirement of data storage. The higher frequency of sampling, defined in [50], is more than 10kHz

sampling frequency for a vibration monitoring system and the SCADA system samples has a frequency of less than 0.002Hz [16].

Techniques that are commonly used for traditional wind turbine condition monitoring including the approaches based on turbine physics and data-based modelling, can be implemented using SCADA data. According to [58], 10 minutes averaged signals often monitored in modern SCADA systems include:

- Active power output (and standard deviation over 10 min interval)
- Anemometer-measured wind speed (and standard deviation over 10 min interval)
- Gearbox bearing temperature
- Gearbox lubrication oil temperature
- Generator winding temperature
- Power factor
- Reactive power
- Phase currents
- Nacelle temperature (1-hour average).

Most modern SCADA systems comprise additional alarm settings based on temperature transducers and based on vibration transducers in the gearbox, generator bearings and the turbine main bearing. Vibration being observed over the 10 minutes average period is the basis of alarms. ReliaWind carried out a research of CMS through SCADA [7].

SCADA combined with other machine learning's techniques represent a powerful tool. The study in [7] proposes and compares two methods to detect and identify incipient faults in key components of wind turbines, such as main bearing, gearbox and blades. The analysis of this SCADA data comprises two methods: Artificial Neural Network (ANN) and mathematical model method. In [59] presents a machine learning methodology to detect and diagnose the delamination of the wind turbine blades. Delamination is the separation of the composite material layers and generates stress concentration in certain points. The techniques applied in this study are: autoregressive Yule-Walker model, K-nearest neighbours and ANN. Most recently, a complete review of machine learning techniques for condition monitoring of wind turbines is presented in [60]. ANN, support vector machines and decision trees are the most common techniques for blade fault detection and generator temperature monitoring.

2.2 Maintenance of Offshore Wind Farms

British Standard (BS) 3811 defines maintenance as “...the combination of all technical and associated administrative actions intended to retain an item or system in, or restore it to, a state in which it can perform its required function”. Internationally, it is defined that the highest priority for O&M is the safety of personnel and to facilitate the remote control access of turbine control systems in order to investigate, rectify and re-set trips where possible [61] [59].

There are different ways of reducing the operation and maintenance costs, for example, by reducing the need for maintenance. Maintenance optimisation can be achieved by designing a simpler wind turbine, reducing the number of components and using components with high reliability. However, even with a very reliable wind turbine, maintenance will be necessary [62] [60][63] [61].

Studies suggest that the cost O&M represents 14% to 30% of an offshore wind farm total operation cost. O&M activities are governed by regulations requirements, condition monitoring techniques available in the market and their associated costs [13]. It is estimated that optimal maintenance could reduce 40-70% of the direct O&M cost and could improve 7% of the turbine availability [5] [17].

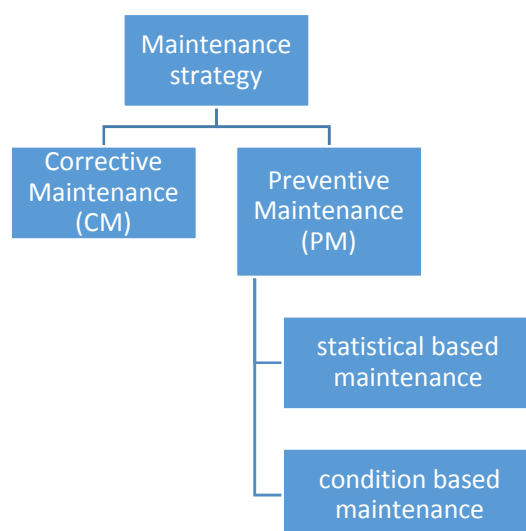


Figure 15. Maintenance strategies. [64,65] [62][3]

The most common maintenance approaches are Corrective Maintenance (CM) activity which is performed after the failure occurs and Preventive Maintenance (PM) activity which is performed before the failure of a component, see figure 3. CM strategy is typically applied when failure consequences do not represent revenue losses or health and safety impact [23]. Failures of critical components of a turbine can be catastrophic with severe operational and Health, Safety and Environmental consequences. Therefore, the feasibility of a CM strategy is given by the consequences of failures on the electricity network and revenue generation [5].

PM activities can be divided into two different techniques; statistical based and condition based preventive maintenance. PM activity following a predefined schedule, e.g. once a year, is called Scheduled Maintenance (SM) and based on statistics of failures. PM activity planned based on sensor information or condition of the component, is called Condition Based Maintenance (CBM) [64] [62][65]. PM strategy, commonly also called Time-Based Maintenance (TBM), includes periodic maintenance actions at regular intervals of time. This strategy is often implemented due to warranty reasons with the OEM and to maintain critical components with known failure data under control. Nevertheless, the selection of the proper length of the interval of time to perform the maintenance tasks has the disadvantages; Figure 16 shows frequent maintenance actions will increase operational costs, it wastes production time and it unnecessary replaces components in good condition [5].

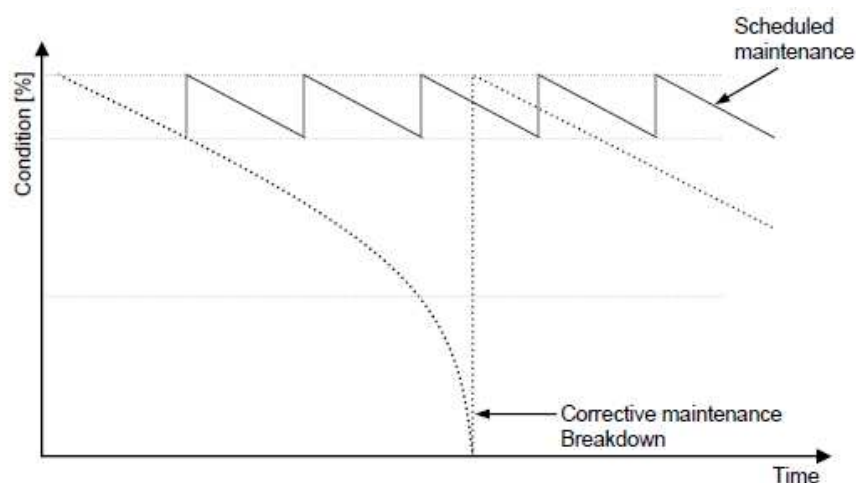


Figure 16. Corrective Maintenance compared to Scheduled Preventive Maintenance [3].

As it is stated before, O&M management of offshore wind turbines has gained big significance with the increase of wind energy capacity installed in the electric power systems. Several

maintenance strategies focused on optimising the cost have been developed by experts. It is important to understand the reliability of a wind turbine to formulate an optimal maintenance strategy however; offshore wind turbine failure statistics are not freely available due to commercial restrictions. In his study Spinato [20] presented results of reliability analysis on a subassembly level based on publicly available databases from Germany and Denmark [64] [62].

In the literature, different approaches for reliability analysis of wind turbines have been proposed. Reliawind project was founded by EU FP7 to improve the design, maintenance and operation of wind turbines. Within Reliawind project a reliability analysis procedure has been outlined to give procedures for performing reliability evaluation of wind turbines.

To effectively manage the reliability and availability of offshore wind turbines, a number of tools and techniques taking into account economic, health, safety and environmental issues have been proposed. These techniques include [5]:

- Reliability-Centred Maintenance (RCM)
- Failure Mode and Effect Analysis (FMEA)
- Hazard and Operability studies (HAZOP)
- Hazard Analysis (HAZAN)
- Fault Tree Analysis (FTA)
- Event Tree Analysis (ETA)
- Critical Task Analysis (CTA)
- Quantified Risk Analysis (QRA)
- Total Productive Maintenance (TPM)
- Risk Based Inspection (RBI)
- Root Cause Analysis (RCA)
- Structured What-if Technique (SWIFT)

The following table summarises the advantages and disadvantages of the three most common maintenance strategies [23]:

Table 10. Maintenance strategies comparison.

Maintenance Strategy	Advantage	Disadvantage
Corrective	Low cost Maximum lifetime of components	High risk of consequential damage Complex spare part logistics Long spare part delay time
Planned	Low downtime Simple spare part logistics	Not maximisation of component life time Higher cost than CM
Condition-Based	Maximisation of component lifetime Low downtime Simple spare part logistics	Complex failure prediction is required Hardware and software Extra cost for the strategy Immature market for wind turbines

2.2.1 Reliability Centred Maintenance (RCM)

The author in [66] [63] defines RCM as “an approach that employs reactive, preventive, and proactive maintenance practices and strategies in an integrated manner to increase the probability that a machine or component will function in the required manner over its design lifecycle with minimum maintenance”.

Large and complex technology systems such as aircraft and wind turbines must be reliable and maintainable in order to operate in both ways, safe and cost-effective. This task requires the application of sound engineering effort from design to decommissioning.

The integration between the RCM with reliability and maintainability engineering practices was first done the 1970s in the airline's industry. RCM is now extensively applied by several industries, including power plants.

The author in [67] [64] states that RCM is based on the premise that more efficient life time maintenance and logistic support programs can be developed using a disciplined decision logic analysis process. This process is focused on the consequences of failure and the necessary preventive maintenance tasks. RCM is technique, that can be applied in every step of the project development, from design to development process and re-assessed after deployment, during operation.

The main tasks of the RCM process are performed based on the following areas:

- Hard-time replacement (HTR): degradation due to age and usage before functional failure can be prevented by replacement or overhaul at a fixed interval or loading cycles.
- On-condition maintenance: degradation before failure is detected by inspections and assessments during a certain period. The inspection interval should be the largest that comprises a reasonable probability of successful detection.
- Condition monitoring: degradation before failure is detected by a sensing system (e.g. temperature, vibration, pressure, etc.). This represents a permanent surveillance using built-in test equipment.

In general, terms, the complete RCM process can be described as follows:

1. Critical component identification using a failure modes analysis tool.
2. Definition and application of the RCM decision logic to each critical component. This will allow the optimal combination of hard-time replacement, on-condition maintenance and condition monitoring tasks. It will also define if a new design is required.
3. Implementation of maintenance tasks and definition of data requirements for logistics analysis.
4. RCM process optimisation using operational data.

The risk assessment tool, FMECA is one of the most relevant data sources since it provides a strong foundation for the RCM decision logic. The Author in [67] [64], states that RCM structure for an operating system might be used as an information management system. RCM is able to register failure and their consequences, assess reliability based on the age of critical assemblies, incorporate new maintenances tasks, assess on-going tasks, and deal with unexpected failures.

The application of the RCM technique comprises design features and operational functions information of the system, its failures and consequences to select the most effective CMS, on-condition maintenance and HTR maintenance tasks. The overall objective is to develop a maintenance strategy focused on the consequences of failure and designed to generate the expected safety and reliability level, while the cost of maintenance is reduced.

RCM of wind turbines

RCM in wind farms is the way to manage turbine downtime and poor performance by failure prevention. It comprises a proactive approach of O&M however, for large wind farms the complexity increases due to the large number of interactions between individual elements.

The authors in [65] present a RCM approach using a sequence of several activities and steps (see Figure 17) that can be summarised in two steps [66] [63]:

- Inductive analysis of potential failures: use of FMEA tool to define critical components or assemblies.
- Application of logical decision diagrams: specification of preventive maintenance activities, replacements, etc.

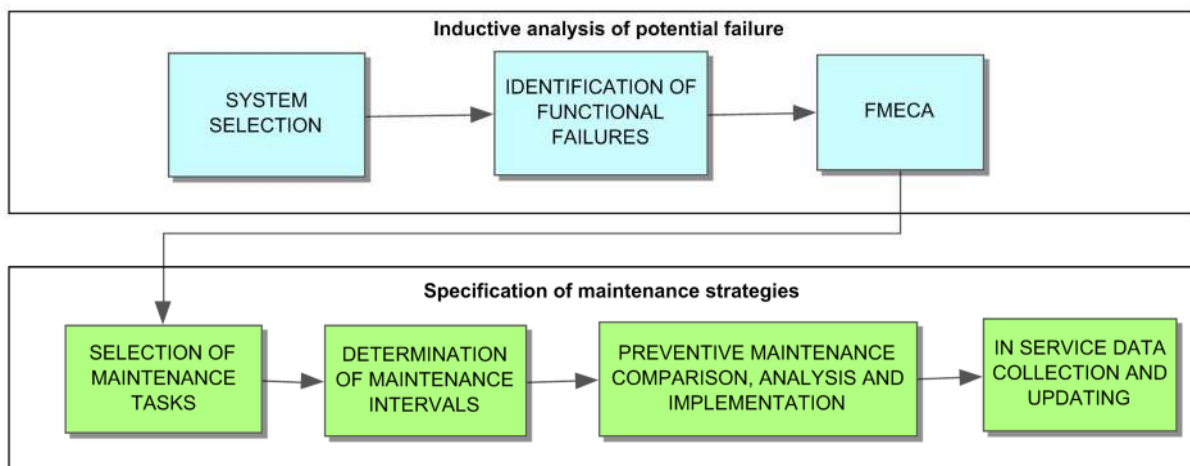


Figure 17. RCM stages [66] [63].

The author in [66] [63] presents the RCM framework described in Figure 18, where it is possible to analyse how RCM stages interact with each other. Data collection and analysis are crucial input for RCM and spans across the lifecycle of the project [66] [63].

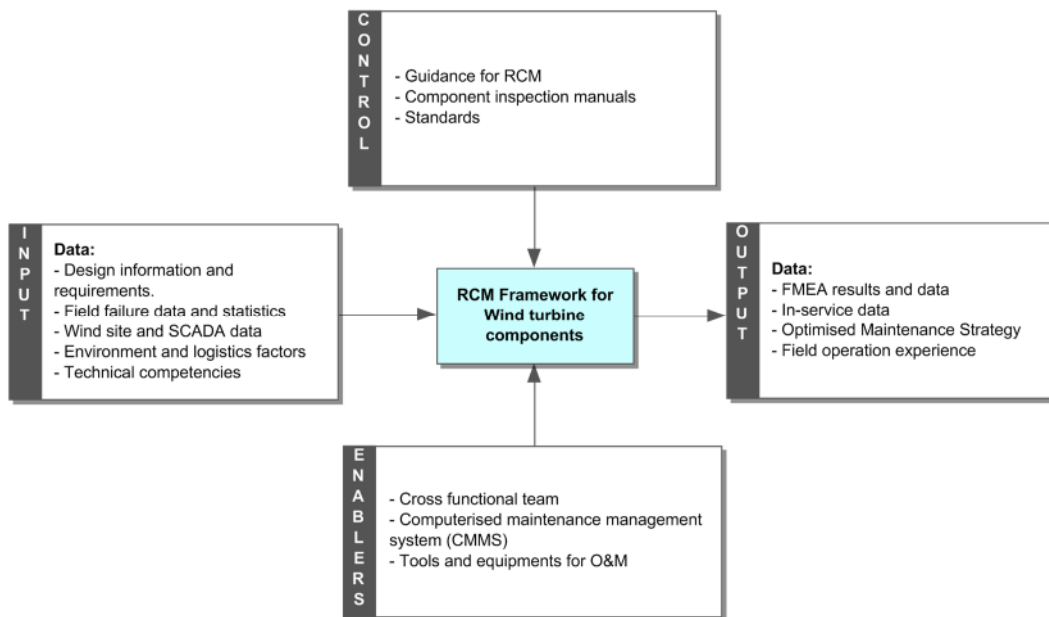


Figure 18. RCM framework [66] [63]

2.2.2 Spare parts management

Spare part management has been identified as a key factor in O&M strategies and can account for between 8.3% and 16.7% of the total O&M costs [68] [65]. Therefore, its successful deployment can lead to cost reductions. Each wind turbine can have around 8000 of components, therefore, to minimise the downtime due to spare part availability, there must be sufficient access to them at all times [69] [66]. There is a lack of understanding of the related information and data. ORE Catapult organisation in [68] [65] compares the offshore wind industry with the aerospace industry, which shares the same asset lifetime, technology complexity level, supply chain and logistics challenges.

The positives impacts of tools and solution related to spare part logistics in the aerospace industry are a reduction of aircraft on-ground time which is equivalent to offshore turbine downtime, reduction of the value of the spare part in inventory, and improving the spare part availability.

There are thousands of components in each offshore wind turbine and to minimize any logistic delay time, the access to replacements need to be expeditious.

The key performance indicators defined in [68] [65] to control the spare part logistics are:

- Unscheduled downtime
- Spare part availability
- Inventory management
- Response time
- Abortive work, parts delayed

2.2.3 O&M Strategy factors

There are three factors used to select an appropriate maintenance strategy for any physical asset such as a wind turbine; failure consequences, predictability of lifetime, and the feasibility of installing CMS on the wind or tidal turbine. A maintenance strategy that is appropriately optimised now may not be optimal in the near future due to the unpredictability of factors such as interest rate, components cost, failure behaviour, etc. Thus, maintenance optimisation is a continuous process which requires periodic evaluation of performance and improving based on previous actions [5].

2.2.4 Condition Based Maintenance

Condition-based maintenance involves continuous monitoring of system data to provide an accurate assessment of the component status of a wind turbine and taking actions based on its observed health. To be able to assess the status of a wind turbine components, it is necessary improved sensor technologies, data collection, storage and processing capabilities, and continuous improvements in algorithms and data analysis techniques. It uses real-time system monitoring and data processing as described in section 2.6. The aim of this approach is to provide an accurate estimation of the remaining useful life and the current condition of the monitored critical component; this is called failure prognosis [49] [27].

Condition monitoring of components enables planning of maintenance prior to failure and will minimise downtime and repair costs since components remaining life will be optimised and the coordination of spare parts will be easy. Additionally, trends and statistical data such as mean time to failure can be provided which is important for getting reliable data for the remaining lifetime of components in the system. With site-specific data the prediction of the remaining time for the components can be more precise [23]. Figure 19 shows a comparison between condition-based, corrective and preventive maintenance strategies.

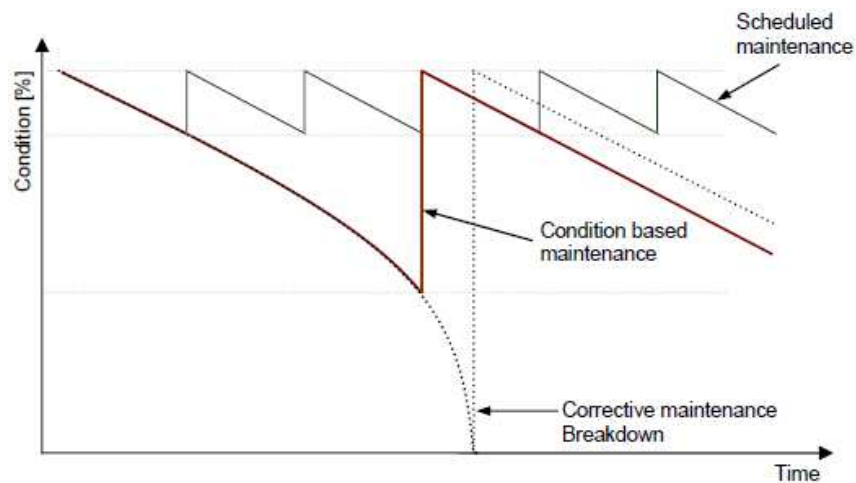


Figure 19. Condition based maintenance compared to scheduled and corrective maintenance. [23] [23]

The Authors in [70] and [65] propose a maintenance strategy selection method to improve the cost effectiveness of offshore wind systems. These methods comprise an algorithm to optimise grouping several maintenance tasks. The algorithm has inputs such as turbine reliability, weather condition, maintenance tasks characteristics, power generation and so on.

2.2.5 Fault Prognostic

The author in [71] [67] reviews some of the most important issues concerning fatigue degradation, test methods for materials characterisation, and how the damage mechanisms behave. Most life prediction models are experiential and are based on macroscopic measurements. There are many empirical relations for predicting fatigue life such as power laws like Baquin's relation, straight fits to S-log N data, Coffin and Manson's relation.

Prognosis is based on the assumption that failure is a process, not an event. Therefore, early detection of the failure will give more flexibility to manage the degradation process [27]. Failure prognosis is the process of generating predictions and pattern understanding of a signal or fault indicator. The final aim is to estimate the remaining useful life (RUL) [72] [68]. The main limitation of failure prognosis is the uncertainties associated with the predictions and it can be approached with to techniques; uncertainty representation and uncertainty management.

Figure 20 shows the probability density function of the RUL generated by a prognosis process, giving a distribution of when is likely the failure occurs in time. At time t_p , the remaining life prediction is made and a maximum allowable probability of failure has to be selected to define

what is called “just on time point” at which it is carried out the corrective maintenance actions [49].

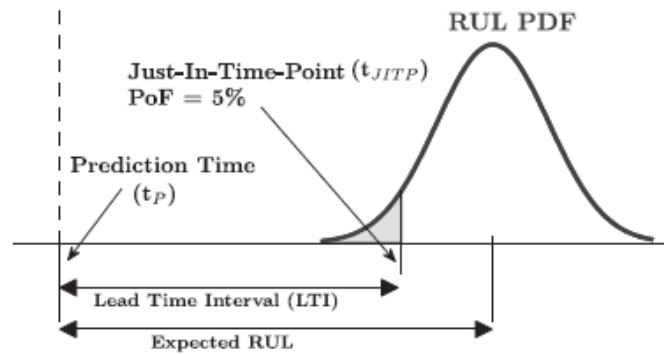


Figure 20. Remaining useful life probability distribution [49].

The lead time interval provides a real-time estimate of the remaining time before a system operates above the maximum allowable probability of failure (PoF). Maintenance actions must be performed before this time elapses. Factors such as safety, criticality and economic considerations determine the maximum allowable probability of failure. [49].

The author in [6] [6] divided prognostic techniques into three categories: experience-based approaches, trending or data-driven approaches and model-based approaches. See Figure 21.

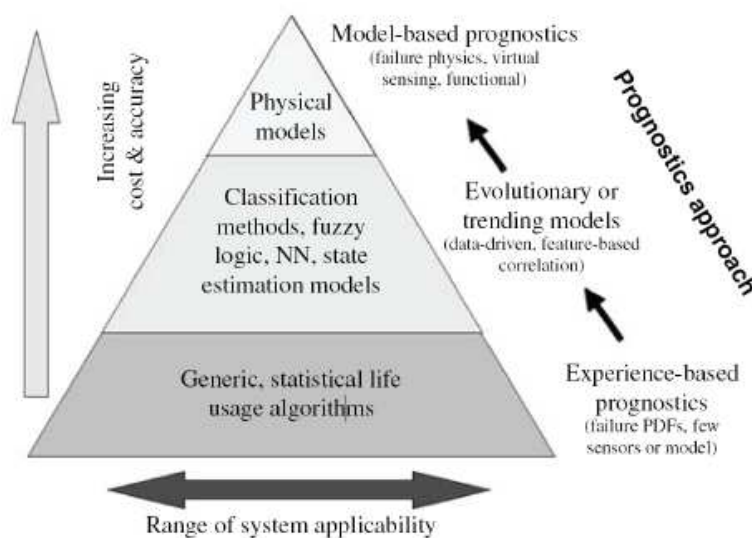


Figure 21. Prognosis techniques [6]

Experience-Based Prognostic Approach is the simplest technique due to it depends on statistical historical failure rates of wind turbine components. Models of components' lifetime can be developed in terms of distributions of failure rates over time using preventive maintenance schedules. Mean time between failures (MTBF), derived from lifetime models, is a parameter used to define the maintenance actions' intervals. This approach does not have any prognostic ability and cannot be considered as really predictive prognostic technique. However, such approaches are used in situations where sensor data is not available and the criticality or cost of the component is low.

On the other hand, a model-based prognostic technique has ability to incorporate physical understanding of the component behaviour, predicting degradation under variable or oscillating loads and operating conditions. It uses the physics of failure models of the system or component under observation. The most popular application of this approach is fatigue models for modelling the initiation and propagation of cracks in structural components.

Finally, the last approach is used when the complexity of the systems under observation does not allow deriving accurate models for prognosis. Data-Based prognostic technique model the relationship between monitored signals, and the remaining life of the system. An example of data-driven techniques is Artificial Neural Networks (ANN) [6].

ANNs are defined in [49] as a tool "to model relationships between input and output variables with a model structure inspired by the neural structure of the brain. The network weights and biases, which define the interconnections between the neurons, are adapted during a training process to maximise the fit between the input and output data on which the models are trained".

The author in [73] summarises the methods to predict the remaining useful life of wind turbines. They are categorised into four groups:

1. Knowledge-based models
2. Life expectancy models
3. Artificial neural networks
4. Physical models

Most of the techniques for failures prognosis are applied to gearboxes, main bearing and, blade and pitch control.

Another Data-Driven approach for fault detection of wind turbines is proposed in [74]. This study uses random forests and xgboost techniques to classify failures.

One of the most relevant limitations of these models representing degradation of components is the type of data available. SCADA data sample does not have the resolution require for some applications. On the other hand, the sensing system installed in a turbine can degrade or improve reliability. Additionally, the condition monitoring system are designed to diagnose a particular component using certain parameters that are not always useful to conclude about the overall health of the turbine.

2.3 Risk Assessment Approach for Offshore Wind Turbines

Quantitative analyses of failure data have shown important features of failure rate values and trends [46]. Failure Mode and Effects Analysis (FMEA) has been extensively used by wind turbine assembly manufacturers for risk and reliability analysis. Basically, each failure mode of the wind turbine is evaluated in the FMEA taking into account Severity (S), Occurrence (O), and the difficulty of detection (D). The combination of the three results in the Risk Priority Number (RPN).

Several limitations are associated with its implementation in offshore wind farms:

- Unreliable data: failure data gathered the data systems such as SCADA system, is often missing or unreliable. The risk assessment regarding severity, occurrence, and fault detection are mainly based on subject matter expert knowledge.
- Uncertainties and assumption: it is difficult for subject matter experts to precisely evaluate the risk factors.
- Factors weights: the relative importance among the risk factors is considered in the evaluation therefore, the results may not necessarily represent the true risk priorities.

To express fuzzy linguistics terms, the author in [75] [69] proposes a grey theory analysis to incorporate the relative importance of the risk factors into the determination of risk priority of failure modes.

The advantages of this approach are:

- An organised framework to combine the qualitative and quantitative data as inputs in the FMEA.
- The relative importance weights of severity, occurrence and detection factors.

A fuzzy-FMEA approach for risk and failure mode analysis in offshore wind turbine systems is proposed in [76] [70]. Fuzzy logic is a tool for transforming the vagueness of human feeling and recognition into a mathematical formula. It also provides a meaningful representation of measurement for uncertainties and vague concepts expressed in natural language. In line with this, there has been a growing trend in FMEA literature to use fuzzy linguistic terms for describing the three risk factors S, O, and D.

A probabilistic model of Risk-based Maintenance is presented in [77] [71]. Here, a prior damage model is combined with data from load measurements, inspections, and the SCADA system to improve the estimate of the probability of failure. To make probabilistic graphical models that represent the relationship between random variables, it is possible to deploy Bayesian networks [16]. Bayesian networks are graphical models based on Bayes's Rule. This rule presents the probabilistic relationship between variables with uncertainties [78] [72].

CHAPTER 3 – FAILURE MODES AND EFFECTS ANALYSIS (FMEA)

A risk assessment is required to identify critical assemblies and components of the Offshore Wind Turbine (OWT). This section comprises a qualitative analysis of failure mechanisms, global and local effects and, the maintenance effort required to improve the condition of the assemblies.

The FMEA comprises almost 500 components with about 1000 failure modes in total. This risk assessment gives details of the failure impacts at the component level. The comprehensive FMEA also delivers two analysis in parallel; operational risk with the Risk Priority Number (RPN) and the criticality analysis with four categories, environment, asset integrity, safety and operation. Additionally, new data sources management tools are designed. This tool allows identifying those areas where more research or real data are required. Finally, this thesis proposes a three-dimensional risk assessment adding to the traditional FMEAs with failure consequence and frequency, the variable failure detectability.

3.1 Introduction

This chapter presents the results of Failure Modes and Effects Analysis (FMEA) conducted for the horizontal axis OWT described in section 3.1.2. The FMEA was performed for the functional modes of each subsystem, assembly and component following the British standard BS EN 60812:2006 described in section 3.2.5. This risk assessment was an iterative process and outcome of a combination of available data and practical experience with the operation of wind farms.

The main objectives of the FMEA are to identify failures with significant impact on the wind turbine operation and to highlight areas of risk for maintainability and availability. Critical components and failure modes will be explored further in Chapter 3 and 4 which are related to physics-based models and data mining. The procedure allocates numerical values from 1 to 5 to each risk associated with a failure, using Severity, Occurrence and Detection as categories. The values of the ranking rise when the risk increases. These are then combined into a Risk Priority Number (RPN), which can be used to analyse the system. By targeting high RPN values the riskiest components and assemblies can be further studied. RPN is calculated by multiplying the Severity, Occurrence and Detection of the risk.

Additionally, this chapter comprises the description of a Criticality analysis to assess the impact of a failure mode from an environmental, financial and reputational point of view.

Based on EN 60812:2006, Criticality can assume different meanings; for the purposes of this study Criticality is defined as “a qualitative measure of the magnitude of the failure mode effect in different categories: Environment, Safety, Asset Integrity and Operation.”

3.1.1 Scope

This analysis delivers an assessment for the proposed Offshore Wind Turbine (OWT) mounted in a monopile foundation. FMEA provides a bottom-up approach to the analysis of each main assembly in order to identify potential failure modes and, the local and global effects in the system. It also provides current monitoring techniques and methods to prevent failure.

The qualitative FMEA will answer the following questions for each assembly's component:

- How can a component fail? How many failure modes each component can have?
- What are the causes of each failure mode?
- What are the effects of the failure on the wind turbine?
- How critical are the effects? How frequent are the effects? Can be the effects detected?
- How is the failure detected?
- What are the critical components/assemblies?

Critical components analysis provides a summary of the selected components whose failure modes can represent a negative impact on the system in different severity categories: asset integrity, environmental impact, operational impact and safety.

The FMEA is intended to be a living tool that will be iterated in order to represent real failure modes and contribute to improve reliability, maintainability, availability and survivability of offshore wind turbines. This tool is also crucial to assess the amount of maintenance required.

3.1.2 Wind Turbine System

Until 2014, 2488 offshore wind turbines were installed representing 8GW of capacity connected to the grid in Europe. In 2018, the total amount of grid-connected offshore wind turbines was 4.545, reaching 18.5GW of installed capacity in 11 European countries. The UK and Germany accumulate more than 14GMW today [11]. 63% of this capacity is installed in the North Sea. 91% of these turbines use a monopile foundation type installed in an average water depth of 22.4m. In terms of wind turbine manufactures, Siemens Company reached 86.2% of market share in 2014 [79] [73]. The market is dominated by Siemens and followed

by Vestas with a percentage of 15% to 20%. Among the population of turbines installed in Europe the turbine configuration with a fully rated power converter, 3 blades, monopile foundation, 3 stages gearbox and induction generator is the most common one. As it is shown in Figure 22, 64% of the turbines use Squirrel Cage Induction Generator (SCIG), 29% Double Fed Induction Generator (DFIG) and 7% Permanent Magnet Synchronous Generator (PMSG). Therefore, 93% of the turbines are using asynchronous generators of which 63% with fully rated power converter as the turbine Siemens SWT 3.6-120 [79,80] [73,74].

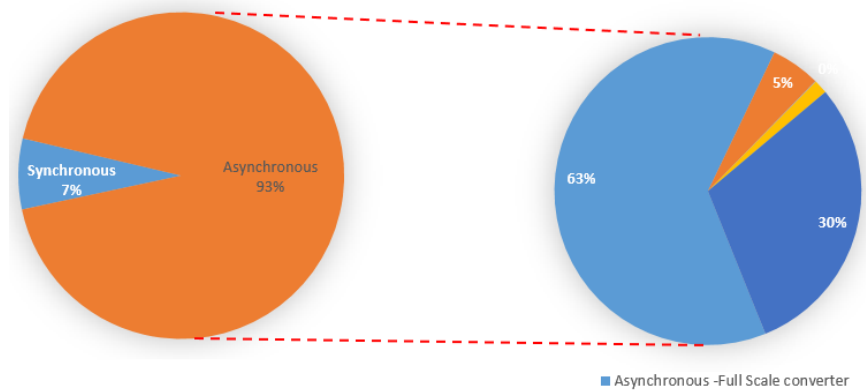


Figure 22. Wind turbine market trends.

Based on the market description above, the turbine configuration of the Siemens SW3.6 corresponds to the most utilised turbine technology of the European offshore wind energy market in 2014. Then, this FMEA is done for the proven technology of the world’s most popular offshore wind turbine. SWT3.6 is an axial three-bladed rotor turbine with pitch regulation and asynchronous squirrel cage generator with fully rated power converter[81] [75].

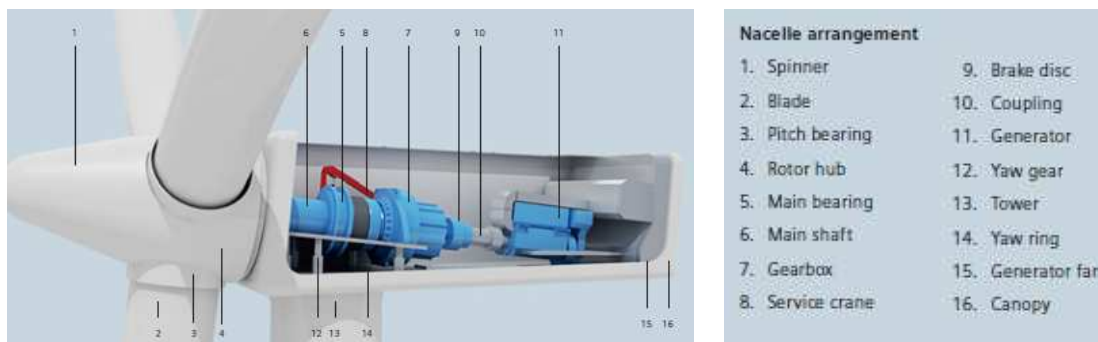


Figure 23. Siemens Turbine SWT 3.6 -120.

3.2 FMEA and FMECA methodology

The FMEA and FMECA are conducted in accordance with the international standard IEC described in the British Standard BS EN 60812:2006 “Analysis techniques for system reliability

- Procedure for failure mode and effects analysis (FMEA)”. This standard provides procedural steps necessary to perform the analyses identifying appropriate terms, assumptions, criticality measures and failure modes. [82] [76]

The analysis consists of the following five main stages:

- Establishment of the basic ground rules for the FMEA/FMECA and defining the scope.
- Defining systems structure including information on different system elements with their characteristics, performances, roles and functions.
- Executing the FMEA using the appropriate worksheet with a pre-defined system boundary and level of the analysis.
- Summarising and reporting of the analysis to include any conclusions and recommendations made.
- Updating the FMEA as the new inputs are incorporated.

3.2.1 Assumptions and Ground Rules

The analysis has been undertaken for the each subsystem and component function. In order to perform the FMEA, the following assumptions and ground rules are defined [83] [77]:

1. The evaluation of the severity, occurrence and detectability will be performed at the component level of the following hierarchical structure which is based on the structure proposed in the project ReliaWind [84] [78]:

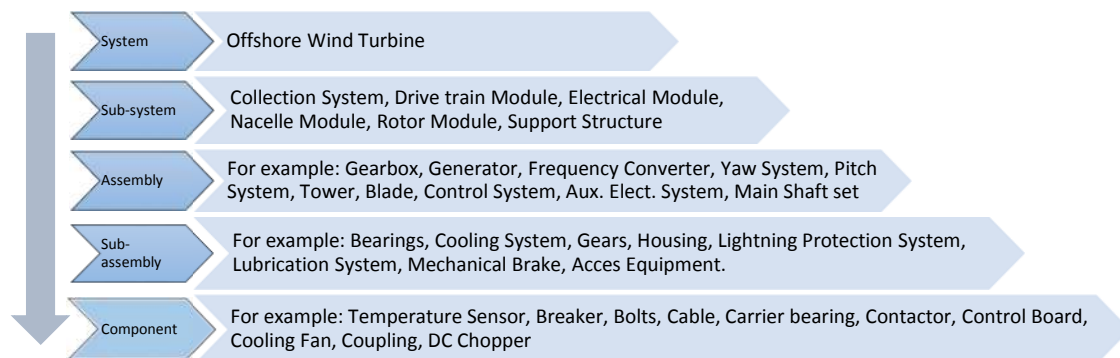


Figure 24. Hierarchical Wind Turbine Structure [84,85] [78,79].

2. Each component’s failure mode will be evaluated for the local and global impact on the system. Local impact is considered as the impact on other components or sub-assemblies directly mechanically, electrically or structurally connected.
3. A failure mode will be allocated a severity level based on the most critical consequence of that failure.

4. A failure mode will be assigned an Occurrence category based on the data available. Occurrence refers to the frequency that a Cause of Failure (CoF) is likely to occur, described in a qualitative way e.g. remote or occasional.
5. Each failure mode identified has a Detection category based on the techniques commercially available. Due to this FMEA forms part of a project to predict failures with greater accuracy, Detection category refers to the likelihood of detecting a failure in terms of “prognostic horizon” or advance warning.
6. The potential failures modes for each component of each subassembly described in Figure 24 are identified. Potential failure modes are assigned based on the following criteria listed in order of relevance:
 - o Numerical data analysis
 - o Expert opinions
 - o Theoretical data analysis
 - o Pre-defined generic failure modes: In the absence of an expert opinion of a particular failure mode, failure modes listed in [86] [80] and Lloyd’s Register’s experts [87] [81] have been used in the FMEA. Generic failure modes were defined to cover all the possible failure modes that can occur in the offshore wind turbine. This is shown in Table 11.

Table 11. Generic OWT Failure Modes.[86] [80][87] [81]

Generic OWT Failure Mode	Description
Brittle Fracture	Failure for metallic component(very rare)
Fatigue Fracture	Failure for metallic component(this would not be as rare as brittle fracture)
Structural Failure	Failure of any part or assembly that forms part of a supporting structure
Electrical Failure	Failure of a part or assembly as a result of an electrical defect
Mechanical Failure	Failure of a part or assembly as a result of a stress related defect
Material Failure	Failure of a part or assembly as a result of a defect/nonhomogeneous composition of the material with which the part is made
Detachment	Failure of a part or assembly where by it is unintentionally no longer rigidly connected to its frame or structure
Electrical Insulation Failure	Failure of a part or assembly with a high resistance to the flow of electrical current, resulting in leakage of current from a conductor
Thermal Failure	Failure of a part or assembly as a result of an incapacity to tolerate any exposed high temperatures, resulting in a reduction in rigidity
Output Inaccuracy	Failure of a part or assembly as a result of a signal output inaccuracy
Misalignment	Failure of a part or assembly as a result of an unintentional change in the parts position or orientation, with particular reference to
Intermittent output	Failure of a part or assembly as a result of an irregular and uncontrollable change or pause of the intended output
Blockage	Failure of a part or assembly as a result of a reduction in flow of a Fluid- typically caused by debris and increased viscosity of the
Abrasion	Failure of non-metallic hoses
Fatigue	Failure of non-metallic hoses
Sudden external damage	Failure of non-metallic hoses (e.g. dropped object).
Prime mover fails	Failure of pumps
Seals fail	Failure of pumps
Electrical Failure	Failure of a part or assembly as a result of an electrical defect
Not working at all	Failure of sensors
Giving false positive	Failure of sensors
Giving false negative	Failure of sensors
Fretting Corrosion	Failure of All gears
Bending Fatigue	Failure of All gears

7. Prevention methods are defined based on the common practice in the offshore wind industry. It is listed all the methods available and defined in the literature review.

Redundant items are considered in this thesis as a prevention method because this strategy allows detecting a failure of a critical component without stopping the operation of the system and giving an alert of deviations from the normal behaviour of the component.

Table 12. Prevention methods. [1][82] [76]

Preventive maintenance tasks
A check of the gearbox and hydraulic system oil levels.
Inspections for oil leaks.
Inspections on the cables running down the tower and their supporting system.
Observation of the machine while running to check for any unusual drive train vibrations.
Inspections of brake disks and brake adjustment.
Inspections of the emergency escape equipment.
Checking the security of fixings, e.g. bolt torque, blade attachment, gearbox hold down, yaw bearing attachment.
Checking high speed shaft alignment.
Checking performance of yaw drive and brake.
Bearing greasing.
Oil filter replacement.
Inspecting overspeed protection systems.
Blade inspection techniques (e.g Torque, acoustic and strain measurement, visual inspection, proximity probe) and cleaning from gradual build up of dirt.
test output regularly
Equipment inspection
lubrication
part replacement
cleaing and adjustments
Alternative means of operation
Redundant Item

- Condition Monitoring Techniques were selected regarding their availability in the market and assigned to the components and assemblies based on studies (Tchakoua et al. 2014, Marquez et al. 2012 and Hameed et al. 2009) and expert opinions. See table 3.

Table 13. Detection Methods associated with the type of failure modes. [22][21] [3] [51]

Subsystem	Component	Failures	Condition Monitoring Method
Rotor	Bearings	Spalling, wear, defect of bearing shells and rolling element	Vibration, oil analysis, acoustic emission, shock pulse method, and performance monitoring
	Shaft	Fatigue, and crack formation, shaft displacement	Vibration analysis
Drive Train	Main shaft bearing	Wear, and high vibration	Vibration, shock pulse method, temperature, and acoustic emission
			Torque, power signal analysis, thermography, acoustic emission, and performance monitoring
	Mechanical Brake	Locking position	Temperature
	Gearbox	Wearing, fatigue, oil leakage, insufficient lubrication, braking in teeth, displacement, and eccentricity of toothed wheels	Temperature, vibration, shock pulse method, particles in oil, and acoustic emission
Generator		Wearing, electrical problems, slip rings, winding damage, rotor asymmetries, bar break, overheating, and over speed	Temperature, vibration, SPM, OM, torque, power signal analysis, electrical effects, process parameters, performance monitoring, and thermography
Auxiliary Systems	Yaw system	Yaw motor problem, brake locked, and gear problem	Motor current
	Pitch system	Pitch motor problem	O&M
	Hydraulic system	Pump motor problems, and oil leakage	O&M, process parameter, performance monitoring
	Sensors	Broken, and wrong indication	Thermography
Electrical System	Control system	Short circuit, component fault, and bad connection	Current consumption, and temperature
			Thermography and visual inspection
	Power electronics	Short circuit, component fault, and bad connection	Current consumption and temperature
	High voltage	Contamination, and arcs	Arc guard, temperature
Tower	Nacelle	Fire, and yaw error	Smoke, temperature and noise measurement, flame detection
			Vibration, shock pulse method, strain measurement, temperature and acoustic measurement and visual inspection
	Tower	Crack formation, fatigue, vibration, and foundation weakness, scour	Capacitive sensors
Transformer		Problem with contamination, breakers, disconnectors, and isolators	Thermography
Wind Turbine			Wind turbine measurements (SCADA)
			Failures cannot be detected remotely (testing will be needed)

3.2.2 Data sources

Failure mechanisms in offshore wind turbines and their consequences arise from several data sources. Using a consistent approach, a knowledge base can be developed in order to assess events in the offshore wind turbine. Disparate sources of data or information are used to develop the FMEA:

- Recognised and peer-reviewed long-term reliability data (for instance from the EU Framework 7 Project, Reliawind)
- Lloyd's Register experience working with wind farm operators which allow having access to expert knowledge of maintenance technicians and managers, maintenance task reports, technicians' logs, marine coordinators' records, vessel skippers' records.
- Reliability data from SCADA databases.
- Reliability data from other industrial sectors for similar components and operational conditions.
- On-going measurements and observations.

3.2.3 Functional Block Diagram

To aid the analysis, symbolic representations such as functional diagrams of the system and operation are very useful. Functional diagrams are created highlighting all the crucial functions of the wind turbine. Blocks representing components are linked together by lines that represent mechanical, electrical or hydraulic inputs and outputs, as described in Table 14.

The diagrams show redundancies and functional interdependencies of the components that allow the analysis of failure through the system.

The block diagram contains the following items:

- Breakdown of the system (Figure 25) into major subsystems, assemblies and components (e.g. Figure 26 and Figure 27) including functional relationships.
- Appropriately labelled block with names, inputs and outputs.
- Redundancies, alternative signal paths and other engineering features which provide protection against system failures.

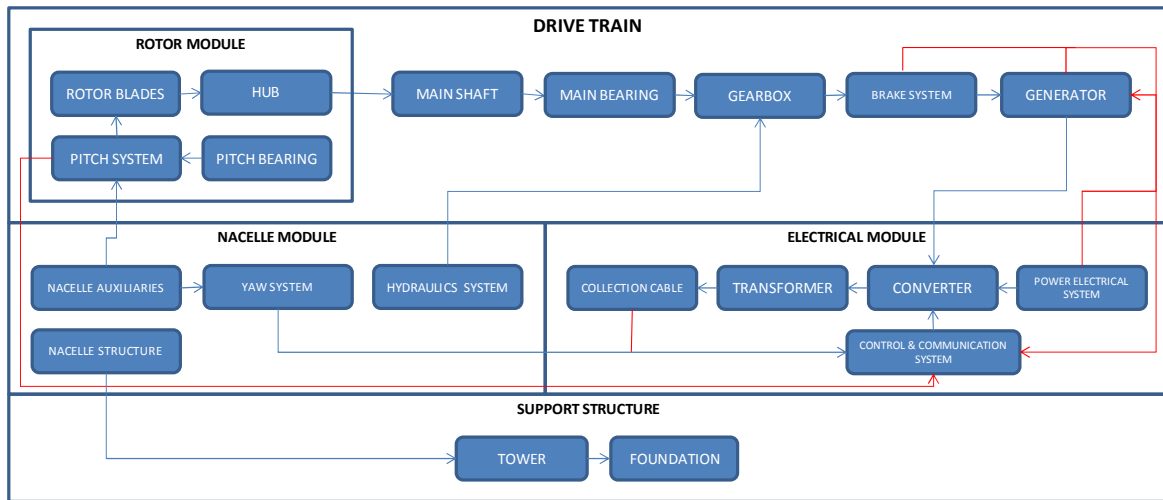


Figure 25. Wind Turbine System Functional Diagram

Table 14. Gearbox Functional Diagram Description

ITEM	DESCRIPTION
Blue lines	Mechanical contact, torque and load transference
Red lines	Hoses
Green lines:	Electrical connections
Blue boxes:	Gearbox components
Red boxes:	Other assemblies
Purple boxes:	Connection components
Orange boxes:	Hydraulic systems

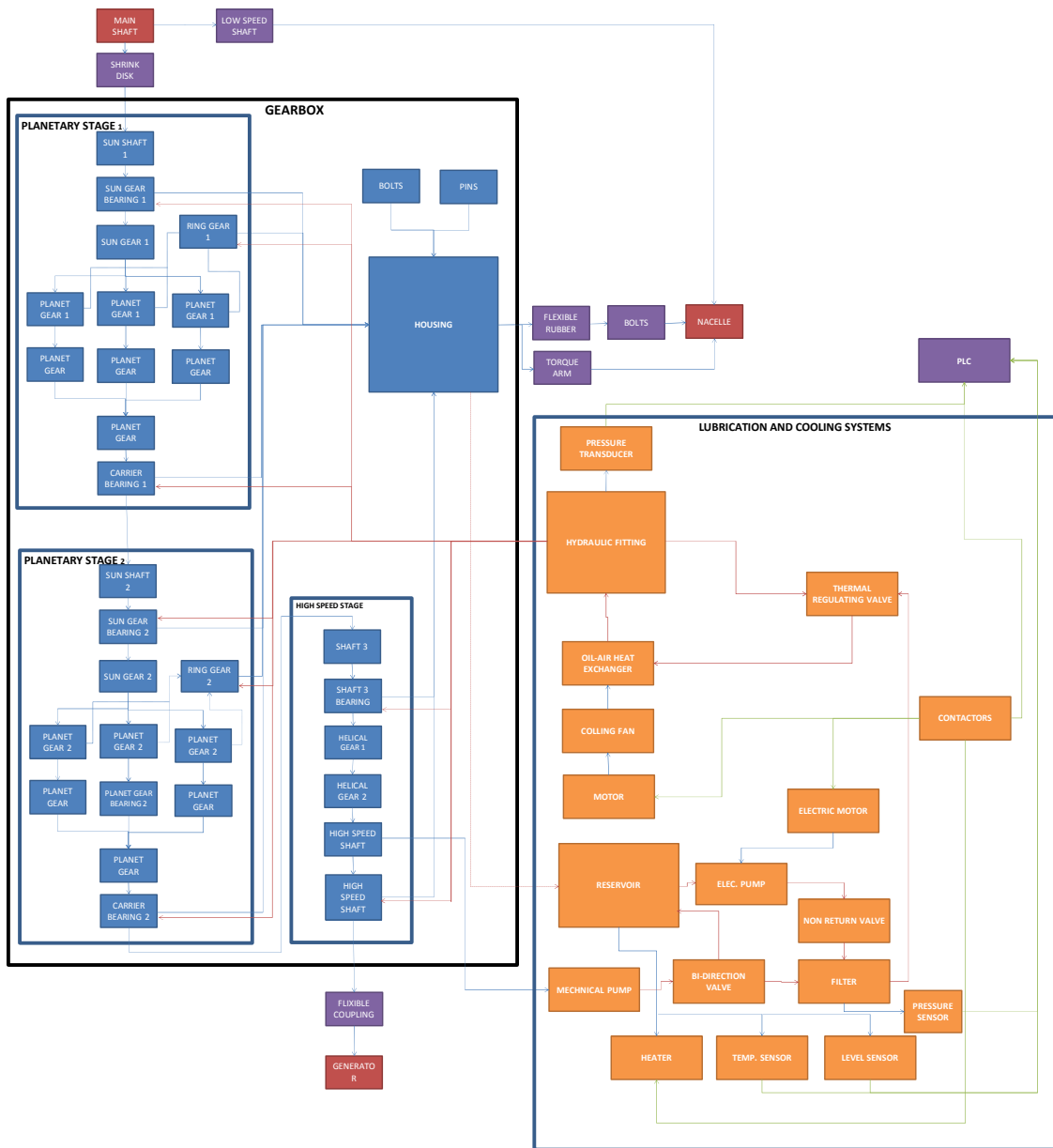


Figure 26. Gearbox Functional Diagram

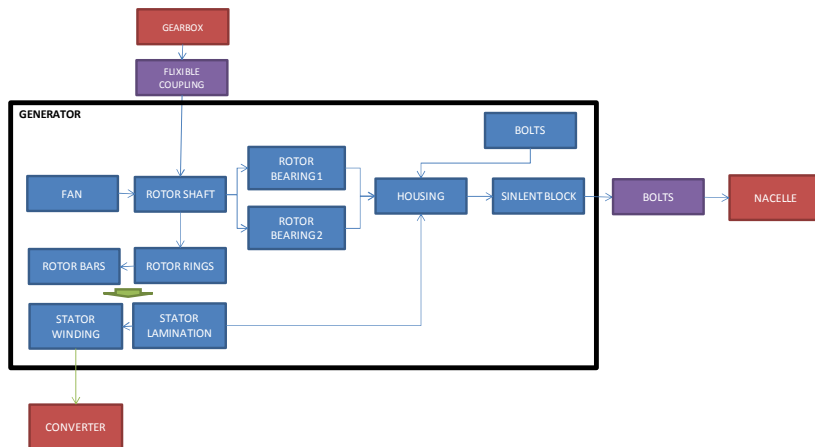


Figure 27. Generator Functional Diagram

3.2.4 FMEA Worksheet

Based on the standard BS EN 60812:2006, terms and definitions are defined to carry out the FMEA:

Item: part or component that can be individually considered.

Failure: termination of the ability of an item to perform a required function.

Failure Local Effect: consequence of a failure mode in terms of the operation, function or status of the item. The expression “local effects” refers to the effects of the failure mode on the system element under consideration.

Failure Global Effect: A failure effect may also influence the next level up and ultimately the highest level under analysis. Therefore, at each level, the effect of failures on the level above should be evaluated. When identifying end effects, the impact of a possible failure on the highest system level is defined and evaluated by the analysis of all intermediate levels

Failure Mode: the way in which an item fails.

Failure Mode Reference Number: The failure mode reference number is a unique identifying number assigned to each component of the system being analysed.

System: a set of interrelated or interacting elements.

Failure Severity: the significance of the failure mode’s effect on item operation, on the item surrounding, or on the item operator.

Detection: For each failure mode, it is determined the way in which the failure is detected and the means by which the user or maintainer is made aware of the failure.

3.2.5 Ratings

The basis of the FMEA is the Risk Priority Number (RPN) which is a multiplication of the numerical values of severity, occurrence and detection ratings assigned to each failure modes.

Severity Classification Definitions

To facilitate the analysis of severity and occurrence ratings and further correlation with previous quantitative surveys or studies it is used reliability concepts based on [3] [3]. The list below described key concepts of reliability to associate a qualitative FMEA with quantitative variables.

- Availability (A): (technical availability: percentage of time that an individual turbine WT or wind farm is available to generate electricity expressed as a percentage of the theoretical maximum.
- Mean time to failure MTTF
- Mean time to repair MTTR
- Logistic delay time LDT
- Downtime MTTR+LDT
- Mean time between failure MTBF = MTTF
- $MTBF=MTTF+MTTR+LDT$
- Failure rate: $\lambda=1/MTBF$
- Repair rate: $\mu=1/MTTR$
- Commercial availability: $A=(MTBF-MTTR)/MTBF=1-(\lambda/\mu)$
- Technical availability: $A=MTTF/MTBF<1-(\lambda/\mu)$

Regarding BS EN 60812:2006, Severity is an assessment of the significance of the failure mode's effect on item operation.

Table 15. Severity Levels

Label	Value	Description
Catastrophic	5	wind turbine inoperable with destructive failure without warning
Critical	4	wind turbine inoperable with equipment damage
Marginal	3	wind turbine operable with significant degradation of performance
Minor	2	wind turbine operable with minimal interference
None	1	no effect on wind turbine operation

The severity ratings in Table 15, give an indication of MTTR, which at the same time is represented by repair rate μ . Downtime is the sum of mean time to repair and the logistic delay time.

Occurrence Classification Definitions

Regarding BS EN 60812:2006, the probability of occurrence of each failure mode should be determined in order to adequately assess the effect or criticality of the failure mode. This parameter is associated with the failure rate. When there is no access to registered failure rates of offshore wind farms, a good starting point for estimation is the failure rates data

available in public databases. The table 16 shows the failure rate from different databases of onshore wind farms.

Table 16. Failure rates (failures/turbine/year) from WSD, WSDK and LWK databases.

	WSD (1291-4285 WT's)	WSDK (851-2345 WT's)	LWK (158-643 WT's)	Average Failure rate	Average MTBF
Electrical system / Grid / Electrics	0.294	0.0468	0.32	0.22	4.54
Rotor or blades / Hub / Blades	0.191	0.0486	0.19	0.14	6.98
Electrical control / Electronics	0.182	0.15	0.239	0.19	5.25
Yaw system	0.108	0.0645	0.116	0.10	10.40
Generator	0.105	0.0497	0.139	0.10	10.21
Hydraulic system	0.0958	0.0451	0.131	0.09	11.03
Gearbox	0.0929	0.0425	0.134	0.09	11.14
Pitch control / Mechanical Control	0.0893	0.0141	0.0834	0.06	16.06
Air brakes / Rotor Brake	0.0411	0.0164	0.0397	0.03	30.86
Mechanical brake	0.033	0.0289	0.0554	0.04	25.58
Main shaft / Bearing	0.0212	0.0145	0.0311	0.02	44.91
Other (Anemometry, Sensors, Others)	0.188	0.209	0.367	0.25	3.93

Table 17 shows the description of the occurrence rating and its association with MTBF.

Table 17. Occurrence Levels

Label	Value	Description
Inevitable	5	failure is almost inevitable, will definitely occur
Frequent	4	repeated failures with regular occurrence
Occasional	3	occasional but not necessarily regular failures
Rare	2	rare and irregular failures
Extremely-Unlikely	1	failure almost never occurs, extremely unlikely

Where $\lambda=1/\text{MTBF}$ is the failure rate.

Detection Classification Definitions

Since the aim of the project, of which this FMEA takes part of, is to optimise the O&M activities by improving the accuracy of failure prognosis, this rating is defined in terms of the prognostic horizon or advance warning. This categorisation allows for identifying hidden failures. Detection classifications are classified from 1 to 5 regarding the following criteria in Table 18

Table 18. Detection Levels

Label	Value	Description
Undetectable	5	Undetectable until failure occurs
Detectable by O&M	4	Detectable by maintenance team in an average of 3 month routine
Detectable by CMS	3	Detectable by safety system when operational parameters are exceeded
Early Prognosis	2	Early prognosis, detectable by the control system during normal production
Detectable	1	Detectable before the turbine starts production

3.2.6 Analysis Flowchart

Figure 28 shows the steps followed by the analyst to allocate the right information for each component in the FMEA. After all the components are listed, the analyst performs the analysis of the components one by one.

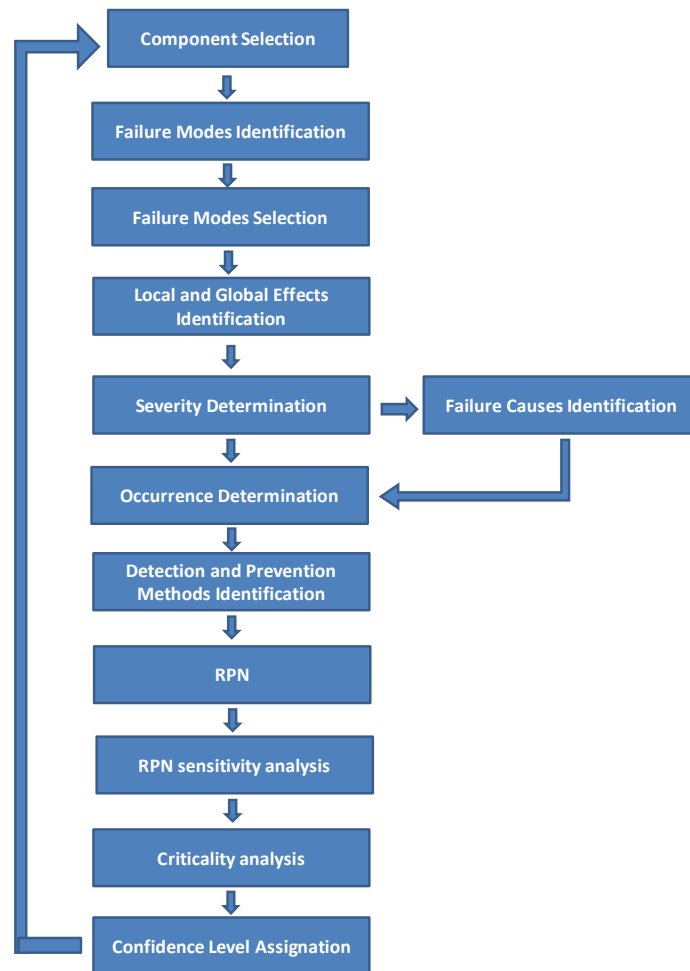


Figure 28. FMEA procedure

The last step is to register the data source used in the assessment by assigning a Confidence Level index described in section 3.5.

3.3 Criticality Analysis

Criticality concept could assume different perspectives; in this study, criticality analysis aims to qualitatively measure the magnitude of a failure effect in the different categories as it is described in Table 19: safety, environment, asset integrity and operation. It considers a wider context than the approach of the FMEA previously described. It comprises environmental, financial and regulatory aspects of wind farm developments. This criticality analysis is

performed in parallel with the assessment of the RPN for each failure mode and component, as shown in an example of the FMEA spreadsheet in Figure 29. In order to have consistency between the criticality and the RPN analysis, the failure frequency remains the same.

Table 19. Criticality Analysis Categories

Severity categories		1	2	3	4	5
S	Safety (Personnel)	zero enjury	slight injury	minor injury	major injury	single fatality
E	Environment	zero effect	slight effect	minor effect	local effect	major effect
A	Assest integrity	zero damage	slight damage	minor damage	local damage	major damage
O	Operation					

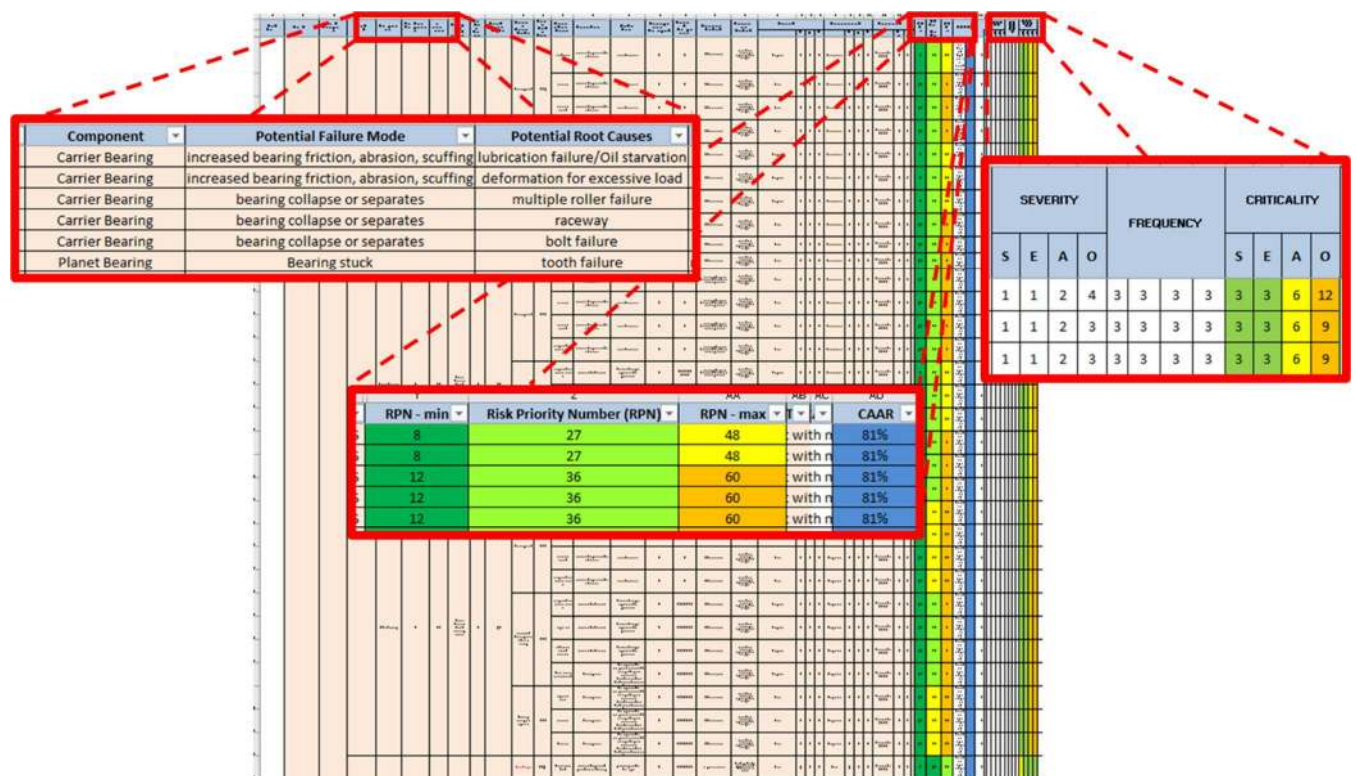


Figure 29. Example of the FMEA spreadsheet.

3.4 Results Analysis

3.4.1 RPN and Failure Contribution

Table 20 shows a summary of the FMEA describing the total number of components per assembly, the average number of failure per component and, the failure contribution of the assemblies. The FMEA comprises 18 main assemblies, 76 sub-systems and 493 components. 963 potential failures modes are identified and classified by the Risk Priority Number (RPN). The failure contribution is the number of the failures modes identified for each assembly out of the total number of failures modes in the turbine.

Table 20. FMEA summary

Assembly	Total Number of Components	Number of Potential Failures	Average Number of Failures per component	FAILURE CONTRIBUTION
nacelle structure	15	15	1.0	2%
power electrical system	15	18	1.2	2%
nacelle auxiliaries	13	26	2.0	3%
foundation/transition piece/tower/cable	25	31	1.2	3%
auxiliaries electrical systems	37	37	1.0	4%
Blade/Hub	38	38	1.0	4%
main shaft	24	47	2.0	5%
hydraulic system	27	49	1.8	5%
pitch system	28	82	2.9	9%
generator	56	83	1.5	9%
control and communication systems	38	84	2.2	9%
yaw system	39	125	3.2	13%
gearbox	46	156	3.4	16%
frequency converter	92	172	1.9	18%
	493	963		

The RPN is calculated multiplying the values of the three ratings for each component; severity, occurrence and detection. Table 21 and Figure 30 show the average, minimum and maximum values of the RPN for each assembly. Some of the components with maximum values of RPN for each assembly are identified.

Table 21. Minimum, average and maximum values of RPN of the components of each assembly.

Assembly	Min RPN	Av RPN	Max RPN	Components with maximum RPN
gearbox	16	30.1	48	shaft bearing
generator	12	27.6	40	sensors
main shaft	12	27.0	40	bearings
auxiliaries electrical systems	10	17.8	40	grid protection relay
control and communication systems	16	28.1	30	sensors
frequency converter	8	38.3	60	capacitors
power electrical system	20	25.0	40	transformer
hydraulic system	18	18.0	18	pressure and level sensors, motor, pump
nacelle auxiliaries	16	29.0	36	anemometer, wind vane
nacelle structure	16	16.0	16	sensors, firefighting system, lightning protection
yaw system	16	30.8	48	brakes
Blade/Hub	12	19.7	24	root structure, paint
pitch system	15	33.9	48	motor, pinions, bearings
foundation/tower/export cable	8	12.0	32	export cable

Figure 30 presents the average RPNs with the standard deviation, which gives an indication of the range of RPN values among the components of one particular assembly. The standard deviation of the RPNs for each assembly is calculated using the following equation:

$$S = \sqrt{\frac{1}{N-1} \sum_{i=1}^N (RPN_i - RPN')^2}$$

Where RPN' is the mean value of the risk priority number, and N is the number of components for each assembly.

The assemblies nacelle structure and hydraulic system have little variations of RPN values while the frequency converter has a wide range of RPN values amongst its components.

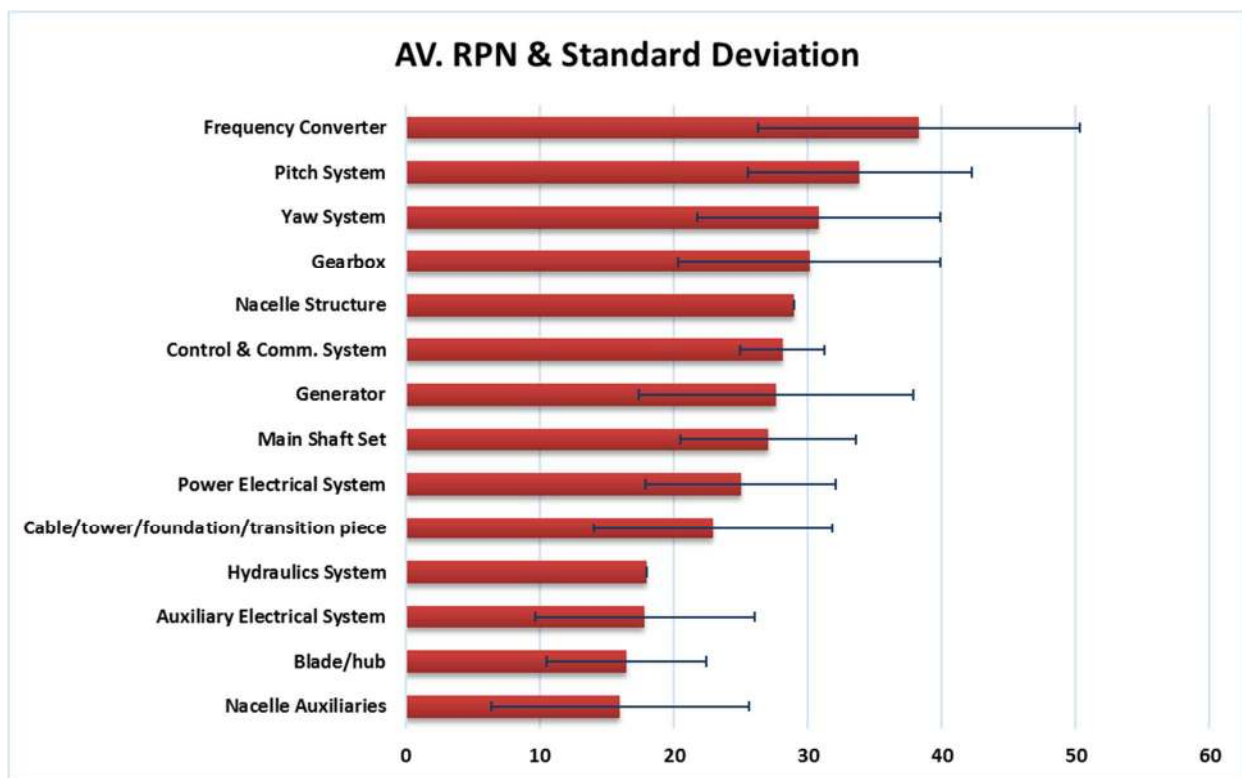


Figure 30. Average RPN per assembly.

In order to identify those assemblies that are critical for the wind turbine, severity ratings are filtered. Those components with “marginal”, “critical” and “catastrophic” impact on the WT’s performance are analysed and highlighted in red in the figure below.

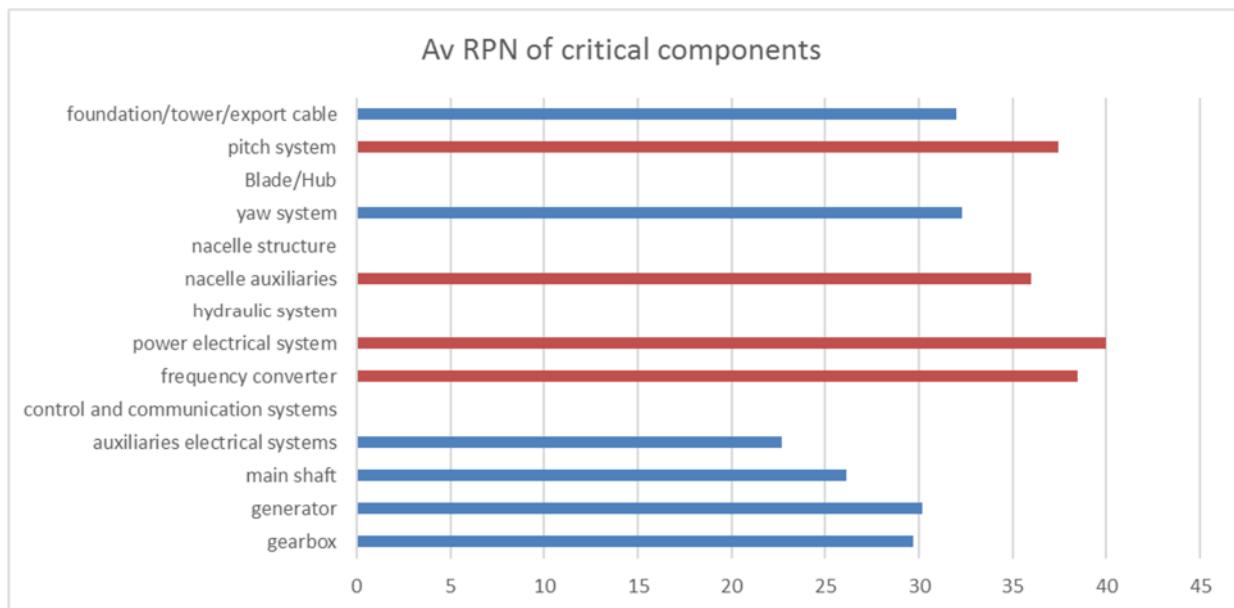


Figure 31. Average RPN of critical components.

Figure 32 presents failure contribution as a percentage of the total number of potential failure modes in the offshore wind turbine. This is compared with the number of failures per component of each assembly. It is possible to see that the frequency converter has the largest failure contribution, but its components have fewer ways in which to fail. On the other hand, assemblies such as pitch system and nacelle structure, represent a lower contribution to the total number of failure however, their components have a wider range of failure mechanism. From the graph, it is possible to conclude that the assemblies with greater failure contribution are frequency converter, gearbox and the yaw system. Amongst these three assemblies, frequency converter has the highest failure contribution of the whole wind turbine system with 18%, however its identified number of failures per component is approximately the half of the number of failures per component of the gearbox with 16% of failure contribution. The number of failure per component could be considered as an indication of component reliability, therefore, if the number of failure per component is high, the estimated reliability of that component could be degraded as it has more chances to fail due to different failure root causes.

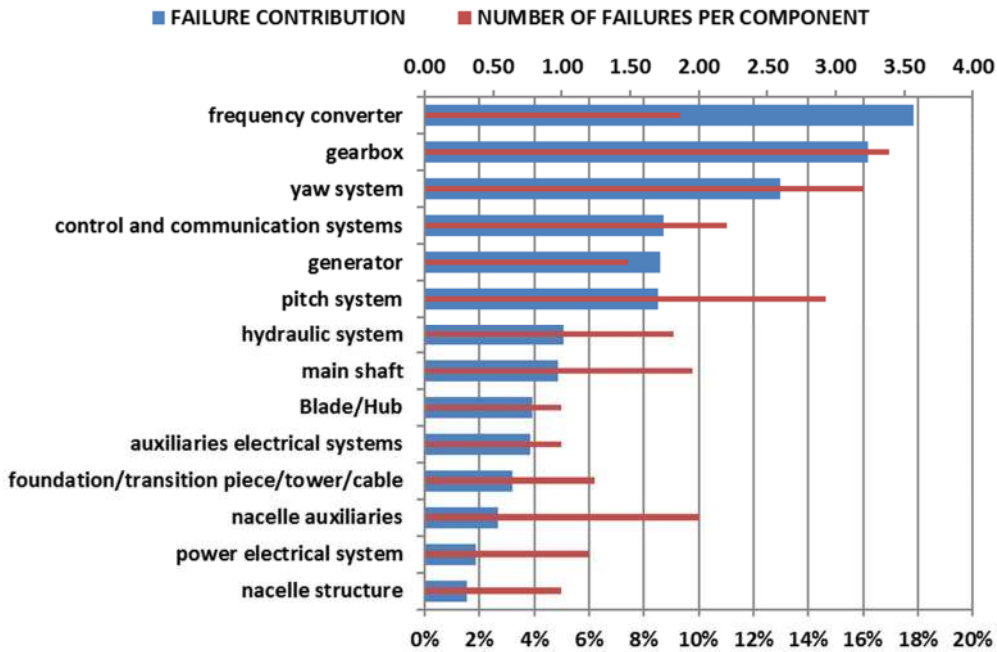


Figure 32. Failure contribution per assembly.

Once critical assemblies are identified, it is necessary to identify how they can fail to put more efforts on avoiding those failures with greater impact on the assembly and therefore, on the turbine operation. The figure below shows that the main failure modes for the gearbox and frequency converter are electrical failures, and most of the main failure modes of the yaw and pitch system are mechanical failure.

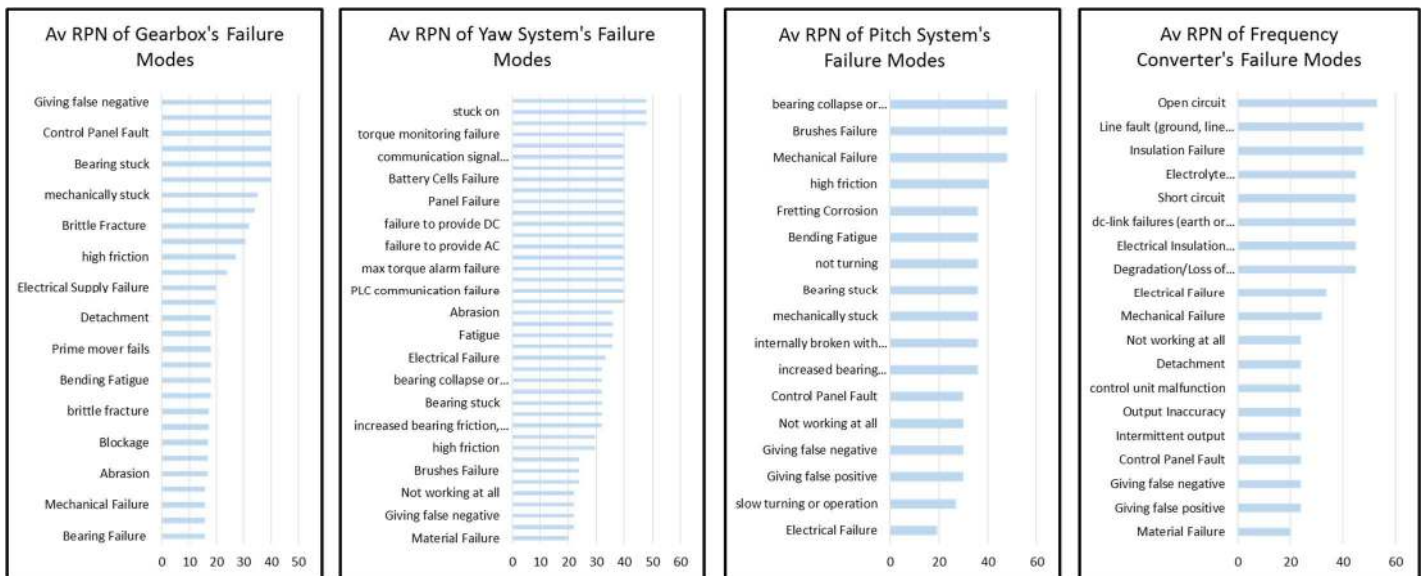


Figure 33. Main failure modes of critical assemblies.

To analyse the failure modes in the FMEA, they are grouped into major families of failures. Figure 34 shows the major failure mode families and the number of events counted per failure type in the FMEA analysis. It is evident that sensor system failure, and electrical failure are the most common type of failures in the wind turbine. Material and mechanical failure is also above average. This graph shows what is the type of failures that could represent the greatest cost in O&M due to their probability of occurrence and where some new strategy could be implemented to focus the effort on that number of the identified failure modes.

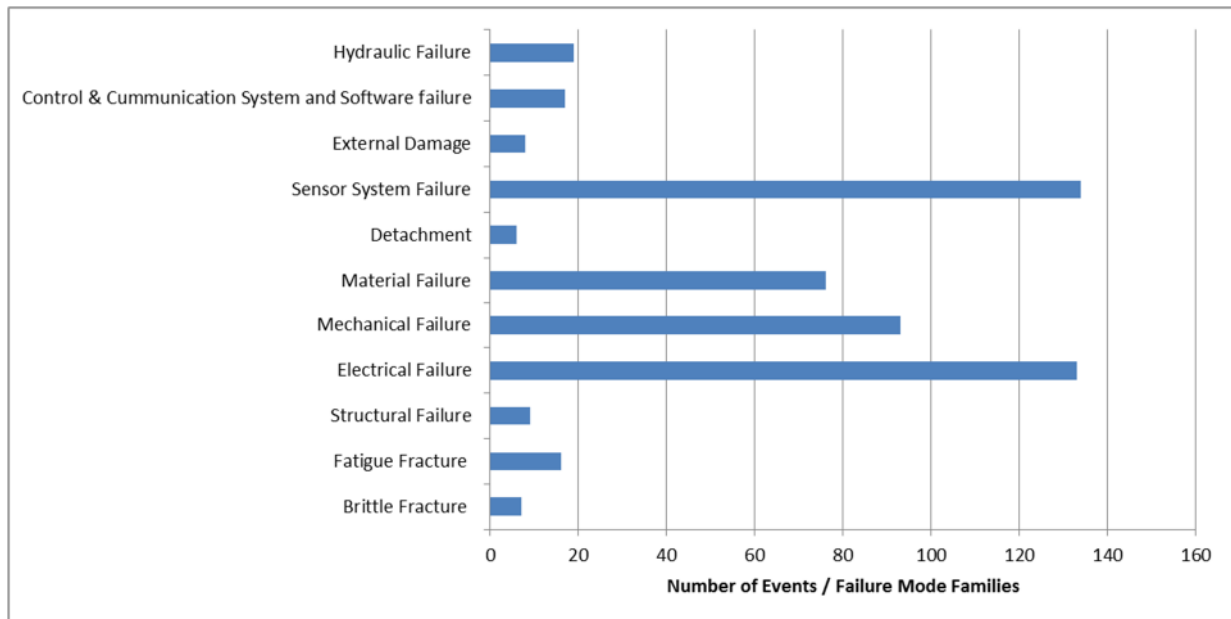


Figure 34. Families of failure modes and their number of events.

Figure 35 shows the unique types of failure modes identified and their RPN in the FMEA. Here it is possible to observe that the majority of the failure in the list has an electrical nature. However, the number of events per failure mode, as it is described above; do not represent the severity of the failure or the impact on O&M activities. The FMEA shows that failure modes with a low number of events like “loose bar” or “shaft scuffing” have high RPN which means that this kind of failure needs to be addressed for further analysis due to their consequences in the system.

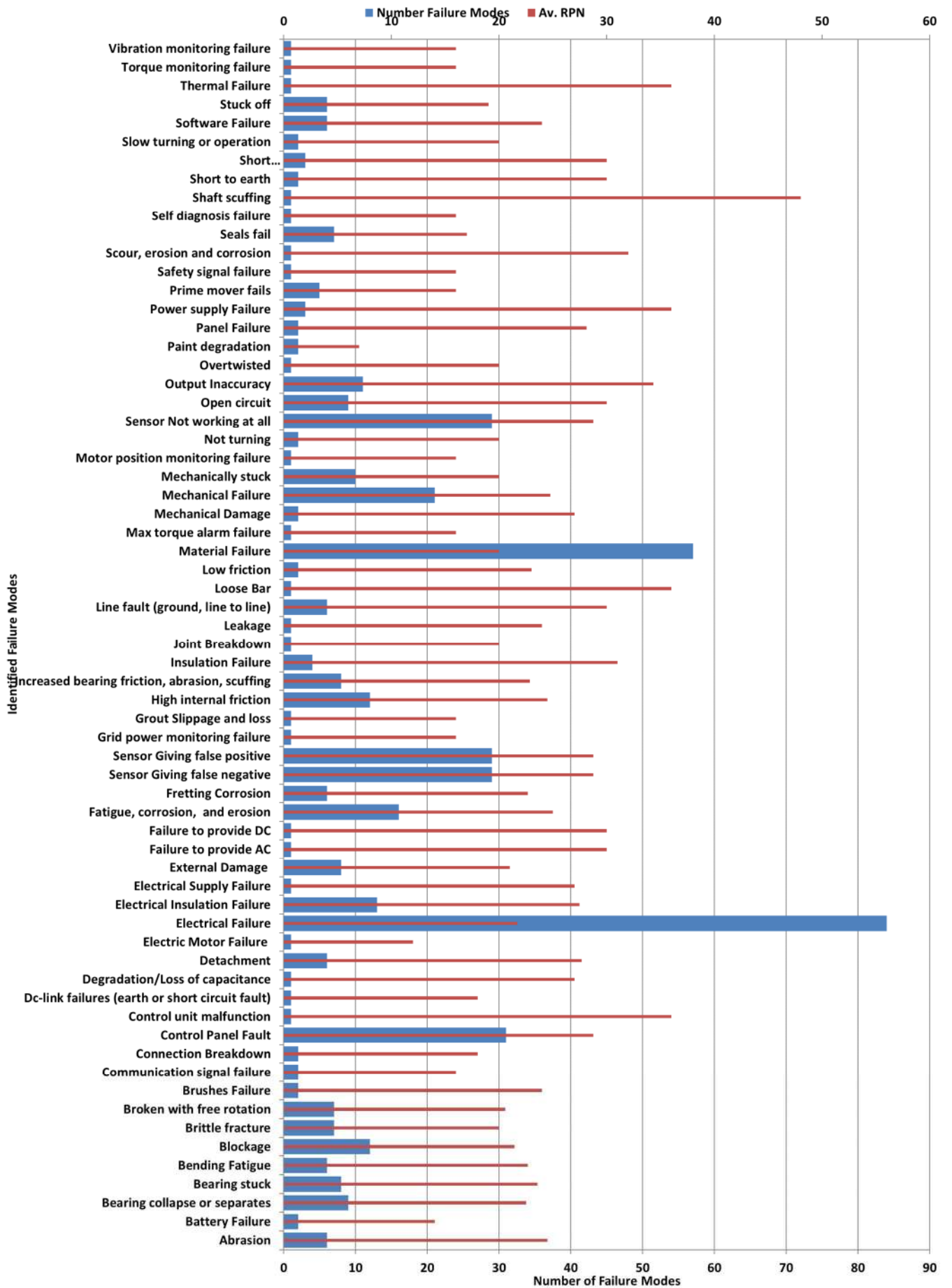


Figure 35. Failure modes and average RPN.

Table 22 is listing the undetectable failure mode identified in the FMEA and their RPN. There are 173 undetectable failures in the entire WT selected by using the detection rating: Undetectable: Undetectable until failure occurs.

Table 22. Undetectable Identified Failure Modes

Undetectable Failure Modes	Count of Failure Modes	Average of RPN
⊕ Battery Cells Failure	1	40.00
⊕ communication signal failure	1	40.00
⊕ Control Panel Fault	19	32.63
⊕ dc-link failures (earth or short circuit fault)	1	45.00
⊕ Degradation/Loss of capacitance	1	45.00
⊕ Detachment	2	10.00
⊕ Electrical Failure	48	26.35
⊕ Electrical Insulation Failure	6	40.00
⊕ Electrical Supply Failure	1	20.00
⊕ Electrolyteevaporation	1	45.00
⊕ failure to charge battery	1	40.00
⊕ failure to provide AC	1	40.00
⊕ failure to provide DC	1	40.00
⊕ Giving false negative	18	32.78
⊕ Giving false positive	18	32.78
⊕ grid power monitoring failure	1	40.00
⊕ Intermittent output	3	23.33
⊕ max torque alarm failure	1	40.00
⊕ Mechanical Failure	1	20.00
⊕ motor position monitoring failure	1	40.00
⊕ Not working at all	18	32.78
⊕ Open circuit	3	46.67
⊕ Output Inaccuracy	4	30.00
⊕ Panel Failure	2	40.00
⊕ PLC communication failure	1	40.00
⊕ Power supply Failure	3	30.00
⊕ safety signal failure	1	40.00
⊕ self diagnosis failure	1	40.00
⊕ Software Failure	6	30.00
⊕ torque monitoring failure	1	40.00
⊕ vibration monitoring failure	1	40.00
⊕ Short circuit	5	41.00

3.4.2 Consequential Damage

The determination of affected components and consequential damage is another capability of the FMEA.

Using a detailed functional diagram of each main assembly, it is possible to determine functional interdependencies between components and therefore, the potential consequential damage and affected components. Each failure mode of a component might affect directly another component. The connection between both components could be mechanical, electrical or hydraulic. An example of failure modes and potentially affected components are shown in the table below.

Table 23. Affected Components associated with failure modes

Assembly	Component	Potential Failure Mode	Affected Component
Auxiliary Electrical System	Grid Protection Relay	Electrical Failure	TRANSFORMER
Control and Communication System	cable	Electrical Insulation Failure	CONTACTOR
Foundation	Monopile	Bending/ Misalignment	TRANSITION PIECE
Foundation	Monopile	Local Buckling	TRANSITION PIECE
Foundation	Monopile	Loss of Structural Integrity/ Deformation	TRANSITION PIECE
Foundation	Monopile	Uprooting	TRANSITION PIECE
Gearbox	Carrier Bearing	bearing collapse or separates	SUN SHAFT
Gearbox	FAN	Bearing Failure	ELC. MOTOR
Gearbox	FAN	brittle fracture	ELC. MOTOR
Gearbox	FAN	Electric Motor Failure	ELC. MOTOR

3.4.3 Failure Detectability and Criticality

The RNP comprises the rating 'detection' to assess each failure mode from a failure prognosis point of view. 173 undetectable failures are identified. Amongst this group of failures, there are 27 failure modes that have been identified as critical in terms of operation (Ref: Severity rating, Critical: wind turbine inoperable with equipment damage) and undetectable in terms of early prognosis. (Ref: Detection rating, Undetectable: Undetectable until failure occurs). See Table 24.

Table 24. Undetectable and Critical failure Modes

Assembly	Component	Potential Failure Mode	Severity (S)	Occurrence (O)	Detection (D)	Risk Priority Number (RPN)
Auxiliary Electrical System	Grid Protection Relay	Electrical Failure	Critical	Rare	Undetectable	40
Frequency Converter	Capacitor	Open circuit	Critical	Occasional	Undetectable	60
			Critical	Occasional	Undetectable	60
			Critical	Occasional	Undetectable	60
			Critical	Occasional	Undetectable	60
	Contactactor	Electrical Failure	Critical	Rare	Undetectable	40
Power Electrical System	Machine Transformer	Electrical Failure	Critical	Rare	Undetectable	40
Yaw System	power cables - yaw motor brake to drive	Open circuit	Critical	Rare	Undetectable	40
		Short to earth	Critical	Rare	Undetectable	40
		Panel Failure	Critical	Rare	Undetectable	40
		Short between cables	Critical	Rare	Undetectable	40
	Power Cables: yaw motor to drive	Open circuit	Critical	Rare	Undetectable	40
		Short to earth	Critical	Rare	Undetectable	40
		Panel Failure	Critical	Rare	Undetectable	40
		Short between cables	Critical	Rare	Undetectable	40
	Battery	Battery Cells Failure	Critical	Rare	Undetectable	40
	inverter	failure to provide AC	Critical	Rare	Undetectable	40
		failure to provide DC	Critical	Rare	Undetectable	40
		Electrical Failure	Critical	Rare	Undetectable	40
		failure to charge battery	Critical	Rare	Undetectable	40
	controller	Electrical Failure	Critical	Rare	Undetectable	40
		torque monitoring failure	Critical	Rare	Undetectable	40
		max torque alarm failure	Critical	Rare	Undetectable	40
		vibration monitoring failure	Critical	Rare	Undetectable	40
		motor position monitoring failure	Critical	Rare	Undetectable	40
		grid power monitoring failure	Critical	Rare	Undetectable	40
		self diagnosis failure	Critical	Rare	Undetectable	40
		PLC communication failure	Critical	Rare	Undetectable	40
		safety signal failure	Critical	Rare	Undetectable	40
		communication signal failure	Critical	Rare	Undetectable	40

Further analysis of the failures has been performed in **Annex 1: FMEA Failure analysis**. Here, graphs show the failures that can be detected by CMS (28), failure detectable by the O&M team (58) and failures able to generate turbine shutdown (24).

3.4.4 Criticality Analysis Results

In this study, criticality analysis was designed to complement the RPN analysis identifying those failure modes that have a negative impact in other areas such as environment and safety. It is also identified the severity of failure in asset integrity and operation to validate the RPN, i.e. acting as a “double check” of the operational consequence of failure.

The values assigned for each category are described in Table 19, and the identified components and failures modes that have a greater impact on the environment and safety are shown in Table 25 and Table 26, respectively.

Those components and failures modes that are not identified by the RPN as severe damage to the personnel or the environment are identified by criticality analysis. For example, the high friction of the components of the gearbox like spur gears could produce risky high temperature for personnel. Leakage on hoses could have a negative impact on the environment or health if it is in direct contact with the skin. There are other dangerous failures modes for personnel in the auxiliary electrical system like live wires with loss of insulation, or mechanical damage in the firefighting system in the nacelle. The results shown in Table 25 and Table 26 allow the analyst to identify failure for components that can be critical for the other wind farm stakeholders: operator, manufacturer, investor, regulators and on. It also shows the ranking for the asset integrity and operational categories. These two categories validate the independent RPN as a combination of both would give the analyst a better approach and an “error checking system” in the allocation of values for severity, occurrence and detection ratings of the RPN.

Table 25. Criticality analysis results – Safety ranking

Assembly	Component	Potential Failure Mode	Potential Root Causes	Safety	Environment	Asset integrity	Operation
Main Shaft Set	Slip Ring	Mechanical Failure	External Accidental Damage	16	4	20	20
Main Shaft Set	Disk	stuck off	mechanically seized	15	6	15	15
Auxiliary Electrical System	Power Point	Electrical Failure	Connection failure	12	3	6	12
Main Shaft Set	Calliper	stuck on	loss of hydraulic pressure	12	3	15	15
Auxiliary Electrical System	Protection Cabinet	Electrical Insulation Failure	Insulation degradation	12	3	6	9
Control and Communication System	contactor	Electrical Failure	Connection failure	12	3	6	12

Table 26. Criticality analysis results – Environment ranking

Assembly	Component	Potential Failure Mode	Potential Root Causes	Safety	Environment	Asset integrity	Operation
Nacelle Auxiliaries	Firefighting System	Mechanical Damage	External Accidental Damage	8	8	10	10
Nacelle Auxiliaries	Firefighting System	Electrical Failure	Connection failure	8	8	10	10
Main Shaft Set	Pad	low friction	Installation Defect	4	8	16	20
Main Shaft Set	Disk	stuck off	mechanically seized	15	6	15	15
Transition Piece	Navigation Light	Electrical Failure	Connection Failure, Aging, Installation Defect	10	6	2	2
Gearbox	Hose	Blockage	Presence of Debris	9	6	3	6
Gearbox	Hose	Abrasion	Maintenance Fault	9	6	3	6
Gearbox	Hose	Fatigue	Low Cycle Fatigue	9	6	3	6

As RPN only combine aspects related to turbine operation, criticality analysis is performed to show an integral analysis with interesting aspects for different wind farm stakeholders.

There are four categories: safety, environment, asset integrity and operation.

To have consistency in both analyses, the operation category in the criticality analysis assumes the same values assigned to the Severity rating in the RPN evaluation. All the categories take into the account a frequency which is also matched to the occurrence rating of the RPN.

Table 27 shows that the assembly “Main shaft set” is the only assembly with high values in all the categories.

Table 27. Criticality analysis summary.

Assembly	Safety	Environment	Asset Integrity	Operation
Auxiliary Electrical System	5.5	2.2	5.8	7.8
Blade	3	3	9.8	9.8
Cable	2	2	10	10
Control and Communication System	4.3	3	3.8	9.6
Foundation	1.9	3.3	7.3	7.3
Frequency Converter	3.6	3	5.6	9.5
Gearbox	3.9	3.3	7.6	10.8
Generator	3.4	2.6	6.7	9.1
Hub	3	3	4.5	6
Hydraulics System	3.1	3.2	5.2	8.9
Main Shaft Set	4.5	3.2	10	11
Nacelle Auxiliaries	3	2.9	9.1	11.6
Nacelle Structure	2	2	4	4
Pitch System	3	4.3	8.7	10.8
Power Electrical System	2.3	2.3	2.3	9.2
Tower	2	3	7.5	7.5
Transition Piece	3.8	3.2	5.8	6.3
Yaw System	2.2	2.2	5.8	6.4

RED: 25th percentile of highest values.

GREEN: 75th percentile of lowest values.

3.4.5 Top 30 chart for failure mechanisms

The FMEA allows determining the top 30 chart of failure mechanisms of a generic offshore wind turbine. The first 10 failures are in the frequency converter, mainly power electronics components at both sides of the converter, generator and grid side. The type of failures is short or open circuit failures due to overheating or insulation degradation. The second ten failures are in the frequency converter but also in the pitch system with a combination of electrical and mechanical failures. Finally, the last ten failures are in the yaw system and frequency converter.

Table 28. Top 30 chart for wind turbine failure mechanism.

Assembly	Potential Failure Mode	Potential Root Causes	Average of Risk Priority Number (RPN)
Frequency Converter	Open circuit	Ageing/degradation in the dielectric material	60
Frequency Converter	Open circuit	Bushing Insulation Lost	60
Frequency Converter	Open circuit	Corrosion (electrodes)	60
Frequency Converter	Open circuit	Increase in the internal pressure	60
Frequency Converter	Open circuit	Insulation degradation	48
Frequency Converter	Insulation Failure	Overheating	48
Frequency Converter	Line fault (ground, line to line)	Insulation degradation	48
Frequency Converter	Line fault (ground, line to line)	Overheating	48
Pitch System	bearing collapse or separates	bolt failure	48
Pitch System	bearing collapse or separates	multiple roller failure	48
Pitch System	bearing collapse or separates	raceway	48
Pitch System	Brushes Failure	Excessive Brush Wear	48
Pitch System	Mechanical Failure	Insufficient Lubrication	48
Yaw System	high friction	Maintenance Fault	48
Yaw System	low friction	Maintenance Fault	48
Yaw System	stuck off	mechanically seized	48
Yaw System	stuck off	Presence of Debris	48
Yaw System	stuck on	loss of hydraulic pressure	48
Yaw System	stuck on	Presence of Debris	48
Frequency Converter	dc-link failures (earth or short circuit fault)	Insulation degradation	45
Frequency Converter	Degradation/Loss of capacitance	Charging/discharging cycles	45
Frequency Converter	Degradation/Loss of capacitance	Excess ripple current	45
Frequency Converter	Degradation/Loss of capacitance	High ambient temperatures	45
Frequency Converter	Degradation/Loss of capacitance	Over voltage stress	45
Frequency Converter	Electrical Insulation Failure	Installation Defect	45
Frequency Converter	Electrical Insulation Failure	Overheating	45
Frequency Converter	Electrolyte evaporation	Internal temperature Increase	45
Frequency Converter	Electrolyte evaporation	Prolonged use-degradation due to nominal operation	45
Frequency Converter	Short circuit	Bushing Insulation Lost	45
Frequency Converter	Short circuit	Charging/discharging cycles	45

3.4.5 Sensitivity Analysis

Sensitivity analysis provides the sensitivity of each output variable such as RPN, to its input variables such as severity and occurrence. It is possible to identify the most influential inputs affecting RPN or other output in the criticality analysis. In this study there are two kinds of sensitivity analysis, the first one is shown in Figure 36, here once the RPN is computed all the ratings are decreased by one value and increased by one value to calculate the minimum and maximum RPN possible. The second sensitivity analysis is only varying the severity and occurrence variables; this is shown in Figure 37.

RPN sensitivity analysis aims to establish the best and worst scenario regarding the estimation of the variables “severity”, “occurrence” and “detection”. This allows determining the impact of an incorrect estimation in the final conclusions given by the analyst.

Severity, occurrence and detection ratings are the inputs of the sensitivity analysis and vary from 1 to 5. The analysis delivers the minimum and maximum values of the RPN based on the nominal or assigned values of the inputs for each failure mode. For example Figure 36 shows the item in the first column of the FMEA spreadsheet: Gearbox-> Carrier Barings->Failure mode: Bearing Stuck->Failure cause: Tooth Failure->RPN:32

RPN - min	Risk Priority Number	RPN - max
9	32	60
6	24	45
12	36	60
3	16	30
8	27	48
9	27	48

Figure 36.Sensitivity Analysis

Once the critical components of the assemblies are identified, the three-variable sensitivity analysis will be performed. This analysis is shown in Figure 37, where the detection variable is assumed to be certain or with a high degree of confidence of the rating. Detection rating is based on techniques commercially available and well recognised in the industry. Then, once the detection variable is defined, the appropriate matrix can be analysed varying severity and occurrence only.

For example: Figure 37 is the sensitivity analysis of the carrier bearing of the gearbox with a failure mode of “bearing stuck” due to a “tooth failure”. The assigned RPN is 32 and the “detection rating” is considered as the low chance that the control system will detect potential cause or mechanism and failure mode, which represents a value of 4. Therefore, the sensitivity analysis is carried out with the fourth matrix. Here we can see that the variation of one unit of either occurrence or severity the RPN would be 40 of 48, which is still in an acceptable “yellow colour band”. The conclusion of this is that even though the analyst, based on the information available, made a mistake allocating the severity or occurrence values, the impact of this specific mistake on the FMEA results is negligible.

If the sensitivity analysis of a particular component shows that varying a value of occurrence or severity makes the colour band turns orange or red, that means that the allocation of the severity and occurrence values need to be analysed with greater accuracy to reduce the impact on the final FMEA results.

DETECTION = 1						DETECTION = 2						DETECTION = 3						DETECTION = 4						DETECTION = 5										
SEVERITY	RPN	OCURRENCE					SEVERITY	RPN	OCURRENCE					SEVERITY	RPN	OCURRENCE					SEVERITY	RPN	OCURRENCE					SEVERITY	RPN	OCURRENCE				
		1	2	3	4	5			1	2	3	4	5			1	2	3	4	5			1	2	3	4	5			1	2	3	4	5
1	1	2	3	4	5	1	2	4	6	8	10	1	3	6	9	12	15	1	4	8	12	16	20	1	5	10	15	20	25					
2	2	4	6	8	10	2	4	8	12	16	20	2	6	12	18	24	30	2	8	16	24	32	40	2	10	20	30	40	50					
3	3	6	9	12	15	3	6	12	18	24	30	3	9	18	27	36	45	3	12	24	36	48	60	3	15	30	45	60	75					
4	4	8	12	16	20	4	8	16	24	32	40	4	12	24	36	48	60	4	16	32	48	64	80	4	20	40	60	80	100					
5	5	10	15	20	25	5	10	20	30	40	50	5	15	30	45	60	75	5	20	40	60	80	100	5	25	50	75	100	125					

Figure 37. Sensitivity Analysis with three variables.

3.4.6 3D Risk Matrix

The 3D risk matrix developed in this study aims to analyse the criticality of failures looking at the risk severity, occurrence and detection ratings at the same time. The 3D risk matrix shows a clear different between failures of the four most critical assemblies: frequency converter, gearbox, pitch system and yaw system. Figure 38 shows an example of the RPN values of one assembly in a 3D graph. RPN values toward the top part of the 3D graph mean that the failures tend to be hidden or undetectable failures. It is possible to see that the frequency converter has value mostly in the top part. The gearbox and the yaw system values tend to be concentrated in the RPN centre, and the yaw system has one value highly undetectable but with very low consequence.

The analysis also delivers the most critical failures per assembly and their number of occurrence. The RPN values are also counted in each 3D matrix.

Assembly: Pitch System

Number of components: 17

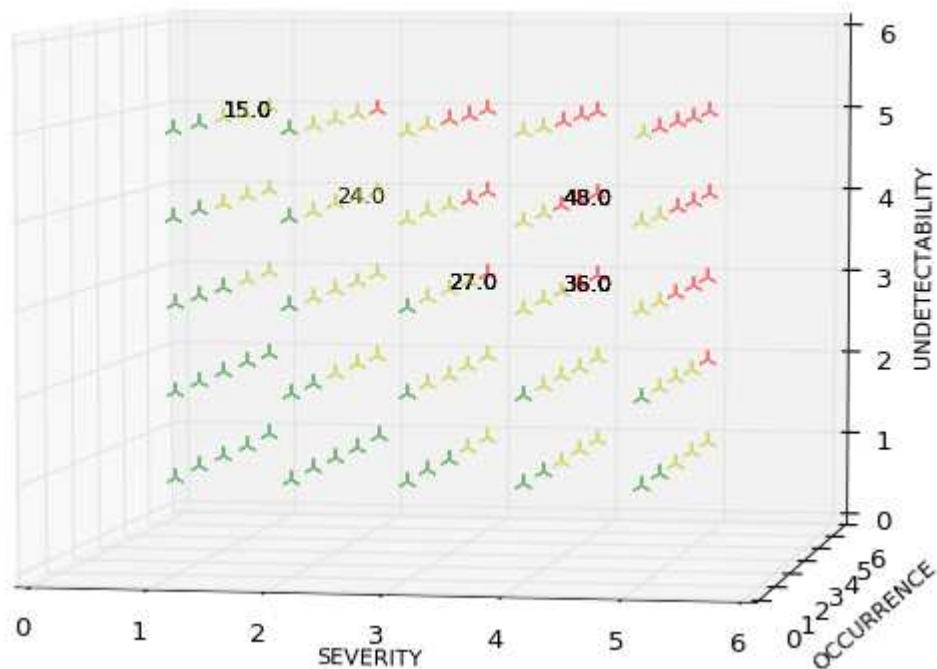


Figure 38. Example of a 3D risk matrix of critical assemblies.

3.4.7 FMEA comparison with European projects

Figure 39 shows a comparison of the failure contribution of each assembly obtained with the FMEA and the average failure rates of onshore wind turbines regarding the WSD, WSDK and LWK databases. Those assemblies with a failure contribution greater than 6% have also the greatest failure rates in the databases. By contrast with the number of failure per components of the gearbox and frequency converter, in this case gearbox has lower value of failure rate than the frequency converter, showing that in an onshore situation the components of the gearbox are more reliable than the components of the frequency converter despite the larger number of failure modes per component.

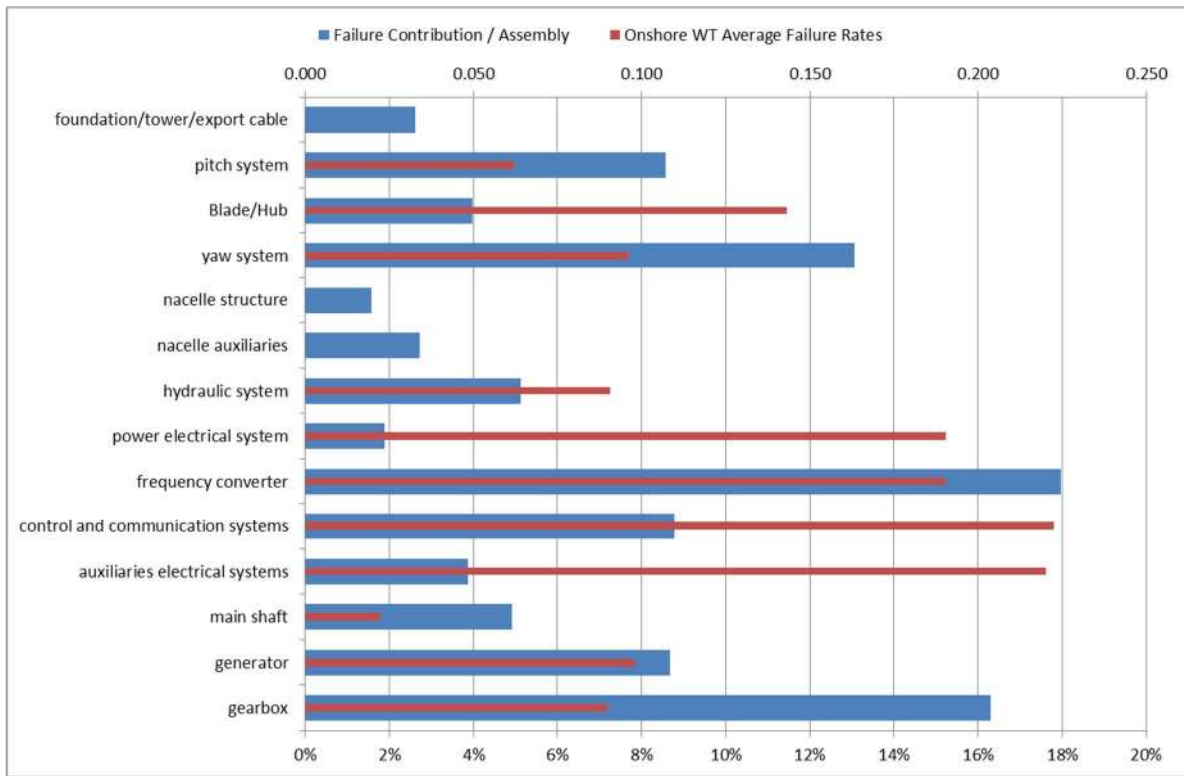


Figure 39. Failure contribution and onshore wind turbine failure rates.

Table 29, Figure 40 and Figure 41 are created to compare the FMEA outputs with the ReliaWind project outcomes. Table 29 shows the approximated values of failure rate and downtime in days of WMEP, LWKF and the Swedish surveys and, the average occurrence and severity rating values assigned. In order to be able to compare the outcomes of the FMEA and the old surveys it was necessary to group the assemblies as it is shown in the table.

Table 29. Comparison with an available database of failure rates(failures/turbine/year)and downtime (days) of onshore WT.

Assembly	WMEP Failure rate 1993-2006	LWKF Failure rate 1993-2006	Swedish Survey Failure rate 1997-2005	WMEP Downtime 1993-2007	LWKF Downtime 1993-2007	Swedish Survey Downtime 1997-2006	FMEA Av. Occurrence /10	FMEA Av. Severity	FMEA assemblies
Electrical system	0.55	0.35	0.10	5.5	1.4	4.5	0.29	3.20	Power electrical system and frequency converter
Electrical control	0.45	0.25	0.05	1.8	1.7	7.8	0.00		Control and communication system
Other	0.25	0.4	0.1	2.6	5.5	2.0	0.29	4.00	Auxiliary electrical system, nacelle auxiliaries, nacelle structure, Foundation & Tower & Cable
Hydraulic system	0.25	0.15	0.05	2.8	1.2	1.8	0.00		Hydraulic system
Yaw system	0.2	0.15	0.05	2.9	2.5	10.9	0.22	3.55	Yaw system
Rotor Hub	0.2	0.1	0	6.9	3.9	0.7	0.00		Hub and pitch system
Mechanical brake	0.15	0.05	0	2.5	3.0	5.2	0.30	4.00	Mechanical brake
Rotor Blades	0.1	0.25	0.04	11.4	3.2	16.0	0.30		Rotor Blades
Gearbox	0.1	0.15	0.05	14.1	6.2	10.7	0.29	3.20	Gearbox
Generator	0.1	0.16	0.02	2.6	5.8	8.9	0.27	2.95	Generator
Drive train	0.05	0.05	0.01	10.7	6.0	12.1	0.22	3.44	High and low speed shaft plus sensors

In order to compare the results of the FMEA and the failure information available in databases shown in table 29, the original graphs are combined in figure 41. Figure 40 is the original graph showing the results of WMEP and LWKF. Here is possible to appreciate that electrical system and control systems have the highest values of annual failure rates and, rotor blades and gearbox represent one of the highest downtime in days of the surveys.

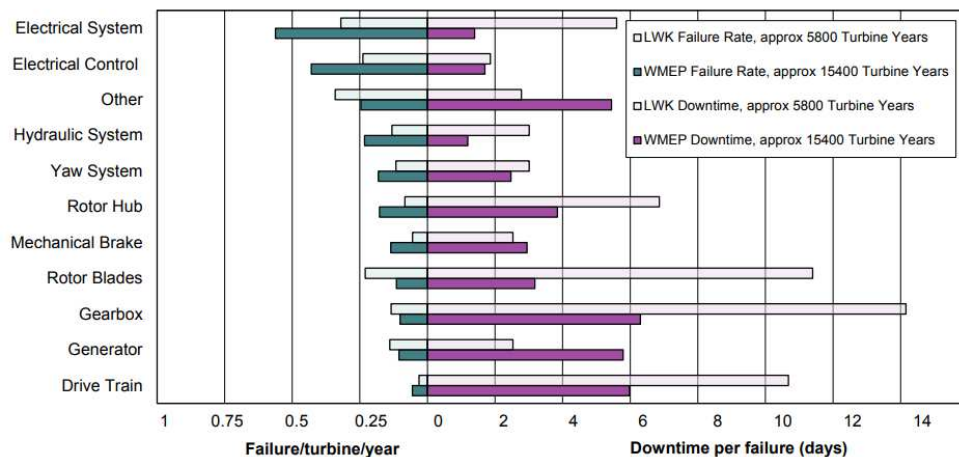


Figure 40. Annual failure frequency and downtime per failure of WMEP, LWKF and Swedish survey.

Figure 41 aims to reproduce the original graph in Figure 40 along with the FMEA outputs. The identified assemblies with highest average values of occurrence rating that vary from 1 to 5 are rotor hub and mechanical brake. On the other hand, the assemblies with highest average values of severity rating are drive train and mechanical brake. To represent in a better way the results of the FMEA, only those components with a significant impact on the turbine performance have been selected. Regarding the Severity rating, values related to “marginal”, “critical” and “catastrophic” represent the significant degradation of performance, equipment damage and destructive failure.

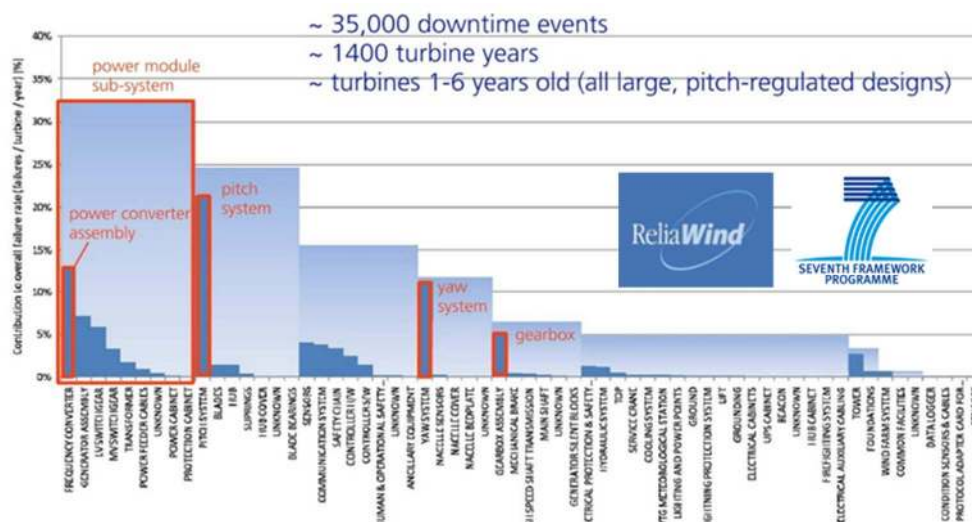
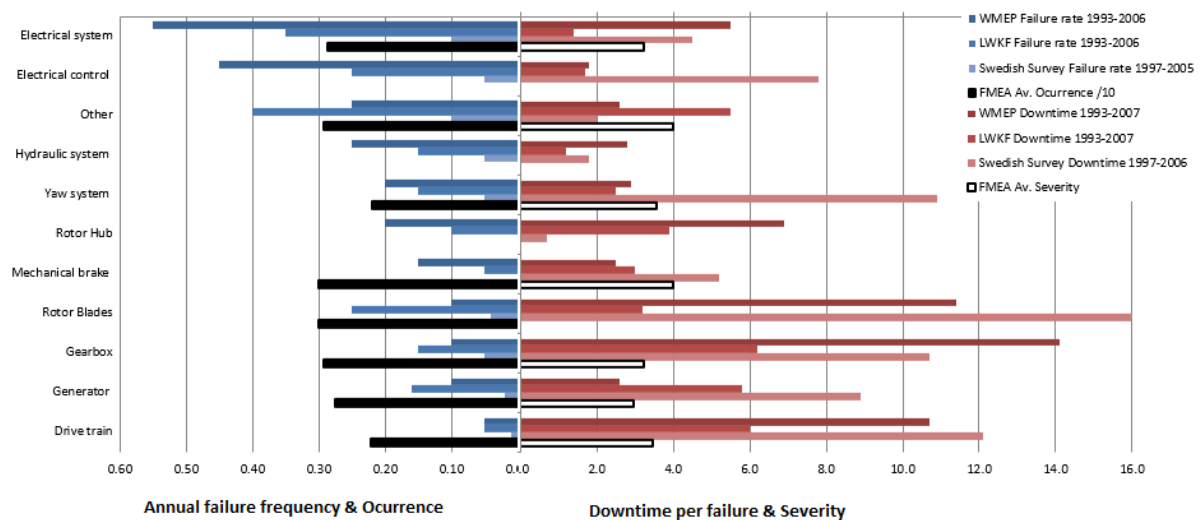


Figure 41. Comparison of occurrence and severity values of the FMEA and the Annual failure frequency and downtime per failure of WMEP, LWKF, Swedish survey and ReliaWind technical report [85].

It is possible to see in Figure 41 that both studies, the FMEA (in red) and the data in WMEP, LWKF and Swedish survey, match with the four most critical assemblies.

3.5 Confidence of the Accuracy of the Assigned Ratings (CAAR)

In order to enable continuous improvement, to ensure consistency and to incorporate new information, a structured audit approach and index have been developed; [Confidence of the Accuracy of the Assigned Ratings \(CAAR\)](#). The main aim of the CAAR index is to answer the question of how confident the analyst of the FMEA is. The main purpose is to standardise the confidence level of the accuracy of the assigned ratings of severity, occurrence and detection for each component and assembly. CAAR index is also a data control strategy registering the type of data source used in each evaluation for each component. The confidence level assessment is based on the availability of the following information and is assessed at the component level. The type of data used in the FMEA is categorised as follows:

- Numerical raw data: quantitative information coming from a data system such as SCADA data.
- Expert review: subject matter expert review of the FMEA spreadsheet in a particular assembly.
- Theoretical data: information available in the literature review with outputs based on theory.
- Analyst judgement: non-expert opinion.

To define criteria on which the confidence can be assessed, it is performed a goal sketching technique, goal decomposition graph, which helps to identify main goals and its sub goal to reach it. The figure below shows a goal decomposition graph where the main goal is to obtain a good accuracy of the assigned ratings of severity, occurrence and detection for each failure mode [88] [82]. In this graph, the main goal can be reached using the analyst judgment (sub-goal) or using expert opinions (sub-goal). The green circle represents that the sub-goal is enough to reach the main goal; in this case, the expert opinion will satisfy the condition to be very confident of the FMEA conclusions. Likewise, the sub-goal “analyst judgement” is divided into two sub-goals: analyst judgement using raw numerical data; and analyst judgement using theoretical data.

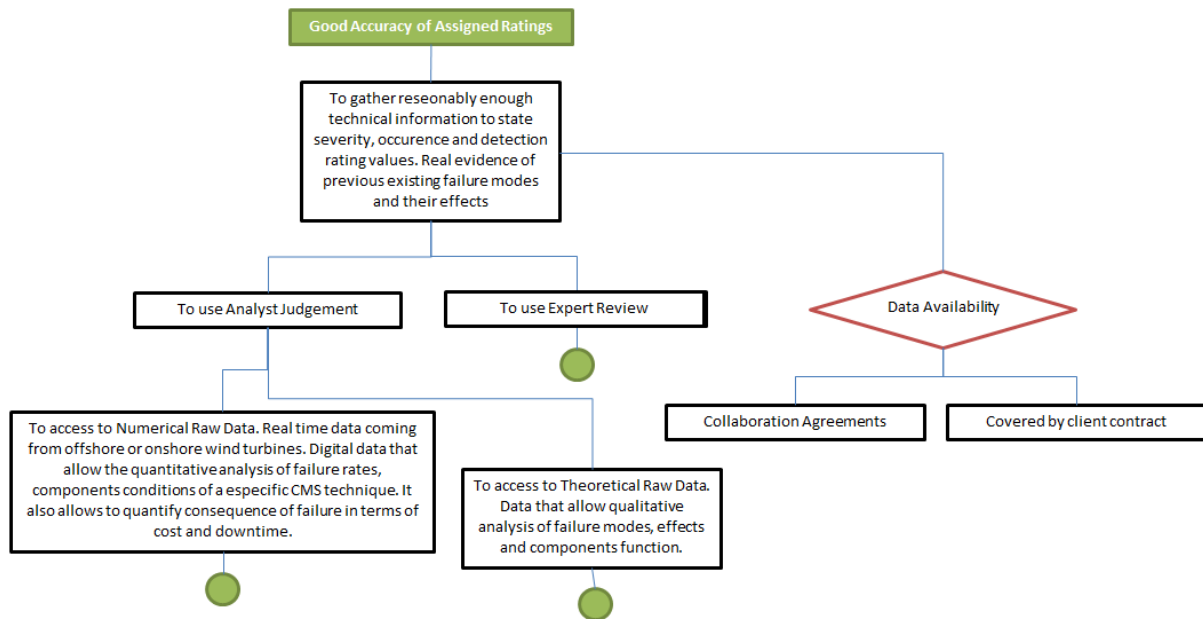


Figure 42. Goal decomposition graph

From the goal decomposition graph, it is clear that there five options to comply with the main goal with different percentages of confidence.

- Numerical raw data (100% Confident)
- Expert review (90% Confident)
- Theoretical data (70% Confident)
- Analyst judgement only (20% Confident)
- No data at all (0% Confident)

To quantify and standardise the confidence level, a flow chart is developed, Figure 43. It is also considered that for all of the options above there are uncertainties associated with processes and different criteria, therefore, “assumptions” is defined as a confidence factor which describes “the confidence that the assumption is sound”. This confidence factor is used in the flow chart shown in Figure 43 and described in Table 30.

Table 30. Confidence factor.

Assumption Level (AL)	Description	multiply by
1	Low Confidence	0.8
2	Moderate Confidence	0.9
3	High Confidence	1

The algorithm described in the flow chart assigns percentages regarding the information availability and the level of assumptions performing the sub-goal to reach the main goal. The final percentage is multiplied by the assumption level (AL) so the CAAR is calculated by:
 $CAAR = \% * AL$.

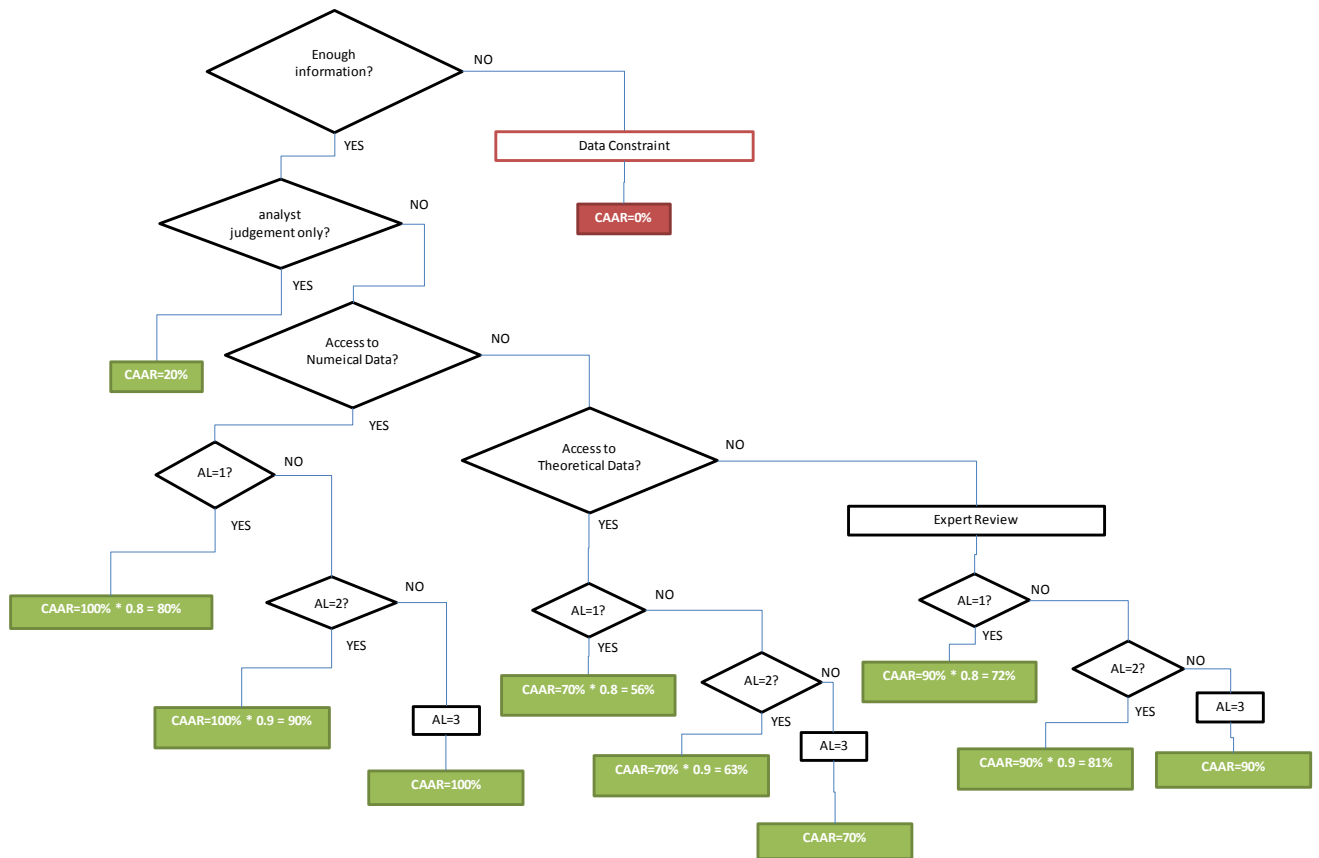


Figure 43. CAAR Flow chart.

All the possible results of the CAAR flow chart are summarised in Table 31. There are three ranges A, B and C with different colours. RPNs in the Range C are considered with a high level of confidence in the accuracy of the assigned ratings. RPNs in Range A and B need to be reviewed further to improve accuracy based on more information.

Table 31. CAAR percentages

	Value	CAAR	Description
A	1	0%	No information at all.
	2	20%	based on analyst judgement only
	3	56%	using theoretical data with low assumption confidence
B	4	63%	using theoretical data with moderate assumption confidence
	5	70%	using theoretical data with high assumption confidence
	6	72%	based on expert judgement with low assumption confidence
C	7	80%	using numerical data with low assumption confidence
	8	81%	based on expert judgement with moderate assumption confidence
	9	90%	using numerical data with moderate assumption confidence or expert judgement high assumption confidence
	10	100%	using numerical data with high assumption confidence

Table 32 shows the result of the CAAR analysis. There are 5 assemblies above 80% of confidence in the accuracy of the conclusions using the data available for this study. This means that the rest of assemblies need to be refined with more information or expert opinions.

Table 32. Average CAAR per assembly

Assembly	Average CAAR
nacelle structure	63%
power electrical system	81%
nacelle auxiliaries	78%
foundation/transition piece/tower/cable	81%
auxiliaries electrical systems	81%
Blade/Hub	63%
main shaft	77%
hydraulic system	77%
pitch system	79%
generator	80%
control and communication systems	79%
yaw system	73%
gearbox	81%
frequency converter	81%

3.6 Conclusion

A risk assessment of an offshore wind turbine is crucial to generate a database of turbine failure rates, failure modes and causes. It is a common tool in the industry to establish inspections intervals. The FMEA tool has been the foundation of this work identifying critical assemblies in terms of operation and consequences of failure. A comprehensive analysis and methodology are proposed to explore the reliability of the components. The definition of the taxonomy of the wind turbine has been essential for the development of this FMEA and to

establish the interfunctional relationship between components. Based on the European project ReliaWind, a comprehensive turbine breakdown was proposed using a hierarchical structure.

The RPN has been developed using three ratings: severity, occurrence and detectability of the failure. The detectability dimension of the analysis allows to explore areas of the condition monitoring system and to identify the type of failures that are difficult to detect.

The FMEA results are the basis for the physics-based and data mining models as well as for the O&M optimisation allowing the determination of consequential damage and local and global effects of failures. Gearbox, pitch system, yaw system and power converter have been identified as the most critical assemblies in the FMEA.

CHAPTER 4 – FAILURE PROGNOSIS BASED ON PHYSICS-BASED MODELS

The critical assemblies identified in the previous chapter, power converter and gearbox, are analysed using physics-based models of the main failure mechanisms. This chapter describes the process and the main assumptions and outputs.

4.1 Introduction

This chapter describes the methodology developed to estimate accumulated damage of critical components. Section 4.2 presents a method to generate future data to estimate the remaining useful life of a particular component of a wind turbine in a particular location. The prognosis process comprises the digital representation of the turbine Siemens SWT3.6-120 and Monte Carlo Markov Chain (MCMC) Simulations. Sections 4.3 and 4.4 present the physics-based model approaches for the gearbox and power converter.

The power converter and gearbox have been identified in the FMEA as one of the most critical assemblies regarding risk to the turbine operation. A method to estimate the remaining useful life (RUL) of a fully-rated power converter and a gearbox in a variable speed wind turbine is proposed.

There are two main sources of data used in the physics-based models are:

- SCADA data commonly available for offshore wind farm operators. This historical data is used to estimate the accumulated damage. This is called “diagnostic model” in Figure 50.
- Wind turbine simulation (FASTv8). These outputs are used to predict damage in the future and the RUL for a particular assembly in a specific location. This is called “prognostic model” in Figure 50.

4.2 Prediction methodology

In order to assess the accumulation of damage within the power converter and gearbox, it is necessary to realistically emulate the same operational conditions in terms of turbine structural and electro-mechanical behaviour, and wind profile. The digital representation of the offshore wind turbine and operation conditions are developed using the aero-hydro-servo-elastic simulator FASTv8 developed by National Renewable Energy Laboratory (NREL). The methodology proposed to create variables in the future for failure prognosis uses a Monte Carlo Markov Chain technique.

4.2.1 Wind Turbine dynamic integrated system in FASTv8

To achieve realistic results, load cases proposed by the IEC 61400-3 (power production category) using FASTv8, are used. The standard proposes some design situations representing the various modes of operation that an offshore wind turbine would experience during its operational life; each design situation leads to a number of Design Load Cases (DLCs). The IEC standard distinguishes two types of load cases, ultimate and fatigue load cases and recommends appropriate load factors to be associated with these load cases to evaluate the structural integrity. The selected load cases are shown in Table 33. A turbulent full-field wind matrix is created by TurbSim [89] [83] as an input to FASTv8.

The analysis is based on the three-bladed horizontal 3.6MW turbine model, variable speed control system, mounted on a monopile with a rigid foundation, induction generator, 3 stage gearbox and fully power converter. Wind condition is site-specific.

Table 33. Design load cases. NTM (Normal turbulence model), NWP (Normal wind profile model), NWLR (Normal Water Level Range), COD (Co-Directional), MUL (Multidirectional)

Design situation	DLC	Wind condition	Waves	Wind and wave directionality	Sea currents	Water level	Other conditions	Type of analysis	Partial safety factor
Power production	1.2	NTM $V_{in} < V_{hub} < V_{out}$	NSS joint probability distribution of H_s, T_p, V_{hub}	COD, MUL	No currents	NWLR or >MSL		F	*
Power production plus occurrence of fault	2.4	NTM $V_{in} < V_{hub} < V_{out}$	NSS $H_s = E[H_s V_{hub}]$	COD, MUL	No currents	NWLR or >MSL	Control, protection, or electrical system faults including loss of electrical network	F	*
Start up	3.1	NWP $V_{in} < V_{hub} < V_{out}$	NSS (or NWH) $H_s = E[H_s V_{hub}]$	COD, MUL	No currents	NWLR or >MSL		F	*
Normal shut down	4.1	NWP $V_{in} < V_{hub} < V_{out}$	NSS (or NWH) $H_s = E[H_s V_{hub}]$	COD, MUL	No currents	NWLR or >MSL		F	*
Parked (standing still or idling)	6.4	NTM $V_{in} < 0.7V_{ref}$	NSS joint probability distribution of H_s, T_p, V_{hub}	COD, MUL	No currents	NWLR or >MSL		F	*
Parked and fault conditions	7.2	NTM $V_{in} < 0.7V_1$	NSS joint probability distribution of H_s, T_p, V_{hub}	COD, MUL	No currents	NWLR or >MSL		F	*
Transport, assembly, maintenance and repair	8.3	NTM $V_{in} < 0.7V_{ref}$	NSS joint probability distribution of H_s, T_p, V_{hub}	COD, MUL	No currents	NWLR or >MSL	No grid during installation period	F	*

In this design situation DLC 1.2, a wind turbine is running and connected to the electric load. DLC 1.2 represents the requirements for loads resulting from the atmospheric turbulence that occurs during normal operation of a wind turbine throughout its lifetime (NTM). DLC 2.4 describes a transient event triggered by a fault or the loss of an electrical network connection while the turbine is producing power. DLC 3.1 includes all the events resulting in loads on a wind turbine during the transients from any standstill or idling situation to power production. DLC 6.4 comprises a number of hours of non-power production time at a fluctuating load appropriate for each wind speed where significant fatigue damage can occur to any components. Finally, DLC 7.2 considers deviations from the normal behaviour of a parked wind turbine, resulting from faults on the electrical network or in the wind turbine [90] [84].

The range of wind speeds may be represented by a set of discrete values, in which case the resolution shall be sufficient to assure the accuracy of the calculation. In general, a resolution of 2 m/s is considered sufficient. Therefore taking into account the cut-in and cut-out wind speeds [81] [75], the wind speeds bin are:

$$V_{in} = 5 \text{ (m/s)}$$

$$V_{out} = 25 \text{ (m/s)}$$

Wind speeds (m/s) to the model are 11 bins:

5	7	9	11	13	15	17	19	21	23	25
---	---	---	----	----	----	----	----	----	----	----

Normal turbulence model (NTM)

For NTM, the representative value of the turbulence standard deviation, σ_1 , shall be given by the 90 % quantile for the given hub height wind speed. This value for the standard wind turbine classes in Table 34, is being given by:

$$\sigma_1 = I_{ref}(0.75V_{hub} + b); b = 5.6\left(\frac{m}{s}\right)$$

Where V_{hub} is the wind speed at the hub height. I_{ref} is the expected value of hub-height turbulence intensity at a 10 min average wind speed. V_{ref} is the reference wind speed average over 10min. A, B and C designate the category for higher, medium and lower turbulence characteristics. I_{ref} is the expected value of the turbulence intensity at 15 m/s.

Table 34. Wind turbine classes [90] [84].

Wind turbine class		I	II	III	S
V_{ref}	(m/s)	50	42,5	37,5	Values specified by the designer
A	I_{ref} (-)	0,16			
B	I_{ref} (-)	0,14			
C	I_{ref} (-)	0,12			

Values for the turbulence standard deviation σ_1 and the turbulence intensity hub σ_1/V_{hub} are shown in Figure 44 and Figure 45. Values for I_{ref} are given in Table 34.

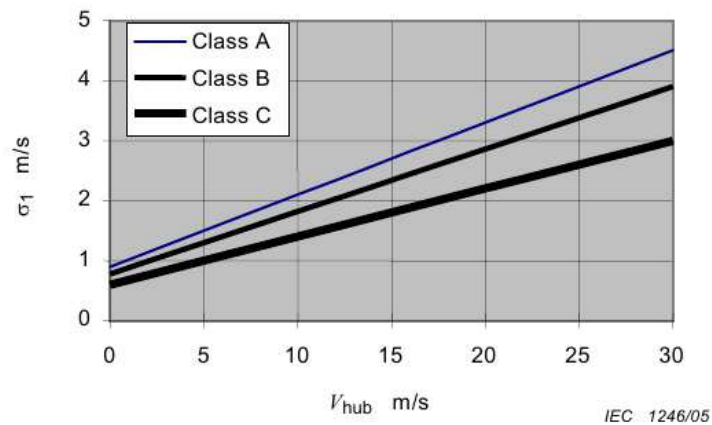


Figure 44. Normal Turbulence Model (NTM): Turbulence standard deviation [91].

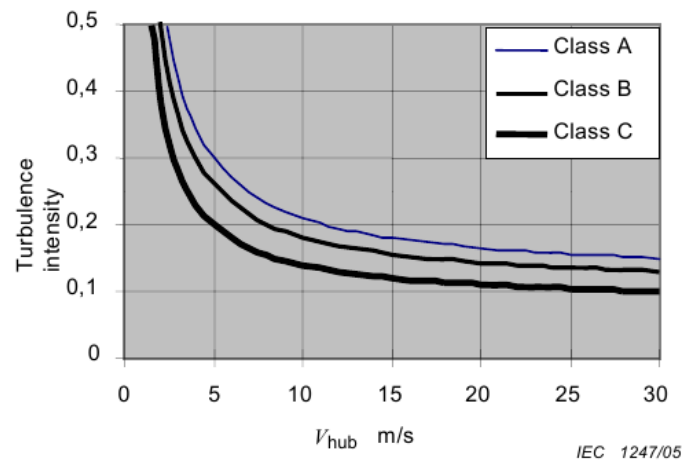


Figure 45. Normal Turbulence Model (NTM): Turbulence intensity [91].

FASTv8 can create a full-field, turbulent-wind simulation. A time series of three-component wind-speed vectors at points in a two-dimensional vertical rectangular grid that is fixed in space is created to represent operational conditions, see Figure 46 [89] [83].

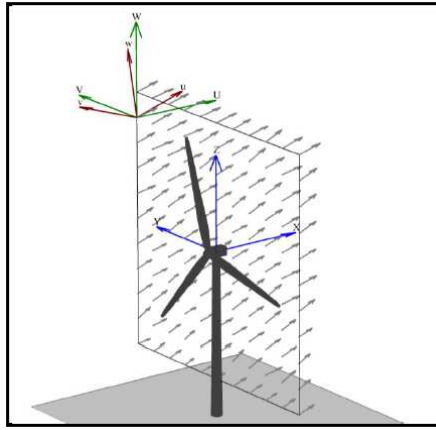


Figure 46. Wind field using FASTv8 pre-processor TurbSim [91].

The detailed explanation of FASTv8 pre-processors is given in **Annex 2: FASTv8 pre-processors**.

FASTv8 outputs

FASTv8 is able to deliver many types of variables from mechanical and structural parameters to electrical variables. For the estimation of the remaining useful life of the gearbox and power converter, the variables power output, low-speed shaft torque, low and high-speed shaft rotational speeds, generator current and generator voltages are selected.

The load case DLC 1.2 represents most of the situations of the turbine operational conditions. Simulations are categorised by Wind speed [m/s], Turbulence intensity [%], Significant Wave Height [m], Wave spectral period [s], Yaw error [deg], and Turbulent wind speed.

For DLC 1.2 there are 66 simulations of 620 second each. For each wind speed, there are six simulations for three different yaw errors (-8, 0, 8 degrees) with two turbulent wind seeds. An example of the outputs is given in Table 35.

Table 35. Example of FASTv8 outputs

DLC	Wind Speed (m/s)	Turbulence Intensity (%)	Significant Wave Height (m)	Wave Spectral Period (s)	Yaw Error (deg)	Seed	Simulated Time (s)	Outputs Variables	Probability of Occurrence derived from SCADA data	Simulation ID
1.2	4	I4	Hs4	Tp4	8	1	620	RotSpeed GenSpeed GenPwr GenTq RotorTq	X%	S1
1.2	4	I4	Hs4	Tp4	8	2	620	RotSpeed GenSpeed GenPwr GenTq RotorTq	X%	S2
1.2	4	I4	Hs4	Tp4	0	3	620	Y%	S3
1.2	4	I4	Hs4	Tp4	0	4	620	Y%	S4
1.2	4	I4	Hs4	Tp4	-8	5	620	Z%	S5
1.2	4	I4	Hs4	Tp4	-8	6	620	Z%	S6
1.2	6
.....	6
.....
1.2	24	I24	Hs24	Tp24	8	1	620	A%	S50
1.2	24	I24	Hs24	Tp24	8	2	620	A%	S51
.....

4.2.2 Generation of future events for failure prognosis

After the simulation of FASTv8, it is necessary to establish a methodology to create a future time series of variables to estimate RUL of the components. This innovative approach starts with the assumption that not all the simulated load cases in Table 33, wind speeds and random seeds are experienced by the turbine in 1-year period. Therefore, it is necessary to derive statistical (probabilities of occurrence) information of load cases and wind speeds from the SCADA data. A decision tree is proposed to filter and identify load cases, wind speeds and turbine operational conditions in the data set. Thus, the probability of each simulation output of FASTv8 is determined and added to Table 35, in red. These probabilities are the input for the Markov Chain Monte Carlo (MCMC) tool to create a random sequence of variables and their respective simulated time until a future year is created.

MCMC tool is selected assuming stationary transition probabilities. A sequence of random elements of some set, such as wind speeds or load cases, can be defined by MCMC if the conditional distribution X_{n+1} given X_1, X_2, \dots, X_n depends on X_n only [92] [85]. Figure 47 shows an example of a transition graph and transition matrix of a discrete MCMC where each event

in the sequence only depends only on the events occurring directly before. For instance, when the current state is load case 1 (LC1), there is a probability of 0.6 to move to LC2, then there is a probability of 0.3 to stay in LC2, a probability of 0.1 to go back to LC1, a probability of 0.4 to move to LC3 and so on. Therefore, it is possible to generate future scenarios of variables by applying MCMC with probabilities distribution of load cases and wind speeds, Figure 48.

The simulation of each load case in FASTv8 gives the same outputs in the time domain which are related to structural loading, bending moments, and operation parameters such as rotational speed, wind speed and direction, shaft torques and power output. These FAST outputs are the inputs for the physics-based models of the gearbox and power converter.

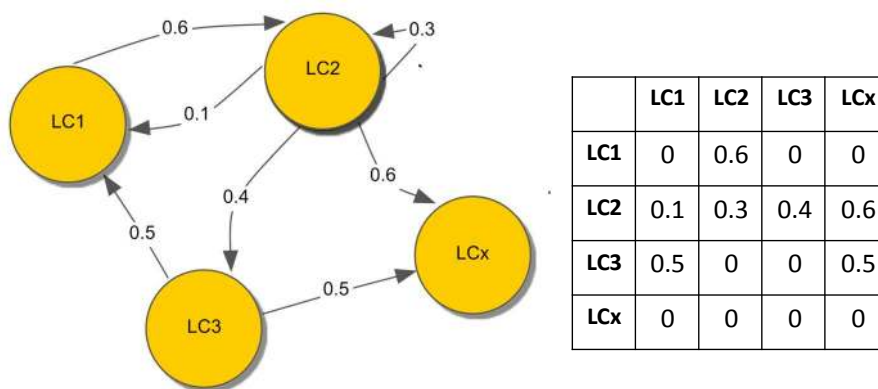


Figure 47. Discrete example of MCMC, transition graph and matrix.

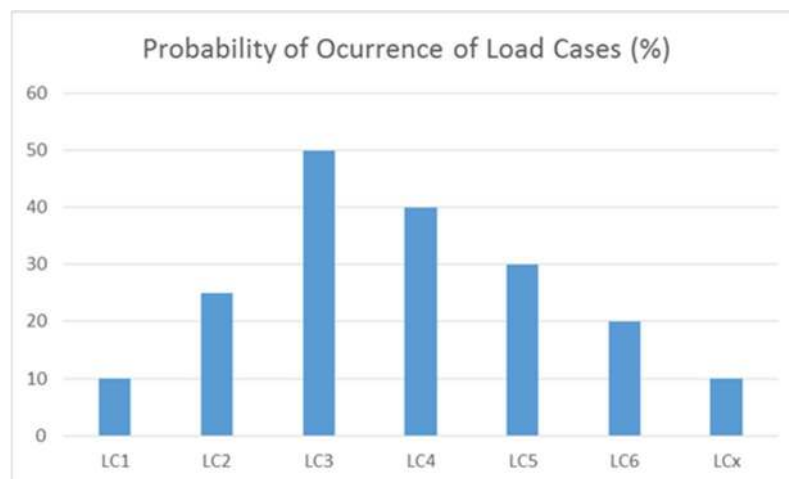


Figure 48. Example of the probability distribution of load cases.

The IEC standard suggests simulation time for each load case (620 seconds with a resolution of 0.05 seconds), these time periods are concatenated in order to generate the whole period (1 year) in the future for prediction purposes. Figure 49 shows an example of a future scenario

of variables such as torque, rotational speed and power output, to be used in the failure prognosis process.

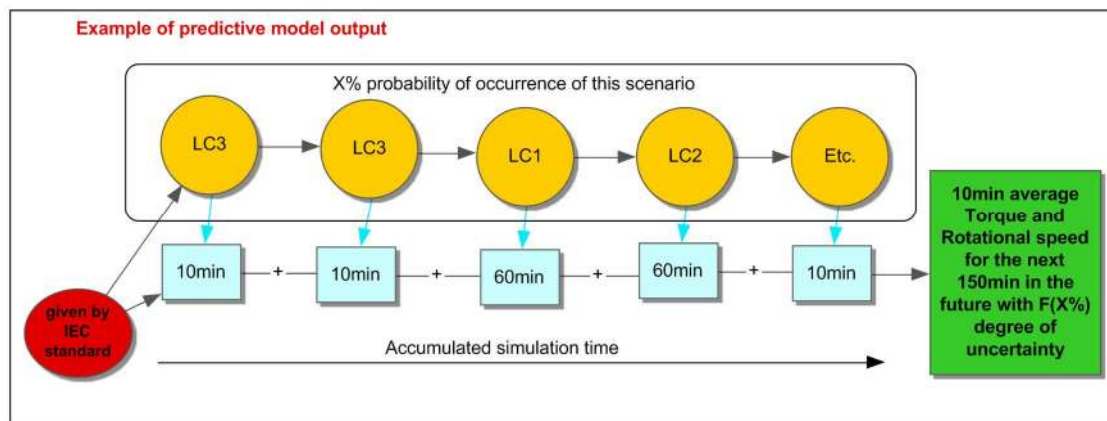


Figure 49. Example of future scenario generation.

4.3 Gearbox physics-model

Figure 50 shows the approach outline for the gearbox. The diagnostic models using historical SCADA data and the predictive model using FASTv8 simulations. Both models will create a load spectrum and result in accumulated damage. The physics-based model of the gearbox is developed in the proprietary software KISSsoft, explained in the next sections.

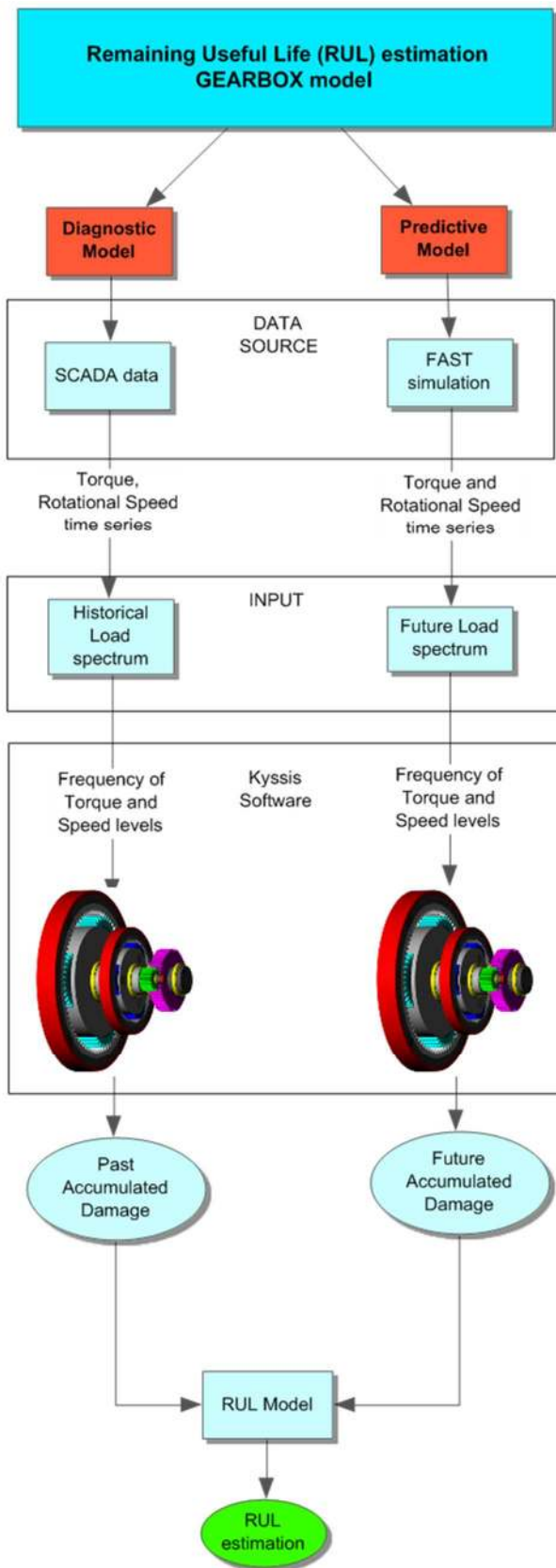


Figure 50. Block diagram of RUL estimation.

4.3.1 Gearbox failure investigation

The complexity of failure interaction is extensively reviewed in the fields of WT reliability. The author in [93], describes three types of failure interactions: first, failure of a component results in the total failures of all other components; second, failure of component 1 increases the failure rate of component 2 and; third, a system can presents a combination of the option 1 and 2. In this study, the overall condition is represented by the failure with the known highest failure rate. A probabilistic approach is proposed in [94], where a Bayesian Network (BN) is used to represent the conditional dependency between failure root causes.

The gearbox to be modelled consists of three stages: two planetary and one parallel stage with helical gears. The load spectrum for failure diagnosis to estimate the current damage and the load spectrum for failure prognosis to estimate the Remaining Useful Life (RUL) are obtained through historical SCADA data and FASTv8 simulation outputs, respectively.

A vulnerability map of the gearbox has been generated to focus the computational efforts on the weakest gearbox parts which represent the health of the assembly. The fatigue damage is estimated by counting load cycles in bearings and gears in conjunction with material S-N curves. The load cycles accumulated in the future for prognosis purposes are estimated using a representative one-year load spectrum based on outputs from FAST simulations of the fatigue load cases described in IEC 61400-1/3.

A gearbox failure investigation was performed to identify the main sources of stress and vulnerable components. The author in [31] presents a detailed analysis of the design of a high-speed gearbox for a 5MW baseline offshore wind turbine. Wind turbine technical specification, environmental conditions, and load response analysis are considered to define the vulnerability map of a 3-stage gearbox; two planetary stages and one parallel stage, in Figure 51. High-Speed Shaft (HSS) bearings, second stage planet bearings, Low-Speed Shaft (LSS) sun gear and third stage gears are the most critical components in term of fatigue damage. The analysed gearbox has an input shaft speed of 12.1 (rpm), and the ratios for this gearbox are given in Table 36. Failure investigation shows that the high-speed shaft bearings are one of the gearbox components with a higher probability of fatigue damage.

Table 36. Gearbox speed ratios [31].

	Ratio
First stage	1:3.94
Second stage	1:6.16
Third stage	1:3.95

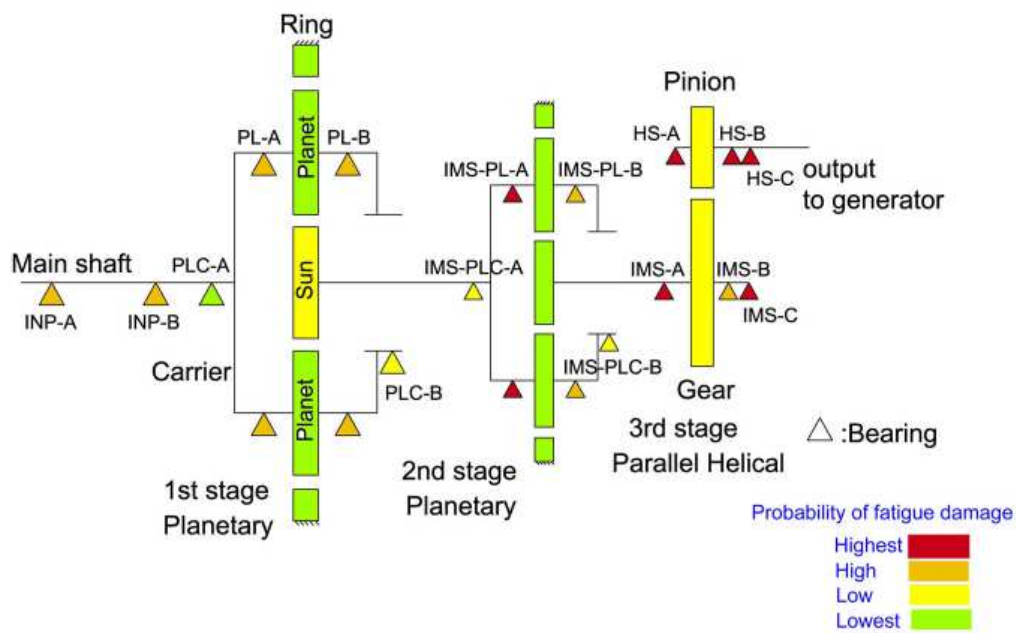


Figure 51. Vulnerability map of a 5MW 3-stage gearbox [31] [31].

Gearbox failure modes and causes are described in [95] [86]. The presence of foreign objects and manufacturing defects are identified as common failure causes. The author in [96] [87] states gearboxes have historically experienced failures in both planet and HSS bearings. The HSS bearings can be replaced on site. However, planet bearings failures require the removal of the gearbox for it to be repaired at the port. For that reason, the gearbox represents 25% of the maintenance cost.

A comparative study between a 2MW 3-stage gearbox prototype and gearbox model was performed in [97] [88]. The results of the tooth root stress for both analyses show the highest values for contact and pitting stress are experienced in the HSS.

In terms of consequences of failure related to the gearbox, the study in [35] [35] found that the HSS bearings and the 2 stage shaft and bearing failures could account for more than 50% of the total gearbox failure cost; see Table 37.

This gearbox vulnerability map ranks the gearbox components from highest to lowest fatigue damage. The gearbox vulnerability map and, conclusions of the literature review allow the most critical components within the gearbox to be identified: the high-speed shaft and second stage bearings and the sun gear of the first stage and the parallel gears of the high-speed shaft.

Table 37. Gearbox failure cost share.

Failure Mode	Share of total failure costs (%)
High-speed shaft bearing failure	27.8
Broken intermediate shaft	21.2
Intermediate shaft bearing failure	10.1
Planet bearing failure	9.6
Broken center post	6.2
High-speed shaft bearing black spot	5.4
Sun gear – broken teeth	5.3
Low-speed shaft bearing failure	5.0
Intermediate shaft bearing failure	4.8
High-speed shaft grinding temper failure	2.3
Broken low-speed wheel	1.2
Oil pump failure	0.8
Intermediate shaft splash plate failure	0.2

4.3.2 Physics-based model of the gearbox

The gears, bearings, and shafts follow the design standard IEC 61400-4 described in [98] [89]. The general gearbox specifications are given in Table 38. The design lifetime is calculated, assuming that the turbine will be operating 60% of the time; it will have a capacity factor of 60%. Damage accumulation is calculated using the respective S-N curves for all mechanical elements and each step of the load spectrum. The damage is accumulated continually and transformed into a lifetime at the end of the analysis. The analysis of the gears is according to DIN, ISO or AGMA standards, the analysis of the bearings according to standard L10 calculation or DIN/ISO 281 [15].

Table 38. 3.6MW Gearbox specification

Parameter	Value
Type	Two planetary, one parallel
Total ratio	1-119
First stage ratio	1-4.9
Second stage ratio	1-5
Third stage ratio	1-4.857
Designed power (MW)	4
Rated input shaft speed (rpm)	13.4
Rated output shaft speed (rpm)	1600
Rated input shaft torque (kNm)	2934
Rated output shaft torque (kNm)	33
System efficiency	0.96
Design Lifetime (hrs) (24x365x20 years)x60%	105120

Torque and shaft diameters are calculated as follows [99] [90]: OWT with an electrical generator of 3.600 kW of power output. The low-speed shaft (LSS) rotates at 12 rpm, and the high-speed shaft (HSS) rotates at 1600 rpm. Maximum stress recommended for solid steel shafts available is 55MPa [12]. The gearbox efficiency at rated power is 0.94, and generator efficiency at rated power is 0.93. Using the terminology described in table 39, the rotational speed (angular velocity) is calculated:

$$w_{LSS} = \frac{2\pi(12)}{60} = 1.256 \text{ rad/sec} \quad (1)$$

$$w_{HSS} = \frac{2\pi(1600)}{60} = 167.46 \text{ rad/sec} \quad (2)$$

Power is calculated:

$$P_{HSS} = \frac{3600}{0.93} = 3870 \text{ KW} \quad (3)$$

$$P_{LSS} = \frac{3870}{0.94} = 4118 \text{ KW} \quad (4)$$

Torque is calculated:

$$T_{HSS} = \frac{P_{HSS}}{w_{HSS}} = \frac{3870 \text{ KW}}{167.46 \text{ rad/sec}} = 23.11 \text{ KNm/rad} \quad (5)$$

$$T_{LSS} = \frac{P_{LSS}}{w_{LSS}} = \frac{4118 \text{ KW}}{1.256 \text{ rad/sec}} = 3278.7 \text{ KNm/rad} \quad (6)$$

The diameter of the shafts to carry a given torque can be calculated by selecting a maximum shearing stress which will be allowed for a given shaft material. This stress take place at $r=r_0$. Based on [99] , the shearing stress in a solid shaft is given by :

$$f_s = \frac{T_r}{J} \left(\frac{N}{m^2} \right) \quad (7)$$

Where r is the distance from the axis of the shaft to point of maximum shearing stress and, J is the shaft's polar moment of inertia.

$$J = \frac{\pi r_0^4}{2} (m^4) \quad (8)$$

Where r_0 is the shaft radius.

The maximum stress is usually selected with a significant safety factor (x2) for designing purposes. The shaft diameter to bear the maximum stress is given by:

$$D_{HSS} = 2r = 2^3 \sqrt{\frac{2T_{HSS}}{\pi f_s}} = 2^3 \sqrt{\frac{2 \times 23110 \text{ Nm/rad}}{3.14 \times 55 \times 10^6}} = 0.13 \text{ m} \quad (9)$$

$$D_{LSS} = 2r = 2^3 \sqrt{\frac{2T_{LSS}}{\pi f_s}} = 2^3 \sqrt{\frac{2 \times 3278700 \frac{\text{Nm}}{\text{rad}}}{3.14 \times 55 \times 10^6}} \quad (10)$$

$$= 1.498\text{m}$$

Likewise, and based on Lloyd's Register rules for main propulsion shafts, the LSS and HSS are calculated as follows to validate the previous calculations [100] [91]:

$$d_{HSS} = Fk \sqrt[3]{\frac{P_{HSS}}{R_{HSS}} \left(\frac{560}{\sigma_u + 160}\right)} (\text{mm}) \quad (11)$$

$$d_{LSS} = 100k \sqrt[3]{\frac{P_{LSS}}{R_{LSS}} \left(\frac{560}{\sigma_u + 160}\right)} (\text{mm}) \quad (11)$$

Where d_{HSS} and d_{LSS} are the diameter of the high and low speed shaft, respectively, k is equal to 1,22 for a shaft is fitted with a continuous liner and is oil lubricated, σ_u is the specified minimum tensile strength of the shaft material, in N/mm^2 , P is the maximum shaft power in kW and R is the rotational speed in rpm. This equations disregard losses in gearboxes and bearings.

The results are shown in Table 39. Both methods concluded that the LSS diameter should be around 15cm and the LSS should have a diameter between 1.5m and 3m.

The gearbox to be modelled consists of three stages: two planetary and one parallel stage gears. This detailed model of the gearbox is achieved by the use of the proprietary software Kissys [101] [92], see Figure 52.

Table 39. HSS and LSS diameter calculation results.

High-Speed Shaft			
Variable	Value	Unit	Description
F	100		For turbine installation
k	1		Shaft with integral coupling
d	500	N/mm2	Minimum tensile strength with vibratory stresses
P_HSS	3870	KW	Power
R_HSS	1200	rpm	Rotational speed
d_HSS	165.4196	mm	Diameter HSS
d_HSS	16.54196	cm	Diameter HSS
Low-Speed Shaft			
Variable	Value	Unit	Description
F	100		For turbine installation
k	1.22		
d	600	N/mm2	Minimum tensile strength with vibratory stresses
P_LSS	4118	KW	Power
R_LSS	12	rpm	Rotational speed
d_LSS	2887.482	mm	Diameter LSS
d_LSS	288.7482	cm	Diameter LSS

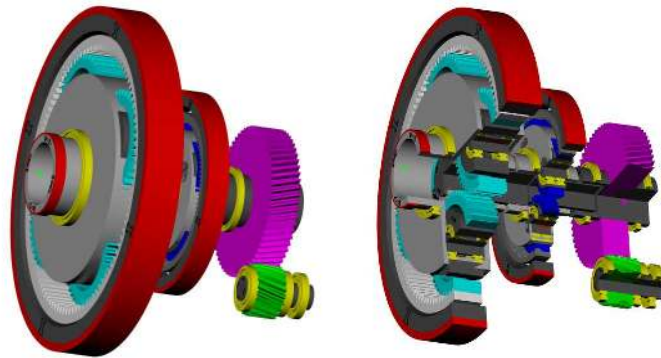


Figure 52. 3D view of Kisssoft gearbox model

There is two parts of the remaining useful life (RUL) model as shown in Figure 50: i) prognostic model using one year historical SCADA data (Table 40) and ii) predictive model using simulations (FASTv8). Both cases will generate a load spectrum of 19 torque bins as an input for the KISSsoft gearbox model defining frequencies (sum of all frequencies = 1), the relative torque and rotational speed.

For each part of the load spectrum, the KISSsoft software calculates the damage for all mechanical elements, using the respective S-N curves. The damage is accumulated continually and being transformed into a lifetime according to DIN, ISO or AGMA standards for gears and according to standard L10 calculation or DIN/ISO 281 for bearings [102] [93]. The RUL of gears is calculated based on the theory that every load cycle produces damage. The amount of damage depends on the stress level, and for lower stress, the damage is considered null. Bending and pitting fatigue life of the gears is an estimate based on the accumulation of discrete damage until failure occurs and using the load spectrum (derived from SCADA and FASTv8 simulations), material fatigue properties given in the KISSsys gearbox model (S-N curves) and the damage accumulation method (Palmgren-Miner rule) described in IEC standards [103] [94].

Table 40. Load spectrum as input for KISSsoft using SCADA data.

Number	Frequency (%)	Speed (rpm)	Power (kW)	Torque (Nm)
1	15	-728	-103	1361
2	4	-762	-217	2723
3	5	-830	-355	4085
4	6	-944	-538	5446
5	6	-989	-705	6808
6	6	-1126	-963	8170
7	5	-1217	-1215	9531
8	5	-1285	-1466	10893
9	4	-1376	-1766	12255
10	4	-1444	-2060	13617
11	3	-1501	-2355	14978
12	2	-1501	-2569	16340
13	2	-1513	-2804	17702
14	2	-1518	-3032	19063
15	2	-1513	-3236	20425
16	2	-1518	-3465	21787
17	2	-1521	-3687	23148
18	3	-1523	-3910	24510
19	2	-1524	-4130	25872

Table 40 shows a load spectrum derived from SCADA of an offshore wind farm in the UK. The rotational speed and torque variation are counted using a rain-flow counting method with 19 bins.

4.3.3 Physics-based model outputs: Gearbox

The most vulnerable components in the gearbox that have been selected for further analysis are the HSS bearings. They are assigned as B1 and B2 in Table 41. The method outlined in ISO 281 for determining the bearing life assumes a constant load. However, methods have been proposed for determining the bearing life when the loading is fluctuating. For example, reference [104] [95] proposes a method for deriving an equivalent mean constant load (from a fluctuating loading). Such a method is incorporated into the proprietary Kissys [14] software. The damage is calculated for each torque bin in Table 40 and then added up to obtain the total damage done in 1 year (historical SCADA data). B1 shows 3.11% of damage or consumed lifetime and, B2 shows 3.45% of damage. Assuming the load spectrum remains similar to the that shown in Table 40, and since the data for this analysis was representative of one year's operation, the remaining useful life for B1 is $100 / 3.11 = 32$ years approximately.

Table 41. Gearbox physics-based model: damage of HSS bearings B1 and B2.

Bin Number	Damage Bearing B1 (%)	Damage Bearing B2 (%)
1	0.30	0.30
2	0.08	0.08
3	0.10	0.10
4	0.12	0.12
5	0.12	0.12
6	0.12	0.12
7	0.10	0.10
8	0.10	0.10
9	0.08	0.08
10	0.08	0.08
11	0.06	0.06
12	0.04	0.04
13	0.04	0.04
14	0.04	0.05
15	0.06	0.07
16	0.07	0.08
17	0.09	0.10
18	0.15	0.18
19	1.36	1.61
Total Damage	3.11(%)	3.45(%)

4.4 Power converter physics-based model

Similar to the methodology proposed for the gearbox, a systematic physics-based method has been proposed to predict the damage accumulation of power converter of offshore wind turbines. The approach was implemented using python codes. The total fatigue life is calculated in two steps shown in Figure 53:

- Historical estimation of pre-existing damage, accumulated during operation (diagnosis model).
- Future estimation of simulated accumulated damage (predictive model).

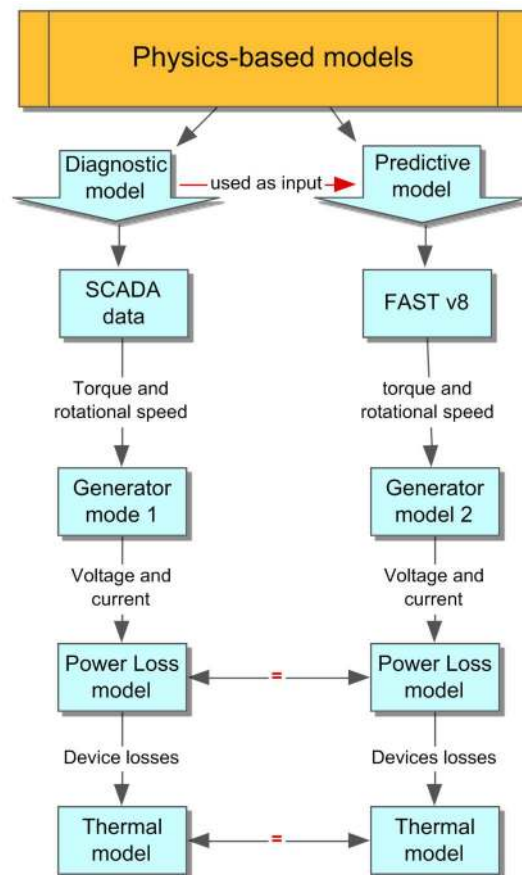


Figure 53. Power converter physics-based approach to estimate accumulated damage.

This section explains each block of the flow diagram shown in Figure 54. The predictive model takes into account the thermal cycling in power electronic components as the main source of stress in the predictive model.

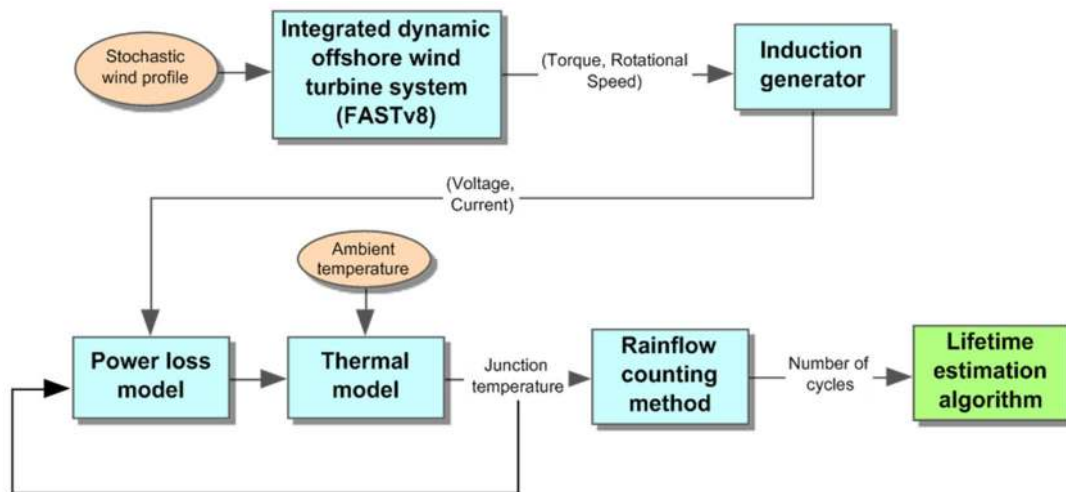


Figure 54. Remaining useful life estimation flow diagram.

4.4.1 Failure investigation of power converter

An Isolated Gate Bipolar Transistor (IGBT) is very similar to a metal oxide semiconductor field effect transistor (MOSFET) driving a gate of a bipolar junction transistor but with superior on-state conductivity. The MOSFET has a gate that is very easy to drive, meaning that it is not drawing too much current. A fully rated power converter, or back to back converter comprises a rectifier (generator side, conversion of AC to DC) and an inverter (grid side, conversion of DC to AC). These two independent systems are connected via a DC link to deal with different and incompatible electrical parameters such as frequency voltage and short-circuit capacity.

The power electronic converter has shown high failure rates in the risk assessment, SCADA data analysis and literature review [105] [96]. Reliability of power electronics is a critical and developing need for offshore wind farm operators; the assessment is essential for design as well as for the lifetime extension which leads to a reduction of energy cost [106] [97].

Damage accumulation or ageing of power converter modules is due mainly due to differing properties of adjacent materials, especially different coefficients of thermal expansion of adjacent layers, see Figure 55. Bond wire lift-off and solder delamination have been identified as the main failure modes [107] [98]. Based on [108] [99], the main source of stress giving rise to failures of power electronic components is temperature cycling. Figure 56 shows that 55% of the failure mechanisms are triggered by thermal activity, followed by vibration with 20%.

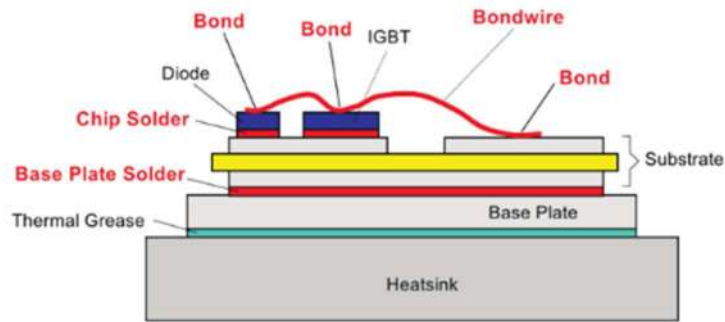


Figure 55. Power converter module structural details [107] [98][109] [100].

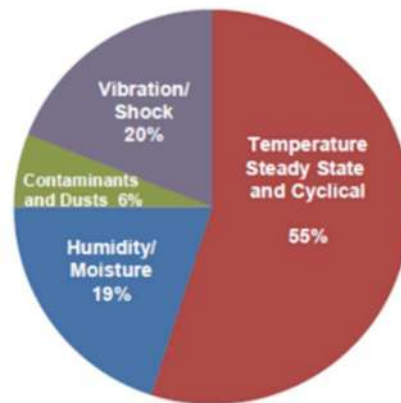


Figure 56. Source of stresses with impact on electronic components [108] [99].

For this project, failure in the IGBTs and diodes on both sides of the power converter due to thermal cycling represent the overall health of the assembly.

4.4.2 Induction generator model

The details of the electrical drive to extract electrical variables are not usually modelled in FAST; instead, the focus is on getting the torque-speed curve correct, which effects turbine loads. For an induction machine, the most sophisticated built-in model available in FAST is the Thevenin-Equivalent Circuit (TEC) model. The analysed turbine uses a squirrel cage induction generator (SCIG); therefore, a model to extract voltage and current variables are proposed to complement FAST simulations.

SCIG is a three-phase induction machine and has three windings in the stator and three windings more in the rotor, although, these can be imaginary. Generators can be described with the same set of the equation than motors, see Figure 57. To simplify the equations, the following hypothesis is commonly used [110] [101]:

- Symmetric and balanced three-phase induction machine, with a single winding rotor (Squirrel cage simple) and constant gap.
- The material is assumed to be linear, that is to say, the iron saturation is discarded.
- The iron magnetic permeability is assumed to be infinite in front of the air permeability, which means that the magnetic flux density is radial to the gap.
- All kind of losses in the iron are neglected.
- Both the stator windings and the rotor windings represent distributed windings which always generate a sinusoidal magnetic field distribution in the gap

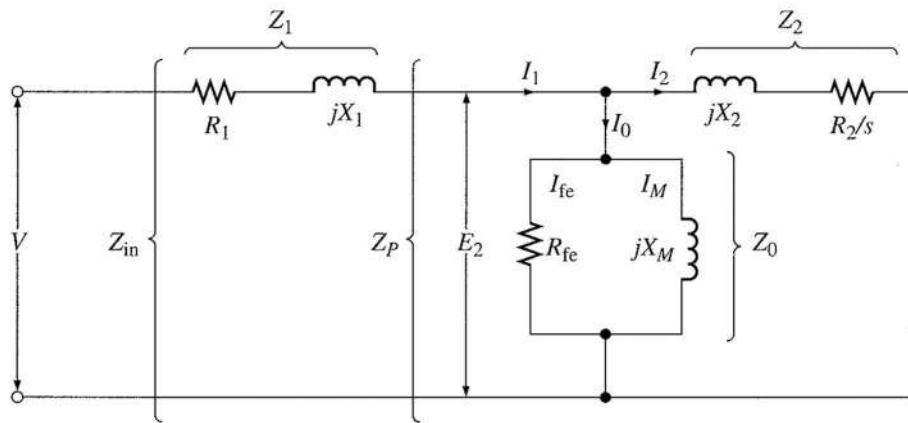


Figure 57. Induction machine simplified equivalent circuit [110].

From the equivalent circuit it is possible to derive the following equations:

$$s = \frac{n_s - n_r}{n_s} \quad (1)$$

$$Z_2 = \frac{R_2}{s} - jX_2 \quad (2)$$

$$Z_P = \frac{Z_2 Z_0}{Z_2 + Z_0} \quad (3)$$

$$Z_{in} = Z_1 + Z_P \quad (4)$$

Where s is the slip which represents the difference between rotational speed (n_r) and magnetic field rotation speed (n_s). R and X is electrical resistance and inductance, respectively. The impedances Z are calculated as an imaginary number using R and X . Rated rotational

speed, magnetic field rotation speed, resistances and inductances and provided by the manufacturer and used to calculate output voltage, current and power factor.

The mechanical input power (P_m) and stator power output (P_s) are computed are based on the general relation between mechanical torque (T_m) and electrical power [111] [102]:

$$P_m = T_m \omega_r; P_s = T_e \omega_s \quad (5)$$

Taking into account the SCIG efficiency (η)

$$P_s = \eta P_m \quad (6)$$

Therefore, AC voltage (V) and current (I) can be derived from the following relationships:

$$V = IZ_{in}; S = P_s + jQ \quad (7)$$

Where S is the complex power, P is electrical active power and Q is reactive power.

4.4.3 Power losses calculation

IGBT and Diode power losses can be divided into conduction losses (P_c), switching losses (P_{sw}) and blocking (or leakage) losses (P_b) which is normally neglected.

$$\text{Power losses} = P_c + P_{sw} + P_b \approx P_c + P_{sw} \quad (8)$$

IGBT Conduction losses can be calculated as follow:

$$u_{CE}(i_c) = u_{CE0} + r_c i_c \quad (9)$$

Where u_{CE0} is the DC voltage source, r_c is the collector-emitter on-state resistance, i_c is the collector current as shown in Figure 58.

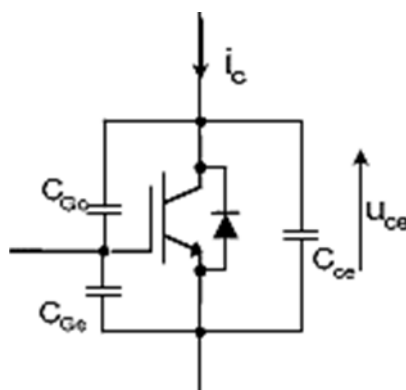


Figure 58. The circuit for the examination of the IGBT switching and conduction losses [112] [103].

The same approach can be used for the anti-parallel diode:

$$u_D(i_D) = u_{D0} + r_D i_D \quad (10)$$

The parameters r_D and r_C can be derived directly from the IGBT Datasheet (see Figure 59 and Figure 60). In order to take into account ambient and junction temperature changes in every simulation step, the u_{CE0} and u_{D0} values are read from the diagram as temperature dependant extrapolating junction temperature values between 25°C and 125°C.

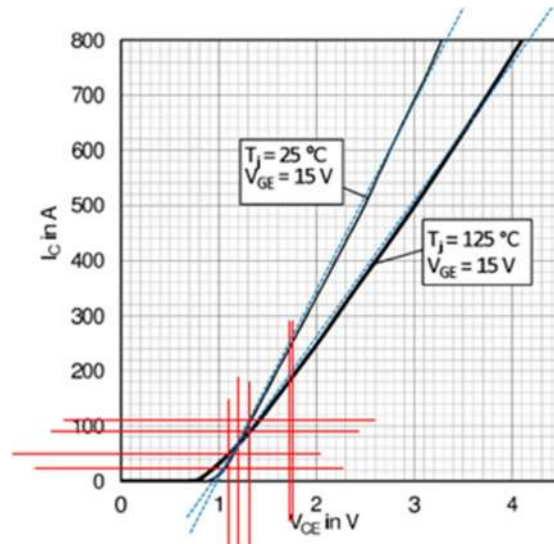


Figure 59. IGBT output characteristics. Red lines are used for slope calculation, and blue lines are curve fitting approximations [113] [104].

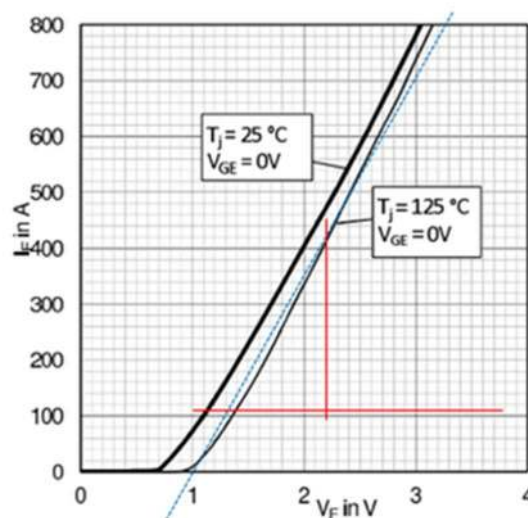


Figure 60. Diode output characteristics. Red lines are used for slope calculation and blue lines are curve fitting approximations [113] [104].

To describe the temperature dependency of the curve for the conduction losses calculation in the IGBTs the coefficients ($a=r_c, b$) can also be made temperature dependent [114] [105].

$$r_c(T_j) = a(T_j) = a_0 + a_{01}T_j \quad (11)$$

$$\text{and, } b(T_j) = b_0 + b_{01}T_j \quad (12)$$

Therefore, the relationship between collector current and voltage is given by:

$$I_C(V_{CE}, T_j) = (a_0 + a_{01}T_j)V_{CE} + (b_0 + b_{01}T_j) \quad (13)$$

With r_c and r_D derived from Figure 59 and Figure 60 are junction temperature dependent.

Based on [112] [103], the switching losses in the IGBT and the diode are a product of switching energies and switching frequency (f_{sw}). This characteristic is given by manufacturers as is shown in Figure 61. As current values would be varying due to a stochastic characteristic of the wind and turbulence intensity, the switching losses will be dependent on the input current using the slope in Figure 61 [115] [106].

$$P_{swM} = (E_{onM} + E_{offM}) \cdot f_{sw} \quad (14)$$

$$P_{swD} = (E_{onD} + E_{offD}) \cdot f_{sw} \approx E_{onD} \cdot f_{sw}$$

Finally, the total power losses in the IGBT and the diode can be expressed as the sum of the conduction and switching losses [109] [100][112] [103]:

$$P_T = P_{CT} + P_{swT} = u_{CE0} \cdot I_{cav} + r_C \cdot I_{crms}^2 + (E_{onT} + E_{offT}) \cdot f_{sw} \quad (15)$$

$$P_D = P_{CD} + P_{swD} = u_{D0} \cdot I_{Dav} + r_D \cdot I_{Drms}^2 + E_{onD} \cdot f_{sw}$$

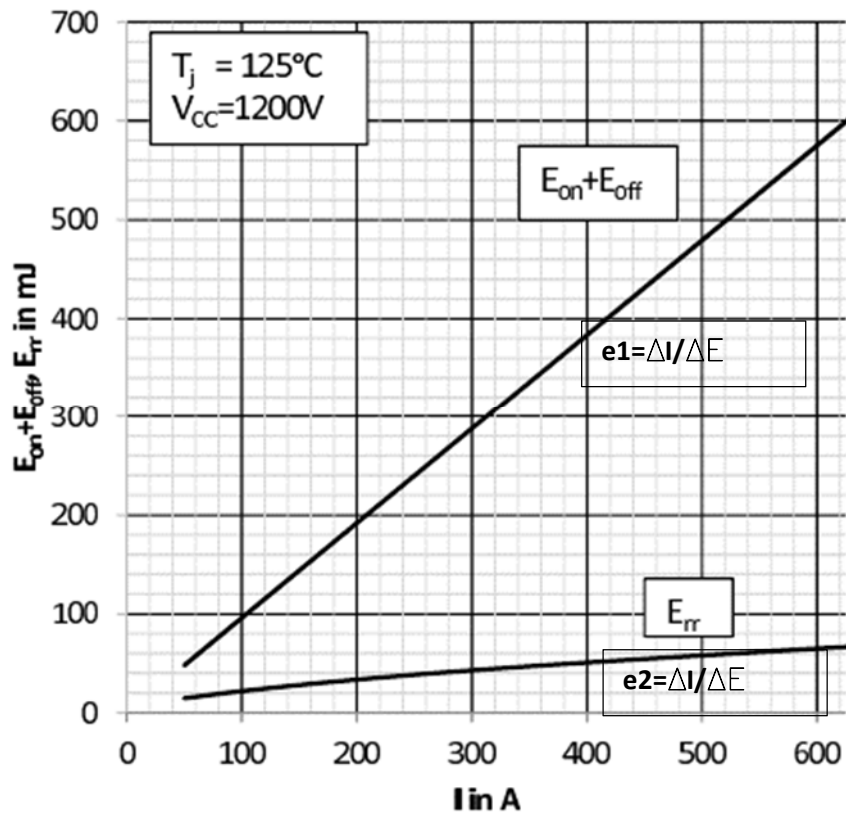


Figure 61. Typical energy losses. e1 and e2 represent slope [113] [104]

4.4.4 Thermal model

Power losses have to be conducted through the connection layers and insulation layers to the heat sink as it is shown in Figure 55. The heat dissipation generated during forward on-state and blocking state and during switching is expressed by the difference of temperatures between the layers described by the following equation:

$$\Delta T_{j-s} = T_j - T_s \quad (16)$$

As mentioned before, different materials used during power converter module construction have different thermal expansion coefficients. This feature of the physics is represented by the thermal resistance and thermal impedance of the material which comprises geometry, conductivity and heat transfer area. The thermal resistance can be calculated as follow:

$$R_{th} = \frac{d}{\lambda \cdot A} \quad (17)$$

Where d is material thickness, λ is heat conductivity and A is heat flow area.

Table 42. Material commonly used on power converters [109] [100].

Material	Heat conductivity λ [W/(m*K)]
Silicon	148
Copper	394
Aluminium	230
Silver	407
Molybdenum	145
Solders	~70
Al ₂ O ₃ -DBC	24
AlN DBC, AlN-AMB	180
AlSiC (75% SiC)	180

Similarly to an electrical circuit, the thermal model of the power converters can be expressed with an equivalent circuit as shown in Figure 62. Here power loss is the input (representing the current in an electrical circuit), the difference in temperature is analogous to the drop in the electrical voltage and thermal resistance is analogous to the electrical resistance.

The temperature differences ΔT over the thermal resistances are calculated for constant power dissipation P_T of the IGBT switches and Diodes inside the power module as follows:

$$\Delta T_{(j-s)} = T_j - T_s = P_T \cdot R_{th(j-s)} \text{ /IGBT switch} \quad (18)$$

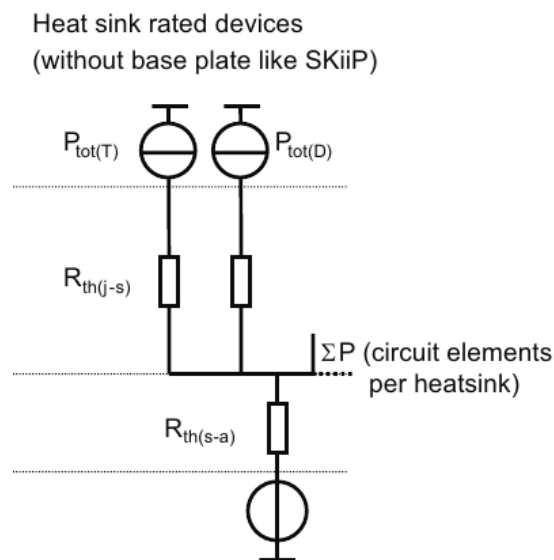


Figure 62. Static thermal model (R_{th}) without base plate [109].

After losses have been calculated, the temperature during stationary operation can be calculated with the aid of thermal resistances R_{th} , final values of the Z_{th} curve given by manufacturers (Figure 63).

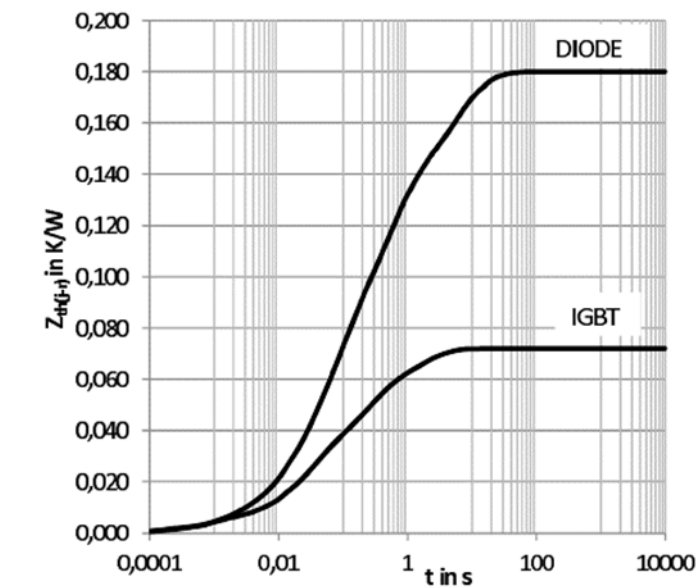


Figure 63. Transient thermal imped. $T (s)$ [9,113] [100,104]

Temperature calculation starts from the ambient temperature T_a outside to the inside as it is shown in Figure 64.

When there is more than one heat source on the heatsink, all the sources are added up. Each loss of electrical power in the electrical circuit represents a source of heat which is input to the heatsink.

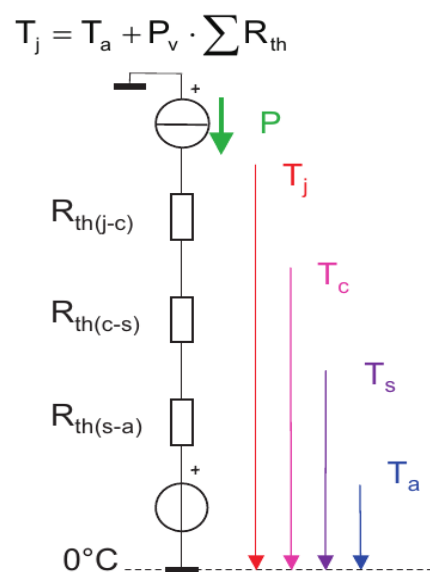


Figure 64. Temperature calculation process [109] [100].

For example, for a power converter with 6 IGBTs and 6 Diodes, the total loss is used to calculate the heatsink temperature, as follows:

$$T_{\text{heatsink}} = n(P_{\text{TotalIGBTs}} + P_{\text{TotalDiodes}}) * R_{\text{heatsink-ambient}} + T_{\text{ambient}} \quad (19)$$

Now the junction temperature T_j for IGBTs and Diodes have been modified a new power loss has to be calculated as it is explained in Figure 65.

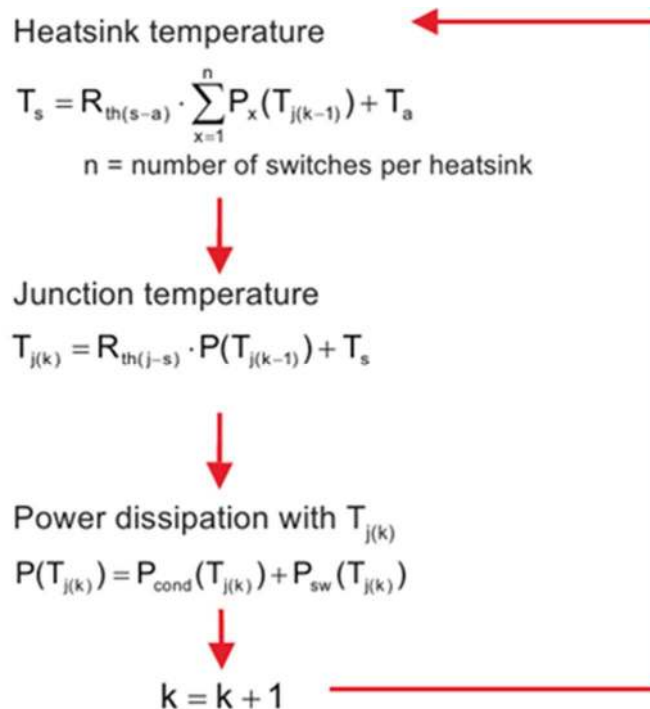


Figure 65. Process to calculate temperatures incorporating ambient temperature in each step [109] [100]

Temperature fluctuations experienced by the internal connections within the power modules produce ageing, through accumulating fatigue damage, caused by thermal stress cycles. As explained before, the fatigue of material is produced by thermal stress due to the different expansion coefficients of the connected materials or adjacent layers. During normal operation at frequencies of few Hz and especially at duty cycle operation, the internal connections of the layers in a power converter module will experience temperature cycling. At frequencies around 100Hz, the temperature variation (ΔT) is small so low energy dissipation is counterbalanced by elastic deformation [109] [100]. Temperature variations have been measured and simulated in [116]; here the author shows two temperature oscillations superimposed. Once, the power modules are in stand by; the temperature is stabilized to 30 °C and every 100 seconds, there is a rise in the temperature of 50°C. When the temperature

reaches the maximum, it is possible to see a higher frequency variation in the temperature of 320ms cycle time. The study concluded that one cycle every 100s is most likely to damage the IGBTs.

Rainflow counting method is applied to estimate the frequency and amplitude ranges of the thermal cycles [108,117,118] [99,107,108]. The rainflow counting method is adapted from material science and applied to power electronics [118] [108]. This method identifies local highs and lows in the data as peaks and valleys where the range between them are all considered to be half cycles. The algorithm pairs the half cycles to generate complete cycles regarding a mean [119] [109].

A script for the ASTM E 1049-85 (2005) Rainflow Counting Method is used as a reference [120] [110].

Based on [106] [97][109] [100], an empirical correlation between a number of cycles to failure N_f and temperature cycling amplitude ΔT_j is given:

$$N_f = A * \Delta T_j^\alpha * e^{\frac{E_a}{k_b T_{jm}}} \quad (20)$$

Where:

- N_f represents the number of cycles to failure of the device.
- ΔT_j is the junction temperature thermal cycle amplitude.
- T_{jm} represents the mean absolute junction temperature.
- A , α and E_a are constant values given by the manufacturer.
- k_b represents Boltzman constant.

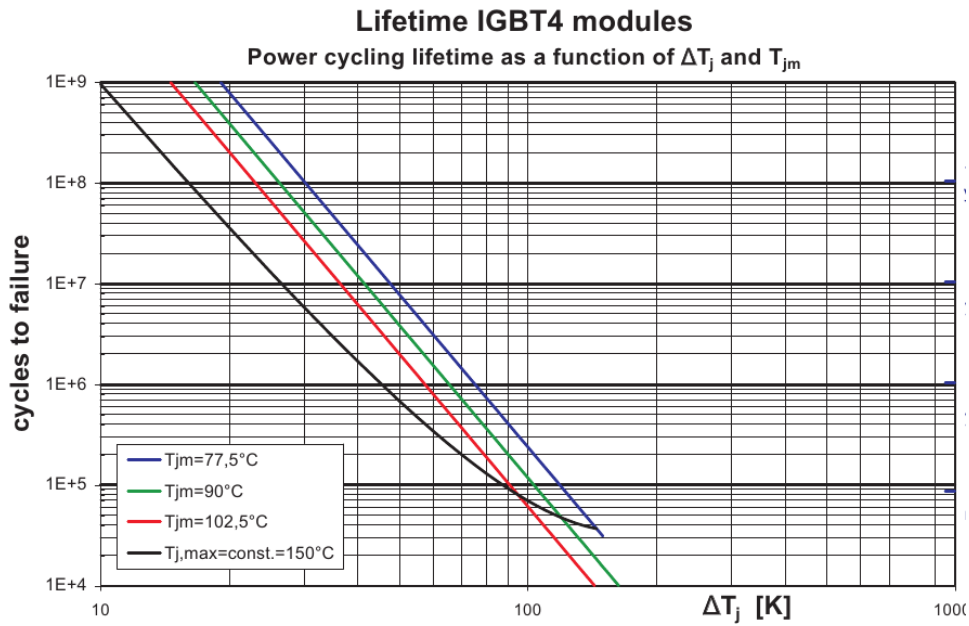


Figure 66. Dependency of the power cycling value n for IGBT4 modules as a function of the temperature cycling amplitude ΔT_j and the mean temperature T_{jm} [109] [100].

The proposed method to estimate the lifetime of power modules is based on Figure 66 which is provided by the manufacturer in [109] [100]. Once temperature cycles are counted using the rainflow counting method, temperature cycling amplitude and the mean absolute junction temperature are calculated.

In Figure 66, an initial point is selected using the counted number of cycles and the calculated ΔT_j . Then, the difference between final cycles to failure for the estimated mean junction temperature curve (blue, green, etc.) at the calculated ΔT_j and the initial point of a counted number of cycles would result in the remaining cycles to failure.

IGBTs and Diodes junction temperature time series are separately analysed and then the lifetimes are combined using the Miner's rule [106] [97].

A cross-multiplication (or rule of three) between counted numbers of thermal cycles associated with a period of prediction (in minutes or hours) and the remaining cycles to failure would result in a predicted failure date.

4.4.5 Physics-based model outputs: Power converter

200,000 seconds derived from the SCADA database have been simulated. Temperatures of the IGBTs and diodes during this period are shown in Figure 67.

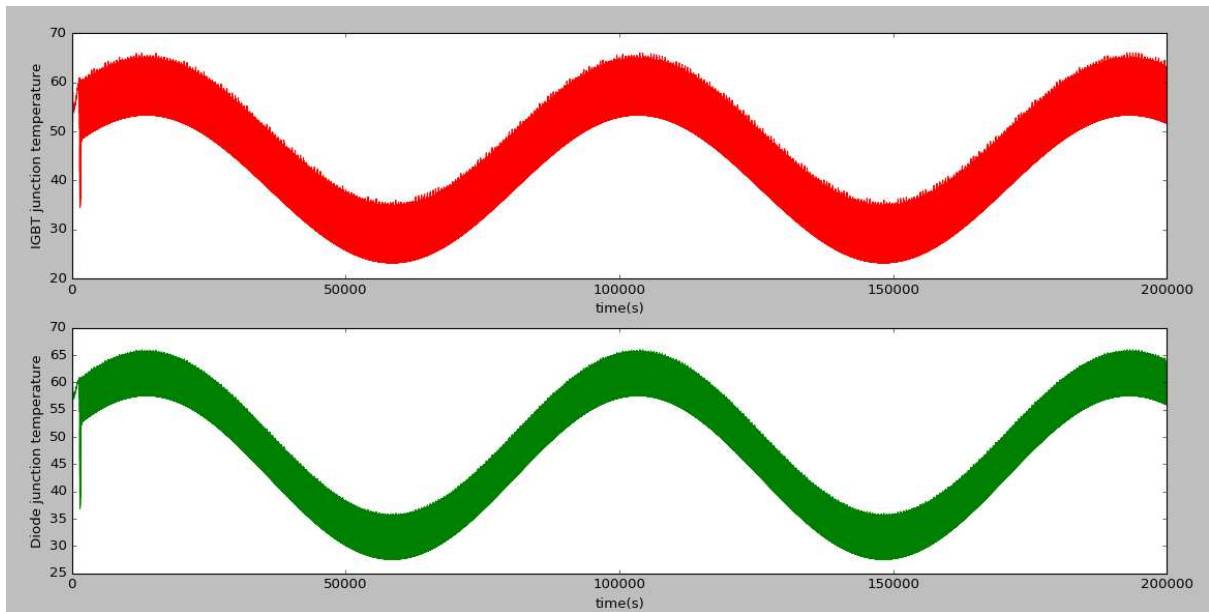


Figure 67. IGBTs and diode temperature.

Figure 68 shows the probability distribution of the IGBT junction temperature, which has a pick value between 50 and 60 degrees Celsius.

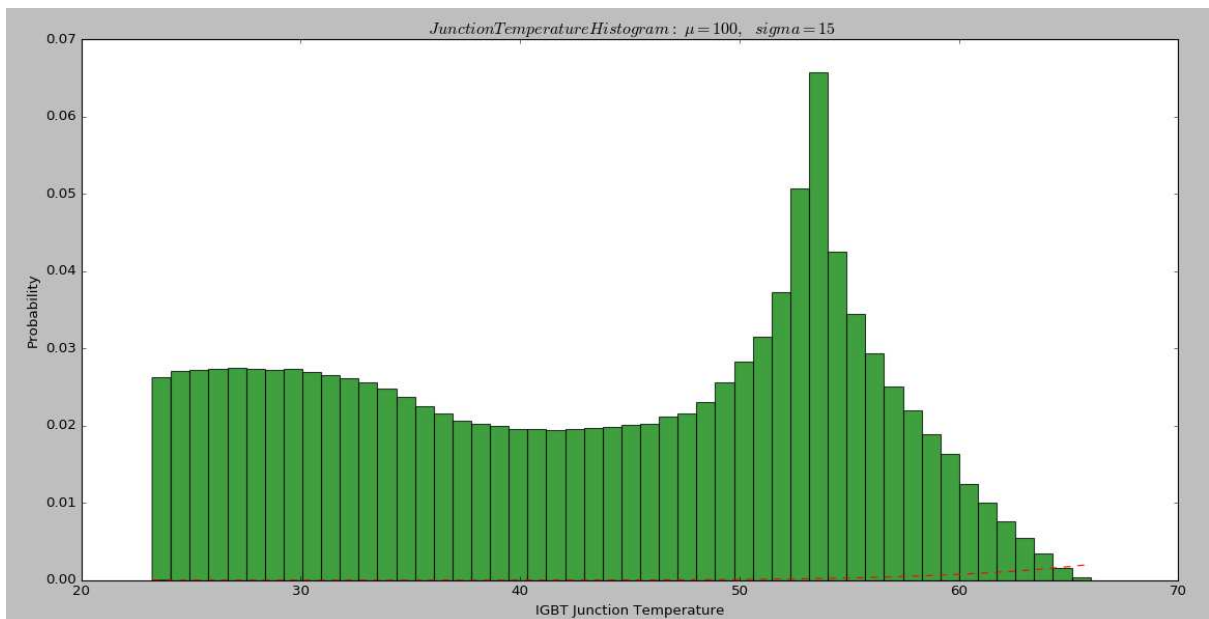


Figure 68. Probability distribution of the IGBT junction temperature.

The estimated damage for a period of two and half days is described in Table 43. Under these operational conditions, there is a total of 75,075 cycles and accumulated damage of 0.00000143%. Since the damage of the power converter is related to the number of cycles for a particular temperature range, It is possible to see that larger estimated damage is generated in the range between 9 and 12 degrees Celsius.

Table 43. Estimated damage of the IGBT.

Range (*C)		DTj(K)	Tjm(K)	cycle count	Number of cycles to failure (Nf)	Estimated Damage
38.5	42.77	4.27	317.61	2	1.25882E+12	1.59E-12
34.22	38.5	4.28	273	0	4.96101E+13	0.00E+00
29.94	34.22	4.28	323.23	0.5	8.40471E+11	5.95E-13
25.66	29.94	4.28	320.65	0.5	1.00455E+12	4.98E-13
21.39	25.66	4.27	322.03	1	9.23656E+11	1.08E-12
17.11	21.39	4.28	318.76	4	1.14684E+12	3.49E-12
12.83	17.11	4.28	322.14	5.5	9.05925E+11	6.07E-12
8.55	12.83	4.28	317.47	16452.5	1.25651E+12	1.31E-08
6.42	8.55	2.13	316.93	9884.5	4.39545E+13	2.25E-10
4.28	6.42	2.14	315.89	31873.5	4.62459E+13	6.89E-10
2.14	4.28	2.14	315.09	16718	4.8987E+13	3.41E-10
1.07	2.14	1.07	331.43	16	5.24991E+14	3.05E-14
0	1.07	2.14	330.84	117	1.6596E+13	7.05E-12
total number of cycles				75075		1.44E-08

4.5 Conclusion

Since statistical-based methods for O&M optimisation do not consider the actual condition of the component, failure date prediction can be at any point in time. This might represent a greater consequential economic cost. Nowadays, data-driven approaches use operational data (CMS or SCADA) to understand the normal behaviour of critical assets or components. When a clear deviation from normal behaviour is identified, a failure can be detected. The predictability of failure in the offshore wind industry is a combination of programming, statistics and subject matter expert knowledge. An inspection might detect a well-developed failure without leaving any time to respond in a cost-effective manner. Accumulated damage determination in the time domain using physics-based models is discussed as one of the methodologies with greater capability to predict failure far in advance, even from the installation date of the component.

The patterns of seasonal variations can change yearly. The procedure described in this chapter allows observed load spectra to be used as inputs, enabling the estimated accumulated damage to be updated throughout the life of the component. The simulated spectra represent future loading scenarios and open up the possibility of using the statistics of the wind climate.

Based on the failure investigation and the vulnerability map of gears and bearings it is noted that bearing failures caused by fatigue damage occurs on several of the shafts in the gearbox, but predominately in the HSS shaft bearings. HSS shaft failures are responsible for 50% of the repair cost in the gearbox.

The load distribution of the three-stage gearbox is calculated using SCADA data and the model. The proposed physics-based model of the gearbox helps to optimise O&M activities by feeding the RUL into the decision-making process of wind farm operators. Around 3% of lifetime consumption is estimated in both HSS bearings, B1 and B2.

A physics-based method to estimate damage accumulation of IGBTs and Diodes and to predict the RUL of power converters have been proposed. The simulations do not require a large computational effort, therefore it is suitable for day-to-day use. The algorithm comprises one glue code and four main pre-processors; generator, power losses, thermal model and the rainbow counting method. The main inputs of the methodology to estimate accumulated damage are the torque and rotational speed in the high-speed shaft. For prediction purposes, the proposed methodology is to calculate the torque and rotational speed using the aero-servo-elastic-hydro simulation tool FAST. FAST uses as inputs the load cases derived from IEC standards representing all the operational conditions an offshore wind turbine may experience at a particular site. A period of two and half days is simulated, which is not long enough to extrapolate the damage for the whole year as it does not include all the operational conditions. The total number of thermal cycles is 75075 and represent very small accumulated damage, 1.44E-08%.

The power losses and junction temperatures depend on the ambient temperature. The power losses and thermal algorithms require information provided by the manufacturer.

Similar to the gearbox, the RUL method of the power converter could be used to inform maintenance decisions to optimise resource allocation considering weather conditions throughout the year. Unexpected failures, which represent huge production losses, as well as time finding failures could be avoided by scheduling maintenance or inspection activities based on the RUL estimation.

CHAPTER 5 – DATA MINING APPROACH FOR THE PITCH SYSTEM

5.1 introduction

Automatic and intelligent systems are needed to minimise human intervention during the operating life. The pitch system has been identified as one of the most critical assemblies in terms of turbine operation. For the pitch system, the limited number of signals available through the SCADA system obstructs the identification of failure causes, the development of physics-based approaches to quantify degradation, estimate risk and hence schedule maintenance tasks. It is clear however, that the health of the pitch system may be discerned from the available data. The challenge is to identify how to combine existing signals. Therefore, machine learning and data mining methodologies have been used to understand the normal behaviour of the pitch system. Observed deviations from normal behaviour in SCADA data can be categorised as positive or negative in terms of the deduced risk profile. Consequently, critical modes of failure of the pitch system have been anticipated in advance.

The initial criteria to select data mining techniques for this project are:

- Ease to understand the codes and interpret the outputs: one of the requirements of the sponsor company is to propose a methodology simple to understand for both, the end user and the developer.
- Cost effective with low computational effort: A super computer is no required and the implementation is done in the open source Python code.
- Unsupervised: taking into account the large amount of data and variables, the first step in this process is to identify how a turbine behaves under certain operational conditions without giving the model inputs.
- Prediction capability: ideally, the proposed methodology needs to be able to diagnose and prognoses failures.

Therefore, the methodology and process in this section are based on simple and commonly used techniques of data mining. The implementation is made in python code.

The proposed method involves an unsupervised one-class Support Vector Machine (SVM), used for novelty detection. Given a set of samples, the SVM detects the soft boundary of that dataset. Many different variables may be incorporated into the analysis as inputs. In two dimensions, the soft boundary can be displayed as a contour. A decision tree is used to take

into account expert knowledge of offshore wind turbine technology and operation and to include more variables to the analysis in three dimensions or more. Figure 69 shows the analysis of 1-year historical data of the wind speed and blade position (2D) and, the addition of a third variable (3D), the oil pressure of the hydraulic system to determine the failure mode. It is possible to associate points in the graph by the time stamp of the original dataset. The final frontier of normal operation is defined and a status variable assigned to the training data (green, yellow, red).

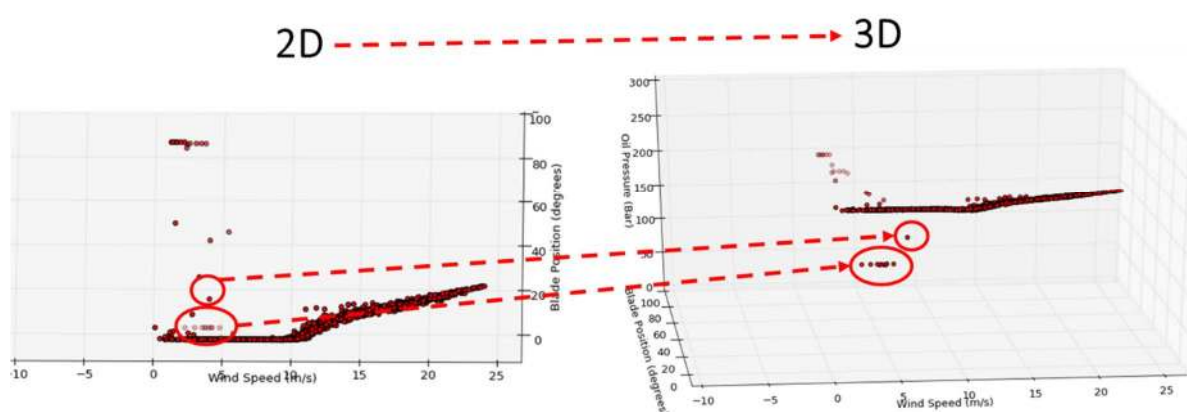


Figure 69. Three-dimensional analysis of the pitch system using one year of historical data.

The classification technique used is the K-Nearest Neighbour (KNN). KNN enables new SCADA data observations to be categorised and operation status to be assigned. The KNN model searches for a number of observations from the training data and then calculates the numerical distance between the unknown “status” of the new observation and the training data. Then the KNN model selects the nearest known status for the new observation. This methodology is less computationally demanding and will allow pitch system anomalies to be identified. More SCADA database variables can then be included in the analysis of anomalies to diagnose the failure mode and cause.

5.1.1 Pitch system technology

Pitch systems can consist of electric or hydraulic power actuators. The generic offshore wind turbine of this project uses a hydraulic pitch system as it is shown in Figure 70.

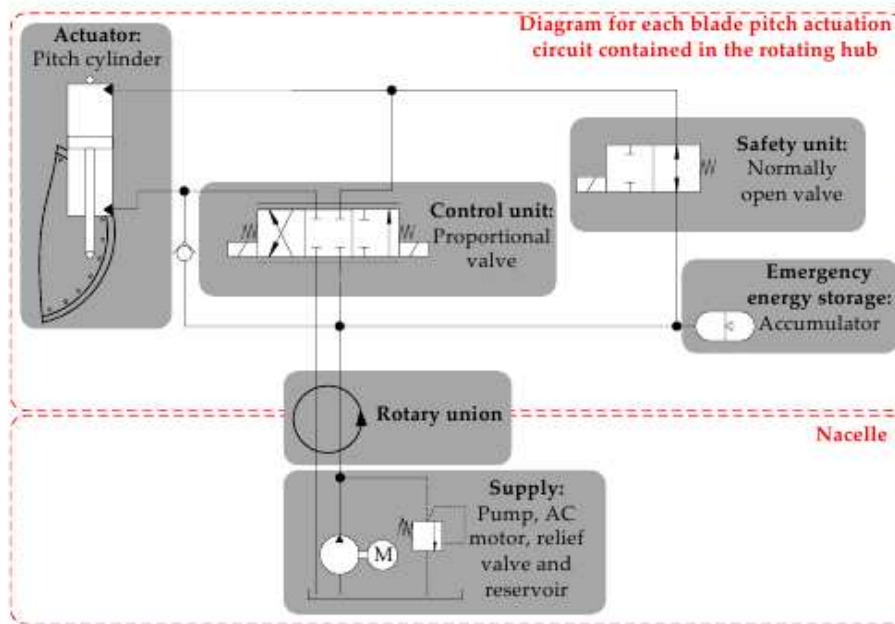


Figure 70. Idealised typical hydraulic pitch system [121] [111].

5.1.2 Data mining approach objectives

The structure of the data mining approach is shown in Figure 71. The general aim of this section is to design and deploy data mining approaches to diagnose failures in the pitch system of an offshore wind turbine as early as possible. The specific objectives are:

- To understand failure modes and causes of the pitch system and their correlation with the available data of the SCADA system.
- To identify normal behaviour and the learnt frontier using an unsupervised Support Vector Machine (SVM) technique.
- To combine Subject Matter Expert Knowledge (SMEK) with SCADA data and the learnt frontier to assign a risk status to the training data.
- To develop a K Nearest Neighbours (KNN) technique to assess new observations or data points based on the created risk status.

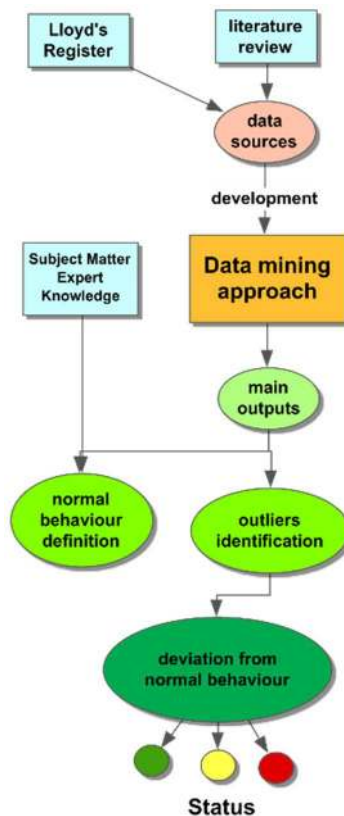


Figure 71. Data mining approach

5.2 Data analysis

The data mining process and analysis is performed using a python code and its machine learning and data analysis tool, scikit-learn. This tool is selected due to it is open source, commercially usable and built-in commonly known python libraries; NumPy, SciPy, and matplotlib.

5.2.1 Data mining process

This section describes a combination of machine learning techniques which is used in the literature as a hybrid classifier. Commonly, SVM and KNN are used together to reduce misclassifications. As one of the main objectives of the data mining approach is to incorporate subject matter expert knowledge into the model, the unsupervised SVM technique is used to identify boundaries and understand turbine behaviour. The proposed data mining process used in this project is described below:

1. Wind turbine and pitch system understanding: First, it is necessary to understand the objectives clearly and identify what are the potential failure modes of the pitch system.
2. To identify data variables in the SCADA system associated with the pitch system failures.

3. To select data mining techniques, assumptions, and constraints.
4. SCADA data understanding (data exploration): This step comprises data collection, including data load and data integration. Next, data exploration is performed using visualisation and Pearson correlation coefficient to identify patterns based on the wind turbine understanding. Then, it is necessary to identify if there is any missing value in the acquired data.
5. Data preparation: This step aims to prepare the final data set. The data identified needs to be formatted into a .csv format to be read by the python code.
6. Modelling: Data mining techniques are selected to be used for the prepared dataset.

5.2.2 SCADA data analysis

There are systems in the offshore wind turbine that have limited access or their knowledge about the multiple dynamic interactions between their subsystems does not exist. The SCADA database is already available and provides a large amount of operational data that can be used to give an indication of the health of the system. The information in the SCADA system varies from status signals to measurement signals such as wind speed, temperatures, pressures, voltages, currents, blade position, etc. [122] [112].

The normal behaviour of systems and changes or deviations from normal behaviour can be detected in an early stage of failure using sophisticated signal analysis techniques. Normal behaviour is established using two input signals from historical operational data during periods where the turbine is normally operating. Correlation of signals is studied to identify those that once are combined they can indicate the system condition. Table 44 shows the results of the Pearson's correlation coefficient test between several SCADA database variables related to the pitch system. The Pearson correlation coefficient is a simple linear analysis. This analysis quantifies the linear relationship between two variables (X and Y), with a series of pairs x_i and y_i , with $i: 1,2,\dots,n$. It varies between +1 and -1 where:

- 1 is total positive linear correlation.
- 0 is no linear correlation.
- -1 is total negative linear correlation.

The Pearson's coefficient r_{xy} is calculated as follows [123] [113]:

$$r_{xy} = \frac{\sum(x_i - \bar{x})(y_i - \bar{y})}{(n - 1)S_x S_y}$$

Where, \bar{x} and \bar{y} are the mean values of X and Y and, s_x and s_y are the standard deviation of X and Y.

Table 44. Pearson correlation coefficient.

	Wind_Speed_ms	Wind_Speed_stddev_ms	Generator_RPM	Yaw_position_degrees	Blade_A_position_degrees	Blade_A_position_stddev	Oil_pressure_Blade_A_Bar
Wind_Speed_ms	1						
Wind_Speed_stddev_ms	0.62799877	1					
Generator_RPM	0.808742898	0.549481447	1				
Yaw_position_degrees	-0.125021943	-0.03954417	-0.068176086	1			
Blade_A_position_degrees	-0.024470984	0.000780576	-0.497982916	0.005892143	1		
Blade_A_position_stddev	0.038812024	0.140537951	-0.042870492	0.00399471	0.128917173	1	
Oil_pressure_Blade_A_Bar	-0.097335886	-0.154429112	0.150686591	-0.001428805	-0.559675413	-0.098140546	1

Table 44 analyses several SCADA variables: wind speed, rotational speed, yaw and blade position and, hydraulic system pressure. As it is expected, there is a clear positive linear correlation between wind speed and rotational speed. But also, it is possible to see in the table a strong negative linear correlation between blade position and rotational speed and, between oil pressure and blade position.

Likewise, Figure 72 visually explores the correlation between turbulence intensity and blade position, wind speed and oil pressure. The turbulence intensity is derived from SCADA data by dividing the standard deviation of 10 minutes wind speeds series by the mean wind speed. The scatter plots in Figure 72 shows variables of a turbine with pitch system failures. The failure was registered and reported on a specific date by the O&M team of a specific offshore wind farm. SCADA data from 6 months before the failure and 6 months after the failure was selected. It is possible to visually inspect the dataset and identify where most of the points are and if there is any outstanding outlier point.

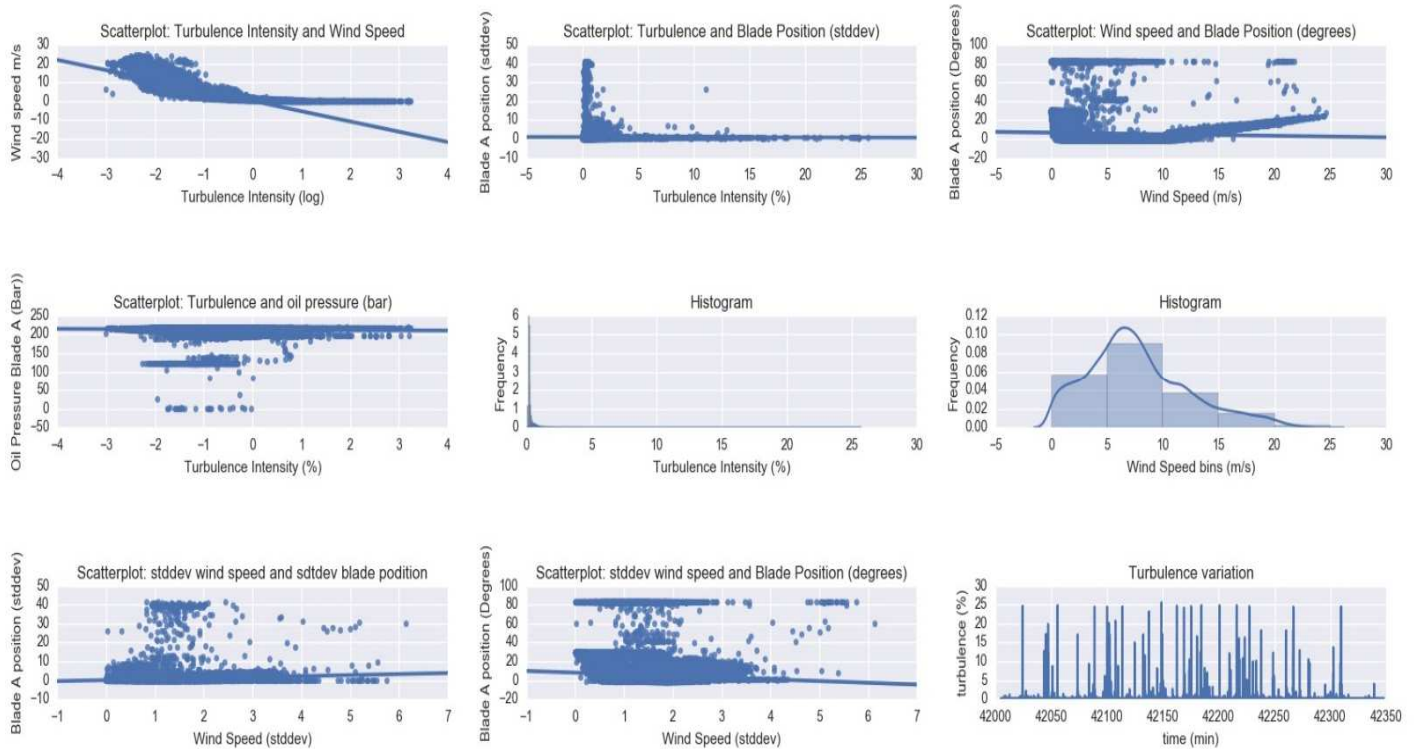


Figure 72. Turbine with pitch system failure

In order to understand turbine behaviour is necessary to cross two data sources: SCADA data and maintenance logs. Using maintenance logs and maintenance team reports, it is possible to identify specific dates of failures of a specific turbine in the wind farm. Therefore, the time variable and turbine ID are used to cross or correlate both sources of information: maintenance logs and SCADA data. The proposed approach is shown in Figure 73. The flow diagram shows the reasoning behind the process. Analysing the O&M reports it is possible to extract failure mode, date and turbine ID. When the failure mode is related to the pitch system, the proper SCADA data variables are selected for the period of time before the identified date of failure.

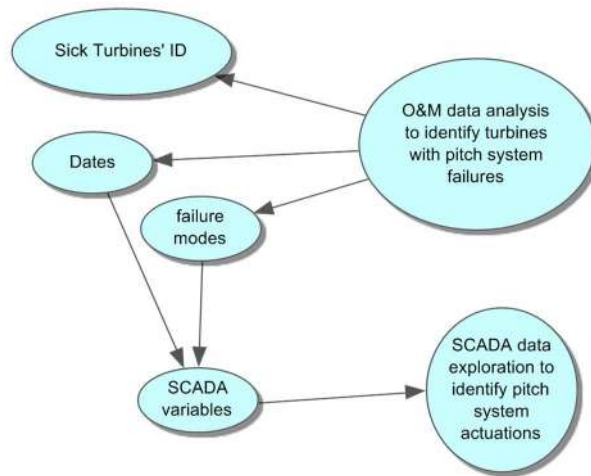


Figure 73. SCADA data and O&M data analysis

5.2.3 Failure investigation outputs

Failure investigation is crucial to understand patterns in SCADA data. First, using the approach described in Figure 73, it is possible to explore SCADA data before a pitch system failure occurs. Figure 74 shows a comparison of 1-year SCADA data between a turbine with a registered pitch system failure and a healthy turbine. It is possible to see that the turbine with a known pitch system failure experienced approximately 10% higher frequency of turbulence intensity during one year before the failure date.

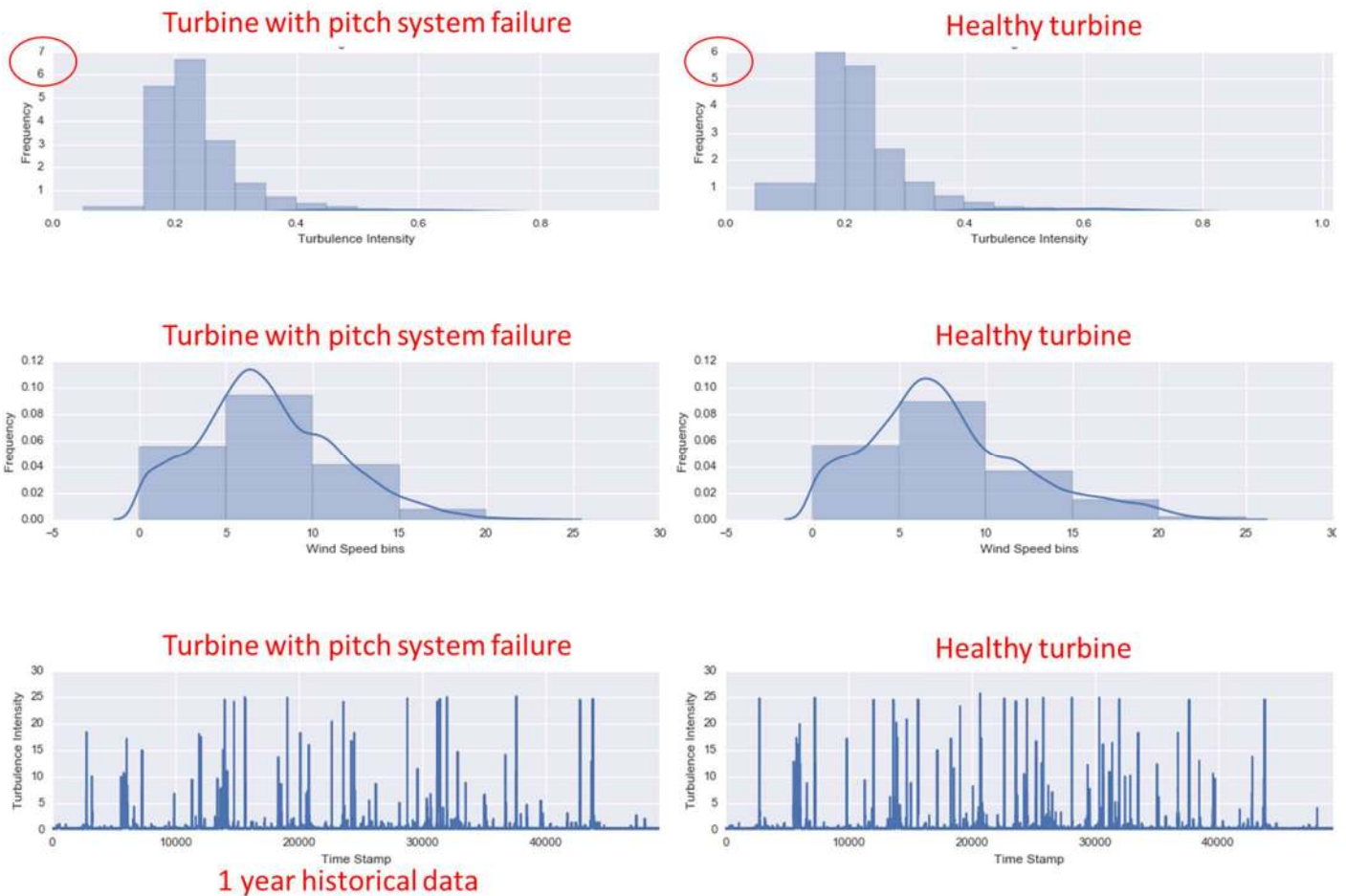


Figure 74. Comparison between healthy turbine and turbine with pitch system failure.

Hydraulic actuators modify the blade pitch or angle during the hydraulic pitch system operation. A hydraulic pump and a pressurised tank providing back up, constantly run to maintain pressure. Springs are used to securing operation safety since, in case of a failure, the blade will pitch to a safe position. Maintenance activities of hydraulic systems mainly involve regular checks for leaks of fluid and to ensure that there is no excessive play in the mechanisms. The pitch system accounts for 20% of the total turbine downtime. Hydraulic pitch systems might present failure modes such as leakage, contamination, component malfunction and electrical faults. Proportional valve leakage is identified as the main failure mode of hydraulic pitch systems [121] [111].

The author in [124] [114] identifies that states in the control system represent potential failures of the active control power system. The most common states are:

- Fault blade load control: this state means that an undue effort was exercised in the blade, the turbine is still operating but with reduced power and the maintenance service needs to rectify the failure.
- Pitch control error: a difference of the angles of the three blades, which leads to the turbine shutdown. The turbine restarts automatically for a number of times before the maintenance service is required.

The main outputs of the failure investigation based on SCADA data analysis, O&M information and literature review, are encoder error, hydraulic system failure, valve failure and actuator failure, Figure 75. The maintenance reports after failure and SCADA data analysis described a generic hydraulic system failure, but non or limited information about the repair actions is provided. On the other hand, in the literature review, the most common failure of the hydraulic pitch system are described. These failures are linked with SCADA data variables such as oil pressure, blade position and wind speed.

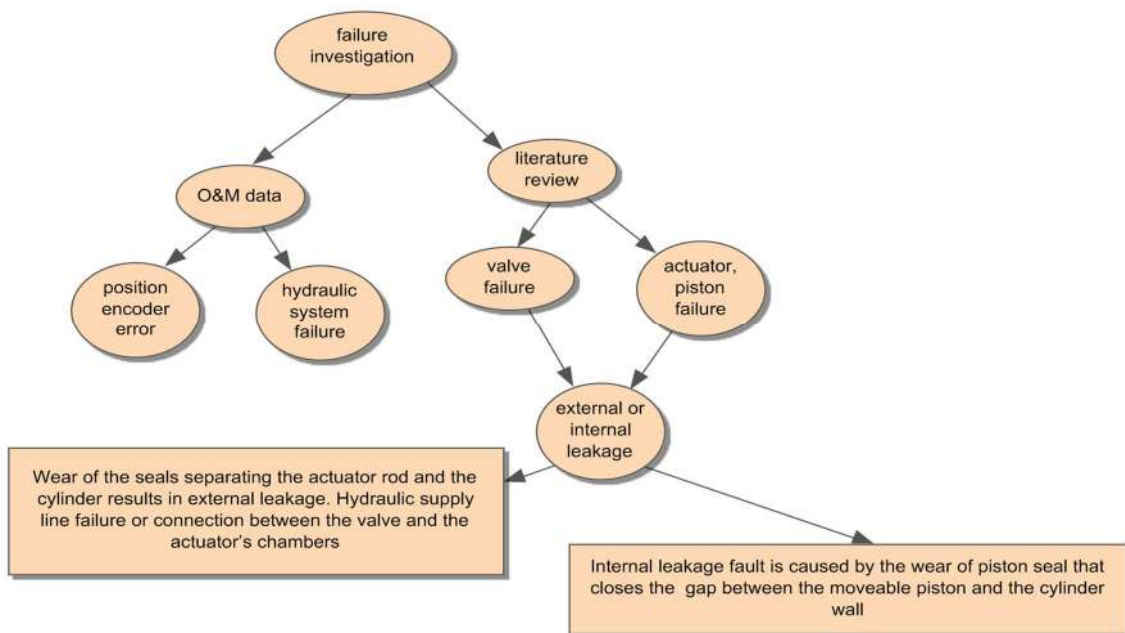


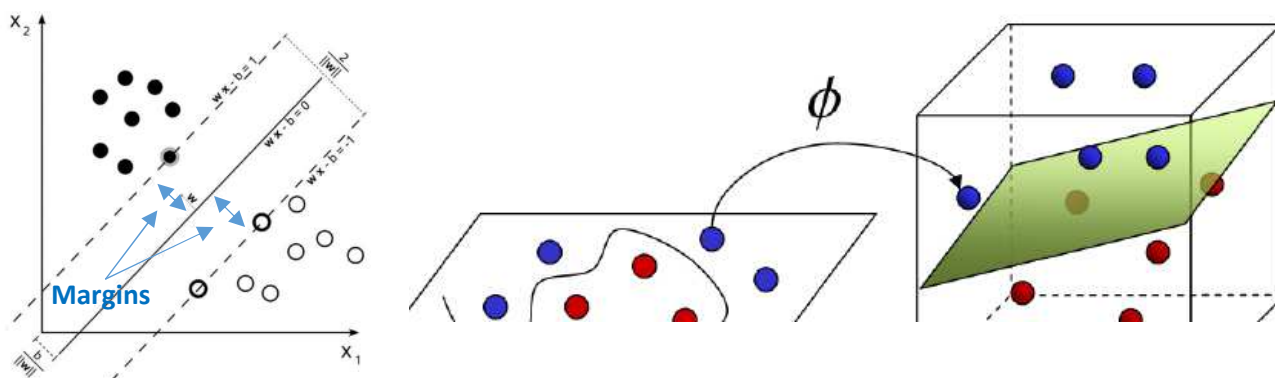
Figure 75. Main findings of the failure investigation.

5.3 Support Vector Machine (SVM)

Due to the design understanding of the relationship of the blade position and wind speed and, the correlation of these variables with the failure modes of the hydraulic pitch system; the

variables to be used in the SVM techniques are the wind speed and the blade position as it is shown in Figure 77.

SVM has been used for data pattern recognition, classification, regression and outliers detection since 1995. The main idea of SVM is to map the input vectors not linearly separable like in Figure 76 (a) into a higher dimensional feature space to use hyperplanes for optimal separation of mapped data like in Figure 76 (b) [16].



a) vector linearly separable

b) Linearly separable data in feature space with hyperplane

Figure 76. SVM data separation with feature space [16].

Support vectors are the data points of observations of SCADA data nearest to the defined hyperplane. Therefore, these points are critical elements of the data set. The further the data points are from the hyperplane, the more confidence there is that the points are classified correctly. The hyperplane can be found by calculating the distance to the nearest data points, known as the margin in Figure 76 (a). The main idea is to select the greatest margin possible. In order to classify the dataset that is not clearly separable, it is necessary to move from 2D to 3D, this process of moving the data to a higher dimension is called kernelling [125] [115]. There are several kernel functions: linear, nonlinear, polynomial, radial basis function (RBF), and sigmoid. The only kernel function that does not require prior knowledge of the data is RBF.

As it is described in section 5.1, this step of the process is unsupervised or without entering the knowledge of the data, therefore, the kernel function selected for this study is RBF which is an exponential function:

$$\text{RBF} = \exp(-\gamma \|x - x'\|^2), \text{ where } \gamma \text{ is the radio greater than } 0 \text{ of the closed ball centred at } x' \text{ in a graph.}$$

The main advantages and disadvantages of SVM technique is shown in Table 45.

Table 45. SVM advantages and disadvantages [126] [116]

Advantages	Disadvantages
Effective in high dimensional spaces	Kernel function choosing is crucial when the number of features is greater than the number of samples
Effective when the number of dimensions is greater than the number of samples	It does not provide probability estimates directly (probability can be derived using a five-fold cross-validation)
Memory efficient as it uses a subset of training points (support vectors)	
The decision functions are versatile as it can be defined by different Kernel functions	

Figure 77 shows the main output of the SMV with an exponential kernel function, RBF with a gamma of 0.01 . One year historical SCADA data is used to asses the methodology. The main frontier or contour is used to understand turbine normal behaviour in combination with subject matter expert knowledge, presented in the following section. The contour is called learn frontier.

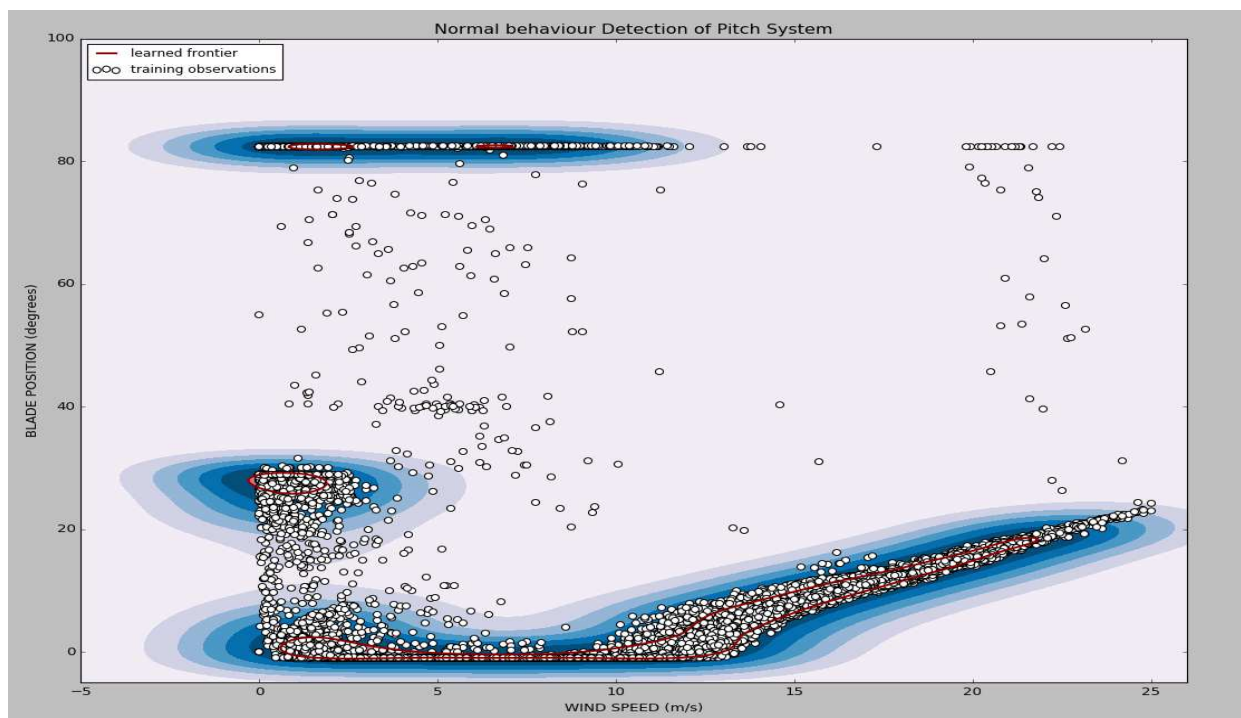


Figure 77. SVM output.

5.4 Decision Tree Algorithm (DTA)

After the learnt frontier in Figure 77 is defined, it is necessary to combine it with technical knowledge of the offshore wind turbine. Now, the methodology and analysis become three-dimensional. Thus, the graph in Figure 77 (wind speed v/s blade position) is divided and analysed in the main sections, as it is shown in Figure 78. These sections are selected identifying the main concentration of points from SVM output. Then, using subject matter expert knowledge, each sections is analysed correlated to a normal or abnormal behaviour based on the original design of the turbine components and control system. The sections and their correlation with the behaviour of the turbine is used in the decision trees methodology.

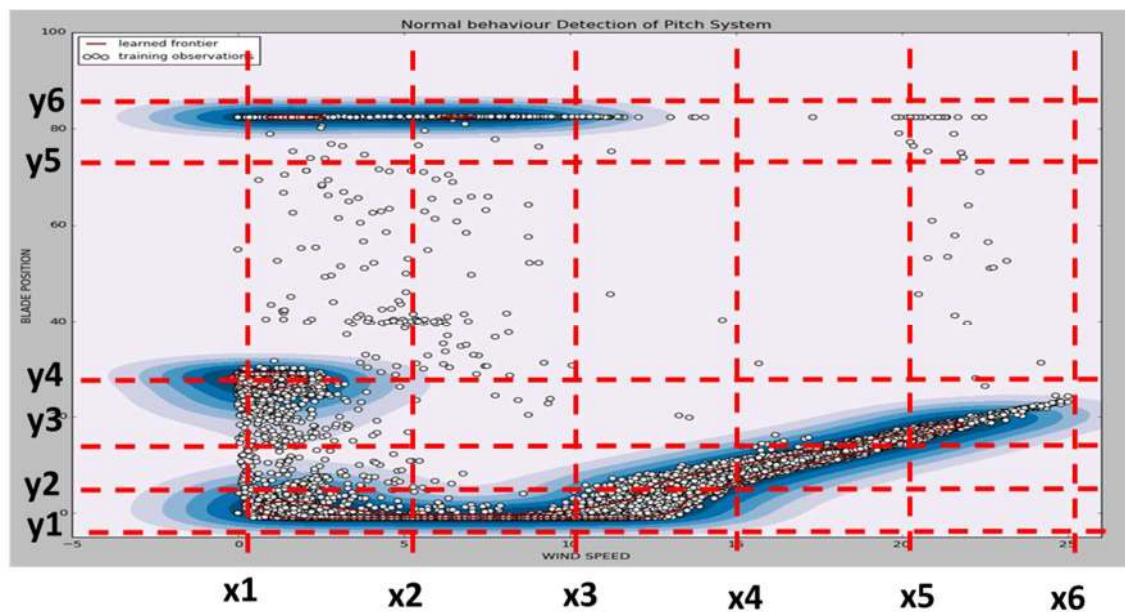


Figure 78. SVM output analysis.

A decision tree algorithm (DTA) is developed to assign a status to the points of the training data in each section of the graph, an example of the flow diagram of the DTA is shown in Figure 79. Green status is normal behaviour, yellow status is abnormal behaviour and red status is a failure. The DTA comprises subject matter expert knowledge to interrogate the data intelligently.

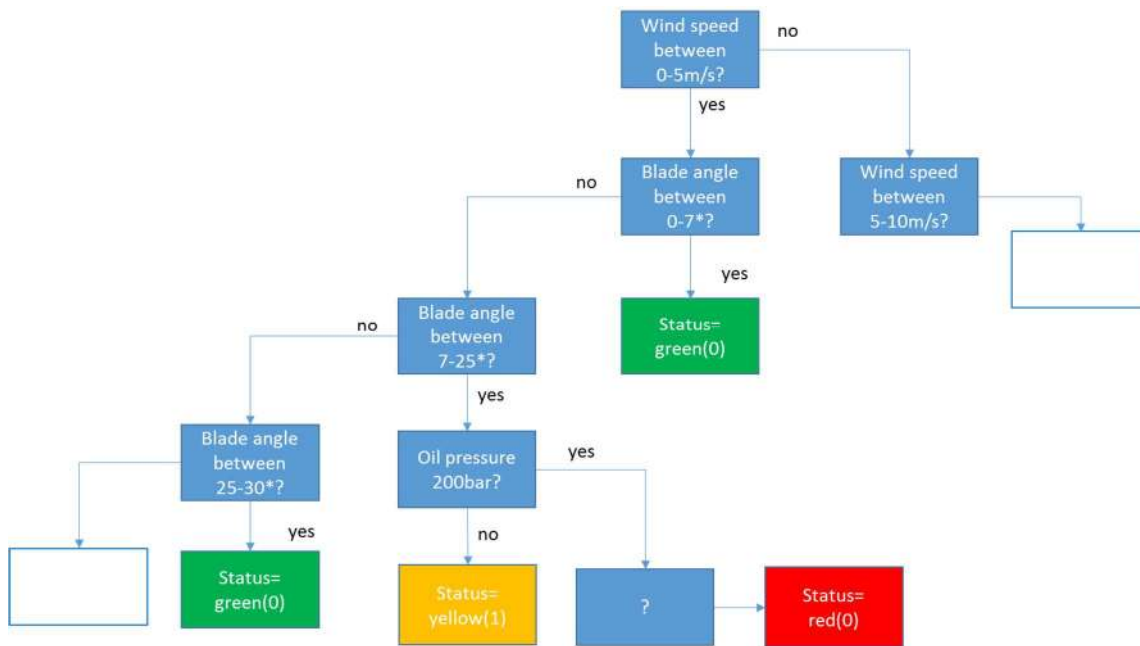
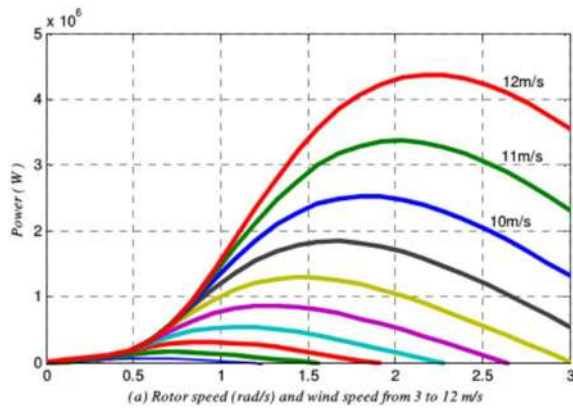


Figure 79. Decision tree to assign a status vector to the training data.

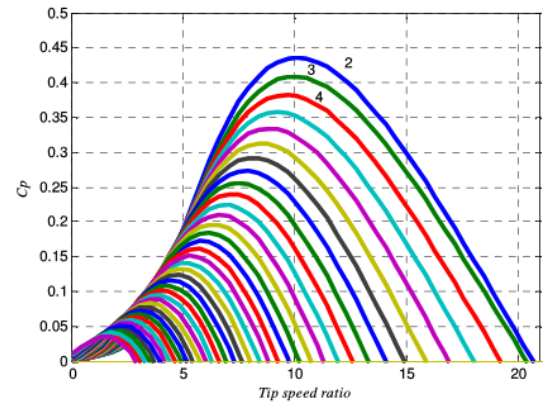
Some of the considerations (subject matter expert knowledge) for this process are:

- There is normally a phase in the start-up where the turbine will wait at ~30deg pitch before deciding whether to go ahead with starting up.
- 12 m/s rated wind speed
- From 12-24m/s – pitch control strategy
- From 0-11m/s – torque control strategy
- Pitch angle - 00° - low wind speed, pre-cut-in
- Pitch angle - 80° - high wind speed cut-out
- Dynamic behaviour, 10min average values is much time. The turbine could be shutting down during this time. Observations or data points in the “transition” areas need to be analysed further, including the time variable.
- The system works against springs that, in case of a failure, will pitch the blade to a safe position.
- The difference in the angles of the blades leads to shut down the turbine.
- A hydraulic pump constantly runs to maintain pressure (200 (bar)), with a pressurised tank providing back-up.
- It is also possible to create lookup tables to incorporate the relationship between variables and methodologies used in control system strategies as it is presented in

[40]. For example; the relationship between power output and wind speed and, the relationship between power coefficient, tip speed ratio and blade position. See Figure 80 a) and b).



a) Power v/s Rotor Speed v/s Wind Speed



b) Power Coefficient v/s Tip Speed v/s Pitch Angle

Figure 80. Wind turbine variables relationship [40].

To manage the large amount of data, a python code of the DTA is developed in this project. The output of the DTA is a new status vector, which is added to the original training data as it is shown in Table 46.

Table 46. New dataset with the status vector.

Training SCADA Data				Decision Tree Output
Wind speed	Blade position	Oil pressure	Power output	STATUS
8.971173	-0.88685	213.6772	1560	GREEN (0)
8.762393	-0.91292	213.9952	1600	GREEN (0)
8.661173	-0.86856	213.7737	1430	YELLOW (1)
8.489378	-1.00364	100.234	1590	RED (2)
.....	

5.5 K-Nearest Neighbours (KNN)

Once the status vector is assigned to the training data, the process requires a simple and fast assessment of the new observations. Additionally, this step needs to comprise a low computational effort. KNN is selected due to it is easy to interpret outputs, it has short

calculation and simulation time and, it has the prediction capability. Once, the training data and the status vector is created in Table 46, new data points are assessed using the KNN technique. This KNN is a two-dimensional (2D in Figure 69) process, analysing only wind speed and blade position points to identify anomalies that might represent failures in the pitch system.

The principle of the KNN technique is to find a number of training data points or predefined samples and estimate the closest distance to the new observation and assign a status label such as green, yellow or red. The distance can be any metric measure such as any standard Euclidean distance.

$$d(x, y) = \sqrt{(x_1 - y_1)^2 + (x_2 - y_2)^2 + \dots + (x_n - y_n)^2}$$

This method is known as non-generalizing machine learning method as it simply remembers all the training data with a fast indexing structure in Python [126] [116].

The “K” is the number of neighbours that are used to assess the status of the new observation. For example: in Figure 81, the new observation (e.g. wind speed vs blade position) is the blue point; red, yellow and green points are the training dataset with a pre-assigned status (green, yellow and red); the number of neighbours to be analysed is K = 5; and the dashed blue circle with the blue point as a centre encloses the five data points on the plane. Four out of five points are red therefore the new observation status is assigned red.

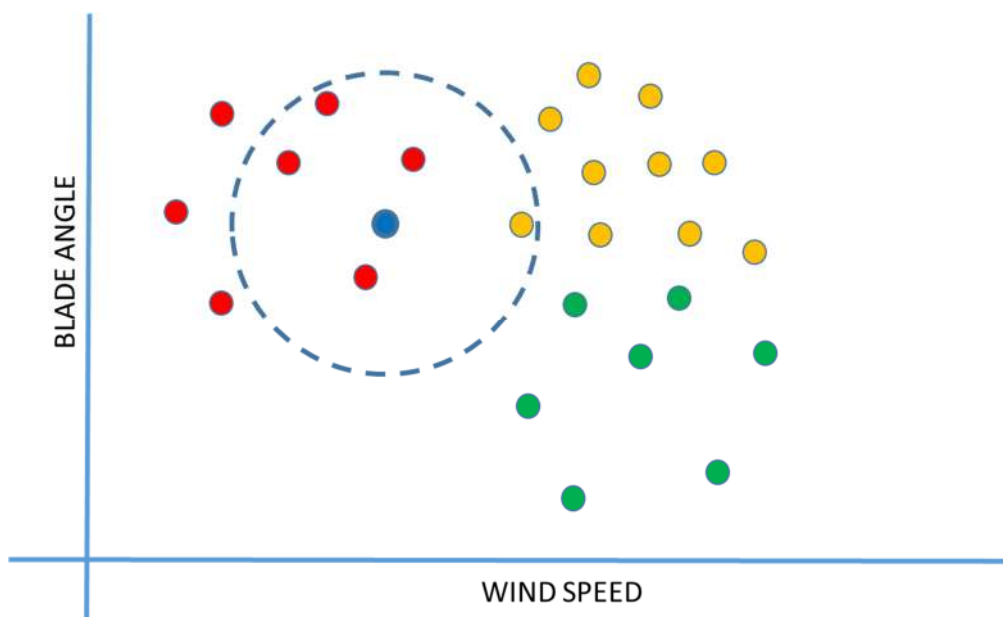


Figure 81. KNN example.

The optimal selection of the value K is highly dependent on the data, a larger K-value would reduce the effects of noise. However, it would make the classification boundaries less distinct [126] [116].

Usually, the nearest neighbours' classification method uses uniform weights, which means that the value assigned to a new observation is calculated from a simple common election of the nearest neighbours. In this study, due to the unknown behaviour of the pitch system, it is better to assign weights to the neighbours based on proximity. In other words, the nearest neighbours contribute more to the status selection. The variable weights = 'distance' in Figure 82, assigns weights proportional to the inverse of the distance from the new observation [126] [116].

5.6 Data mining approach outputs

The main output of the KNN technique is shown in Figure 82. The 3-class classification is performed using a K-value of 10 and assigning weights to the proximity of neighbours to the new observation. Green areas represent the normal behaviour of the pitch system; yellow areas represent potential failure events or component (variable) transition from one state to another. Finally, red areas represent anomalies in one or two variables, a failure in the hydraulic pitch system (e.g. low oil pressure < 200 (bar)). The background colour tells what the predicted response value (status) would be. The KNN method with the new status vector is applied to 1 year SCADA data of a turbine with a failure in the pitch system known in the wind farm maintenance logs. Before 17 days, the wind speed is less than 5 m/s and the blade angle registered in SCADA is around -0.9 degrees (Figure 82-A). During the day 17, an angle of 50 degrees is identified with a wind speed of 2.9 m/s (Figure 82-B), which is detected as red status (2) by KNN algorithm. In day number 22, the oil pressure decreased from an average of 208 bar to an average of 123 bar. The wind speed and blade angle associated with this event are detected by the method (Figure 82-C). Finally, figure 82 D and E shows the simulation of 6 months and one year, respectively. The new data points with low pressure or abnormal behaviour defined in the DTA were located near neighbours with yellow and red status.

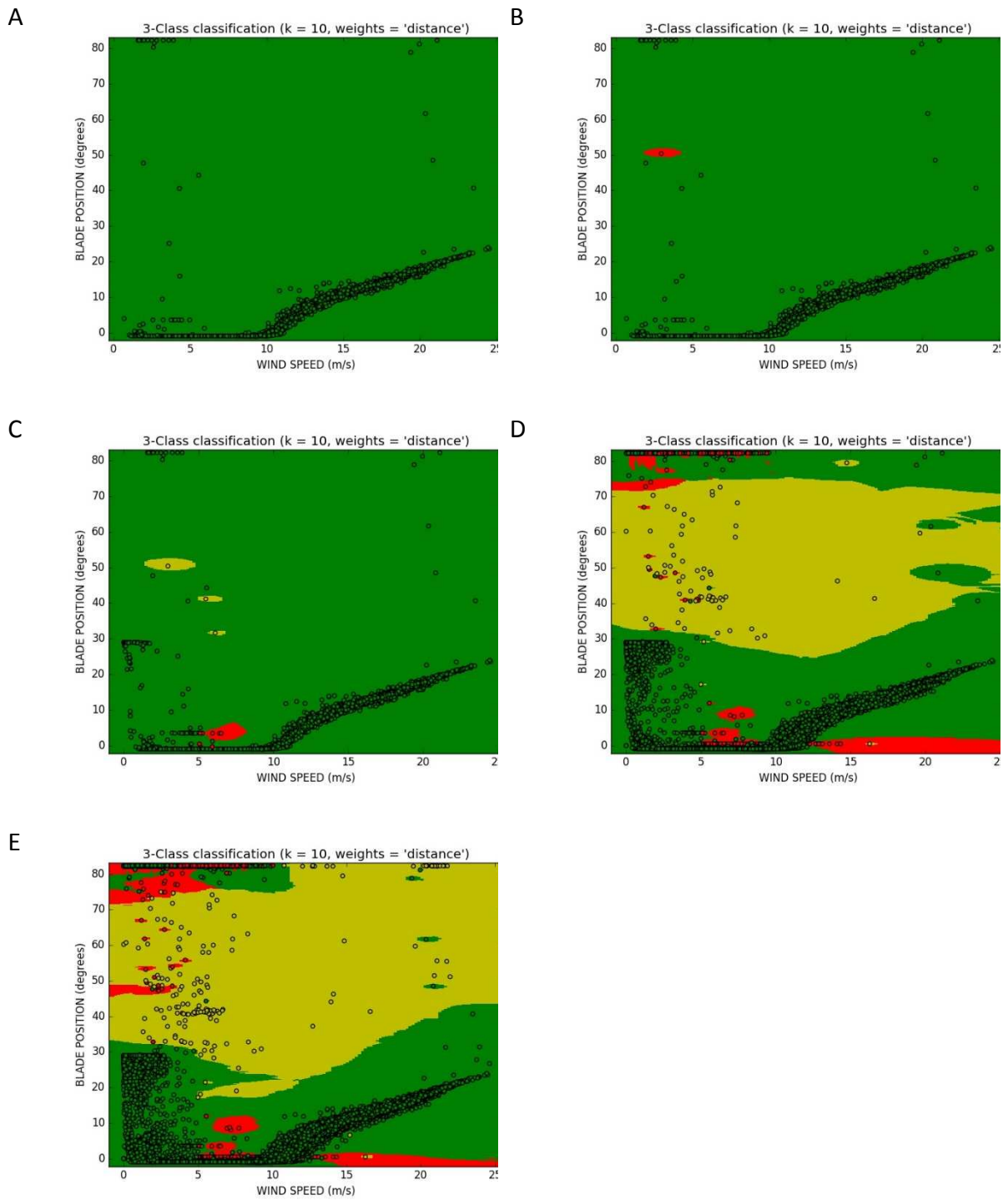


Figure 82. KNN main output

5.7 Conclusion

The pitch system failure modes and causes representing the overall condition were identified in the literature review. External leakage due to wear in the seals between the actuator rod and the cylinder, hydraulic supply line failure, valve connection failure, and internal leakage due to the wear of the piston seal are the most common failures. The development of algorithms representing the physics of failure using the SCADA data available is challenging. The SVM technique is applied to determine the normal behaviour of a known healthy turbine. This algorithm delivered a learnt frontier boundary which was analysed to establish the normal behaviour. However, the uncertainty accompanying the outputs is not calculated. The learnt frontier shows areas in the relationship between wind speed and blade position that are understandable only knowing the control philosophy of the turbine.

Subject matter expert knowledge of the offshore wind turbine is required to analyse the learnt frontier and assign conditions status to the variables pair. A decision tree algorithm is proposed to analyse the data based on the learnt frontier. The data is analysed in sections of the wind speed and blade position and interrogated using more variables; oil pressure and power output. These sections (e.g. 0-5m/s of wind speed and 0-10 degrees of blade position) may be reduced to improve the resolution of the analysis. The training data is 1 year of SCADA data. Each dataset point (wind speed, blade position) is interrogated by the decision tree and assigned a status value green if it is normal, yellow if it is abnormal and red if it is a failure.

The accuracy of this approach may be calculated by validating the model using historical SCADA data and maintenance logs with pitch system failures.

The final step of the proposed methodology is to interrogate new observations in real time using the KNN techniques. The KNN algorithm will use the training data with the status vector to assign a status to the new observation (wind speed and blade position). The main advantages of this approach are that it needs only two variables to detect abnormal behaviour. Therefore, it requires less computational effort and it is straightforward to implement. The accuracy of the KNN method also needs to be refined using more than one-year historical SCADA data for several turbines operating in different operational conditions.

Even though, data mining is a tool widely used in O&M of offshore wind farms, the combination of the decision tree and KNN methodologies is a novel alternative that allows

improving the accuracy of the analysis process by including subject matter expert and reducing computational effort.

CHAPTER 6 - O&M COST MODEL

6.1 Introduction

The O&M cost model is the final step in this project. It integrates the FMEA, physics-based models and data mining technique outputs to estimate availability and maintenance costs of a particular turbine in a specific location. Figure 83 shows the whole process to optimise O&M; the tools developed in previous chapters and the cost model, potential improvements for operators and, the main source of uncertainties. Profit maximisation comes from three different sources: improvements of turbine availability, reduction of maintenance costs and from, mean waiting time (due to logistics and weather) reduction.. The investment in maintenance efforts impacts the availability of the turbine and reduces the indirect cost of loss of revenue. The cost of maintenance increases exponentially near 100% availability (Figure 89). Knowing that there is a trade-off between turbine availability and maintenance cost, reaching an optimum at around 95% based on the SPARTA project outputs the O&M optimisation relays on the optimal maintenance strategy identification. This is an optimal combination of preventive, predictive and corrective strategy. Turbine reliability and meteorological conditions are identified as the main source of uncertainties. However, failure prognosis and data mining also comprise probabilities and assumptions that need to be taken into account.

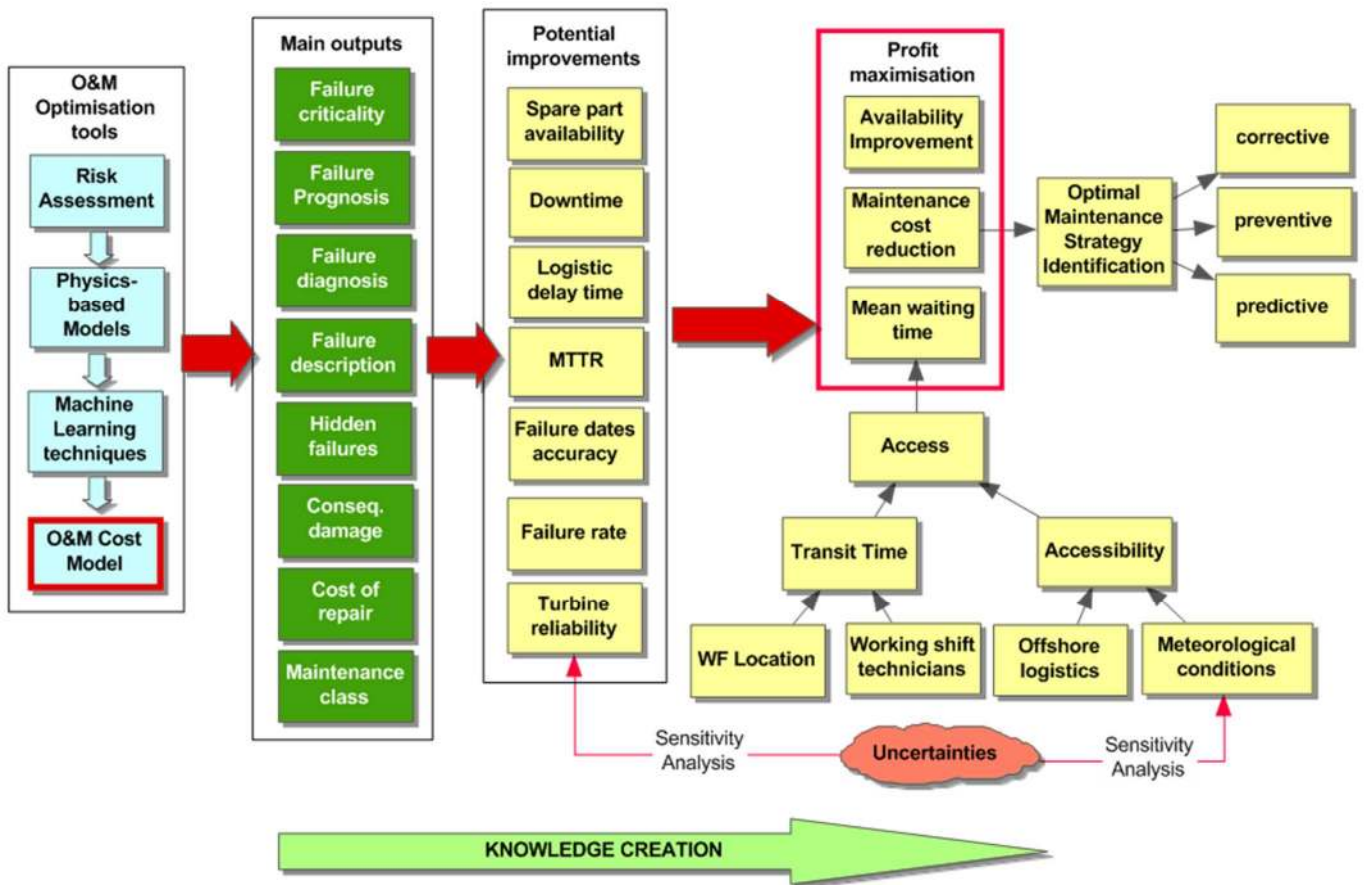


Figure 83. O&M optimisation tools and outputs.

6.1.2 Objectives

The O&M cost model can assist owners and operators of offshore wind farms to better estimate and control the costs of offshore wind farms integrating the approaches described in previous chapters. The final objective of this tool is to be a decision support system, a computer algorithm that analyses the measured data and visualises it in order to support the decision-making process.

Since O&M costs are driven by mainly unexpected failures and corrective maintenance [118], the task is to predict with greater accuracy if failures will occur, how many and what costs are associated with these failures on the short, medium and longer term. An O&M cost model uses the experience and data from the offshore wind farm as well as physics-based models, probabilistic models and data mining models to diagnose and predict accumulated damage and then, to update the cost estimates during the operating life.

The specific objectives are:

- To develop two maintenance strategies. First, an O&M strategy without failure prognosis outputs and second, an O&M strategy incorporating the physics-based models and probabilistic approaches to failure diagnosis and prognosis.
- To estimate the logistic delay time.
- To estimate the downtime of the turbine.
- To estimate the loss of production in kWh and monetary loss
- To estimate the turbine availability.
- To estimate the cost of repair including labour and vessels cost.
- To estimate hidden CO₂ emissions. Offshore wind farms comprise hundreds of turbines and the trend indicates that the number will increase in the future, therefore, the CO₂ emissions of vessels need to be considered into the decision-making process of operators during the project life cycle [1] [1] [127] [117].

6.1.3 O&M cost model outline

The process to include and compute the inputs and partial outputs are described in Figure 84. The O&M model was wholly implemented in Microsoft Excel. As the data that was used comes from different sources, the model will have input blocks to define and modify the original inputs. The input blocks are shown in yellow in the O&M cost model outline:

- Input block 1 – Maintenance classes: All maintenance actions, equipment, costs and logistics information for each failure mode are classified. O&M resources: labour, crew transport strategy, spare parts logistics, etc.
- Input block 2 – Wind turbine database: the FMEA is the basis to create the wind turbine database. Turbine breakdown model at a component level, critical assemblies regarding risk to the operation, component IDs and manufacturer, installation date, failure modes and causes. It also comprises the maintenance class per failure to include information such as repair equipment, MTTR, number of technicians to repair, repair actions, spare part availability.
- Input block 3 – Digital sensors: these inputs come from the previous chapters of physics-based models for the gearbox and power converter and, data mining approach for the pitch system. Physics-based failure predictions estimate the accumulated damage per assembly per turbine, remaining useful life and estimated

failure date. Data mining tool gives an indication when failure starts. The data mining model provides failure diagnosis with an alarm with low, medium and high failure risk.

- Input block 4 – Power output: wind probability distribution of the site derived from SCADA and, the power curve of the turbine Siemens SWT3.6MW-120.
- Input block 5 – Wind farm information: Wind farm characteristics: layout, distance from the port, inter-turbine distances, number of turbines and, turbine location, etc. This block will allow estimating of travels times, fuel consumption, CO₂ emissions and so on.
- Input block 6 – Meteorological simulation: wave height, wind speed and direction, lightening, visibility, safety thresholds. The final output is the mean delay time in days per month.
- Input block 7 – O&M Strategy: selection of maintenance activities and intervals based on failure rates and criticality of the components, condition monitoring system and digital sensors.
- Input block 8 – O&M information: information related to the O&M strategy and the wind farm characteristics such as number and type of vessels and, number and shift of technicians.
- Input block 9 – Economic parameter prediction: fuel cost, spare part cost, labour cost and electricity sales price.

Results of the O&M cost model

The main outputs of the O&M cost model are time-varying cost estimations, green blocks (input and outputs) and pink bubbles (maintenance strategies) in Figure 84.

- Optimal maintenance strategy selection. Three types of maintenance are considered (Figure 87): Annual time-based maintenance, condition-based maintenance including digital sensors, risk-based maintenance and unscheduled maintenance.
- Turbine downtime and availability, loss of production, revenue losses, cost of repair and CO₂ emissions.

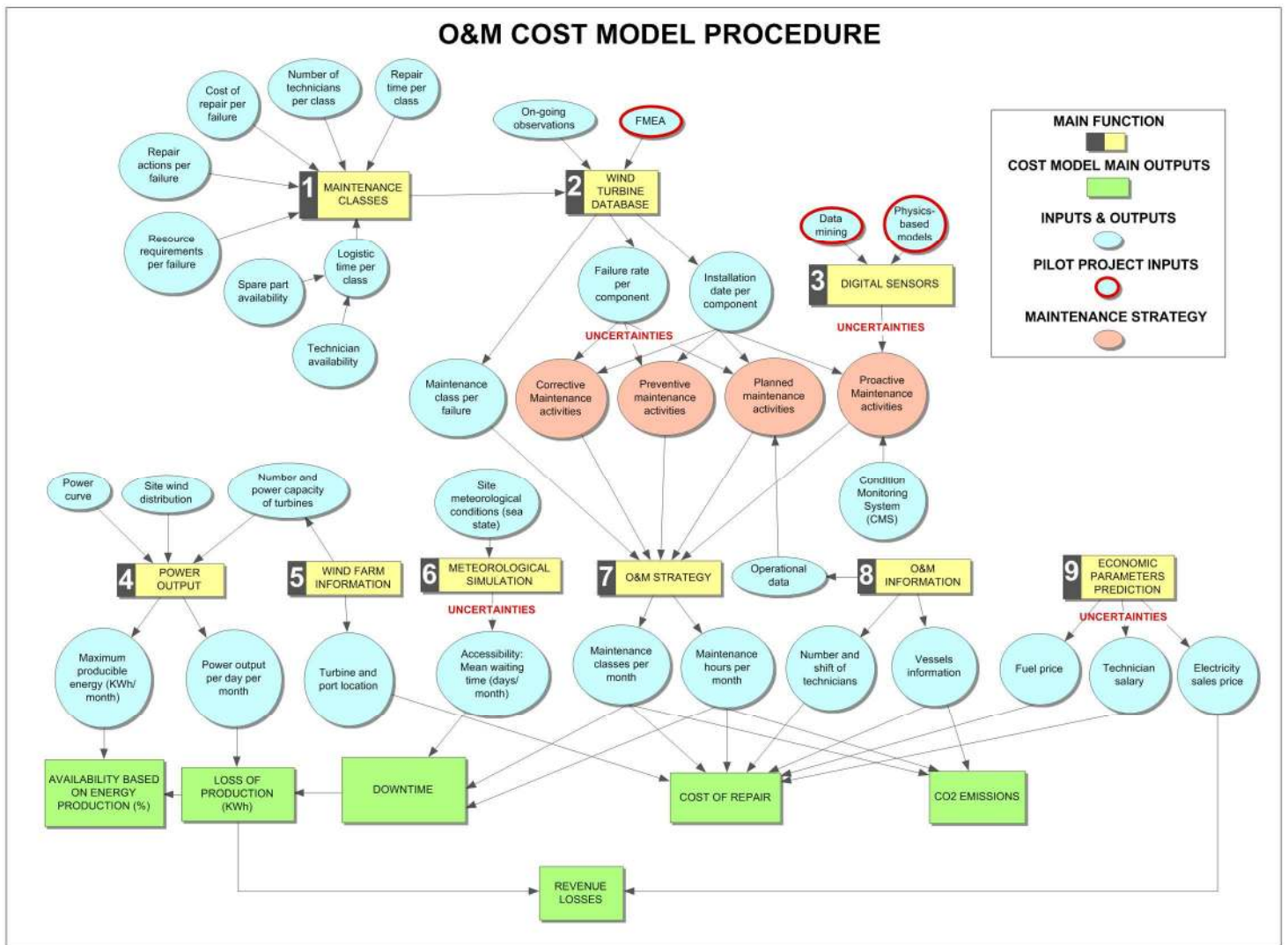


Figure 84. O&M cost model outline.

6.2 O&M of offshore wind farms

The O&M optimisation of offshore wind farms is integrated into the asset management framework proposed by Lloyd's Register shown in Figure 85. The flow diagram describes the process that needs to be taken to performed asset integrity service of offshore wind farms. The figure identifies three key phases: integrity goals definition, risk understanding and risk management. O&M optimisation factors such as FMEA, strategy, condition monitoring etc. can be identified in all the three key phases.

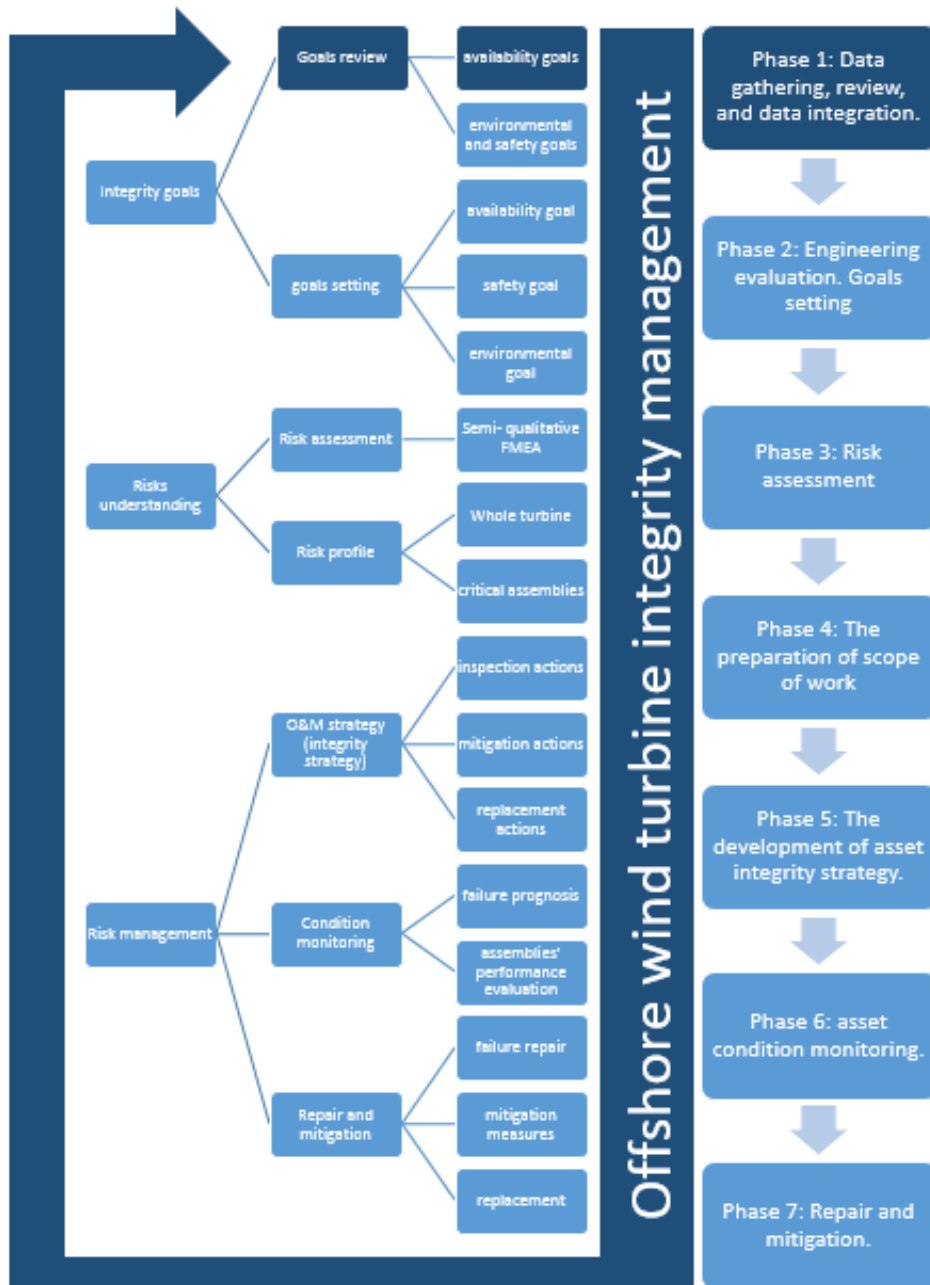


Figure 85. Asset integrity management of offshore wind turbines.

The analysis of market segmentation and market strategy allows the identification of the requirements for the asset management tool and, therefore for O&M optimisation. The main drives of asset management are:

- To understand offshore turbine operation under certain conditions
- To understand failure mechanisms in order to design a preventive maintenance strategy

- To identify hidden failure to reduce downtime and unscheduled maintenance activities
- To optimise O&M resources such as vessels, technicians, ports, spare parts and equipment.

6.2.1 Key offshore wind energy O&M market trends

Based on previous studies [128] [118] [129] [119] [130] [120] and [131] [121], key offshore wind energy market trends are identified and used as a reference to develop the O&M cost model:

- Average OPEX of a typical offshore wind turbine is £70,000/MW/year.: “The estimated OPEX for a typical offshore wind turbine ranges from £60,000 / MW/year (E&Y, 2009) to £87,500 /MW/year (BVG Associates, 2012). These figures do not include leases paid to The Crown Estate (TCE), Transmission Network Use of System (TNUoS) charges or operational insurance premiums”[128] [118].
- Catapult 2015. Studies suggest that the cost of O&M represent between 15% and 30% of the LCOE [128] [118].
- Reliability target of main components: O&M products need to focus on increasing reliability and availability to maximise energy production or to the minimise levelised cost of energy (LCOE).
- Offshore wind farms out of the warranty period (~2700 turbines in 2020 in Europe): offshore wind farm operators or asset owners have to use a tool to optimise O&M.
- Unscheduled maintenance activities represent an important percentage of O&M resources. Based on the SCADA data analysis,unscheduled maintenance hours can reach 40% of the total time of maintenance. Additionally, 21% of the total time is recorded as a fault-finding maintenance activity [130] [120].
- The reduction of unscheduled maintenance tasks might be accelerated by implementing an integral O&M approach considering the risk to the operation, failure prognosis, weather forecasting and financial models.
- A lack of effective interpretation of data increases reactive activities and therefore, the cost of O&M.

- O&M activities represent between 15% to 30% of the LCOE and 60% of the OPEX [131] [121].
- The OPEX breakdown is described in the following table [129] [119]:

Table 47. OpEx breakdown[129] [119].

Item	Value (%)
Crane barges or vessels	25
Part and consumables	15
Vessels and logistics	11
Service provider profit and risk margin	10
technicians	8
insurance	9
Balance of plant maintenance	3
Onshore based personnel	1
Onshore service base	1
Other OpEx	17

- When estimating the costs of O&M of offshore wind farms, maintenance costs can be categorised as follows:
 - Costs of unscheduled maintenance to repair failures
 - Costs of scheduled preventive maintenance activities
 - Costs of scheduled major replacements of the wind turbine. Major replacement activities need to be included in the cost model as they affect the component or assembly reliability and therefore the maintenance cost estimation.

6.2.2 O&M logistics

Based on the reports [128] [118][129] [119][132] [122][133] [123], a typical maintenance team and logistics are described in Figure 86.

The distance from the port, port facilities and weather conditions at the location govern the O&M logistic strategy [132] [122]. Commonly there are three options:

- Port-based work boats;

- Port-based work boats plus helicopter support;
- Fixed or floating offshore base (e.g. ‘motherships’).

Table 48 describes different scenarios for the utilisation of different vessels.

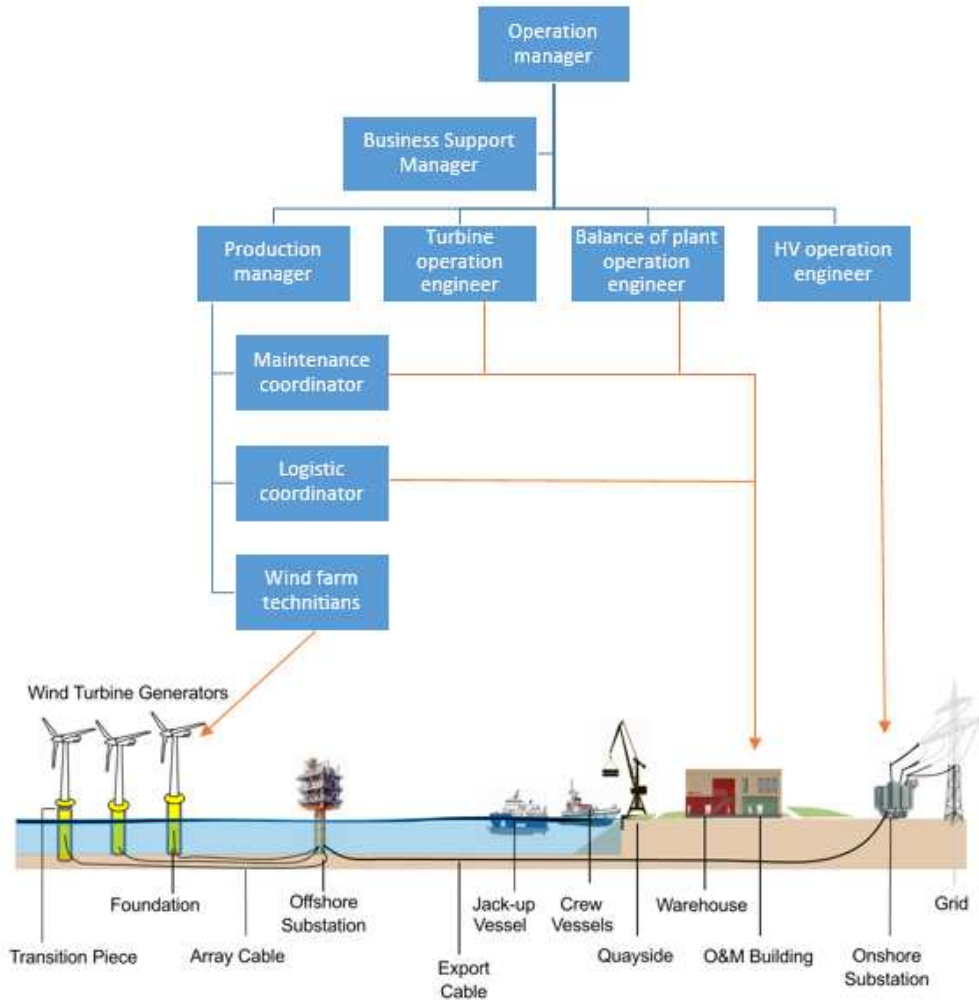


Figure 86. Maintenance team and logistics [117].

Table 48. Vessels utilization features [132] [122].

O&M strategy	Relative cost	Operability (weather conditions)	Transit speeds	Distance port to wind farm
Work boats: based at a coastal port.	Low	Limited: maximum wave height of 1.5m.	Slow: ~20knots	Less than 75km
Helicopter access for work boat support or primary access.	High	High: Visibility restrictions only	Quick: ~135knots	
Fixed or floating offshore base.	High	High	NA	More than 75km

The operation comprises monitoring, controlling and coordinating the day to day activities including remote monitoring, port facilities management, vessels for crew transfer and electricity sales.

- Monitor & control the turbines
- Monitor & control the HV and auxiliary systems
- Control the turbines, HV systems and BOP to facilitate maintenance & repair activities

Maintenance takes into account all the actions required to efficiently run turbines and balance of plant. The balance of plant comprises all infrastructural and facilities of an offshore windfarm with the exception of the turbine and all its elements. The balance of plant therefore mainly comprises of the following items.

- Crane pads/ Hard standings
- Foundations
- Substation Civil and Electrical
- Road upgrades and Construction
- Cabling to substation and Grid
- SCADA
- Transformers
- Miscellaneous Costs

Maintenance comprises preventive (scheduled) and corrective (unscheduled) activities of repair and inspections. See Figure 87.

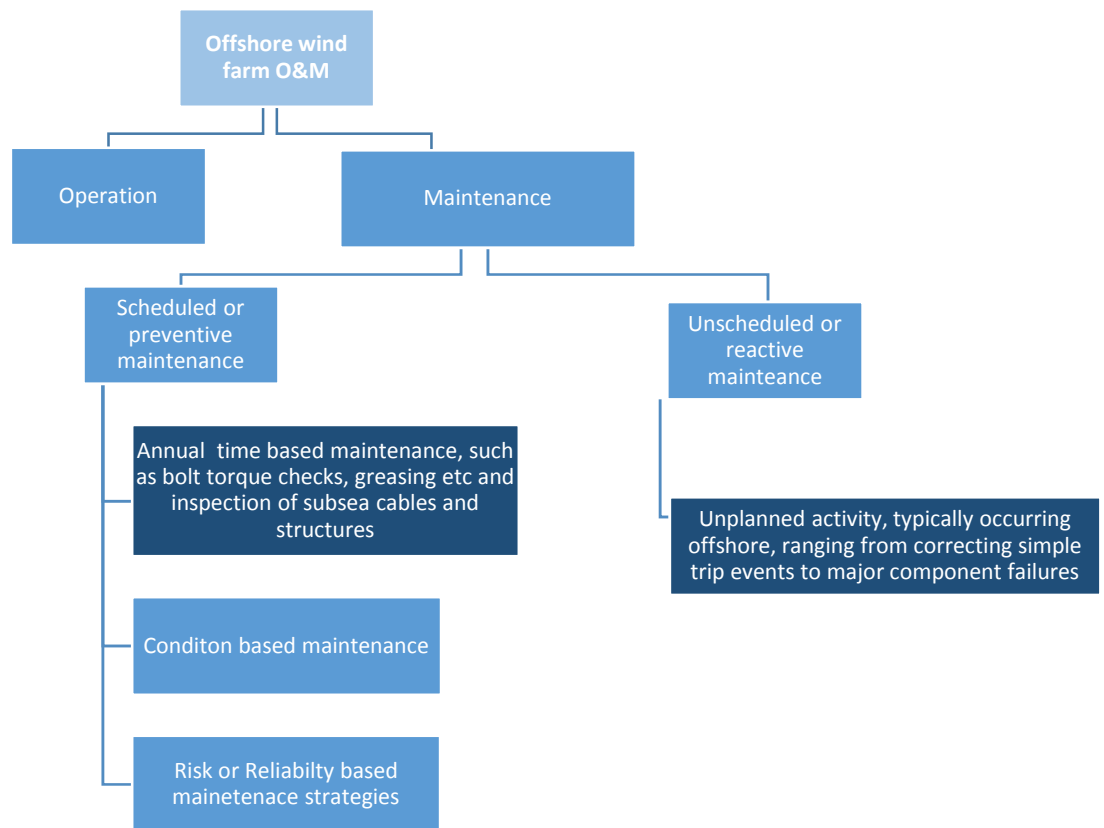


Figure 87. Maintenance strategies.

6.2.3 Spare part management

As described in the literature review, spare part management is a crucial part of O&M optimization. It accounts for a range between 8.3% and 16.7% of the total O&M costs [68] [65]. The positive impacts that are identified in spare part logistics improvements are offshore turbine downtime reduction, reduction of the value of the spare part in inventory and, spare part availability improvements.

The key performance indicators that depend on effective spare part management are:

- Unscheduled downtime
- Spare part availability
- Inventory management
- Response time
- Abortive work, parts delayed

Based on [134] [124], 70% of the time the spare part is available in the local depot which represents no delay in the O&M logistics, 25% of the time the spare part is available in another depot which represents 1 day of delay and, 5% of the time the spare part is not available and need to be ordered with the manufacturer which can represent until 7 days of logistics delay time.

6.3 O&M optimization overview

An offshore wind turbine has thousands of components; each of them may fail in different ways. Figure 88 shows a holistic view of the prognosis and diagnosis of failure modes and their impact on the O&M strategy. Different failure modes, failure mode 1, 2 and 3 in the figure, have a different mean time to repair (MTTR) and consequently different turbine downtime. There are several ways to predict and diagnose failure modes and they have different technical and economic implications. For example, the statistical-based approach is inexpensive. However, it is only able to predict failure events after they occur. Inspections are quite reliable, but they can only detect a failure when it is already advanced. New condition monitoring systems are more accurate for failure prognosis and allow more time to plan maintenance activities before failure, however; they might also reduce or degrade turbine reliability with the incorporation of more systems. Data mining and physics-based models are inexpensive and have the capability to diagnose and predict failures; nevertheless, they require considerable engineering effort and validation.

Figure 88 gives an example of the O&M optimisation challenge. It correlates failure modes with access windows and maintenance strategies. For example, access windows are defined using the significant wave height under a certain safety threshold for a specified period. The planned maintenance activities are already set for the whole period. Failure mode 1 occurs during a no-access period; therefore, it will comprise loss of production and potential consequential damage of other components. Choosing one of the failure prognosis and diagnosis techniques with enough time in advance, failure mode 1 might be avoided if it is included in planned maintenance 2.

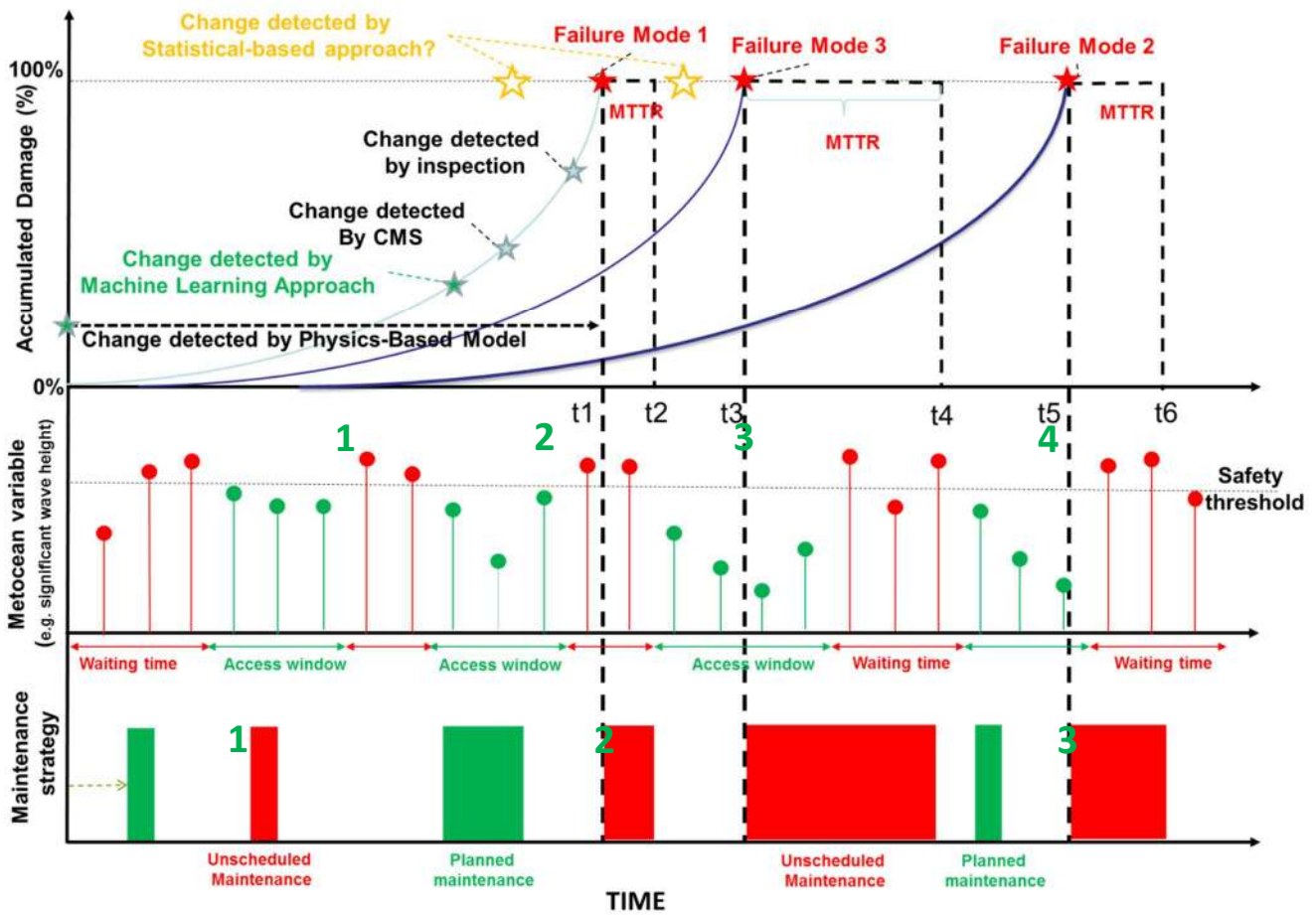


Figure 88. Prediction of accumulated damage techniques, accessibility and O&M strategy.

There is a trade-off between O&M cost reduction and availability improvement. Figure 89 shows qualitatively that after a certain point of availability improvement or maintenance effort, the cost of maintenance starts rising again. The direct cost of O&M such as vessels, spare part and technicians increases exponentially with maintenance efforts to improve availability. The indirect costs, such as loss of production, decrease linearly with the maintenance efforts. Therefore, based on [123] there is a point in the graph around 95% availability where the cost of O&M starts increasing again.

Turbine availability depends on wind farm characteristics such as turbine location and turbine age. The report in [135] [125] shows that availability improves with age and decreases with the distance to the port.

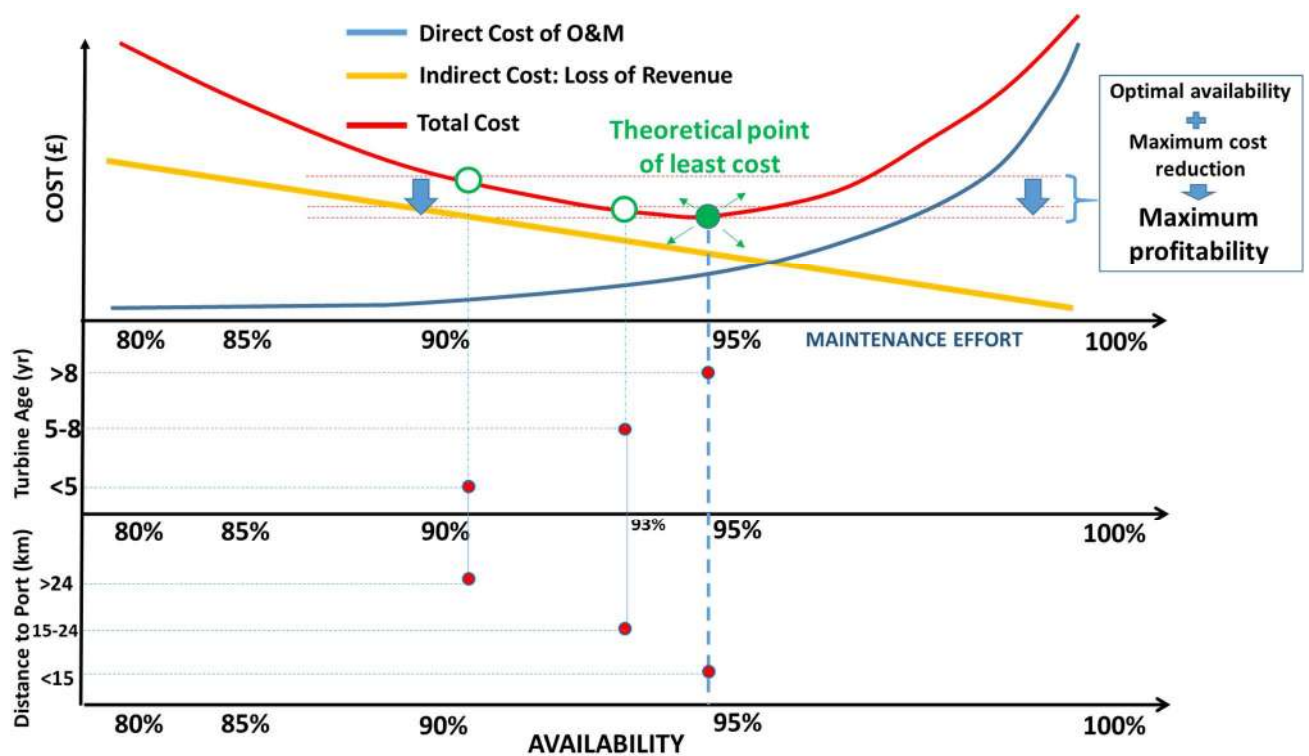


Figure 89. Optimal maintenance costs, turbine availability, distance to port and turbine age [117].

To optimise O&M, it is necessary to predict a failure and access window far enough in advance. The necessary resources to repair a failure will depend on the wind farm and turbine characteristics. Logistical delay time improvements will also contribute to optimise O&M by reducing the waiting time for technicians and spare parts.

6.4 O&M cost model

6.4.1 General description

This cost model is based on the methodology proposed in [136] [126] and developed in Microsoft Excel using a fictitious offshore wind farm with 24 turbines. The O&M cost model includes a wind farm model with actual specific wind farm data, and damage accumulation algorithm (time-dependent variable) for each turbine in the offshore wind farm.

In case of a failure event, the next process is adopted for this cost model:

1. Alarm will be notified (operation office)
2. The operator needs to decide between the following:
 - a. Turbine can be restarted remotely without a visit to the turbine
 - b. A visit is required to determine whether the turbine can be restarted without maintenance or whether maintenance activities are required first.

3. Operator organise repair actions
4. Time to Repair (TTR) is divided into the following periods:
 - a. Logistics time: crew, spare part and equipment are ready to depart.
 - b. Waiting time: period of time that the weather does not allow safe access to the turbine.
 - c. Transit time: travel time from port to the turbine.
 - d. Repair time: the time needed to repair the failure.
 - e. Return time: travel time to return to port.

6.4.2 Maintenance classes, repair actions and spare part availability

Maintenance classes are crucial for the development of this O&M cost model. They are assigned to every single failure mode identified in the FMEA to correlate the failures with costs and resources necessary to repair them, as well as the logistic delay time.

Each failure mode and its associated repair actions are classified based on repair actions, crew and equipment required to repair. The maintenance classes are defined in Table 49 and Table 50 based on studies in [137] [127], [136] [126] and Lloyd's Register experience with offshore wind farm operators.

Table 49. Maintenance classes' description (continuous) [79][124][125]

Class	Value	Visit to turbine	Type of repair	Vessel required	Number of technicians	Spare parts requirements
A	1	remote reset – no visit to the turbine required	remote reset	no vessel	0	no parts
B	2	turbine visit (inspection) – manual reset may be required on site – minor part replacement, top up lubrication, replace consumables such as filters	manual reset	CTV	2	no parts or minor parts or consumables, carried by technicians
C	3	second visit required – possibly additional trouble-shooting required – incorrect tools or spares carried on first visit	minor-medium repair	CTV	3	larger parts lifted in bag using on-board crane (either turbine davit crane or standard crane on CTV)
D	4	overnight stoppage of turbine – repair which cannot be fixed immediately – may take longer than a single day – may need rope-access to less accessible external parts of turbine	major repair	CTV/FSV	4	specialist spare parts (may be small or large)
E	5	Major turbine outage – specialist vessels required to be chartered from the spot market, such as jack-up barge.	major replacement	specialist vessel/HLV	6	significantly large items, entailing significant logistical requirements for transport and transfer to turbine – heavy-lift crane required – examples include blade, gearbox, main bearing, transformer
F	6	visit to the turbine due to planned maintenance	planned maintenance	CTV	2	minor parts or consumables, carried by technicians or larger parts lifted in bag using on-board crane (either turbine davit crane or standard crane on CTV)
G	7	annual service	annual service	CTV	3	minor and larger parts or consumables, carried by technicians or larger parts lifted in bag using on-board crane (either turbine davit crane or standard crane on CTV)

Table 50. Maintenance classes' description[79][124][125]

Class	Spare part weight (kg)	Spare parts availability	Spare part logistic time (days)	Weather window	Repair time (days)	Min spare part Cost (£)	Max spare part Cost (£)
A	<2000	no parts	0	no delay due to weather	0.167	£ -	£ -
B	<2000	spare parts available on board SOV	0	technician transfer CTV to turbine – duration of tasks between 1 and 4 hours	0.167	£ -	£ 500.00
C	<2000	spare parts available from port or near onshore warehouse	0	each task between 4 and 8 hours each	0.33	£ 500.00	£ 20,000.00
D	<2000	spare parts available at port or potentially order readily-available, generic part from supplier	1	2 or more separate weather windows each of several hours duration	1.5	£ 20,000.00	£ 74,000.00
E	>2000	long logistical delay – spare parts ordered from supplier, possibly bespoke part from Siemens or single supplier	7	several days for each visit, reasonable weather required over several weeks or months	5	£ 74,000.00	£ 340,000.00
F	<2000	spare parts available on board SOV	0	no delay due to weather	4	£ 1,000.00	£ 19,000.00
G	<2000	spare parts available on board SOV	0	no delay due to weather	2	£ 1,000.00	£ 19,000.00

It is also necessary to describe how the repair is going to be carried out and how the equipment is going to be used. This process is used to estimate the time to repair a failure in the maintenance classes. An example of this process for maintenance class B is shown in Table 51.

Table 51. Repair actions per maintenance class[79].

Event	Maintenance Class B
1	travel of access vessel with 2 technicians and spare part
2	transfer of technicians from vessel to turbine
3	inspection of failure and decision of replacement
4	in case of replacement, spare part is lifted using the internal crane in the platform
5	failed component is removed from the turbine using the internal crane in the nacelle
6	spare part is mounted using the internal crane in the nacelle
7	failed component is moved from the platform to the vessel using the crane
8	return to port

6.4.3 Wind turbine database

The wind turbine database comprises information for all the turbines in the offshore wind farm. It contains the location of each turbine and a comprehensive hierarchical breakdown of components of each turbine based on the FMEA previously developed. The FMEA is the base of the wind turbine database. The information per component is complemented with operation data such as installation date and manufacturer per component, maintenance class per failure mode, turbine ID and SCADA systems detection methods. An example of the database spreadsheet for each wind turbine in the wind farm is given in Figure 90.

Assembly	Assembly description	Sub-Assembly	Installation date
frequency converter	frequency converter master & slave – 2x3MW – NetConverter generator side converter – module		01/01/2015
pitch system	pitch regulation with variable speed – independent pitch sys pitch rams		01/01/2015
pitch system	pitch regulation with variable speed – independent pitch sys hydraulic pitch pawl		01/01/2015

Potential Failure Mode	Failure Mode Refer	Potential Root Causes	Maintenance Class
IGBT/Diodes failure, electrical failures	FEI10	thermal stress	class B turbine visit
leak	FAR40	failure of seal	class C second visit required
unknown status	FAR67	sensor failure	class C second visit required

Global Effects	Consequential Damage?	Affected Component	Detection Method	Prevention Method	Failure rate/year
switched to operate at I no		power converter	SCADA error raised (141010)	forced outage	2
excessive loads, failure none		pitch ram	inconsistency between blade	inspection, accurate records, accu	1
manual reset required none		pitch pawl sensor	SCADA error raised (103004)	none	0.111111111
switched to operate at I no		power converter	SCADA error raised – multiple planned	corrective action	2
switched to operate at I no		power converter	SCADA error raised (141049)	forced outage	1

Figure 90. Example of the wind turbine database.

The failure rate is assigned to each failure mode and cause using the occurrence rating which was defined using operation data and offshore wind farm operators experience. The failure frequency in Table 52 is given by technicians of an offshore wind farm.

Table 52 Failure rate based on FMEA occurrence rating.

Value	Failure Rate/year	Label	Description	Failure frequency
1	0.040	Extremely-Unlikely	failure almost never occurs	25 years (once per turbine lifetime)
2	0.111	Rare	irregular and unlikely failures	8–10 years
3	0.286	Occasional	occasional but not necessarily regular failures	2–5 years
4	1.000	Frequent	repeated failures with regular occurrence	12 months
5	2.000	Inevitable	failure is almost inevitable, will definitely occur	1–6 months

The wind turbine database will be used to establish the O&M strategy by selecting those failures and components that may require maintenance actions within a period.

6.4.4 Digital sensors

The digital sensors are the outputs of the physics-based and data mining models explained in chapter 3 and 4 respectively. Table 53 shows the digital sensors for all the assemblies. Only the outputs of the gearbox, power converter and pitch system digital sensor are considered within the O&M cost model.

Table 53. Digital sensors as inputs of the O&M cost model

Assembly	Sub-assembly or Component	Failure Mode	Maintenance Class	Accumulated Damage (%/year)	Remaining Useful Life (months)	Estimated Failure Date (month/year)	Condition (green, yellow, red)
hydraulic station							
induction generator							
gearbox	HSS bearings	deformation due to fatigue	class E	4%	288	2039	
control system							
rotor lock							
tower							
transformer							
electro- magnetic rotor							
frequency converter	PC-Module	Diode, IGBT	class B	60%	4	Aug-17	
generator main bearing							
yaw system	Gears		Class E	50%	12	Jan-18	
switchgear							
mechanical brake							
generator cooling system							
blade							
pitch system	Hydraulic system	leakage	class B				yellow
nacelle auxiliary structure							
transition piece							
nacelle primary structure							
foundation							
generator stator							
lightning protection							
pitch bearing							
nacelle auxiliaries							
power export cable							
hub							

6.4.5 Maintenance strategies

In order to analyse the cost of repair, availability and loss of production, using the digital sensors developed in previous chapters, a case study is established and presented in the following.

Wind farm and operational data

The wind farm case study of 86MW is based on a group of turbines of a real offshore wind that is anonymised. The turbines are selected taking into account the original position of the turbines within the wind farm design as well as 1 year SCADA data. The fictitious wind farm used for this study is described in Table 54. The calculations of the main outputs: availability, downtime, costs and other KPIs, are performed for one turbine only.

Table 54. Wind farm characteristics.

Item	Value	Unit
Distance to Port	30	km
Inter-turbine distance in a line	1	km
Distance between turbine lines	1	km
Number of turbines	24	
Turbine power capacity	3.6	MW
Wind farm MW installed	86.4	MW

The operational data in the O&M cost model is used to indicate the percentage of corrective maintenance activities that a real offshore wind turbine can experience. This information is used to set up the number of unexpected failures and the corresponding component in the case study (Table 55). The unscheduled and scheduled hours per year allocated per turbine are derived from 1 year SCADA data.

Table 55. Percentage of scheduled and unscheduled maintenance hours.

Turbine	Unscheduled (hrs/yr)	Scheduled (hrs/yr)	Unscheduled (%)	Scheduled (%)
WT1	12.65	94.11	12%	88%
WT2	29.84	67.84	31%	69%
WT3	4.8	7.92	38%	62%
WT4	30.52	95.85	24%	76%
WT5	26.31	103.83	20%	80%
WT6	17.97	84.98	17%	83%
WT7	27.52	68.92	29%	71%
WT8	18.3	57.73	24%	76%
WT9	32.02	27.27	54%	46%
WT10	18.54	81.32	19%	81%
WT11	15.74	40.86	28%	72%
WT12	14.14	95.66	13%	87%
WT13	48.45	138.85	26%	74%
WT14	27.3	78.61	26%	74%
WT15	15.78	19.15	45%	55%
WT16	12.13	91.57	12%	88%
WT17	94.47	70.81	57%	43%
WT18	52.24	67.86	43%	57%
WT19	19.25	54.4	26%	74%
WT20	17.81	93.5	16%	84%
WT21	61.18	75.88	45%	55%
WT22	25.41	67.42	27%	73%
WT23	36.11	55.2	40%	60%
WT24	42.25	79.61	35%	65%
Average	29.20	71.63	29%	71%

O&M information

More information about the O&M resources of the wind farm is required to establish a strategy since technical capabilities of the items such as vessels' maximum wave height, and fuel consumption are essential for the O&M process [138] [128].

Table 56. O&M information [138] [128].

Number of helicopters	0					
Number of crew transfer vessels	2					
CTV speed	24	knots	1.852	km/hr / Knot	44.448	km/hr
Fuel Consumption	446	litres/hour				
Charter rate	3250	£/day				
CO2 emissions	2.68	kgCO ₂ /l	Diesel			
Operation wave height	1.5	m				
Jack-up barge	1					
Charter rate	80000	£/day				
Total number of technicians available	7					
Single shift of technicians	12	hr	8am-8pm			

O&M strategies

Case study: Current O&M situation – at the beginning of a wind farm project the O&M strategy is usually set-up based on assumptions and estimations using generic data. This strategy comprises a time-based and unplanned corrective maintenance. Typically, turbines are being visited twice a year, and the duration of each visit is between 3 to 5 days (4 days average). The case study comprises 24 Siemens 3.6MW turbines with a total capacity of 86.4 MW located 30km offshore.

When a component is not maintained in time or properly, component degradation increases and eventually, the component will experience a failure. Therefore, unplanned corrective maintenance is carried out. Based on 1 year of operation data, each of the 24 turbines has a certain percentage of unscheduled and scheduled maintenance hours, which is used to set up the baseline case study. When the component is maintained in time, the maintenance activity is performed during the period of low wind speeds and vessels are ready to depart immediately. In this situation, the logistic waiting time of the turbine is zero.

Technicians have on average a working day shift of 10 hours, constant throughout the year during the daylight. The total number of staff reported (onshore and offshore) ranges between 0.37 to 0.75 persons per turbine and 60% of them are technicians [139] [129].

Therefore, a wind farm of 24 turbines should have an average of 12 staff in total and 7 turbine technicians.

The power curve of the turbine and 1-year historical wind speed data from the SCADA system are used to estimate the total electricity production in kWh at given wind speeds per month.

Based on Figure 87, there are two categories of maintenance:

- Scheduled maintenance
 - Annual time-based maintenance: Class G in maintenance classification (Table 49)
 - Condition Based Maintenance (CBM): Power converter (Class B)
 - Risk-Based Maintenance: Pitch system and gearbox (Class F)
- Unscheduled maintenance
 - Unplanned activity: based on Table 55, the average percentage of unscheduled maintenance hours per year is around 30%.

Table 57. Planned maintenance based on component condition and risk.

Assembly	Maintenance Class
Power converter (RBM)	B
Gearbox (CBM)	F
Pitch system (RBM)	F
Annual service	G

Table 58 shows that the assemblies gearbox and pitch system have a planned maintenance activity, which comprises a visit to the turbine with minor parts carried by technicians in the CTV and lifted by the turbine crane. Maintenance class F take place in April (after winter) and August (necessary inspection during summer time to be prepared before). Based on O&M operational data and previous failure reports, the power converter is likely to experience more than one failure per year. Therefore Table 58 shows a maintenance class B in April for the power converter. Finally, the annual service for WT1 is selected in the summertime where the waiting time due to weather conditions is expected to be zero.

Table 58. Case study: scheduled maintenance WT1.

CASE STUDY - WT1		REPAIR TIME												
Scheduled Maintenance (Repair Time per turbine)	Maintenance Class	Jan.	Feb.	March	Ap.	May	Jun.	Jul	Aug	Sep.	Oct.	Nov	Dec	Repair Time TOTAL(hr)
Time-Based Maintenance	Class F				96				96					192
Condition Based Maintenance	Class B				4									4
Annual Service	Class G						48							48
Total number of hours of Repair Time		0	0	96	4	0	48	0	96	0	0	0	0	244

Table 59 shows the unscheduled maintenance activities assumed for the WT1 due to failure or abnormal behaviour in the power converter and pitch system assemblies. It is assumed to expect a power converter failure in June and a pitch system failure during winter in December.

Table 59. Case study: unscheduled maintenance WT1.

Assembly	January	February	March	April	May	June	July	August	September	October	November	December
Power converter						Class B						
Pitch system												Class C

Optimised case study: integration of predictive maintenance with “digital sensors” into the original case study. Tools to estimate the damage of critical components are used, and failures class B and C in Table 59 are reduced or eliminated. Table 60 shows that the unscheduled maintenance class B for the pitch system is carried out in April instead of June as scheduled maintenance and, the unscheduled maintenance class C of the pitch system is now carried out in August as scheduled maintenance class B.

Table 60. Case study: digital sensors application.

Assembly	January	February	March	April	May	June	July	August	September	October	November	December
power converter				Class B		Class B						
pitch system								Class B				Class C

6.4.6 Meteorological conditions

The calculation of the mean waiting time for an access window, shown in Figure 91, is based on the study in [140] [130]. The number of days per month in the figure describes the delay time due to the availability of technicians and spare part. The calculation process is described below and the values of the mean waiting time are adopted for the offshore wind farm in the O&M cost model.

Accessibility – weather windows

Weather data is a key input for the O&M cost model. A concise model of the weather conditions will ensure that the O&M strategy is modelled more realistically with more accurate cost estimations.

A Monte Carlo based approach, Markov Chain model (MCMC) has been proposed to determine accessibility and to estimate the power capture and therefore the loss of revenue. MCMC is a probabilistic approach using a dataset with sea states able to produce a time series of the meteorological variables [140] [130].

Time series variables:

- Significant wave height

Wind speed 10m above sea level is also necessary to establish a 24 hours period where significant wave height and wind speed remain under safety threshold. This parameter will vary based on wind farm location and vessels characteristics.

MCMC has been created using a SCADA dataset with a 1-year period at 10-minute intervals. In order to identify sea states, it is necessary to define bins of the parameters. The range of the data bins gives the resolution of the values since a greater or smaller number of data points will fall into each bin:

- Significant wave height: 0.25m to 9.75m with steps of 0.5m
- Wind speed: 0m/s to 25m/s with steps of 1m/s

The dataset is also organised in months to identify seasonal changes in the sea states. A fundamental property of MCMC is to determine a “sea state” at any given point based on the previous “sea state” at a previous interval. Therefore, the monthly data comprises 5 days of the previous and next month, and for each 24-hour interval, the next interval sea state is recorded.

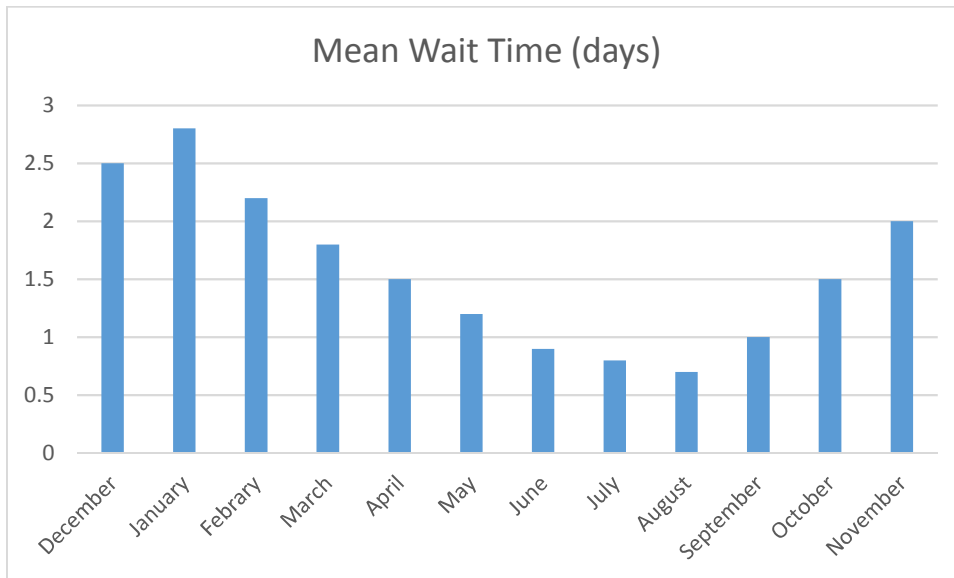


Figure 91. Mean waiting time per month [140] [130]

The average number of hours of daylight derived from [141] [131] is shown per month in Table 61. The daylight hours per month is used to assess if one day is enough to repair a failure based on the shift of technicians and repair actions description.

Table 61. Mean waiting time and daylight hours

Month	Mean Wait Time (days)	Av. Hours of Daylight	Season
December	2.5	8	winter
January	2.8	8	winter
February	2.2	9	winter
March	1.8	11	spring
April	1.5	13	spring
May	1.2	15	spring
June	0.9	16	summer
July	0.8	16.5	summer
August	0.7	16	summer
September	1	14	autumn
October	1.5	11	autumn
November	2	10	autumn

6.4.7 Wind turbine power output

Wind speed distribution

Using 1-year historical SCADA data a wind speed distribution is plotted in Figure 92 at hub height.

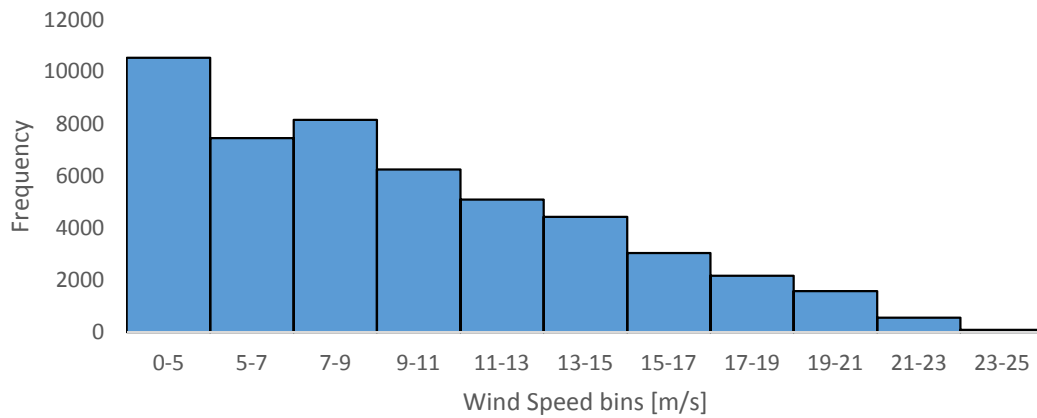


Figure 92. Wind speed histogram for one year.

This wind speed distribution is further analysed by month and with wind speed bins of 1 m/s as it is shown in Table 62. Frequency corresponds to 10 minutes averaged measurements.

Table 62. Wind speed frequency per month.

Wind Speed (m/s)	Frequency – Jan (31days)	Frequency - Feb (28 days)
1	65	294
2	61	153
3	60	124
4	132	151
5	157	189
6	152	210
7	207	210
8	286	255
9	368	265
10	313	283
11	272	265
12	219	275
13	280	262
14	243	239
15	213	168
16	221	143
17	205	116
18	224	132
19	225	140
20	226	96
21	148	33
22	101	17
23	38	10
24	28	1
25	19	0

Power curve

Using the power curve in Figure 93 provided by the manufacturer, it is possible to derive the power generation per wind speed in Table 62, for the turbine Siemens 3.6MW.

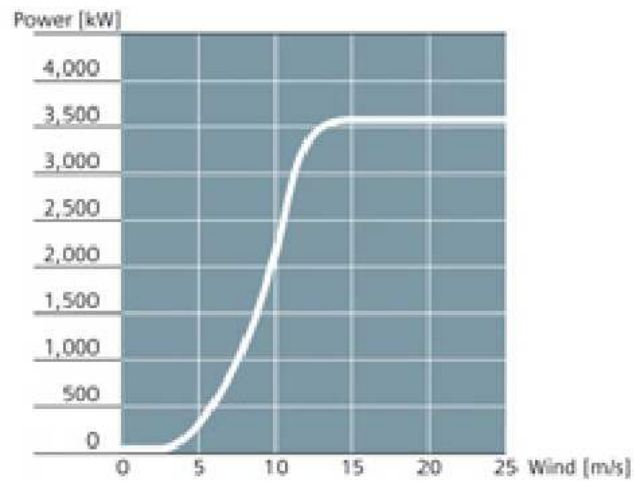


Figure 93. Siemens 3.6MW power curve [81].

Power output per wind speed and per month

Finally using the power output per wind speed of the Siemens 3.6MW turbine and the wind speed frequency per month previously calculated, the maximum energy generation is estimated per month as is shown in Table 63.

Table 63. Power output per wind speed and month.

Wind Speed (m/s)	Power (W)	January [kWh]	February [kWh]
1	0	0	0
2	0	0	0
3	33.9	339	700
4	135.1271834	2973	3401
5	302.04528	7904	9514
6	551.0542439	13960	19287
7	898.5722484	31001	31450
8	1361.017467	64875	57843
9	1954.808073	119895	86337
10	2696.36224	140660	127178
11	3600	163200	159000
12	3600	131400	165000
13	3600	168000	157200
14	3600	145800	143400
15	3600	127800	100800
16	3600	132600	85800
17	3600	123000	69600
18	3600	134400	79200
19	3600	135000	84000
20	3600	135600	57600
21	3600	88800	19800
22	3600	60600	10200
23	3600	22800	6000
24	3600	16800	600
25	3600	11400	0
	Total Energy Produced (kWh)	1978806	1473911

To estimate the loss of production per day, it is necessary to know the number of days per month. The final output of the power output calculation, the average energy production per day is shown in Table 64.

Table 64. Average energy production per day.

Number of days	Month	Total Energy (kWh)	Average Energy Production(kWh/day)
31	January	1978806	63832
28	February	1473911	52640
31	March	1643181	53006
30	April	1130137	37671
31	May	1459698	47087
30	June	1244976	41499
31	July	1440903	46481
31	August	1159981	37419
30	September	1223373	40779
31	October	1252838	40414
30	November	2032466	67749
31	December	2438144	78650

Figure 94 shows the theoretical maximum energy production (kWh) required to estimate the availability based on energy generation.

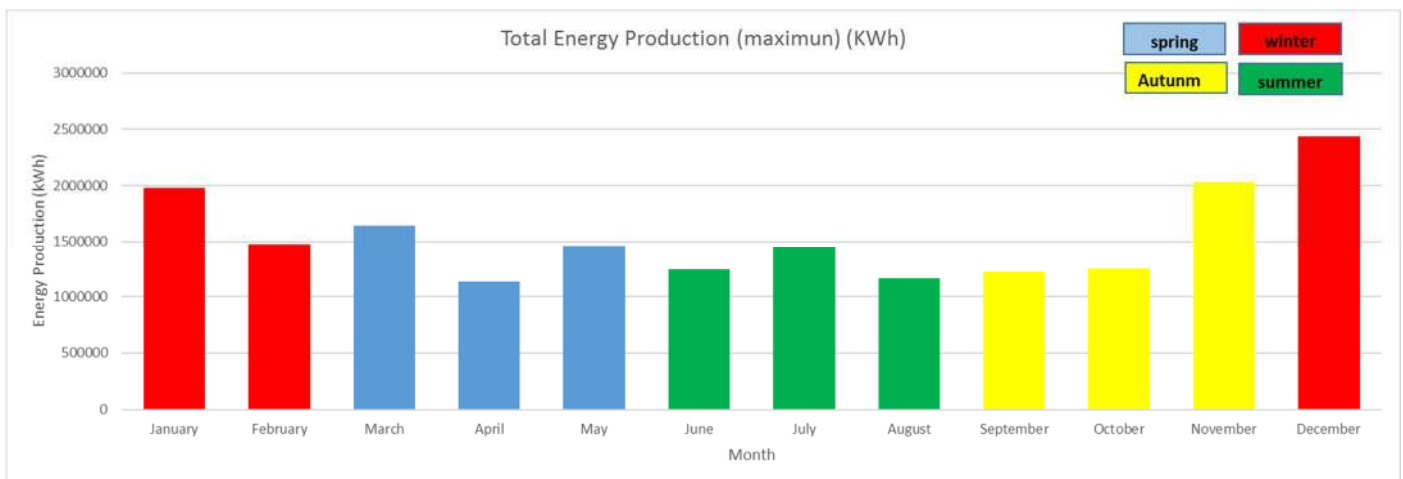


Figure 94. Total theoretical maximum energy production per month.

6.4.8 Economic parameters

The electricity sales price is highly affected by subsidies available. One of the main policy mechanisms to incentive investment in offshore wind is the UK Contract for Difference (CfD). The offshore wind industry was classified as a less-established technology due to the allocation of CfD. A CfD is a private law bilateral contract between generators and the government owned Low Carbon Contract Company (LCCC). Based on [142], “the contract offers generators a fixed price over (typically) a 15-year period by paying them the difference between the CfD’s strike price and a market reference price.” It is possible to see in two rounds of actions a decrement of the prices. However, it is not clear that the low prices reflect

a decline in the technology cost or an increase in the supply chain efficiency. In this case, developers expect that by the delivery year, O&M efficiencies are reached [142]. The author in [143] states that due to the O&M and construction challenges the offshore industry heavily subsidised. However, huge efforts need to be done to reduce the cost of energy since there is no clarity of how long the public support will be available. The study in [144] explores the impact of government subsidies on the economic feasibility of the offshore wind farms. The levelised cost of energy (LCoE) is critical for developers to calculate a strike price for CfD.

The values of the electricity sales price have significant differences between European countries, see figure 95. In the UK, the offshore wind tenders and auctions between 2010 and 2018 have winning prices between £76/MWh and £223/MWh. For this study, the offshore wind farm, Neart na Gaoithe, announced in 2015 and to be commissioned in 2019, is selected as a reference. This project has a winning price of £188/MWh approximately [145].

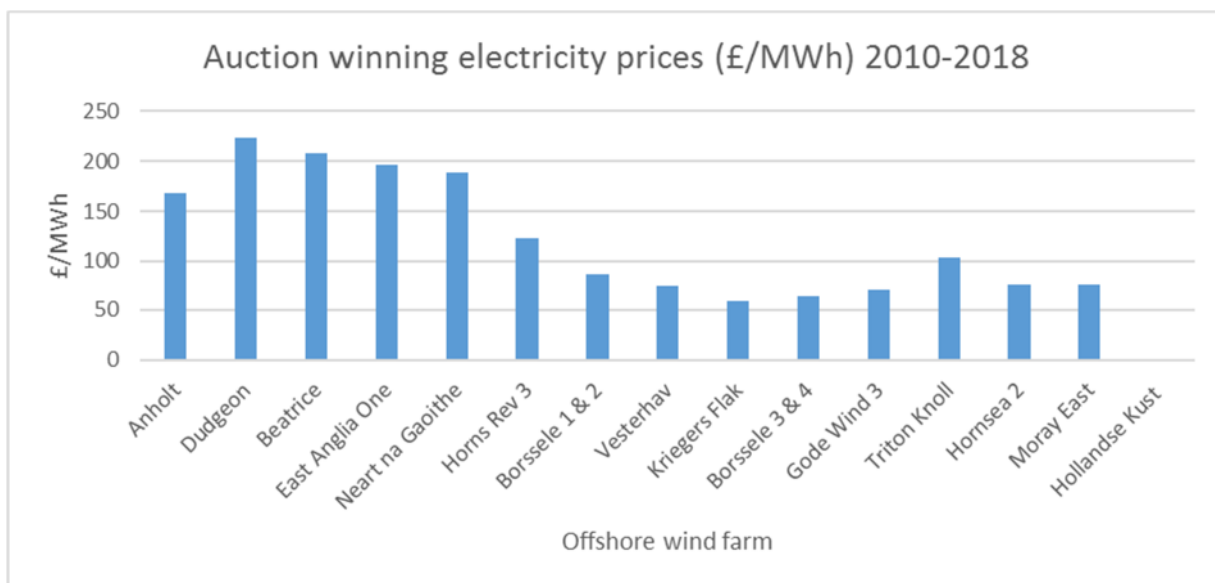


Figure 95. Electricity sales price [145]

Table 65 shows the values for the electricity sales price, fuel cost and technicians’ salary per month to be used in the O&M cost model. The fuel cost and technician costs are considered fixed for the calculation period [138] [128].

Table 65. Economic parameters per month

Parameter	Unit	Value
Electricity sales price	£/MWh	188
Fuel cost	£/litre	0.83
Salary (Technicians)	£/hr	70

6.4.9 O&M costs model outputs

Main Assumptions

In order to develop the O&M cost model the following assumptions were taken:

- No offshore operation can be carried out with wind speeds over 12m/s
- No offshore operation can be carried out with a wave height over 1.5m
- The wind farm operator owns the vessels.
- Electricity sales price is predicted based on previous values. It can introduce more uncertainties to the model which, can be combined with weather and turbine reliability uncertainties.
- Time for a technician to be available is average 6 hours.
- Operational data – unscheduled and scheduled maintenance hours are derived from SCADA data.
- Weather windows – based on the study [140] [130] using Monte Carlo technique.
- The installation date for all the components in the wind turbine database is 01/01/2015.

Case study

The case study with the current scheduled and unscheduled maintenance strategy is established in Table 58 and Table 59 respectively. The outputs are calculated for WT1 for a period of 1 year. Table 66 shows the downtime, loss of production, availability and revenue losses for the wind turbine WT1 during a period of 1 year. The downtime is the sum of logistic time (time for the technicians and spare part to be available), waiting time (weather windows as an average number of access days per month), transit and return time (travel time in the vessel) and, repair time. The loss of production is calculated using the average energy production per day in each month and the downtime. The availability is calculated based on the theoretical producible energy in kWh and the loss of production due to the failures. The revenue losses per month are calculated using the electricity sales price prediction and the loss of production per month

Table 66. O&M outputs: downtime, loss of production and revenue losses due to scheduled maintenance.

Scheduled Maintenance (Class B)	January	February	March	April	May	June	July	August	September	October	November	December
Logistics time (hr)				6								
Waiting time (hr)				36								
Transit time (hr)				0.67								
Repair time (hr)				4								
Return time (hr)				0.67								
Sub TOTAL (hr)	0	0	0	47.3	0	0	0	0	0	0	0	0
Scheduled Maintenance (Class F)	January	February	March	April	May	June	July	August	September	October	November	December
Logistics time (hr)			6					6				
Waiting time (hr)			43.2					43.2				
Transit time (hr)			0.67					0.67				
Repair time (hr)			96					96				
Return time (hr)			0.67					0.67				
Sub TOTAL (hr)	0	0	146.5	0	0	0	0	146.5	0	0	0	0
Scheduled Maintenance (Class G)	January	February	March	April	May	June	July	August	September	October	November	December
Logistics time (hr)						6						
Waiting time (hr)						21.6						
Transit time (hr)						0.67						
Repair time (hr)						48						
Return time (hr)						0.67						
Sub TOTAL (hr)	0	0	0	0	0	76.9	0	0	0	0	0	0
TOTAL Downtime due to scheduled maintenance (hr/month)	0	0	96	4	0	48	0	96	0	0	0	0
Theoretical Produccible Energy (KWh)	1978806	1473911	1643181	1130137	1459698	1244976	1440903	1159981	1223373	1252838	2032466	2438144
Average Energy Production(KWh/day)	63832	52640	53006	37671	47087	41499	46481	37419	40779	40414	67749	78650
Loss of Production(KWh)	0	0	212023.3505	6278.539254	0	82998.38877	0	149674.9088	0	0	0	0
Availability (based on Energy)	100%	100%	87%	99%	100%	93%	100%	87%	100%	100%	100%	100%
Revenue Losses (£)												

Table 67 presents the costs related to the maintenance classes of the case study. The cost of the spare part is calculated using the average value of the components described in each maintenance class and based on [134] [124] [137] [127] [147] [133] and operational data. The labour cost is calculated with the number of hours that a technician needs to spend waiting for access to the turbine, travel time and repair time. The salary is considered fixed during the whole year at £70 per hour. The vessel cost calculation only considers fuel consumption and not rental cost since it is assumed the wind farm operator owns the vessels. The fuel price is estimated fixed for the whole period at £0.83 per litre. The total cost of repair due to scheduled maintenance activities is £177,075per year for the turbine WT1. Finally, the hidden CO₂ emissions are calculated using the vessels' fuel consumption, the travel time and 2.68 kgCO₂/lt of CO₂ emissions [138] [128].

Table 67. O&M outputs: spare part, labour and vessel cost due to scheduled maintenance.

Cost of Spare Part	January	February	March	April	May	June	July	August	September	October	November	December
Spare part cost (Class B) (£)				250								
Spare part cost (Class F) (£)			10000					10000				
Spare part cost (Class G) (£)						10000						
Total Spare Part Cost (£/month)	£ -	£ -	£ 10,000	£ 250	£ -	£ 10,000	£ -	£ 10,000	£ -	£ -	£ -	£ -
Labour Cost	January	February	March	April	May	June	July	August	September	October	November	December
Wages (£)	£ -	£ -	£ 19,676.98	£ 5,788.98	£ -	£ 14,899.48	£ -	£ 19,676.98	£ -	£ -	£ -	£ -
Cost of Vessel	January	February	March	April	May	June	July	August	September	October	November	December
Fuel Consumption (Litres)	0	0	602.1	602.1	0.0	602.1	0.0	602.1	0	0	0	0
Rental cost	0	0	0	0	0	0	0	0	0	0	0	0
Fuel cost (£/month)	£ -	£ -	£ 500	£ 500	£ -	£ 500	£ -	£ 500	£ -	£ -	£ -	£ -
Total Cost / month												
Hidden CO2 Emissions (KgCO2)	0	0	1613	1613	0	1613	0	1613	0	0	0	0

The same calculations are performed for the unscheduled maintenance activities of the case study of the WT1. Table 68 shows two maintenance classes, i) class B and C for the power converter and ii) the pitch system, respectively. The total cost due to unscheduled maintenance activities during one year of operation of WT1 is £89,069.

The total values of the O&M cost model outputs are summarised in Table 69. The total downtime for one year is 352 hours, which represents a loss of production of 754MWh and an average wind turbine WT1 availability of 95%. The total cost of repair, including revenue losses, is £266,144. Due to O&M operations during one year, around 10 tonnes of CO₂ are emitted into the atmosphere.

Table 68. O&M outputs: downtime, loss of revenue and costs due to unscheduled maintenance.

Corrective Maintenance (Class B)	January	February	March	April	May	June	July	August	September	October	November	December
Logistics time (hr)						6						
Waiting time (hr)						21.6						
Transit time (hr)						0.67						
Repair time (hr)						4						
Return time (hr)						0.67						
Sub TOTAL (hr)	0	0	0	0	0	32.95	0	0	0	0	0	0
Corrective Maintenance (Class C)	January	February	March	April	May	June	July	August	September	October	November	December
Logistics time (hr)												6
Waiting time (hr)												60
Transit time (hr)												0.67
Repair time (hr)												8
Return time (hr)												0.67
Sub TOTAL (hr)	0	0	0	0	0	0	0	0	0	0	0	75.35
Downtime due to CM (hr)	0	0	0	0	0	32.95	0	0	0	0	0	75.35
Total Downtime (hr/yr)	108											
Loss of Production(KWh)	0	0	0	0	0	56974.75	0	0	0	0	0	246927.30
Revenue Losses (£)	£ -	£ -	£ -	£ -	£ -	£ 6,267.22	£ -	£ -	£ -	£ -	£ -	£ 41,978
Cost of Spare Part	January	February	March	April	May	June	July	August	September	October	November	December
Spare part cost (Class B) (£)						250						
Spare part cost (Class C) (£)												10250
Total Spare Part Cost (£)	£ -	£ -	£ -	£ -	£ -	£ 250.00	£ -	£ -	£ -	£ -	£ -	£ 10,250
Labour Cost	January	February	March	April	May	June	July	August	September	October	November	December
Wages (£)						£ 4,612.98						£ 15,823.48
Cost of Vessel	January	February	March	April	May	June	July	August	September	October	November	December
Fuel Consumption (Litres)						602.05	0	0	0	0	0	602.05
Rental cost	0	0	0	0	0	0	0	0	0	0	0	0
Fuel cost (£/month)	£ -	£ -	£ -	£ -	£ -	£ 499.70	£ -	£ -	£ -	£ -	£ -	£ 499.70
Total Cost / month	£ -	£ -	£ -	£ -	£ -	£ 11,629.91	£ -	£ -	£ -	£ -	£ -	£ 68,551
Hidden CO2 Emissions (KgCO2)	0	0	0	0	0	1613	0	0	0	0	0	1613

Table 69. O&M outputs: summary of the case study.

Downtime	Units	January	February	March	April	May	June	July	August	September	October	November	December	YEAR
Logistics time	hr	0	0	6	6	0	12	0	6	0	0	0	6	36
Waiting time	hr	0	0	43.2	36	0	43.2	0	43.2	0	0	0	60	226
Travel time	hr	0.0	0.0	1.3	1.3	0.0	2.7	0.0	1.3	0.0	0.0	0.0	1.3	8
Repair time	hr	0	0	96	4	0	52	0	96	0	0	0	8	256
TOTAL Downtime	hr	0.0	0.0	96.0	4.0	0.0	80.9	0.0	96.0	0.0	0.0	0.0	75.3	352
Loss of Production	KWh	0	0	212023	6279	0	139973	0	149675	0	0	0	246927	754877
Energy Production	KWh	1978806	1473911	1431158	1123859	1459698	1105003	1440903	1010306	1223373	1252838	2032466	2191217	17723536
Availability (based on KWh)	%	100%	100%	85%	99%	100%	87%	100%	85%	100%	100%	100%	89%	95%
Revenue Losses	£	£ -	£ -	£ 39,860	£ 1,180	£ -	£ 26,315	£ -	£ 28,139	£ -	£ -	£ -	£ 46,422	£ 141,917
Spare Part Cost	£	£ -	£ -	£ 10,000	£ 250	£ -	£ 10,250	£ -	£ 10,000	£ -	£ -	£ -	£ 10,250	£ 40,750
Labour Cost	£	£ -	£ -	£ 19,677	£ 5,789	£ -	£ 19,512	£ -	£ 19,677	£ -	£ -	£ -	£ 15,823	£ 80,479
Transport Cost	£	£ -	£ -	£ 500	£ 500	£ -	£ 999	£ -	£ 500	£ -	£ -	£ -	£ 500	£ 2,998
TOTAL cost of repair (1/turbine)	£	£ -	£ -	£ 70,037	£ 7,719	£ -	£ 57,077	£ -	£ 58,316	£ -	£ -	£ -	£ 72,996	£ 266,144
TOTAL cost of repair (1/turbine)	£ /KWh	£ -	£ -	£ 0.0489	£ 0.0069	£ -	£ 0.0517	£ -	£ 0.0577	£ -	£ -	£ -	£ 0.0333	£ 0.0150
Hidden CO2 Emissions	TonnesCO2	0.0	0.0	1.6	1.6	0.0	3.2	0.0	1.6	0.0	0.0	0.0	1.6	9.7

Finally, it is possible to see in Figure 96 that the revenue losses represent around 53% of the total cost of repair, followed by labour cost and spare part cost.

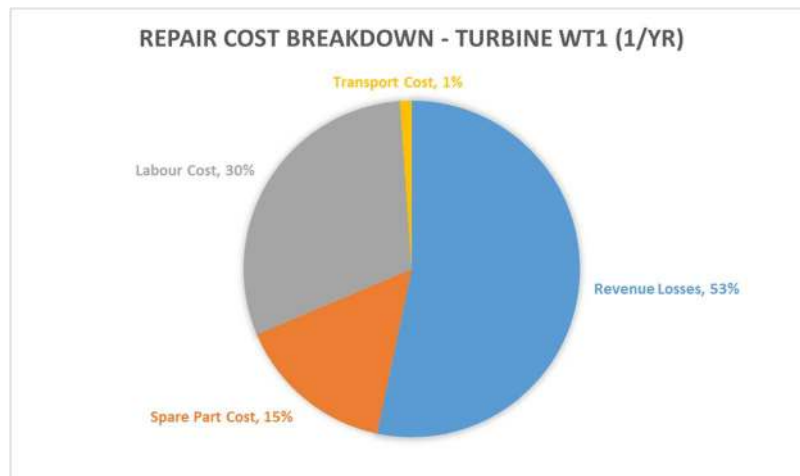


Figure 96. Repair cost breakdown for WT1.

Optimised case study

The optimised case study integrates the digital sensors into the decision-making process of the O&M strategy.

Based on the digital sensor of the power converter (physics-based model), assuming 60% of damage accumulation with an expected failure date within 8 months (August), the maintenance activity to avoid a power converter failure now is part of the scheduled maintenance. Based on Table 58, there is a scheduled maintenance related to the annual service (maintenance class F). In April there are 13 hours of daylight and the annual service and travel time takes only 6 hours, therefore, it is possible to perform a maintenance class B during that scheduled activities. The described scenario represents waiting time due to weather and no logistics delay time. It only increases the time spent on the turbine by technicians.

It is assumed that the digital sensor of the pitch system (data mining) predicted yellow status at the beginning of the period. The failure mode is unknown, therefore, a visit to investigate the pitch system condition is required before winter. A maintenance class B is included in the scheduled maintenance of the case study. An entirely new offshore activity is planned to avoid the failure of the pitch system during winter, which is classified as maintenance class C in Table 60.

Table 70 shows a reduction of 28.47% of the total downtime with an improvement of 1.64% of turbine availability in one year applying. This represents a reduction of £86,071 in the revenue losses. With the use of digital sensors, the total cost of repair fell from £266,144 to £149,102.

Table 70. Comparison between the case study and the optimised case study.

Downtime	Case study (year)		Case study + digital sensors (year)	
Logistics time (hr)	36	30	6	reduction
Waiting time (hr)	226	134	91	reduction
Travel time (hr)	8	7	1	reduction
Repair time (hr)	256	252	4	reduction
TOTAL Downtime (hr)	352	252	28.47%	reduction
Loss of Production (kWh)	754877	463490	38.60%	reduction
Energy Production (kWh)	17723536	18014923	1.64%	improvement
Availability (based on kWh)	95.5%	96.8%	1.3%	improvement
Revenue Losses	£ 141,917	£ 55,846	£ 86,071	reduction
Spare Part Cost	£ 40,750	£ 30,750	£ 10,000	reduction
Labour Cost	£ 80,479	£ 60,007	£ 20,471	reduction
Transport Cost	£ 2,998	£ 2,499	£ 500	reduction
TOTAL cost of repair (£/turbine)	£ 266,144	£ 149,102	117042	reduction

CHAPTER 7 – CONCLUSIONS AND DISCUSSIONS

7.1 General

This chapter summarises the research and project development. It covers the whole spectrum of O&M optimisation process, from data analysis and decision-making process to O&M optimisation outputs. Further work is also described for each part of the project.

The project was focused on the development of tools to optimise O&M of offshore wind farms. A literature review and market research were performed to identify failure mechanisms and commercially available solutions that have been critical for the turbine operation. Physics-based models to estimate damage accumulation of the gearbox and power converter are presented. A data mining approach is proposed for the pitch system integrating subject matter expert knowledge. Finally, an O&M cost model is proposed to compare costs and turbine availability with and without the use of intelligent approaches for failure diagnosis and prognosis in the maintenance strategies.

The main contributions of the thesis are listed below:

- a) Through the application of the FMEA tool, it was identified that the gearbox, power converter, yaw system and pitch system are the most critical assemblies for the offshore wind turbine.
- b) A data control index CAAR was proposed in the FMEA to register the data and information used to assign the severity, occurrence and detection rating. The CAAR index aims to secure a consistent evaluation process and allows future iterations to improve the RPN based on the data source.
- c) A physics-based model of the gearbox is proposed to determine the damage accumulation in the bearings of the high-speed shaft.
- d) A physics-based model of the power converter is proposed to determine the thermal cycling and accumulated damage in the power electronic components - IGBTs and diodes.
- e) A data mining approach using SVM and KNN techniques is proposed as an alarm system. The methodology integrates turbine knowledge to identify deviations from normal behaviour. The main output is an alarm for the pitch system status (green, yellow and red indicators) based on the risk to the turbine operation.

- f) An O&M cost model is developed to assess maintenance strategies by analysing the turbine availability, loss of production, revenue losses, turbine downtime, cost of repair, and CO₂ emissions. Maintenance strategies are set up using conventional approaches and compared with maintenance strategies integrating the physics-based models and data mining approach. Significant reduction in time and costs are observed using the last approach.

6.2 Conclusions

At present, the offshore wind energy industry target is to reduce the levelised cost of energy (LCoE) by 40%. Operation and Maintenance (O&M) activities can contribute up to 30% of the LCoE, so automatic and intelligent systems are needed to minimise human intervention during the operating life. Statistical approaches have been used to integrate the operational experience into failure prognosis. However, statistical methods do not consider the actual condition of the component; hence, the predicted date of failure, which is based on statistics, can even be after the actual failure occurs, leading to consequential damages.

Offshore wind turbines tend to be larger than those used onshore in order to improve the MW/turbine ratio, to reduce CAPEX and to improve OPEX. However, there is a price to pay during turbine installation and O&M which involves hiring vessels and associated personnel, and in the worst case scenario where component replacement is necessary, a crane vessel is required for installation.

Risk assessment of the Siemens SWT3.6 turbine has been the foundation of this work. A comprehensive analysis and method are proposed to study the performance of the components of offshore wind turbines from a reliability point of view. The FMEA has been a useful tool to analyse critical assemblies regarding risk to turbine operation and to identify their components, failure modes and causes. The definition of the taxonomy of the wind turbine is crucial for the development of this FMEA and project. Based on the European project ReliaWind, a comprehensive turbine breakdown was proposed using a hierarchical structure. It is the basis for the FMEA, physics-based models and failure investigation. It allows the determination of consequential damage and local and global effects of failures.

The FMEA outputs have been compared with standard failure rates and reliability information of previous studies. The most critical assemblies identified in this study are consistent with the outputs of publicly available reports such as the European project ReliaWind where the

pitch system, power converter and gearbox are also identified as critical. However, it is important to compare the failures rates and modes of the same type of turbines operating under similar operational conditions. The publicly available reports comprise a wide range of turbine manufactures and rated power. Additionally, the O&M strategy has an important impact on the turbine reliability, even if it is the same type turbine in the same wind farm.

On the other hand, optimisation of O&M based on the condition of components is explored. The literature review shows that a condition monitoring system aims to enhance the availability of expensive critical assets and reducing overall O&M costs. A condition based maintenance approach aims to reduce maintenance costs by reducing the number of planned maintenance actions. Specialised technicians will only perform maintenance tasks when there is evidence of abnormal behaviour. The process of condition monitoring can be divided into three phases; first, detecting an unusual operation condition that is outside of the right theoretical behaviour of a healthy turbine. Second, a failure diagnosis and, thirdly, the remaining useful life of the identified component is forecasted based on physics of failure.

Maintenance optimisation is a continuous process since a particular maintenance strategy may be optimal now, but it may not be in the future. Previous studies identified the three main factors to select an appropriate maintenance strategy: the consequence of failure, the predictability of lifetime, and the feasibility of using condition monitoring systems to detect the failure. Maintenance optimisation comprises periodic assessment of performance due to the uncertainty related to factors such as spare part costs, degradation patterns, operational conditions and so on.

Condition-based maintenance requires an accurate assessment of the status of the wind turbine. Therefore it is necessary to improve sensing technologies, data management systems and real-time data analytics algorithms. This robust and reliable data management system (sensors, data collection and processing) is the base for making informed maintenance decisions. Likewise, there is no certain healthy state of the component due to variations in environmental and operational conditions and their influence on the monitoring system.

This project responds to what the offshore wind market is asking for, a more accurate and intelligent approach to optimise O&M activities. A maintenance policy with a proactive approach has been compared with a preventive and corrective approach. Digital sensors

inform the decision-making process of wind farm operators and maintenance activities are planned to avoid greater turbine downtime and consequential damages.

Overall, during this research project, it has been identified that maintenance optimisation depends on a significant number of factors affecting LCoE and the turbine availability:

- CAPEX factors: turbine design and manufacturing. Installation of new condition monitoring systems might affect initial investment and degrade turbine reliability. New design approaches of critical components may have a positive impact on critical components reliability and maintainability.
- Maintenance strategies and cost of repair. Different maintenance strategies may have an impact on the component lifetime maximisation.
- Operations and logistics. Vessels strategy, number and shift of technicians, spare part availability and cost, are factors that influence the LCoE.
- Turbine reliability. Failure rates and component maintainability.
- Wind farm characteristics such as distance from the port, number and power rating of turbines and capacity factor.
- Accessibility and weather prediction techniques.

Physics-based models

Statistical approaches are used to integrate the previous experience into failure prognosis. However, statistical methods do not consider the actual condition of the component. Therefore, failure date prediction based on statistics can be at any point in time, even after the actual failure date, with the respective consequential economic cost. Data-driven approaches use operational data such as Condition Monitoring Systems (CMS), inspections or SCADA data to study the behaviour or patterns of several parameters. When a clear deviation from normal behaviour is identified, a failure can be detected. An inspection might detect a well-developed failure without leaving any time to respond in a cost-effective manner. Accumulated damage determination in the time domain using physics-based models is discussed as one of the methodologies with greater capability to predict failure far in advance, even from the installation date of the component.

Gearbox

Although seasonal variations will be similar from one year to the next for any particular turbine, there will be differences. The procedure proposed for the gearbox model allows

observed load spectra to be used as inputs, enabling the estimated accumulated damage to be updated throughout the life of the component. Furthermore, load spectra obtained from simulations may also be used as inputs. These simulated spectra represent future loading scenarios for the gearbox. This opens up the possibility of using the statistics of the wind climate, the variability of material resistance and manufacturing quality to be used to derive input spectra, which are representative of the specific component in operation. By matching these spectra with their respective probabilities of occurrence, a distribution function may be derived to estimate the probability of failure. Inspection, repair or replacement of the affected part might reasonably be scheduled when the probability of failure at a pre-determined future date is expected to exceed a threshold value established by the wind farm operator. In principle, the same threshold value, specifying the failure probability, may be used for every failure mode in every component of the wind turbine, enabling a rational approach to all aspects of maintenance management.

Based on the failure investigation and the vulnerability map of gears and bearings it is noted that bearing failures caused by fatigue damage occurs on several of the shafts in the gearbox but, predominately in the HSS shaft bearings. HSS shaft failures are responsible for 50% of the repair cost in the gearbox. The main factors that influence the downtime are the availability of spare parts, distance to site, transport system, weather conditions and service action at the wind turbine. It is proposed that predictions of remaining useful life may be used to optimise the maintenance strategies.

Key elements of the physics-based approach to estimate damage accumulation of gears have been provided including a description of the diagnostic and predictive models. The load distribution of the three-stage gearbox is calculated using SCADA data and the model provided by KISSsoft AG allows rapid calculation, multiple failure modes analysis and an integrated approach for damage accumulation and RUL estimation.

The proposed physics-based model of the gearbox helps to optimise O&M activities by feeding the RUL into the decision making process of wind farm operators taking into account all characteristics of the wind climate, including wind gusts and turbulence. Around 3% of lifetime consumption is estimated in both HSS bearings, B1 and B2.

Power converter

A physics-based method to estimate damage accumulation of IGBTs and Diodes and to predict the RUL of power converters have been proposed. The simulations do not require a large computational effort, therefore it is suitable for day-to-day use. The algorithm comprises one glue code and four main pre-processors; generator, power losses, thermal model and the rainbow counting method. The main inputs of the methodology to estimate accumulated damage are the torque and rotational speed in the high-speed shaft. For prediction purposes, the proposed methodology is to calculate the torque and rotational speed using the aero-servo-elastic-hydro simulation tool FAST. FAST uses as inputs the load cases derived from IEC standards representing all the operational conditions an offshore wind turbine may experience at a particular site. A period of two and half days is simulated which is not long enough to extrapolate the damage for the whole year as it does not include all the operational conditions.

The power losses and junction temperatures depend on the ambient temperature. The power losses and thermal algorithms require information provided by the manufacturer. A method to extract information from look-up tables and graphs is proposed to make the models that are temperature dependent in every simulation step.

Similar to the gearbox, the RUL method of the power converter could be used to inform maintenance decisions to optimise resource allocation considering weather conditions throughout the year. Unexpected failures, which represent huge production losses, as well as time spent finding failures could be avoided by scheduling maintenance or inspection activities based on the RUL estimation.

Data mining approach

Reliability, maintainability and availability continuously improve through wind turbine design. However, there is a balance between design cost and improvements. Sometimes, the cost of research and development of the turbine can be more expensive than the income generated by the turbine output improvement. Therefore, it makes sense to look at the O&M optimisation from a wind farm point of view rather than from an individual turbine. However, this approach may require a large amount of data collected from the wind farm. Normal behaviour and common patterns may be identified using cognitive computing elements such as data mining and machine learning.

The pitch system has been identified as one of the most critical assemblies in terms of turbine operation. However, the development of a physics-based approach to identify failures is limited by the variables available in the SCADA databases related to the health of the pitch system. Therefore, machine learning and data mining methodologies are approaches to understand the pitch system normal behaviour and identify SCADA data observations that might represent early stage pitch system failure.

The main result is the identification of outliers that might represent an incipient failure in the pitch system. The normal behaviour and boundary are defined using offshore wind turbine parameters such as blade position, wind speed, wind turbulence, power output, and the pitch system hydraulic oil pressure. The alarm is a green, yellow or red flag for every new observation status, which indicates if there is abnormal behaviour of the pitch system, or not.

Pitch system failure modes and causes were explored. External leakage due to wear in the seals between the actuator rod and the cylinder, hydraulic supply line failure, valve connection failure, and internal leakage due to the wear of the piston seal are the most common failures. The development of algorithms representing the physics of failure using the SCADA data available is challenging. The SVM technique is applied to determine the normal behaviour of a known healthy turbine. This algorithm delivered a learnt boundary which was analysed to establish the normal behaviour. However, the uncertainty accompanying the outputs is not calculated. The learnt frontier shows areas in the relationship between wind speed and blade position that are understandable only knowing the control philosophy of the turbine.

Subject matter expert knowledge of the offshore wind turbine is required to analyse the learnt frontier and assign conditions status to the variables pair. A decision tree algorithm is proposed to analyse the data based on the learnt frontier. The data is analysed in sections of the wind speed and blade position and interrogated using more variables; oil pressure and power output. These sections (e.g. 0-5m/s of wind speed and 0-10 degrees of blade position) may be reduced to improve the resolution of the analysis. The training data is 1 year of SCADA data. Each dataset point (wind speed, blade position) is interrogated by the decision tree and assigned a status value green if it is normal, yellow if it is abnormal and red if it is a failure.

The accuracy of this approach may be calculated by validating the model using historical SCADA data and maintenance logs with pitch system failures.

The final step of the proposed methodology is to interrogate new observations in real time using the KNN techniques. The KNN algorithm will use the training data with the status vector to assign a status to the new observation (wind speed and blade position). The main advantages of this approach are that it needs only two variables to detect abnormal behaviour. Therefore it requires less computational effort and it is straightforward to implement. The accuracy of the KNN also needs to be validated using historical SCADA data.

O&M cost model

As described before, it is difficult to predict the failure before they occur to maximise the component usage and reduce the cost of maintenance. Specific damage accumulation information is required to achieve optimal maintenance strategy. Today, this information can be gathered using regular inspections and condition monitoring systems. However, the cost of gathering this information for all the turbines in a wind farm is high. Therefore, in this scenario, there is a trade-off between the cost of the monitoring system implementation, inspections, preventive maintenance and the reduction of the cost of unplanned corrective maintenance. The O&M cost model aims to understand the impact of digital sensors instead of the condition monitoring system, on the O&M optimisation process. Digital sensors such as the proposed physics-based and data mining models represent a cost-effective input for the decision-making process.

The thesis presented factors of the O&M strategy that can be optimised:

- Failure prognosis horizon by the use of digital sensors.
- Number of vessels available. There are two options, vessels can be part of the wind farm operation strategy, or they can be rented to a subcontractor. Both have economic advantages and disadvantages.
- Number of technicians available. For the case study, technicians have on average a single shift of 10 hours throughout the year during the daylight. A total number of staff (onshore and offshore) of 0.37 to 0.75 persons per turbine is estimated. 60% of the total number of staff are technicians. Therefore, a wind farm of 24 turbines should have an average of 12 staff in total and 7 turbine technicians. More technicians will have a positive impact on the delay time due to their increased availability.
- Preventive maintenance intervals or margins. Wind speed limit can be reduced from 12 m/s to a lower wind speed and the timescale to perform preventive maintenance

can be extended from 6 months to 12 months so the loss of production can also be reduced.

- Reduction of unscheduled maintenance activities using a more accurate failure prediction and including new repair actions in the planned maintenance.
- To use more reliable components. The work presented in the FMEA section shows that not only were critical assemblies identified, but also critical failure modes per component, undetectable failures and commercially available prevention methods. This information is useful to iterate in new design and maintenance solutions.
- To change the type of vessel to improve accessibility. This will change the safety threshold for the weather window estimation. The use of new vessels for wind farms further offshore, new maintenance strategies including an offshore base may be established.

The work presented also identified potential benefits for wind farm operators or owners:

- O&M strategy after the warranty period. The complete understanding of the factor affecting turbines reliability and availability. Additionally, this project delivers a holistic view to optimise O&M by improving availability and reducing maintenance cost.
- To determine O&M budget for future periods. O&M cost model is a tool that can be used to estimate the necessary resources required in the future. The accuracy of the prediction of weather windows, economic parameters, and failure events will be determined by a combined probability of the models.
- To improve O&M strategy based on operational experience. Operational experience of the turbines, wind farm and onshore activities are crucial to improve predictions and approaches to the decision-making process. SCADA data, maintenance logs, spare part management strategy are some of the main inputs with potential automation in further work.
- Profitability assessment of the wind farm. Potential investors will take decisions based on the future profitability of the wind farm. Variables such as loss of production, cost of repair and availability are outputs of the O&M cost model.
- Spare part stock optimisation. It is seen in this project that spare part management takes a considerable percentage of the O&M total cost. There is room for

improvements, and the O&M cost model can identify the delay time due to poor spare part availability.

- Buying v/s renting vessel decision. The cost of running vessels is calculated using fuel cost, travel time and vessel capabilities. However, the O&M cost model does not compare the cost of owning or renting a vessel.
- “Hidden” CO₂ emissions. Today, the trend is to deploy wind farms with a large number of turbines. Maintenance actions will require a considerable amount of fuel for technicians transfer to the turbines. The CO₂ emissions become relevant to comply with regulations and standards.

6.3 Further work

FMEA

The FMEA tool developed in this project can be easily developed further by incorporating new approaches and techniques. The consequential damage examination of failure modes looks at the correlation of one failure mode in a specific component causing a new failure mode in another component. This analysis may be performed using the functional block diagram. Additionally, failure modes correlations between two or more failures can be identified using the consequential damage analysis. Two failure modes can lead to catastrophic failure. Therefore, it is important to identify them in order to take the necessary actions to prevent them occurring at the same time.

This thesis investigated a particular offshore wind turbine technology. A FMEA for different turbine configurations, e.g. turbines using direct drive generator and jacket support structure, would expand the turbine knowledge of this project.

The risk priority number comprises severity, occurrence and detection rating with the same level of importance. An interesting area that can be further developed is to apply some weightings to the ratings. The relative importance of the risk priority number elements may be considered in the evaluation to represent the true risk priorities in the results.

This study explores the risk to operation integrating three factors to the risk priority number. Usually, risk analysis is performed in two dimensions taking into account severity and failure frequency only. A 3D risk matrix is proposed to be used as an indicator of criticality allowing the analysis of failure detectability amongst the components.

Finally, the FMEA proved to be a good source of turbine information. The inputs and outputs such as functional block diagram, failure modes per component and local effects are important for knowledge creation for the turbine technology and operational conditions. An interesting area to explore would be the development of a tool that is able to harness the created knowledge of turbines with different configurations based on the FMEAs. A Digital Subject Matter Expert using machine learning techniques and a database of FMEAs may be able to create new FMEAs for different technologies and answer intelligent questions about the turbines.

Physics-based models

The prediction model described in Chapter 3 needs to be implemented. FAST simulations were carried out only for the load case 1.2. Monte Carlo Markov Chain model aims to be implemented using all the FASTv8 simulations representing the fatigue damage in the turbine. A future scenario in the time domain may be created using historical data of weather conditions of the site under investigation. This future scenario will better represent the dynamic behaviour of the turbine and the potential failure mode events. Further information about the installation date, the current condition of the represented critical components, and long-term wind climate data are necessary to more accurately predict potential dates and the associated probability of failures.

Both, the gearbox and power converter model require validation with actual data. Even though the SCADA systems are standard services in the wind industry, the number and type of variables available differ from one wind turbine technology to another. Likewise, the models developed in this project are only representing the operational behaviour of the Siemens SWT3.6 turbine.

Data mining

To explore the yellow and red status assigned with the KNN approach, it is possible to create look up tables to incorporate the relationship between variables and methodologies used in control system strategies. For example; the relationship between power output and wind speed and, the relationship between power coefficient, tip speed ratio and blade position. The correlation between more than 3 variables will allow the diagnosis of the failure.

The combination of the SVM, decision tree algorithm and KNN techniques comprises a high level of uncertainty. The uncertainty for each section needs to be quantified in order to deliver

a complete solution. Further works will comprise uncertainty quantification and model validation.

O&M cost model

As is described in chapter 5, Due to time constraints and the uncertainty involved in the parameters and calculations, some model blocks assume values from previous publications to calculate the final outputs and test the proposed approach integrating the accumulated damage and data mining models

The final accumulated damage of the physics-based models only quantified the damage for the period of simulation. The total accumulated damage since the assembly or component was installed is not available. Therefore, the outputs of the physics-based model do not represent the final consumed life of the item. The digital sensors outputs are the input of the predictive maintenance strategy in the O&M cost model. These inputs take into account an assumption of the total accumulated damage for the gearbox and power converter at the beginning of the period. Thus, a failure date prediction is made within a year. The criteria is set up to perform a predictive maintenance is based on the predicted failure date, which may occur during winter. Winter season comprises a higher mean waiting time to access the turbine, resulting in a higher downtime and loss of production. Previously planned maintenance activities might be used as “opportunistic maintenance”, which means recycling resources already compromised to repair or maintain the gearbox or power converter before the predicted failure date. The budget for that planned maintenance is only increased by the cost of the spare part for the new maintenance activity, but it does not comprise downtime and loss of production. It is also important to mention that the daylight, the maintenance actions duration and the technicians’ shift are also considered to make sure the technicians can perform two maintenance activities on the same day.

Prediction of weather windows is described in this study but was not implemented. Further improvement will be to run simulations of Monte Carlo Markov Chain to estimate the mean waiting time per month for a particular wind farm location. The mean waiting time in days per month used in this work is based on previous research projects for wave energy converters. Additionally, the safety threshold selected for the mentioned study may vary using specific O&M information regarding vessel type and navigation technology.

The O&M model proposed a methodology to quantify the combined probability of the inputs and integrate it with the main output of the model; availability per turbine, loss of production, cost of repair and turbine downtime. Each section of this work comprises the probability of occurrence, even the deterministic approaches. The physics-based models were designed to quantify the accumulated damage and remaining useful life. The main source of uncertainty of the physics-based models is included through the prediction model using FASTv8. The prediction approach comprises two main probability inputs: first, the pre-processor to recreate a turbulent wind profile requires site wind probability distribution. Second, the MCMC approach to create a future scenario in the time domain requires the probability of occurrence of each load case and wind speed from SCADA data. On the other hand, the data mining approach comprises uncertainties in the three phases, the SVM, the decision tree and the KNN. They contribute to the probability of occurrence of each component status. Finally, the FMEA in the O&M model represents the basis of the wind turbine database. This database contains the failure rate per failure mode, which is derived from the occurrence rating of the RPN.

As described before, the FMEA represents the basis to generate a wind turbine database with complete information of each component including maintenance class, installation date, failure rate, manufacturer, failure modes and causes, prevention and prediction methods, and so on. This database needs to be continuously updated with operational data, so better decisions are taken. SCADA data can inform the failure rate per component, new condition monitoring systems are deployed to improve local and global effects and, installation of new spare parts play a key role in the accuracy of the failure prediction. Additional future work for the dataset is the decoupling of the cost of spare parts from maintenance class. The cost of spare parts should be individually identified in the wind turbine database. Thus, the O&M cost model outputs would predict a more accurate cost of repair.

The decision-making process of the maintenance strategy itself is based on the failure rates, critical assembly identification, and available resources. However, there is no standard methodology to set up activities combining planned, corrective and proactive maintenance activities. Future work in this matter can comprise a decision tree algorithm recognising the inputs from either digital sensors or probability estimations automatically, and the effect that planned maintenance activities had on the reliability of the components.

Finally, this O&M cost model analyses the impact of the use of digital sensors on O&M optimisation for one turbine. Future work needs to be done to analyse each of the turbines and the wind farm as a whole, so resources and inputs are realistically distributed. Automation of the O&M cost model is proposed using a python code able to read each function block in the model, inputs and process the outputs. The final step is to work on the visualisation and interpretation of the outputs, so the decision makers are adequately informed.

REFERENCES

1. Karyotakis A. On the optimisation of operation and maintenance strategies for offshore wind farms. University College of London. 2011.
2. IRM. A risk management standard. The Institute of Risk Management. London. 2002;
3. Tavner P. Offshore Wind Turbines: Reliability, Availability & Maintenance. IET Digital Library. UK. 2012.
4. Myhr A, Bjerkseter C, Ågotnes A, Nygaard TA. Levelised cost of energy for offshore floating wind turbines in a life cycle perspective. *Renewable Energy*. 2014;66(C):714–28.
5. Andrawus JA. Maintenance optimisation for wind turbines. The Robert Gordon University. UK. 2008.
6. Vachtsevanos GJ, Lewis F, Hess A, Wu B. Intelligent fault diagnosis and prognosis for engineering systems. Wiley Online Library; John Wiley & Sons, Inc. ISBN: 978-0-471-72999-0. 2006.
7. Kaidis C. Wind Turbine Reliability Prediction: A Scada Data Processing & Reliability Estimation Tool. Uppsala University. 2014.
8. Tavner P, Xiang J, Spinato F. Reliability analysis for wind turbines. *Wind Energy*. Wiley Online Library; 2007;10(1):1–18.
9. Dowell J, Zitrou A, Walls L, Bedford T, Infield D. Analysis of Wind and Wave Data to Assess Maintenance Access to Offshore Wind Farms. European Safety and Reliability Association Conference. University of Strathclyde. Glasgow. 2013.
10. Amirat Y, Benbouzid MEH, Al-Ahmar E, Bensaker B, Turri S. A brief status on condition monitoring and fault diagnosis in wind energy conversion systems. *Renewable and Sustainable Energy Reviews*. Elsevier; 2009;13(9):2629–36.
11. WindEurope. Offshore Wind in Europe: Key Trends and Statistics 2018. Via Internet (1010 2018) < <https://windeurope.org/wp-content/uploads/files/about-wind/statistics/WindEurope-Annual-Offshore-Statistics-2017.pdf>. 2018;
12. Oelker J. Global Wind 2016 report: Offshore Wind. Stiftung Offshore Windenergie; GWEC. UK. 2016.
13. Brauer SA. Damage Identification of an Offshore Wind Turbine Jacket Support Structure. Institutt for marin teknikk. NTNU. 2014;
14. Feng Y, Tavner P, Long H. Early experiences with UK Round 1 offshore wind farms. *Proceedings of the Institution of Civil Engineers: energy*. Thomas Telford; 2010;163(4):167–81.
15. Sinha Y, Steel JA, Andrawus JA, Gibson K. A SMART software package for maintenance optimisation of offshore wind turbines. *Wind Engineering*. SAGE

- Publications; 2013;37(6):569–77.
16. Wang Y. Wind turbine condition monitoring based on SCADA data. University of Strathclyde. Glasgow. 2014.
 17. Smarsly K, Hartmann D, Law KH. A computational framework for life-cycle management of wind turbines incorporating structural health monitoring. *Structural Health Monitoring*. Sage Publications Sage UK: London, England; 2013;12(4):359–76.
 18. L.W.M.M. Rademakers HBMZG van B. Assessment and optimisation of operation and maintenance of offshore wind turbines. ECN Wind Energy. Netherlands. 2003.
 19. TheCrownState. Offshore wind operational report. Retrieved from www.thecrownstate.co.uk/en-gb/what-we-do/on-the-seabed/energy. 2018;
 20. Spinato F. The reliability of wind turbines. Durham theses, Durham University. Available at Durham E-Theses Online: <http://etheses.dur.ac.uk/1918/>. 2008.
 21. Tchakoua P, Wamkeue R, Ouhrouche M, Slaoui-Hasnaoui F, Tameghe TA, Ekemb G. Wind Turbine Condition Monitoring: State-of-the-Art Review, New Trends, and Future Challenges. *Energies*. Multidisciplinary Digital Publishing Institute; 2014;7(4):2595–630.
 22. García Márquez FP, Tobias AM, Pinar Pérez JM, Papaalias M. Condition monitoring of wind turbines: Techniques and methods. *Renewable Energy*. 2012;46(C):169–78.
 23. Ribrant J. Reliability performance and maintenance—a survey of failures in wind power systems. KTH School of Electrical Engineering. 2006;59–72.
 24. Entezami M. Novel operational condition monitoring techniques for wind turbine brake systems. The University of Birmingham. 2013.
 25. Lambert J, Chambers A, Sinclair I, Spearing S. 3D damage characterisation and the role of voids in the fatigue of wind turbine blade materials. *Composites Science and Technology*. Elsevier; 2012;72(2):337–43.
 26. Caselitz P, Giebhardt J. Rotor condition monitoring for improved operational safety of offshore wind energy converters. *Journal of Solar Energy Engineering*. American Society of Mechanical Engineers; 2005;127(2):253–61.
 27. Hyers R, McGowan J, Sullivan K, Manwell J, Syrett B. Condition monitoring and prognosis of utility scale wind turbines. *Energy Materials*. Maney Publishing; 2006;1(3):187–203.
 28. Heap R. Wind Farm Owners: How To Cut The Impact Of Gearbox Failure [Internet]. 2015 [cited 2016 16–2]. Available from: <http://www.awordaboutwind.com/blog-post/wind-turbine-gearbox-failure/>
 29. Abramson S. Condition based monitoring adds bottom-line value. *Power Engineering*. PennWell Publishing Corp.; 2011;115(4):60–2.

30. Smith P. Data: Component fault rates analysed [Internet]. 2014 [cited 2016]. Available from: <http://www.windpowermonthly.com/article/1302791/data-component-fault-rates-analysed>
31. Nejad AR, Guo Y, Gao Z, Moan T. Development of a 5 MW reference gearbox for offshore wind turbines. *Wind Energy*. Wiley Online Library; 2015;
32. Tian Z, Ding Y, Ding F. Maintenance optimization of wind turbine systems based on intelligent prediction tools. *Innovative computing methods and their applications to engineering problems*. Springer; 2011. p. 53–71.
33. Dupuis R. Application of oil debris monitoring for wind turbine gearbox prognostics and health management. *Proceedings of the Annual Conference of the Prognostics and Health Management Society*. 2010.
34. Budny R. Fixing Wind-Turbine Gearbox Problems [Internet]. 2014 [cited 2016]. Available from: <http://www.machinedesign.com/sites/machinedesign.com/files/uploads/2014/06/Roma-x-wind-gearing.png>
35. Van den Broek T, van Bussel G, Hofemann C, Boussion C. Cost-sensitivity Analyses for Condition Monitoring Systems for Gearboxes. [Netherland]: Delft University of Technology; 2014.
36. Tavner P. Review of condition monitoring of rotating electrical machines. *Electric Power Applications*, IET. Durham University. UK; 2008;2(4):215–47.
37. Yang W, Tavner P, Court R. An online technique for condition monitoring the induction generators used in wind and marine turbines. *Mechanical Systems and Signal Processing*. Elsevier; 2013;38(1):103–12.
38. Pliego Marugán A, García Márquez FP, Pinar Pérez JM. Optimal Maintenance Management of Offshore Wind Farms. *Energies*. Multidisciplinary Digital Publishing Institute; 2016;9(1):46.
39. Ahadi A. Wind Turbine Fault diagnosis Techniques and Related Algorithms. *International Journal of Renewable Energy Research (IJRER)*. 2016;6(1):1347–56.
40. Hwas A, Katebi R. Wind turbine control using PI pitch angle controller. *IFAC Proceedings Volumes*. Elsevier; 2012;45(3):241–6.
41. Michalis P, Saafi M, Judd M. Capacitive sensors for offshore scour monitoring. *Proceedings of the ICE-Energy*. Thomas Telford; 2013;166(4):189–97.
42. Saeed A. Online condition monitoring system for wind turbine. 2008.
43. Verbruggen T. Wind Turbine Operation & Maintenance based on Condition Monitoring WT-Ω. ECN, Energy research Center of the Netherlands) Final report, ECN-C-03-047. 2003;

44. Wisznia R. Condition Monitoring of Offshore Wind Turbines. KTH School of Industrial Engineering and Management. Sweden. 2013;
45. Sinha Y. Optimisation of offshore wind farm maintenance. Robert Gordon University; PHD Thesis. Available from <http://openair.gu.ac.uk>. UK. 2016.
46. Li Y. Discussion on the principles of wind turbine condition monitoring system. Materials for Renewable Energy \& Environment (ICMREE), 2011 International Conference on. 2011. p. 621–4.
47. Wiggelinkhuizen E, Verbruggen T, Braam H, Rademakers L, Xiang J, Watson S. Assessment of condition monitoring techniques for offshore wind farms. Journal of solar energy engineering. American Society of Mechanical Engineers; 2008;130(3):031004.
48. McMillan D, Ault G. Condition monitoring benefit for onshore wind turbines: sensitivity to operational parameters. IET Renewable Power Generation. IET; 2008;2(1):60–72.
49. Butler S. Prognostic algorithms for condition monitoring and remaining useful life estimation. National University of Ireland, Maynooth. 2012;
50. Crabtree CJ, Zappalá D, Tavner PJ. Survey of commercially available condition monitoring systems for wind turbines. Durham University School of Engineering and Computing Sciences and the SUPERGEN Wind Energy Technologies Consortium; 2014;
51. Hameed Z, Hong YS, Cho YM, Ahn SH, Song CK. Condition monitoring and fault detection of wind turbines and related algorithms: A review. Renewable and Sustainable Energy Reviews. 2009;13(1):1–39.
52. Wiggelinkhuizen E, Verbruggen T, Braam H, Rademakers L, Xiang J, Watson S, et al. CONMOW: Condition monitoring for offshore wind farms. 2007 European Wind Energy Conference and Exhibition. 2007. p. 118–22.
53. Sharma DM, others. Condition Monitoring of Wind Turbines: A Review. Global Journal of Researches In Engineering. International Journal of Scientific & Engineering Research, Volume 4, Issue 8. 2013;13(6).
54. Jablonski A, Barszcz T, Bielecka M. Automatic validation of vibration signals in wind farm distributed monitoring systems. Measurement. Elsevier; 2011;44(10):1954–67.
55. Christensen JJ, Andersson C, Gutt S. Remote condition monitoring of Vestas turbines. Technical Track—Operation \& Maintenance, Proceedings EWEC, Marseille, France. 2009;
56. Du L, Zhe J. A high throughput inductive pulse sensor for online oil debris monitoring. Tribology International. Elsevier; 2011;44(2):175–9.
57. Caselitz P, Giehardt J. Advanced maintenance and repair for offshore wind farms using fault prediction techniques. Proceedings of the world wind energy conference.

- 2002.
58. Kim K, Parthasarathy G, Uluyol O, Foslien W, Sheng S, Fleming P. Use of SCADA data for failure detection in wind turbines. ASME 2011 5th International Conference on Energy Sustainability. 2011. p. 2071–9.
 59. Jiménez AA, Muñoz CQG, Márquez FPG, others. Machine learning for wind turbine blades maintenance management. *Energies*. MDPI, Open Access Journal; 2017;11(1):1–16.
 60. Stetco A, Dinmohammadi F, Zhao X, Robu V, Flynn D, Barnes M, et al. Machine learning methods for wind turbine condition monitoring: A review. *Renewable energy*. Elsevier; 2018;
 61. El-Thalji I, Liyanage JP. Integrated asset management practices for offshore wind power industry: a critical review and a road map to the future. *International Offshore and Polar Engineering Conference (ISOPE)-2010 Beijing, China, June 20-26, 2010*. 2010. p. 934–41.
 62. Utne IB. Maintenance strategies for deep-sea offshore wind turbines. *Journal of Quality in Maintenance Engineering*. Emerald Group Publishing Limited; 2010;16(4):367–81.
 63. Scheu M, Matha D, Hofmann M, Muskulus M. Maintenance strategies for large offshore wind farms. *Energy Procedia*. Elsevier; 2012;24:281–8.
 64. Bangalore P. Load and Risk Based Maintenance Management of Wind Turbines. Chalmers University of Technology; 2014.
 65. Zhu W, Castanier B, Bettayeb B. A dynamic programming-based maintenance model of offshore wind turbine considering logistic delay and weather condition. *Reliability Engineering & System Safety*. Elsevier; 2019;106512.
 66. Igba J, Alemzadeh K, Anyanwu-Ebo I, Gibbons P, Friis J. A systems approach towards reliability-centred maintenance (RCM) of wind turbines. *Procedia Computer Science*. Elsevier; 2013;16:814–23.
 67. Anderson RT, Neri L. *Reliability-centered maintenance: management and engineering methods*. Springer Science & Business Media; 2012.
 68. Conaill Soraghan AL. Spare Parts Management in Offshore Wind Leveraging good practice from the aerospace industry. *Catapult Offshore Renewable Energy*. 2017.
 69. Council GWE. Global wind energy council: Wind turbine in numbers [Internet]. [cited 08-08/17]. Available from: <http://www.gwec.net/global-figures/wind-in-numbers/>
 70. Nguyen TAT, Chou S-Y. Maintenance strategy selection for improving cost-effectiveness of offshore wind systems. *Energy conversion and management*. Elsevier; 2018;157:86–95.
 71. Gamstedt K, Andersen SIS. Fatigue degradation and failure of rotating composite structures-Materials characterisation and underlying mechanisms. Risø National

- Laboratory, Roskilde, Denmark. 2001.
72. Orchard ME, Vachtsevanos GJ. A particle-filtering approach for on-line fault diagnosis and failure prognosis. *Transactions of the Institute of Measurement and Control*. SAGE Publications; 2009;31(3-4):221–46.
 73. Leite G de NP, Araújo AM, Rosas PAC. Prognostic techniques applied to maintenance of wind turbines: a concise and specific review. *Renewable and Sustainable Energy Reviews*. Elsevier; 2018;81:1917–25.
 74. Zhang D, Qian L, Mao B, Huang C, Huang B, Si Y. A data-driven design for fault detection of wind turbines using random forests and xgboost. *IEEE Access*. IEEE; 2018;6:21020–31.
 75. Dinmohammadi F, Shafiee M. A fuzzy-FMEA risk assessment approach for offshore wind turbines. *Int J Progn Health Manag*. 2013;4:1–10.
 76. Yang Z, Bonsall S, Wang J. Fuzzy rule-based Bayesian reasoning approach for prioritization of failures in FMEA. *Reliability, IEEE Transactions on*. IEEE; 2008;57(3):517–28.
 77. Nielsen JJ, Sørensen JD, others. Challenges for Risk-based Maintenance Planning for Offshore Wind Turbines. *The Twenty-first (2011) International Offshore and Polar Engineering Conference (ISOPE)*. 2011. p. 451–7.
 78. Plumley CE, Wilson G, Kenyon A, Quail F, Zitrou A. Diagnostics and prognostics utilising dynamic Bayesian networks applied to a wind turbine gearbox. *International Conference on Condition Monitoring and Machine Failure Prevention Technologies, CM \& MFPT 2012*. 2012.
 79. EWEA. *The European offshore wind industry - key trends and statistics 1st half 2015*. Wind Europe. Belgium. 2015.
 80. LORK. *Offshore Wind Farms Map* [Internet]. [cited 2016]. Available from: <http://www.lorc.dk/offshore-wind-farms-map/list?sortby=NumberOfTurbines&sortby2=&sortorder=desc>
 81. Siemens. *Siemens Wind Turbine SWT 3.6-120* [Internet]. Siemens; 2015. Available from: www.siemens.com/energy
 82. Commission IE, others. *Analysis Techniques for System Reliability: Procedure for Failure Mode and Effects Analysis (FMEA)*. International Electrotechnical Commission; 2006.
 83. DiVenti A. *Failure Mode Effect Analysis (FMEA) & Critical Items List (CIL) GLAST LAT Anti-Coincidence Detector (ACD) Report*. Maryland; 2002.
 84. Wilkinson M, Hendriks B, Spinato F, Harman K, Gomez E, Bulacio H, et al. *Methodology and results of the ReliaWind reliability field study*. *European Wind Energy Conference and Exhibition 2010, EWEC 2010*. 2010. p. 1984–2004.

85. Wilkinson M, Hendriks B. Reliability focused research on optimizing wind energy systems design, operation and maintenance: tools, proof of concepts, guidelines & methodologies for a new generation. 2011.
86. Tavner P, Higgins A, Arabian H, Long H, Feng Y. Using an FMEA method to compare prospective wind turbine design reliabilities. European Wind Energy Conference and Exhibition 2010, EWEC 2010. 2010. p. 2501–37.
87. Register L. Wind Turbine and FMEA Consultancy Report. Lloyd's Register. UK. 2015.
88. Boness K, Finkelstein A, Harrison R. A method for assessing confidence in requirements analysis. *Information and Software Technology*. Elsevier; 2011;53(10):1084–96.
89. Jonkman BJ. TurbSim user's guide: Version 1.50. National Renewable Energy Laboratory Golden, Colorado; 2009;
90. Commission IE, others. Wind turbines: Part 3: Design requirements for offshore wind turbines. IEC 61400-3; 2009.
91. Commission IE, others. Wind Turbines-Part 1: Design Requirements. IEC 61400-1 2007.
92. Geyer C. Introduction to Markov Chain Monte Carlo. *Handbook of Markov Chain Monte Carlo*. Springer. London. 2011;3–48.
93. Qiu Q, Cui L, Yang L. Maintenance policies for energy systems subject to complex failure processes and power purchasing agreement. *Computers & Industrial Engineering*. Elsevier; 2018;119:193–203.
94. Shafiee M, Sørensen JD. Maintenance optimization and inspection planning of wind energy assets: Models, methods and strategies. *Reliability Engineering & System Safety*. Elsevier; 2017;
95. Budny R. Fixing Wind-Turbine Gearbox Problems [Internet]. [cited 2017 9–1]. Available from: <http://machinedesign.com/mechanical-drives/fixing-wind-turbine-gearbox-problems>
96. Nathan S. Direct approach: improving wind turbine drivetrain reliability [Internet]. [cited 2017 9–1]. Available from: <https://www.theengineer.co.uk/direct-approach-improving-wind-turbine-drivetrain-reliability/>
97. Nam JS, Park YJ, Kim JK, Han JW, Nam YY, Lee GH. Application of similarity theory to load capacity of gearboxes. *Journal of Mechanical Science and Technology*. Springer; 2014;28(8):3033–40.
98. International Organization for Standardization I 61400-4: 2012. Wind Turbines-Part 4: Design Requirements for Wind Turbine Gearboxes. ISO Geneva; 2012;

99. Johnson GL. Wind energy systems. Prentice Hall. Electronic edition. Manhattan, KS. Citeseer; 2001.
100. Lloyd's-Register. Rules and regulations for the classification of ships. Lloyd's Register. London; 2016.
101. KISSsoft-AG. KISSsys description [Internet]. [cited 2017 9–1]. Available from: http://www.kisssoft.ch/english/downloads/instructions_kissys.php
102. KISSsoft A. Lifetime analysis of a 4MW Wind Turbine Gearbox using Kisssys. Private Publication. Switzerland; 2016.
103. BSI. BS ISO 6336-6:2006 - Calculation of load capacity of spur and helical gears. 2006.
104. Khonsari MM, Booser ER. Applied tribology: bearing design and lubrication. Second Edition. John Wiley & Sons Ltd.; 2008.
105. Ma K, Zhou D, Blaabjerg F. Evaluation and Design Tools for the Reliability of Wind Power Converter System. Journal of Power Electronics. 2015;15(5):1149–57.
106. Givaki K, Parker M, Jamieson P. Estimation of the power electronic converter lifetime in fully rated converter wind turbine for onshore and offshore wind farms. Power Electronics, Machines and Drives (PEMD 2014), 7th IET International Conference on. 2014. p. 1–6.
107. Degrenne N, Ewanchuk J, David E, Boldyrjew R, Mollov S. A Review of Prognostics and Health Management for Power Semiconductor Modules.
108. Wang H, Zhou D, Blaabjerg F. A reliability-oriented design method for power electronic converters. Applied Power Electronics Conference and Exposition (APEC), 2013 Twenty-Eighth Annual IEEE. 2013. p. 2921–8.
109. SEMIKRON. Application Manual Power Semiconductors. ISLE Verlag, a commercial unit of the ISLE Association. Germany. 2011.
110. Garcia JLD. Modeling and Control of Squirrel Cage Induction Generator with Full Power Converter Applied to Windmills. Universitat Politècnica de Catalunya. Spain. 2009.
111. Petersson A. Analysis, modeling and control of doubly-fed induction generators for wind turbines. Chalmers University of Technology; UK. 2005.
112. Graovac D, Purschel M. IGBT power losses calculation using the data-sheet parameters-Application note. 2014-08-01] <http://www.infineon.com>. 2009;
113. Semikron. SKIIP semikron datasheet. ISLE Verlag, a commercial unit of the ISLE Association. Germany. 2014.
114. Drogenik U, Kolar JW. A general scheme for calculating switching-and conduction-losses of power semiconductors in numerical circuit simulations of power electronic systems. Proceedings of the 2005 International Power Electronics Conference

- (IPEC'05), Niigata, Japan, April. 2005. p. 4–8.
115. Semikron. SkiiiP 513 semikron datasheet. ISLE Verlag, a commercial unit of the ISLE Association. Germany. 2014.
 116. Künzi R. Thermal Design of Power Electronic Circuits. CERN in the Proceedings of the CAS-CERN. CAS-CERN Accelerator School: Power Converters, Baden, Switzerland, 2016.
 117. Lei T. Doubly-fed induction generator wind turbine modelling, control and reliability. The University of Manchester, Manchester, UK; 2014;
 118. Ikonen M, others. Power cycling lifetime estimation of IGBT power modules based on chip temperature modeling. Acta Universitatis Lappeenrantaensis. Lappeenranta University of Technology; 2012;
 119. Manwell JF, McGowan JG, Rogers AL. Wind energy explained: theory, design and application. John Wiley & Sons; 2010.
 120. Irvine T. Vibration data python: rainflow fatigue [Internet]. [cited 01-08/16]. Available from: <https://vibrationdatapython.wordpress.com/?s=rainflow>
 121. Liniger J, Pedersen HC, Soltani M. Reliable Fluid Power Pitch Systems. Proceedings of the ASME, Bath 2015 Symposium on Fluid Power & Motion Control. 2015.
 122. Schlechtingen M, Santos IF, Achiche S. Wind turbine condition monitoring based on SCADA data using normal behavior models. Part 1: System description. Applied Soft Computing. Elsevier; 2013;13(1):259–70.
 123. Fischer K, Stalin T, Ramberg H, Thiringer T, Wenske J, Karlsson R. Investigation of converter failure in wind turbines. Elforsk report. 2012;12:58.
 124. Carvalho M, Nunes EP, Telhada J. Maintenance costs of a pitch control device of a wind turbine. Proceedings of the World Congress on Engineering 2013 (WCE 2013). 2013. p. 569–74.
 125. Cortes C, Vapnik V. Support-vector networks. Machine learning. Springer; Kluwer Academic Publishers, Boston. Manufactured in The Netherlands. 1995;20(3):273–97.
 126. Louppe G, Varoquaux G. Scikit-Learn: Machine Learning in the Python ecosystem. University of Liege, Belgium. 2013;
 127. Cole S, Martinot P, Rapoport S, Papaefthymiou G, Gori V. Study of the benefits of a meshed offshore grid in Northern Seas region: Final Report. European Commission. 2014;
 128. Newman M. Operations and maintenance in offshore wind: key issues for 2015/16. Catapult offshore Renewable Energy. UK. 2015;
 129. Hassan GG. A guide to UK offshore wind operations and maintenance. Scottish Enterprise and The Crown Estate. UK. 2013;

130. Spring M, Sepulveda M, Davies P, Gaal G. Top 30 Charts of wind turbine failure mechanisms. Proceedings of the EWEA Annual Event. Paris; 2015.
131. EON. Wind Turbine Technology and Operations Factbook. E.ON Climate & Renewables GmbH. Germany. 2013.
132. Carlos Aras CME karavina HA katherine B. Balance of plant of wind projects [Internet]. [cited 10-10/16]. Available from: http://www.esru.strath.ac.uk/EandE/Web_sites/11-12/Wind_BOP/methodology.html#data.
133. WEU. Onshore O&M strategy configuration report 2015. Wind Energy Update. UK Available from: www.windenergyupdate.com/operation—maintenance-onshore-wind-report—series/strategies—index.php. 2015.
134. Dewan A. logistic & Service Optimization for O&M of Offshore Wind Farms. Delf university of Technology. Netherlands. 2014.
135. SPARTA. System Performance, Availability and Reliability Trend Analysis. The Crown State. ORE Catapult. London. 2017.
136. Rademakers L, Braam H, Obdam T, vd Pieterman R. Operation and maintenance cost estimator (OMCE) to estimate the future O&M costs of offshore wind farms. European offshore wind 2009 conference Stockholm. 2009.
137. Carroll J, McDonald A, McMillan D. Failure rate, repair time and unscheduled O&M cost analysis of offshore wind turbines. Wind Energy. Wiley Online Library; 2015;
138. Dalgic Y, Dinwoodie IA, Lazakis I, McMillan D, Revie M. Optimum CTV fleet selection for offshore wind farm O&M activities. ESREL 2014. University College of London. UK. 2014;
139. Martin R, Lazakis I, Barbouchi S. Analysis of input factors to operations and maintenance of two offshore wind farm case studies; a screening process. Renewable Power Generation Conference (RPG 2014), 3rd. 2014. p. 1–6.
140. Gray A, Johanning L, Dickens B. A Markov chain model to enhance the weather simulation capabilities of an operations and maintenance tool for a wave energy array. EWTEC; University of Edinburgh. UK. 2015;
141. Average hours of daylight in Britain through out the year [Internet]. [cited 2017 Mar]. Available from: <http://www.projectbritain.com/weather/sunshine.htm>
142. Welisch M, Poudineh R. Auctions for allocation of offshore wind contracts for difference in the UK. Oxford Institute for Energy Studies; UK. 2019;
143. Ahsan D, Pedersen S. The influence of stakeholder groups in operation and maintenance services of offshore wind farms: Lesson from Denmark. Renewable energy. Elsevier; 2018;125:819–28.
144. Joshi S, McKeogh E, Dinh V. Levelised cost of offshore wind energy in Ireland at different deployment scales and lifetime. The Fifth International Conference on

- Offshore Energy and Storage, Ningbo, China. 2018.
145. Lacal-Arántegui R, Yusta JM, Domínguez-Navarro JA. Offshore wind installation: Analysing the evidence behind improvements in installation time. *Renewable and Sustainable Energy Reviews*. Elsevier; 2018;92:133–45.
 146. BusinessElectricityPrices. Retail versus wholesale electricity sales prices [Internet]. [cited 2017 Mar]. Available from: <https://www.businesselectricityprices.org.uk/retail-versus-wholesale-prices/>
 147. Martin R, Lazakis I, Barbouchi S, Johanning L. Sensitivity analysis of offshore wind farm operation and maintenance cost and availability. *Renewable Energy*. Elsevier; 2016. p. 1226–36.

FAILURE MODES DETECTED BY O&M TEAM

56 
Giving false positive

55 
Giving false negative

55 
Not working at all

51 
Control Panel Fault

35 
Material Failure

27 
Electrical Failure











10 
mechanically stuck

8 
high friction

4 
Short circuit

3 
Blockage

FAILURE MODES -> TURBINE SHUTDOWN

24		<i>bearing collapse or separates</i>
20		<i>high friction</i>
17		<i>mechanically stuck</i>
5		<i>increased bearing friction, abrasion, scuffing</i>
5		<i>Material Failure</i>
3		<i>Fatigue</i>
2		<i>Detachment</i>
1		<i>Brushes Failure</i>
1		<i>Electrical Failure</i>
1		<i>Electrical Insulation Failure</i>

FAILURE MODES DETECTED BY CMS

28		<i>Bearing stuck</i>
26		<i>increased bearing friction, abrasion, scuffing</i>
21		<i>bearing collapse or separates</i>
9		<i>Material Failure</i>
7		<i>Electrical Failure</i>
5		<i>Blockage</i>
4		<i>Electrical Insulation Failure</i>
4		<i>Fatigue</i>
4		<i>high friction</i>
4		<i>mechanically stuck</i>
3		<i>Detachment</i>

Annex 2: FASTv8 pre-processors

FAST Pre-processor AeroDyn

AeroDyn is a time-domain wind turbine aerodynamics module that has been coupled into the FAST version 8 multi-physics engineering tool to enable aero-elastic simulation of horizontal axis wind turbines. Aerodynamic calculations within AeroDyn are based on the principles of actuator lines, where the three-dimensional (3D) flow around a body is approximated by local two-dimensional (2D) flow at cross sections, and the distributed pressure and shear stresses are approximated by lift forces, drag forces, and pitching moments lumped at a node in a 2D cross section.

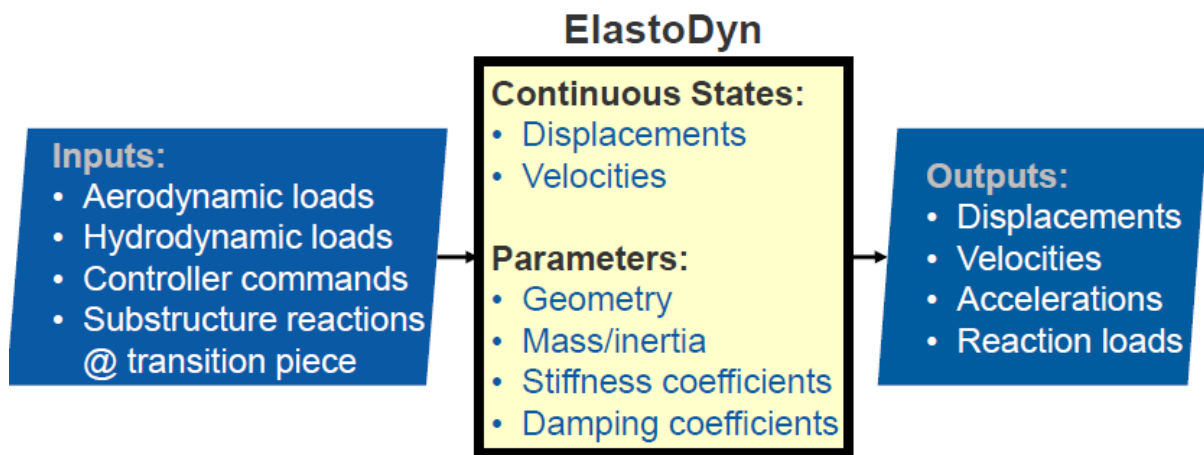
Wind and structural calculations take place outside of the AeroDyn module and are passed as inputs to AeroDyn by the driver code. AeroDyn consists of four sub models: (1) rotor wake/induction, (2) blade airfoil aerodynamics, (3) tower influence on the wind local to the blade nodes, and (4) tower drag.

The primary AeroDyn input file defines modeling options, environmental conditions (except freestream wind), airfoils, tower nodal discretization and properties, as well as output file specifications.

Airfoil data properties are read from dedicated inputs files (one for each airfoil) and include coefficients of lift force, drag force, and pitching moment versus angle of attack (AoA), as well as unsteady airfoil aerodynamic (UA) model parameters. Blade nodal discretization, geometry, twist, chord, and airfoil identifier are likewise read from separate input files (one for each blade). AeroDyn uses the SI system (kg, m, s, N). Angles are assumed to be in radians unless otherwise specified.

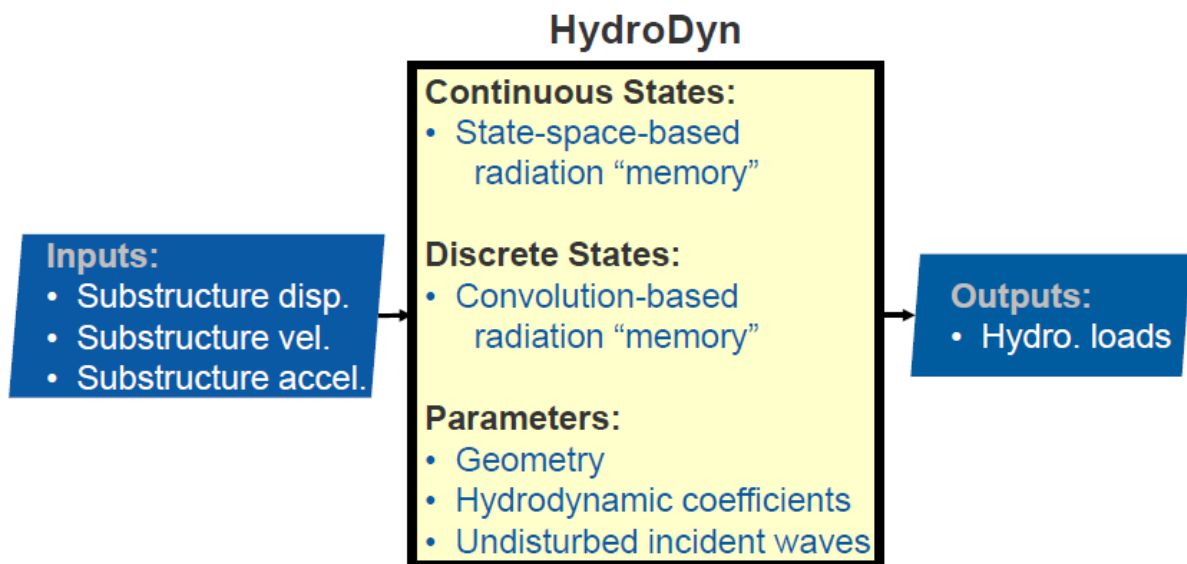
FAST Pre-processor ElastoDyn

ElastoDyn is the Structural-Dynamics Module.

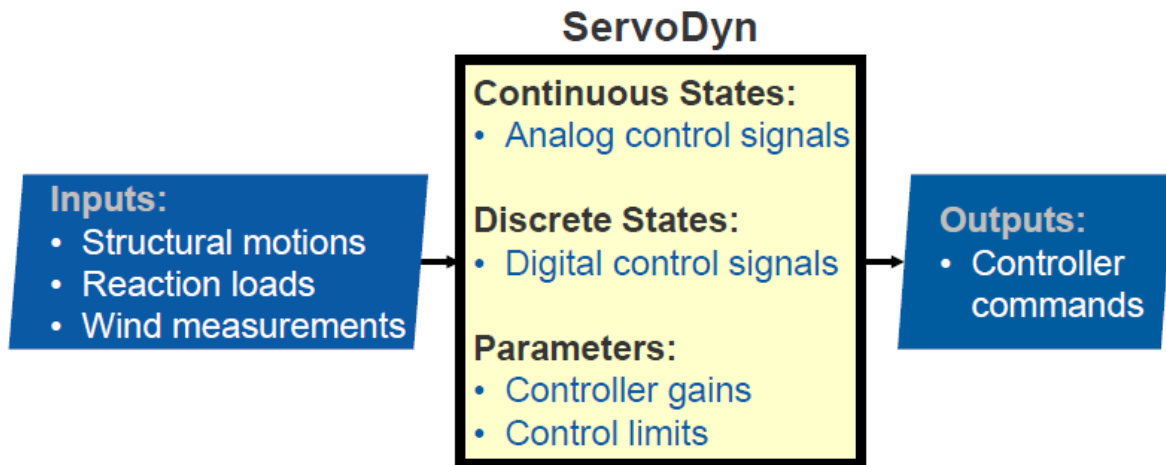


FAST Pre-processor HydroDyn

HydroDyn is a time-domain hydrodynamics module of FAST. HydroDyn allows for multiple approaches for calculating the hydrodynamic loads on a structure: a potential-flow theory solution, a strip-theory solution, or a hybrid combination of the two. Waves generated internally within HydroDyn can be regular (periodic) or irregular (stochastic) and long-crested (unidirectional) or short-crested (with wave energy spread across a range of directions).



FAST Pre-processor ServoDyn



FAST Pre-processor TurboSim

TurbSim is a stochastic, full-field, turbulent-wind simulator. It uses a statistical model (as opposed to a physics-based model) to numerically simulate time series of three-component wind-speed vectors at points in a two-dimensional vertical rectangular grid that is fixed in space. TurbSim output is used as input into AeroDyn. AeroDyn's InflowWind module uses Taylor's frozen turbulence hypothesis to obtain local wind speeds, interpolating the TurbSim-generated fields in both time and space.

